

**New catalysts for amine alkylation reactions
promoted by hydrogen borrowing**

Roberta Lanaro

Submitted in accordance with the requirements for the degree of
Doctor of Philosophy

The University of Leeds
School of Chemistry

June 2015

The candidate confirms that the work submitted is his/her own and that appropriate credit has been given where reference has been made to the work of others.

This copy has been supplied on the understanding that it is copyright material and that no quotation from the thesis may be published without proper acknowledgement.

The right of Roberta Lanaro to be identified as Author of this work has been asserted by her in accordance with the Copyright, Designs and Patents Act 1988.

Acknowledgements

First, I would like to thank Steve for his invaluable guidance, for all the ideas and advice throughout the entire project and for his support over the past three and a half years. I must also thank my co-supervisors: Paddy McGowan and John Blacker for their ideas and advice, particularly in the organometallic and kinetic fields. I would like to thank my industrial supervisor, Lianne Frodsham, for her support and help throughout the project and for her supervision during my CASE placement in AstraZeneca.

I would like to thank the University of Leeds, Kocienski Bequest and AstraZeneca for funding.

I must thank the technical staff in the University of Leeds, particularly Ian Blakeley and Tanja Marinko-Covell for the elemental analyses and Helena Shepherd and Chris Pask who recorded all the X-ray crystal structures of my complexes. I would particularly thank Chris for his help in the elucidation of the structures. I must also thank the MChem student Ashley Thompson for all of her hard work.

I would like to thank all the present and past members of the Marsden's group who made amazing these three and a half years here in Leeds. First, I would like to thank the original members: David, John Li, Mary, James, Nic and Dan for their invaluable help and advice, for the tea breaks and the (often random) discussions. I would like to thank the amazing post-doc team: Tarn, Mark, Tony, Andrea, Ignacio and James for all of the suggestions and proofreading of reports and thesis. Thank you to the new PhD members, Seb and Gayle. I'll miss you all! I would also like to thank the "additional" members Chris for the good laugh at the pub and at the Christmas meals and Carlo for sharing our AZ meetings and placement.

I would like to thank my family for all of the support and encouragement throughout this time, despite not being particularly happy of me living abroad. Finally, thank you to Gabri to be always present and supporting over these three and a half years and to share with me sorrows and joys of the PhD.

Abstract

N-Alkylation of amines with alcohols mediated by borrowing hydrogen is a useful synthetic tool for the preparation of functionalised amines. Specifically, alcohols can be temporarily converted into carbonyl compounds by the metal-catalysed removal of hydrogen. The carbonyl compounds are more reactive than the precursor alcohols and can react *in situ* with amines to give imines. The metal catalyst returns the borrowed hydrogen to the imines, giving the alkylated amines.

Chapter 1 outlines the potential for the atom-efficient hydrogen borrowing processes, giving an overview of the main transformations that can be carried out using this interesting methodology. A preliminary investigation of the reaction mechanism gave us useful information for the synthesis of more robust catalysts for these processes.

As a result, a new family of rhodium and iridium complexes was synthesised, which contained a modified Cp* ligand bearing an amine on the tethered chain. Two iridium catalysts were found to be the most active among our family of monomeric complexes. More than 20 substrates containing aryl, heteroaryl and alkyl groups were prepared in 62-99% yields; among them, primary and secondary alcohols and primary and secondary amines have been used. Furthermore, a broad range of functional groups were tolerated, such as halides, nitriles, ethers, esters, amides, sulphonamides and carbamates. Furthermore, the development of a recyclable rhodium complex and a chiral iridium catalyst were attempted.

To conclude, Chapter 5 describes the catalytic activities of three dicationic monomers. The *N*-alkylation of amines on water was explored. The procedure works well for a range of substituted alcohols and amines; in total, 10 compounds have been isolated in good to excellent yield (> 69%).

Contents

Acknowledgements	iii
Abstract	iv
Contents	v
Abbreviations	viii
Chapter 1. Introduction	1
1.1 Alkylation of Amines with Alcohols promoted by Hydrogen Borrowing.....	1
1.2 History.....	5
1.3 Ruthenium-catalysed N-Alkylation with Alcohols	6
1.4 Iridium-catalysed N-Alkylation with Alcohols.....	8
1.5 Mechanistic studies for the alkylation of amines catalysed by [Cp*IrCl ₂] ₂	13
1.6 N-Alkylation by Alcohols Catalysed by other Metal Complexes.....	19
1.7 Formation of N-Heterocycles.....	22
1.8 N-Alkylation of Amides, Carbamates and Sufonamides with Alcohols.....	26
1.9 N-Alkylation of Amines with Alcohols affording Chiral Compounds.....	28
1.10 Project Aims.....	31
Chapter 2. Initial Attempts to Study the Reaction Mechanism.....	33
2.1 Evaluation of the Active Iridium Catalyst: Amine-Coordination or Carbonate-Coordination.....	33
2.2 Determination of the Reaction Order: Amine	37
2.3 Determination of the Reaction Order: Alcohol	38
2.4 Determination of the Reaction Order: Catalyst.....	40
2.5 Conclusions	41
Chapter 3. Synthesis of New Complexes	42
3.1 Introduction	42
3.2 Synthesis of New Monomeric Rhodium(III) Catalysts.....	44
3.3 Modification of Rhodium(III) Complex 67: Secondary Amine	50

3.4 Modification of Rhodium(III) Complex 67: Tertiary Amine	54
3.5 Modification of Rhodium(III) Complex 67: Iodide as Halide ligand	61
3.6 Modification of Rhodium(III) Complex 67: Dicationic Rhodium Monomer	61
3.7 Modification of Rhodium(III) Complex 67: Synthesis of Monomer containing a Fluorous Tag	63
3.8 Synthesis of New Monomeric Iridium(III) Complexes	67
3.9 Modification of Iridium(III) Complex 102: Secondary Amine	70
3.10 Modification of Iridium(III) Complex 102: Tertiary Amine	72
3.11 Modification of Iridium(III) Complexes 102 and 105: Iodide as Halide Ligand	74
3.12 Modification of Iridium(III) Complex 102: Chiral Iridium Complexes	75
3.13 Modification of Iridium(III) Complex 102: Dicationic Iridium Complexes	79
3.14 Conclusions	84
Chapter 4. Catalytic Activity of Rhodium and Iridium Complexes	85
4.1 Activity of Rhodium Complexes with Respect to Length of Side Chain	85
4.2 Activity of Rhodium Complexes with Respect to the Substitution on Tethered Amine	86
4.3 Activity of Rhodium Complexes with Respect to the Halide Ligands	88
4.4 Solvent Tolerance and Catalyst Loading using Catalyst 67	89
4.5 Activity of Iridium Complexes with Respect to the Substitution on Tethered Amine and with Respect to the Halide Ligands	91
4.6 Comparison between Catalysts 67 and 102	93
4.7 Solvent Tolerance and Catalyst Loading using Catalyst 102	94
4.8 Effects of Water, Bases and Acids in the Catalytic System	99
4.9 Substrate Scope using Catalyst 102: Secondary and Tertiary Amines	103
4.10 Substrate Scope using Catalyst 102: Functional Groups	106
4.11 Substrate Scope: Racemisation	112
4.12 Substrate Scope using Catalyst 102: Amino alcohols	115
4.13 Synthesis of Chiral Amines using Iridium Catalysts 113 and 119	120
4.14 Activity of Rhodium Catalyst 101 and Attempts to Recycle	123
4.15 Mechanistic studies	125
4.16 Conclusions	133
Chapter 5. Improved Catalytic Activity using Dicationic Rhodium and Iridium Complexes	138
5.1 Activity of Dicationic Rhodium Complex 93	138
5.2 Activity of Dicationic Iridium Complexes 120 and 122	139
5.3 Screening of Solvents and Catalyst Loading	142

5.4 Activity in Water of Rhodium and Iridium Catalysts and Substrate Scope.....	146
5.5 Catalyst recovery.....	151
5.6 Conclusion	155
Chapter 6. Experimental.....	158
6.1 General Considerations	158
6.2 General Procedures	160
6.3 Experimental Procedures	165
6.4 Supplementary data.....	228
References	229

Abbreviations

α	<i>alpha</i>
Å	Angstrom
β	<i>beta</i>
δ	Chemical shift
Ac	Acetyl
ap	Apparent
aq.	Aqueous
Ar	Aryl
b.p.	Boiling point
BINAP	(1,1'-Binaphthalene-2,2'-diyl)bis(diphenylphosphine)
Bn	Benzyl
BnOH	Benzyl alcohol
Boc	<i>tert</i> -Butyloxycarbonyl
br	Broad
Bu	Butyl
C	Celsius
cod	1,5-Cyclooctadiene
cot	1,3,5,7-Cyclooctatetraene
Cp	Cyclopentadienyl
Cp*	Pentamethylcyclopentadienyl
CPME	Cyclopentyl methyl ether
d	Doublet
DCM	Dichloromethane
DFT	Density functional theory
DMF	<i>N,N</i> -Dimethylformamide
DMAP	<i>N,N</i> -Dimethylaminopyridine
DMSO	Dimethylsulfoxide
DPEphos	Bis[(2-diphenylphosphino)phenyl] ether
dppe	Ethylenebis(diphenylphosphine)
dppf	1,1'-Bis(diphenylphosphino)ferrocene

d.r.	Diastereomeric ratio
EDC	N-(3-Dimethylaminopropyl)-N'-ethylcarbodiimide
EDG	Electron-donating group
<i>e.e.</i>	Enantiomeric excess
eq	Equivalent
ES	Electrospray
ESI	Electrospray ionisation
Et	Ethyl
EWG	Electron-withdrawing group
F-SPE	Fluorous solid phase extraction
FC-72	Perfluorohexane
FC-75	Perfluoro(butyltetrahydrofuran)
GC	Gas chromatography
h	Hours
HPLC	High-performance liquid chromatography
HRMS	High-resolution mass spectrometry
Hz	Hertz
IRF	Internal response factor
<i>J</i>	Coupling constant
<i>k</i>	Rate constant
KIE	Kinetic isotope effect
ln	Natural logarithm
M	Molar
m	Multiplet
<i>m-</i>	<i>Meta</i>
Me	Methyl
min (or mins)	Minutes
mp	Melting point
NHC	<i>N</i> -Heterocyclic carbene
NMP	1-Methyl-2-pyrrolidinone
NMR	Nuclear magnetic resonance
<i>o-</i>	<i>Ortho</i>
<i>p-</i>	<i>Para</i>

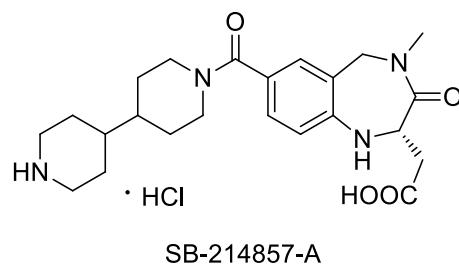
Ph	Phenyl
ppm	Parts per million
Pr	Propyl
psi	Pound-force per square inch
q	Quartet
RDS	Rate determining step
RT	Room temperature
SCRAM	η^5 -(pentamethylcyclopentadienyl)iridium(III) diiodide dimer
<i>t</i>	Tertiary
TFAA	Trifluoroacetic anhydride
THF	Tetrahydrofuran
TLC	Thin layer chromatography
Ts	<i>p</i> -Toluenesulfonyl
UV	Ultraviolet
Xantphos	4,5-Bis(diphenylphosphino)-9,9-dimethylxanthene

Chapter 1. Introduction

1.1 Alkylation of Amines with Alcohols promoted by Hydrogen Borrowing

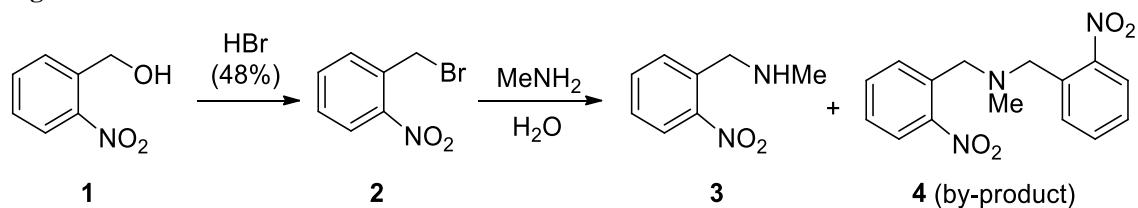
The chemistry of amines, amides and other nitrogen-containing compounds plays a central role in organic synthesis. A great number of natural, pharmaceutical and agrochemical compounds have a C-N bond and for this reason, several methods have been developed to prepare them. Particularly, we focus our attention on the synthesis of amines. There are numerous reactions which give amines as products, including reductive amination processes from carbonyl groups and amination of aryl halides.¹ Among all the reactions to make amines that are carried out efficaciously in the pharmaceutical industry, *N*-alkylation processes using alkyl halides or tosylates are the most used (36%), followed by reductive amination (20%) and *N*-alkylation of amides and reduction (10%).² Nucleophilic substitutions (S_N2) are still widely used, even though alkylating reagents are often genotoxic and the requirement that only a minute level of genotoxic impurities are permitted in drug candidates discourages these substitutions late in the synthesis.² The reduction of amines and amides is often carried out using flammable or toxic reducing reagents, such as lithium aluminium hydride, borane or sodium cyanoborohydride, which also lead to complex work-up procedures and to the generation of a high level of waste.² The following example shows some of the difficulties found in scaling up these processes. Lotrafiban, SB-214857-A, was a potential drug candidate molecule which acted as a non-peptidic glycoprotein IIb/IIIa receptor antagonist to prevent platelet aggregation and thrombus formation (Figure 1).³

Figure 1



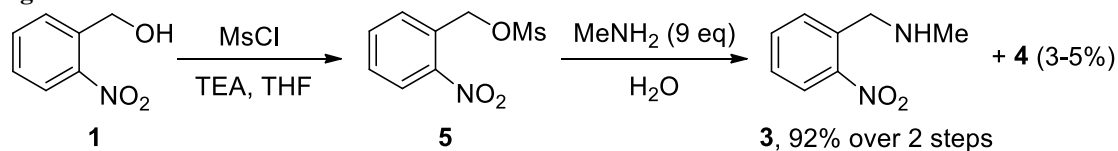
The development of this drug halted during phase III clinical trials, but by that stage several routes have been developed to manufacture the drug in multi-ton scale.² The intermediate *N*-methylaminomethylnitrobenzene **3** was initially prepared starting from 2-nitrobenzyl alcohol by bromination using concentrated hydrobromic acid and a nucleophilic substitution with aqueous methylamine (Figure 2). The methylamine was used in excess to avoid the formation of the dialkylated product **4**.³

Figure 2



Since these reaction conditions were quite harsh and the intermediate **2** was lachrymatory and not thermally stable, further optimisations were necessary in order to improve the sustainability of this process. Thus, 2-nitrobenzyl bromide **2** was replaced with the corresponding mesylate **5**. Even though the reaction conditions were milder, the mesylate was not isolated and it was added directly to a large excess of methylamine to synthesise **3** (Figure 3).³

Figure 3



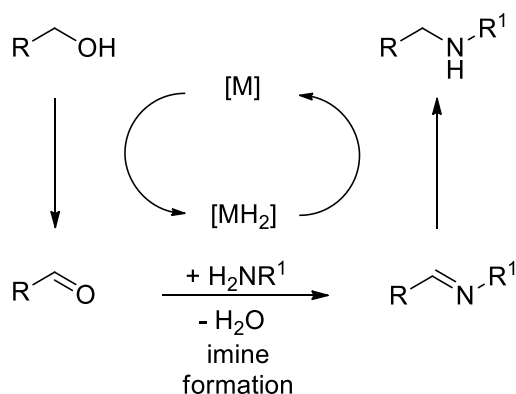
The optimisation of the reaction conditions led to preparation of **3** in high yield (92% over two steps) and the formation of the dialkylated amine **4** was reduced down to 3-5% yield. However, compounds **5** and **2** were less stable and less safe to handle than the corresponding benzyl alcohol **1** and the amine had to be used in large excess (9 equivalents) to avoid the overalkylated product **4**. Besides, a stoichiometric amount of waste was formed both in the first and second step of the synthesis (respectively, triethylammonium chloride and methanesulfonic acid), which underlines the low atom efficiency of such processes.

In the last few years, the rise of green chemistry has highlighted the need to develop strategies that increase the sustainability of such processes.⁴ One of these strategies replaces highly reactive reagents such as alkyl halides or tosylates with less reactive reagents such as alcohols, ROH. Effectively, the use of alcohols as alkylating agents is beneficial as these reagents are readily available, highly stable, low in toxicity, easily stored, low in cost and relatively high in atom efficiency.⁵

Generally, alcohols are not used as alkylating reagents because the hydroxyl group is not a good leaving group. However, they can be activated by catalytic dehydrogenative oxidation to generate *in situ* a more reactive carbonyl species, which can react as an electrophilic or a nucleophilic species.⁶ If the carbonyl compound or its derivative is subsequently reduced under the reaction conditions, this protocol is known as a hydrogen autotransfer process^{7,8,9} or borrowing hydrogen.¹⁰ The additional reactivity of the ketone is exploited by imine formation and reduction to an amine, alkene formation and reduction to a C-C bond and enolisation, electrophilic trapping and reduction to a functionalised alcohol.⁶

The general mechanism for the first pathway, which leads to carbon-nitrogen bond-formation reactions, is shown in Figure 4.

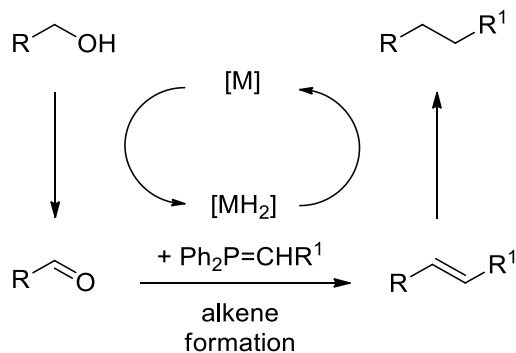
Figure 4



The first step is the abstraction of hydrogen from the starting alcohol by a catalyst to form the corresponding carbonyl compound. The following step is a condensation reaction between the new carbonyl compound and the amine, which leads to imine or iminium formation. Finally, the abstracted hydrogen is returned and incorporated into the final product. The atom efficiency of such process is really high as the only by-product is water. The other two reaction pathways lead to the formation of new C-C bonds. In the first case,

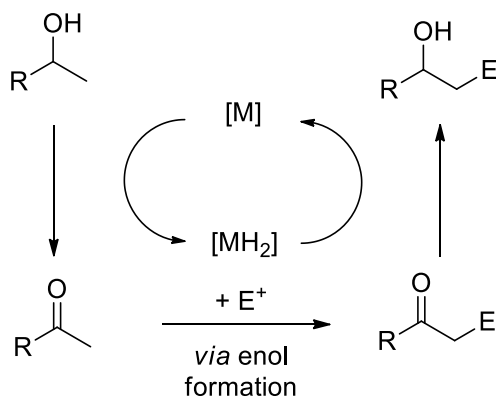
the carbonyl compound generated from the dehydrogenation of the alcohol reacts in a Wittig reaction to give an alkene, which is then reduced *in situ* to the corresponding alkane (Figure 5).¹⁰

Figure 5



In the last pathway, the alcohols are functionalised in the β -position (Figure 6). Effectively, the oxidation to a carbonyl compound provides an opportunity to access enol/enolate chemistry, which can react with an electrophile. Again, the abstracted hydrogen is incorporated into the final product to afford the β -substituted alcohol.

Figure 6



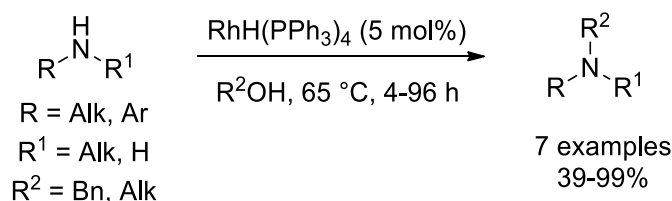
Within this introduction, we will cover the synthesis of alkylated amines mediated by borrowing hydrogen, as shown in the general mechanism reported in Figure 4.

1.2 History

In the literature, both heterogeneous and homogeneous catalysts have been reported to promote this reaction.^{1,4} Heterogeneous catalysts have some advantages over homogeneous ones, such as their greater ease of recovery from the reaction mixture. However, high pressures and temperatures are often required and, therefore, the use of homogeneous catalysts frequently allows reactions to occur at a lower temperature and with higher selectivity than heterogeneous catalysts.

Grigg and co-workers reported the first hydrogen borrowing reaction *via* homogeneous catalysis in 1981.¹¹ The authors achieved the *N*-alkylation of amines by alcohols using both metal halide-triphenylphosphine mixtures, to generate metal-phosphine complexes *in situ*, and preformed metal-phosphine catalysts. Iridium, ruthenium and rhodium complexes have been examined and the best results were obtained with the preformed rhodium-phosphine complex RhH(PPh₃)₄ (Scheme 1). The substrate scope was quite limited because, since the alcohols were used in large excess, only relatively volatile alcohols were used.

Scheme 1

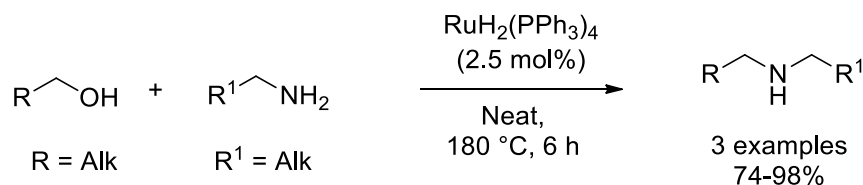


Since this first example reported by Grigg *et al.*, great efforts have been made to develop better catalysts for the alkylation of amines. Several other complexes were synthesised and tested in hydrogen borrowing reactions. The catalysts which gave the best activities and yields can be divided into two main families. The first one is ruthenium-based; some of the results obtained with these catalysts are reported in the next section. The second main class contains an iridium atom as the metal centre and we will focus on this family in Section 1.4.

1.3 Ruthenium-catalysed *N*-Alkylation with Alcohols

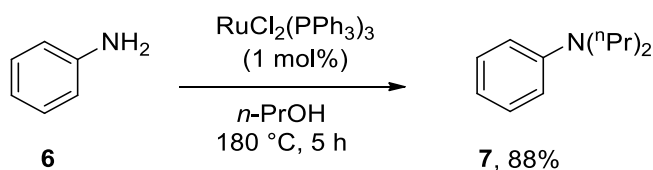
In 1982, only one year after Grigg's paper,¹¹ Murahashi and co-workers demonstrated that aliphatic amines were competent substrates for *N*-alkylation with alcohols using a $[\text{RuH}_2(\text{PPh}_3)_4]$ catalyst (Scheme 2).¹²

Scheme 2



Aryl amines did not work in this catalytic system; nevertheless, the authors managed to successfully use aminoarenes in good yields using a similar catalyst, $[\text{RuCl}_2(\text{PPh}_3)_3]$, as shown in a representative example in Scheme 3.⁴

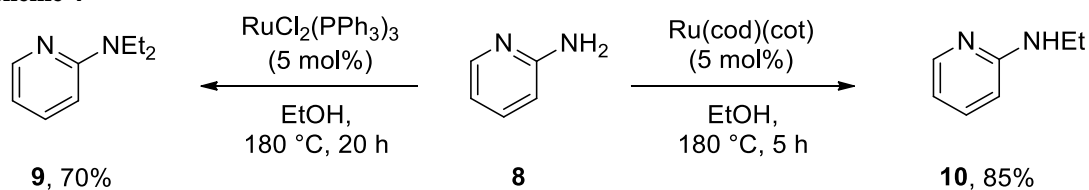
Scheme 3



The substrate scope in these two examples was still quite limited and the reaction conditions were harsh, requiring a high temperature (180 °C).

The group of Watanabe demonstrated that different ruthenium catalysts show widely varying selectivity in *N*-alkylation reactions. Indeed, depending on the complex employed and the conditions used, both mono- and dialkylated amines could be prepared. For instance, ruthenium complex $[\text{Ru}(\text{cod})(\text{cot})]$ was the most selective for monoalkylation of heteroaromatic amines, whereas the previous catalyst $[\text{RuCl}_2(\text{PPh}_3)_3]$ promoted the formation of tertiary amines (Scheme 4).¹³

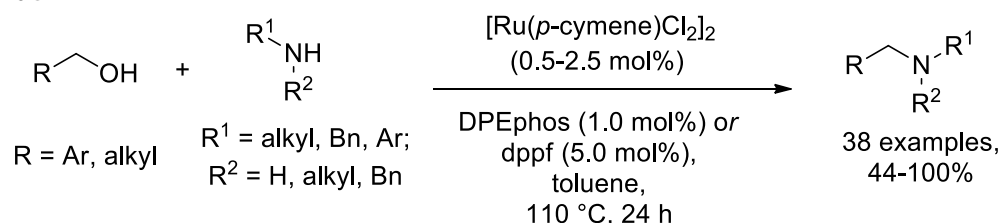
Scheme 4



Watanabe identified this reactivity as an advantage of the alcohol activation strategy: choosing the right catalyst, the secondary amine formed by alkylation of a primary amine did not react further, particularly using non-polar solvents.² The synthesis of secondary amines *via* alkylation using halide or tosylate is difficult because over-alkylated by-products are often observed.

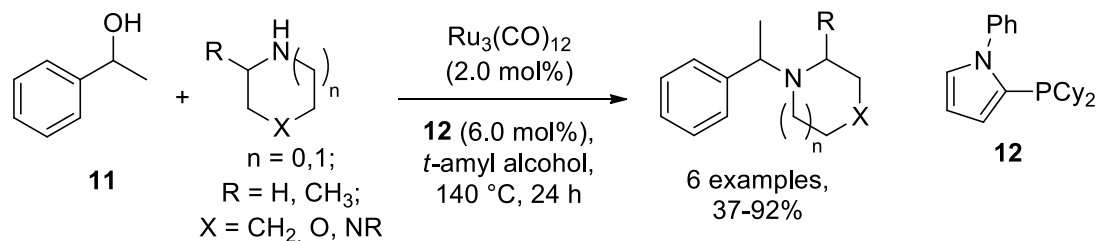
More recently, better catalytic systems have been reported. Williams and co-workers demonstrated that $[\text{Ru}(p\text{-cymene})\text{Cl}_2]_2$, activated by the addition of either bis(diphenylphosphino)ferrocene (dppf) or DPEphos, was an active catalyst system for the alkylation of amines by primary alcohols, as shown in Scheme 5.^{14,15} The addition of an additive was paramount to achieve good yield, because, when $[\text{Ru}(p\text{-cymene})\text{Cl}_2]_2$ was used alone as the catalyst, the *N*-alkylation proceeded slowly.

Scheme 5

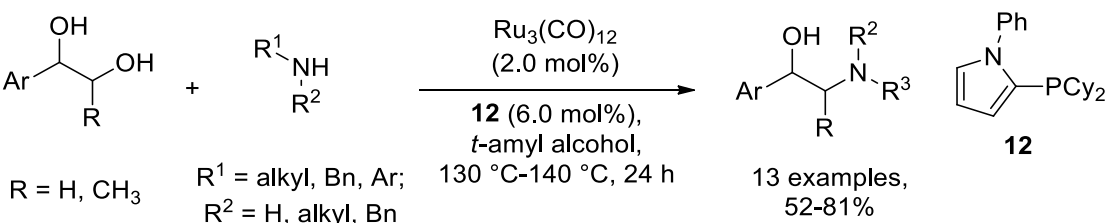


This catalytic system showed a quite broad tolerance of functional groups but unfortunately, it did not work when secondary alcohols were used as the substrate. *N*-Alkylation with secondary alcohols is more difficult than with primary alcohols because ketones are poorer electrophiles than aldehydes, in spite of the oxidation potential of secondary alcohols making dehydrogenation of these more favourable than primary alcohols.⁴

Beller and co-workers further improved this family of ruthenium complexes, reporting that $[\text{Ru}_3(\text{CO})_{12}]$ promotes the *N*-alkylation of primary and secondary amines using both primary and secondary alcohols.^{16,17} To obtain higher yields, a phosphine ligand was added in a catalytic amount; good results were obtained using both tri(*o*-tolyl)-phosphine¹⁶ and 2-(dicyclohexylphosphanyl)pyrrole **12** (Scheme 6).¹⁷

Scheme 6

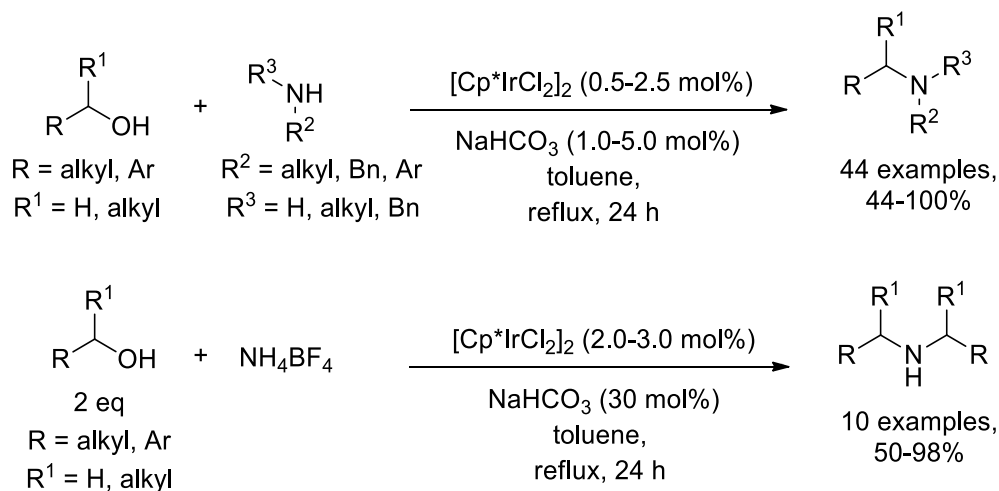
Beller and co-workers also demonstrated the applicability of this catalytic system, which was able to promote the selective monoalkylation of vicinal diols with secondary amines and anilines. This system was selective for amination at primary hydroxyl groups or sterically less hindered secondary hydroxyl groups (Scheme 7).¹⁸

Scheme 7

1.4 Iridium-catalysed *N*-Alkylation with Alcohols

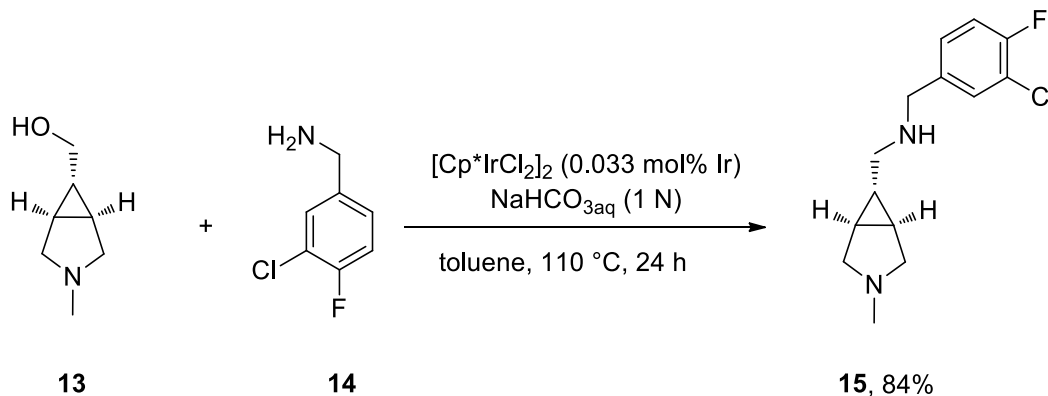
In the literature, iridium complexes have been reported to catalyse different reactions, such as carbon-carbon forming reactions, as well as isomerisation and hydrogen autotransfer reactions.^{19,20} In the last two decades, iridium catalysts were also applied in hydrogen borrowing, showing a great activity and generally achieving higher yields than those obtained with ruthenium complexes. The iridium complex most widely used for this reaction is the dimeric η^5 -(pentamethylcyclopentadienyl)iridium(III) dichloride $[\text{Cp}^*\text{IrCl}_2]_2$, which was largely studied by Yamaguchi and co-workers.^{19,21,22,23} This iridium dimer has been efficaciously used in the *N*-alkylation of primary and secondary amines as well as in the multialkylation of ammonium salts, as shown in Scheme 8. Primary and secondary alcohols could be used, through with bulky substrates the catalyst loading was increased up to 5 mol% of iridium in order to obtain the products in high yield. The functional groups that could be tolerated were quite broad and included both electron-withdrawing and electron-donating groups, such as ethers, esters, halogens, nitro and nitrile groups.

Scheme 8



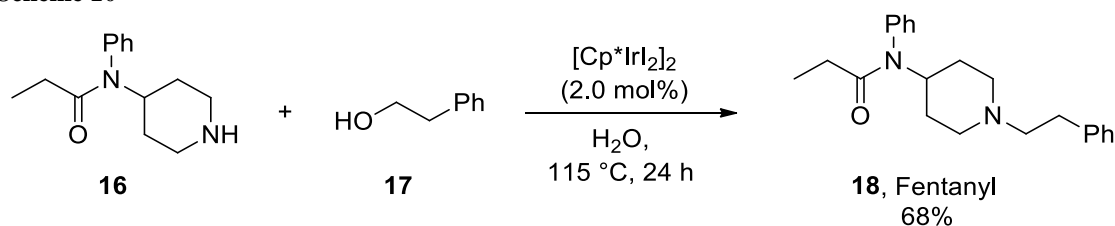
Recently, the first kilogram-scale application of this technology was reported in the synthesis of a GlyT1 inhibitor.²⁴ Using [Cp*IrCl₂]₂, the reaction was optimised to isolate compound **15** in high yield using a catalyst loading lower than 0.05 mol% of iridium (Scheme 9).

Scheme 9

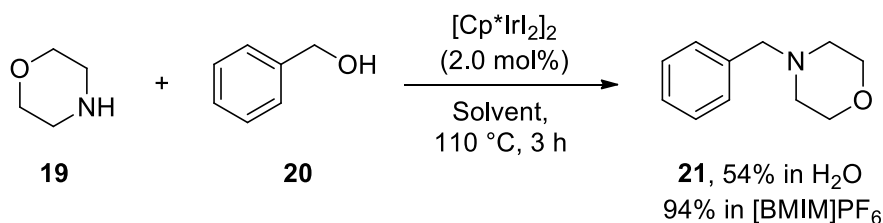


Other iridium complexes have showed a better activity in protic solvents, such as water and *t*-amyl alcohol.

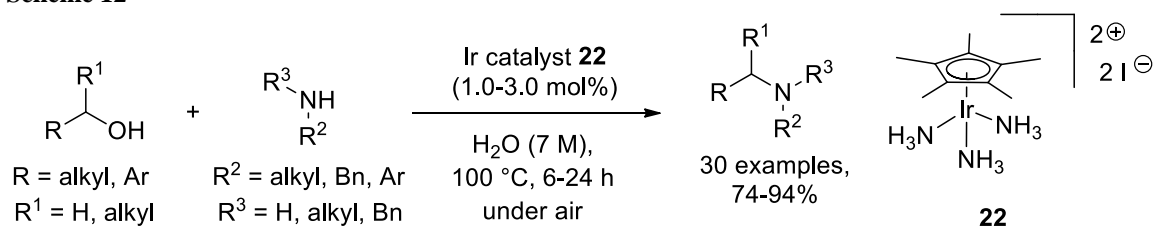
One of the first examples was the dimer [Cp*IrI₂]₂, (SCRAM), which gave good yields in water and proceeded without adding base.^{25,26} Williams and co-workers have demonstrated the applicability of the amine alkylation chemistry using SCRAM to the synthesis of pharmaceutically relevant compounds. Fentanyl, which is an analgesic with 100x greater potency than morphine, was synthesised in 68% yield (Scheme 10). Both of the starting materials are commercially available.²⁶

Scheme 10

Williams and co-workers reported that SCRAM could be used not only in water, but also in ionic liquids. During their exploration of the substrate scope, it was found that tertiary amines were synthesised with higher yields in ionic liquids than in water, as shown in a representative example in Scheme 11.²⁶

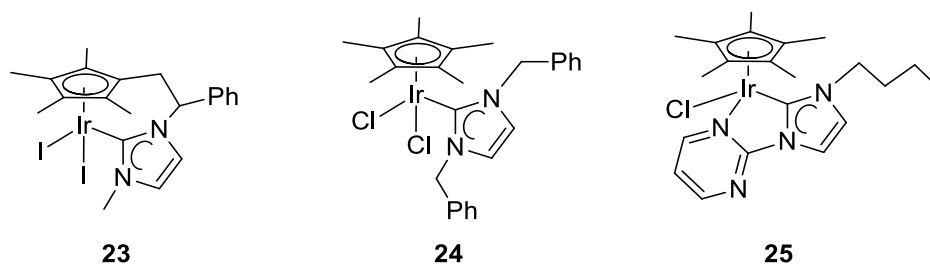
Scheme 11

Recently, a monomeric iridium catalyst **22** has showed high activity in the *N*-alkylation reaction using water as the solvent (Scheme 12).²⁷ The substrate scope was broad; however, a high concentration is required (7 M) in order to achieve high yields and secondary alcohols could efficaciously be used only for the alkylation of primary amines.

Scheme 12

The groups of Peris^{28,29} and Crabtree³⁰ tried to improve the activity of the catalysts used in borrowing hydrogen synthesising new iridium complexes containing *N*-heterocyclic carbenes (NHCs) (Figure 7). This class of ligands had previously led to significant advances in several catalytic reactions, such as the metathesis of olefins and Pd-catalysed cross-coupling reactions.³¹ The yields obtained with these catalysts were comparable to results obtained with [Cp*IrCl₂]₂, but the substrate scope was more limited.

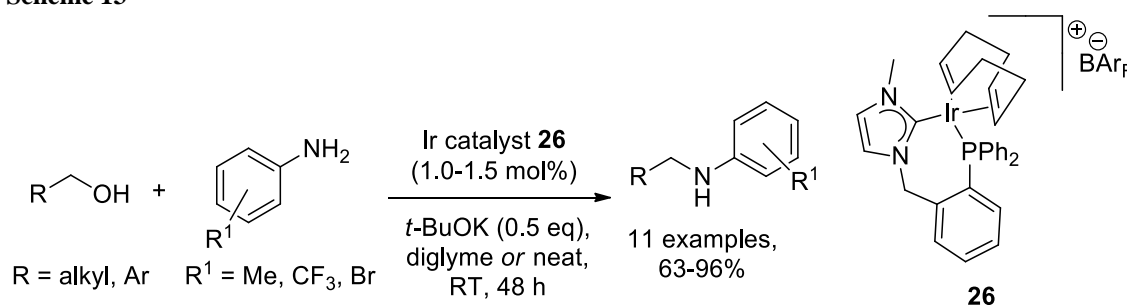
Figure 7



The catalyst **23** was the first example of this class of compounds and it has been used to alkylate anilines with primary alcohols isolating the products in moderate yield (6 examples, 47-85% yield).²⁸ The similar iridium complex **24** showed a slightly better activity in the alkylation of primary amines with primary and secondary alcohols. The substrate scope was again quite limited and the alcohol was often used in excess in order to obtain good yields and decent selectivity (7 examples, 35-95% yield).²⁹ Finally, the iridium complex **25** promoted *N*-alkylation of aliphatic and aromatic primary amines with an equimolecular amount of a primary alcohol. Again, the substrate scope was quite limited (6 examples, 25-98% yield).³⁰

Interestingly, Andersson and co-workers demonstrated that NHCs could be efficaciously used in borrowing hydrogen, reporting the first iridium-catalysed *N*-alkylation of anilines at room temperature.³² A cationic iridium complex containing a bidentate NHC-phosphine ligand and BAR_F (BAR_F : *tetrakis*(3,5-bis(trifluoromethyl)phenyl)borate) as the counterion was used as a catalyst, as shown in Scheme 13.

Scheme 13

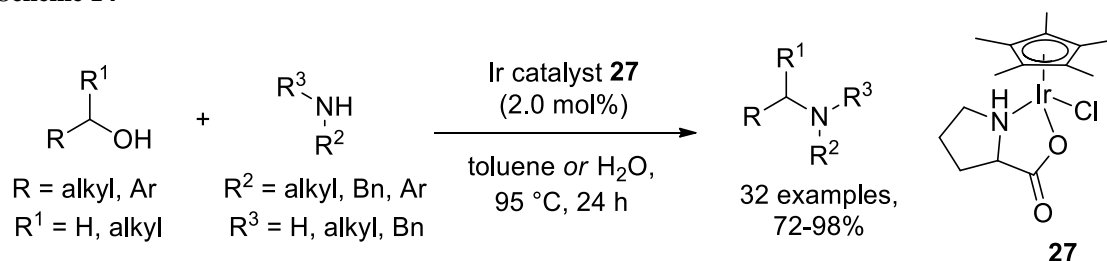


Catalyst **26** promoted the reaction in good yield (63-93%) at room temperature, either using diglyme as the solvent or neat. The long reaction time, 48 hours, could be decreased to 24 hours by increasing the temperature to 50 °C, achieving comparable yields. Unfortunately, the substrate scope was quite limited. Only primary alcohols have been

used and, among them, benzyl alcohols worked better than aliphatic substrates, for which the catalyst loading had to be increased to 1.5 mol% of iridium. Additionally, the amine tolerance was also quite poor and only anilines afforded the corresponding products in good yield. However, this was the first example in which hydrogen borrowing reactions were carried out at room temperature.

Recently, Limbach and co-workers reported a new family of iridium complexes active in hydrogen borrowing. They prepared five different complexes containing five different aminoacidate ligands. The best results were achieved when the complex was coordinated to a proline, as shown in Scheme 14.³³

Scheme 14

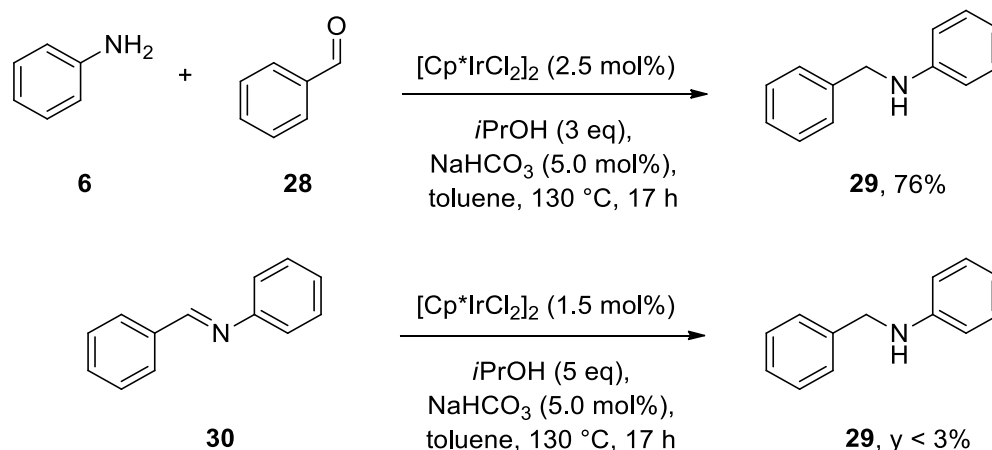


Complex **27** generally promoted the reaction in good yield (72-98%) for a broad range of substrates. Interestingly, comparable yields were achieved both in toluene and in water and therefore, the catalyst could be used efficaciously in non-polar and polar solvents. Primary amines worked better than secondary ones and the reactions could be run at lower temperature with these substrates (95 °C instead of 130 °C). Several substituents could be tolerated and again, they included aromatic and aliphatic groups, halogens, esters and ethers. However, the functional group tolerance was not as broad as that observed previously by the group of Fujita and some electron-withdrawing groups (*e.g.* nitro and nitrile groups) were not reported in the paper among the substrates.²² Additionally, bulky amines such as *tert*-butylamine and cyclohexylamine did not work and the corresponding products were obtained in poor yield.

1.5 Mechanistic studies for the alkylation of amines catalysed by $[\text{Cp}^*\text{IrCl}_2]_2$

The catalyst which gives the best functional group tolerance and the highest yields is the iridium dimer $[\text{Cp}^*\text{IrCl}_2]_2$, which is also the most widely used catalyst for the outlined hydrogen borrowing processes. Therefore, efforts were made to study the reaction mechanism using this complex. Yamaguchi and co-workers performed some experiments to understand if the synthesis of the imine was metal-assisted (Scheme 15).²² In a first experiment, the reaction of aniline **6** with benzaldehyde **28** in the presence of a hydrogen donor (2-propanol) gave *N*-benzylaniline **29** in 76% yield, whereas, in a second reaction, benzylideneaniline **30** with 2-propanol gave only a trace amount of *N*-benzylaniline **29**. These results suggest that uncoordinated imine could not be transfer hydrogenated by the present catalytic system; therefore, the formation of benzylideneaniline **30** has to occur in the coordination sphere of iridium to give *N*-benzylaniline **29**.

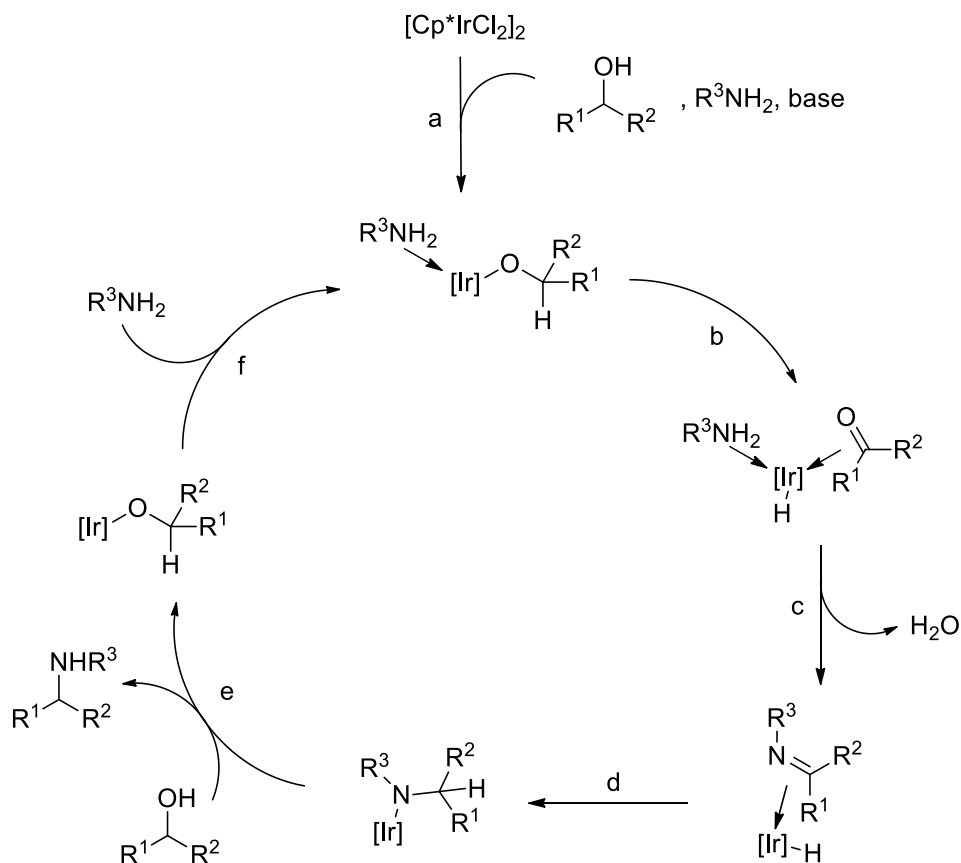
Scheme 15



Furthermore, when a chiral secondary alcohol was used as a substrate with an amine, the racemic alkylated amine was obtained, in agreement with *in situ* generation of a carbonyl during alcohol activation.

On the basis of these results, the authors proposed the following possible mechanism for the iridium-catalysed *N*-alkylation of primary amines with primary and secondary alcohols, shown in Figure 8.²²

Figure 8

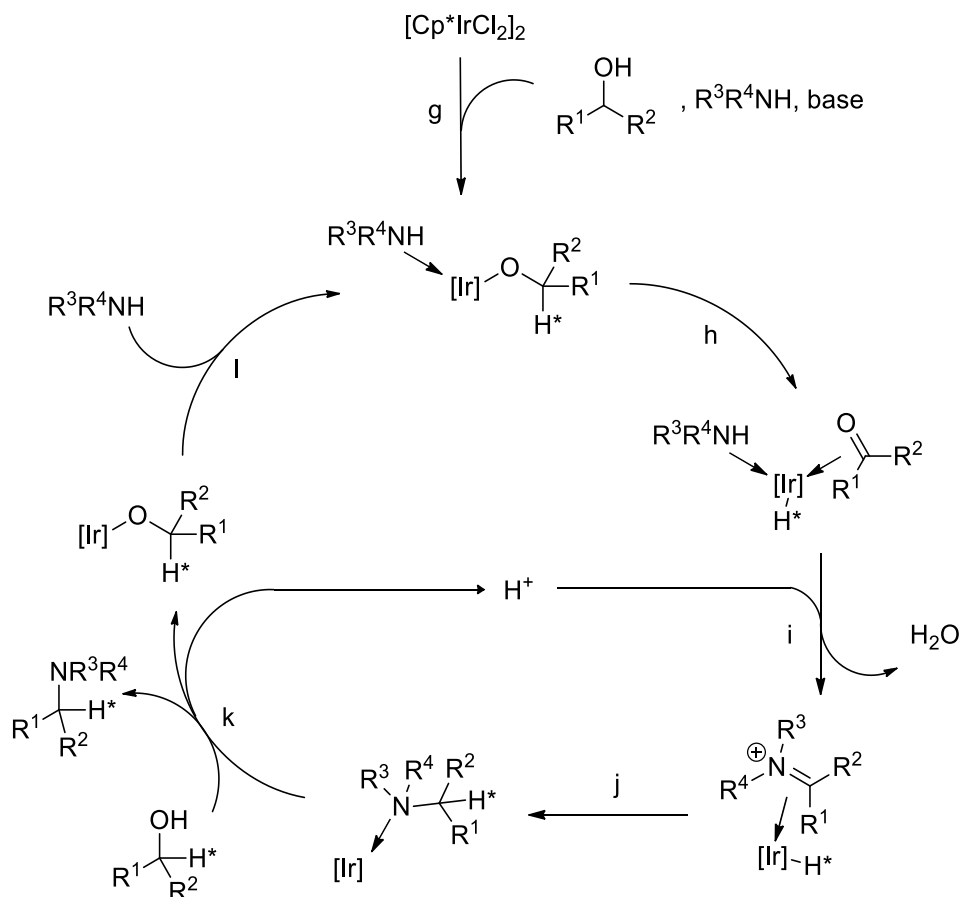


The first step (a) would involve the formation of alkoxo-iridium species coordinated with an amine. The second step (b) would occur to afford an iridium hydride species coordinated with the aldehyde, followed by the imine condensation in the coordination sphere of iridium (step (c)), forming an imine-coordinated iridium-hydride intermediate. Step (d) would be the reduction of the C=N double bond of the imine by the coordinated hydride. The last step would be the amide-alkoxide exchange with the release of the product (step (e)). Finally, coordination of the amine would occur to regenerate the catalytically active species (step (f)). In this cycle, catalytic intermediates would be trivalent iridium species, in accord with the previous literature.²²

A possible mechanism for the iridium-catalysed *N*-alkylation of secondary amines with primary and secondary alcohols is shown in Figure 9. The proposed steps are similar to those reported previously for the primary amine mechanism: the oxidation of the alcohol gives the corresponding carbonyl group (step (h)), which is followed by a condensation between a secondary amine and the aldehyde (or ketone) affording an iridium-hydride species coordinated by an iminium ion (step (i)). The final steps are the reduction of the

C=N double bond with the coordinated hydride (step (j)), the release of the product (step (k)) and the regeneration of the active catalytic species (step (l)).²²

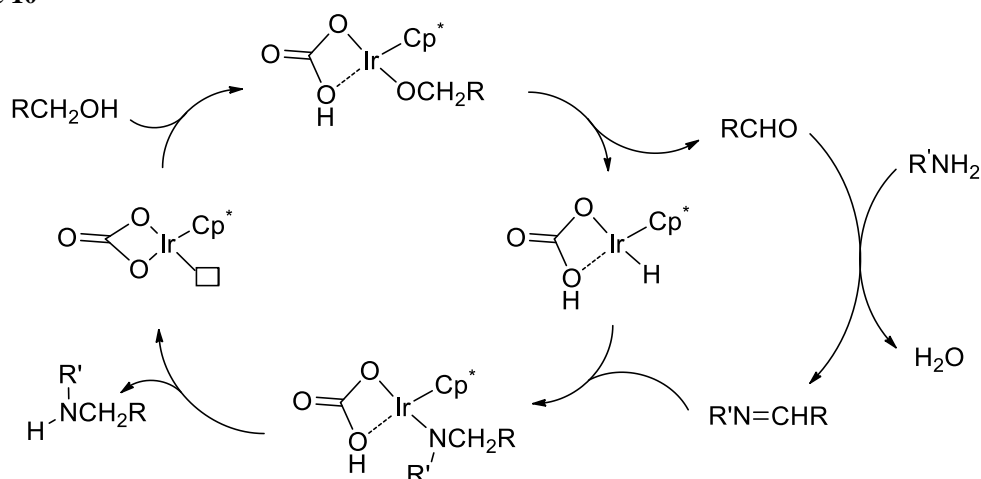
Figure 9



Three mechanistic investigations have been performed on the alkylation of amines with primary alcohols catalysed by the dimer $[\text{Cp}^*\text{IrCl}_2]_2$. The first one was proposed by Crabtree and co-workers³⁴, the second one by Madsen *et al.*³⁵ and the last one by Zhao *et al.*³⁶ Crabtree's work, performed using density functional theory (DFT) calculations, was based on postulating that $[\text{Cp}^*\text{Ir}(\text{CO}_3)]$ was the active catalyst generated *in situ* from potassium carbonate and the dimer $[\text{Cp}^*\text{IrCl}_2]_2$. This study showed that the calculated reaction energetic barriers were consistent with the experimental requirements of elevated temperatures. Three different complexes could be formed *in situ* and they have been explored in their calculation: the neutral monomer $[\text{Cp}^*\text{IrCl}_2]$ and the two complexes coordinating respectively an amine or a carbonate. The presence of a carbonate as an ancillary ligand has been found to decrease the energetic barrier in different steps. It participated in the alcohol dehydrogenation by removing the proton and, in the last step,

it donated the proton for the reduction of imine. Furthermore, the proposed mechanism of reaction was composed of three multistep processes: the first was the iridium-catalysed oxidation of the alcohol, the second was the nucleophilic addition of the amine to the formed aldehydes, and the third was the iridium-catalysed reduction of the imine to the final amine. The amine dissociation from the metal centre was a highly energetic step; therefore a high temperature had to be used to overcome this barrier. Furthermore, the dehydrogenation of the alcohol *via* proton transfer had a lower energetic barrier than the related one with the amine; this was related to the weaker Ir-O π -bond in the alkoxy intermediate relative to the Ir-N π -bond in an amido intermediate. Moreover, the imine is more easily hydrogenated to the secondary amine than the aldehyde and these preferences contribute to favouring the overall reaction pathway. Figure 10 shows the proposed mechanism.

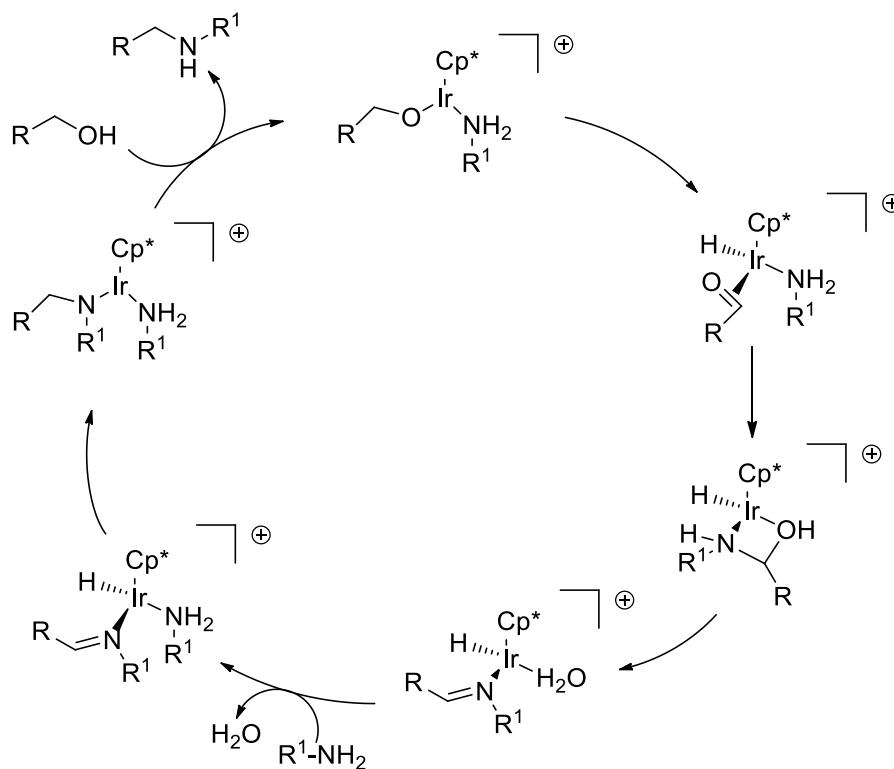
Figure 10



Madsen and co-workers proposed a different catalytic cycle, based on a combination of experimental and computational studies.³⁵ A Hammett study with *para*-substituted benzyl alcohols gave a good σ correlation with the standard values; it showed that neither radicals nor cations were involved in the RDS and the negative slope indicated that a small positive charge was built up in the dehydrogenation process. A different Hammett study using *para*-substituted anilines was carried out to analyse the imine reduction step. The best correlation was achieved using the standard σ values and the negative slope indicated that, also in this step, a small positive charge was built up in the transition state. The authors proposed that the rate-determining step could be either the formation of the carbonyl group in the dehydrogenation step, the nucleophilic addition to form the

hemiaminal or the elimination of water, which was different from the results reported by Crabtree, which suggested that the rate determining step was the amino dissociation from the metal centre.³⁴ Combining these results with others achieved by computational studies, the catalytic cycle shown in Figure 11 was proposed. The group of Madsen proposed a metal-amine coordination, instead of a metal-carbonate coordination and the following metal-catalysed steps: the synthesis of the hemiaminal, the dehydration to achieve the imine and the last reductive step to obtain the amine.³⁵

Figure 11

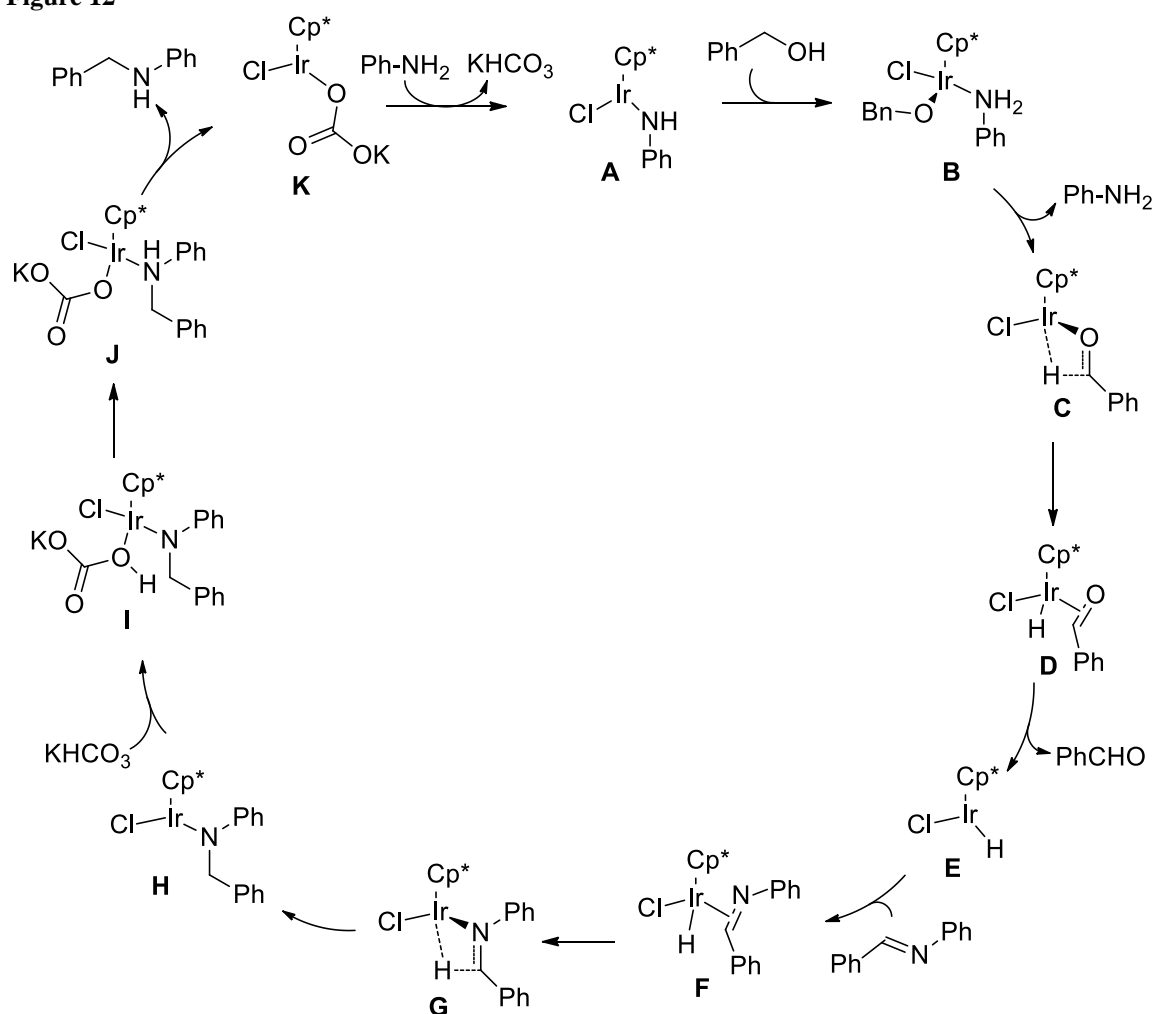


The group of Madsen also reported that this reaction was first order with respect to the alcohol and to the amine, achieving a global second order reaction. Besides, the kinetic isotope effect (k_H/k_D) was found to be 2.48 when it has been calculated using [1',1'-²H₂] benzyl alcohol in competition with *p*-methoxybenzyl alcohol and 1.94 using [1',1'-²H₂] benzyl alcohol in competition with *p*-chlorobenzyl alcohol. Since the k_H/k_D is greater than one, the isotope effect is normal; besides, these values are typical for a primary KIE, in which the bond is broken in the rate determining step, but there would also be a stabilisation of the formed hydride.^{35,37} These results confirm their previous hypothesis, for which the rate-determining step could be either the formation of the

carbonyl group, the nucleophilic addition to form the hemiaminal or the elimination of water.³⁵

Recently, Zhao and co-workers have proposed a third mechanism, based on DFT calculations for the reaction between benzyl alcohol and aniline.³⁶ Inner and outer sphere coordination pathways were considered for the first time during the calculations; Figure 12 reports the favoured catalytic pathway that the authors proposed. Two different inner sphere pathways were suggested as favoured, one for the oxidation of the alcohol and the second for the imine reduction.

Figure 12



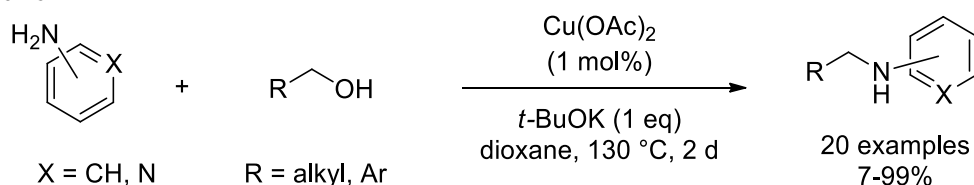
The first step of the catalytic cycle was the formation of the active iridium species **A**, in which one of the chloride ligands has been formally displaced by PhNH^- . Proton transfer between the alcohol and the amine led to the formation of **B**, which then underwent dehydrogenation to form the aldehyde. The free energy barrier of activation for the β -H

elimination was high, which accounts for the high temperature required to obtain an acceptable reaction rate. They proposed that the formation of the imine was not metal templated. The iridium-hydride species **E** was then able to hydrogenate the imine to the corresponding amine. Finally, the authors proposed the proton transfer pathway from **H** to **J** was catalysed by potassium carbonate, which acted as a proton donor. This inner sphere hydrogen transfer pathway gave the lowest Gibbs free energy and the lowest enthalpy among all the other energy profiles considered. The final steps of the proposed catalytic cycle were the dissociation of the amine and the formation of the active catalyst **A**. The authors also suggested that the imine reduction was the driving force of the reaction.³⁶

1.6 *N*-Alkylation by Alcohols Catalysed by other Metal Complexes

Recently, efforts were made to develop new hydrogen borrowing processes using cheap and readily available metals, such as iron and copper, which were highly attractive alternatives for expensive and often toxic heavy metals.³⁸ Thus, new cheaper catalysts have been used to promote the *N*-alkylation reaction using alcohols as a source of electrophiles. Copper(II) acetate with 1 equivalent of base (potassium *tert*-butoxide or potassium hydroxide) was found to be an efficient catalyst for the *N*-alkylation reaction in high yield. Scheme 16 shows the general methodology.

Scheme 16

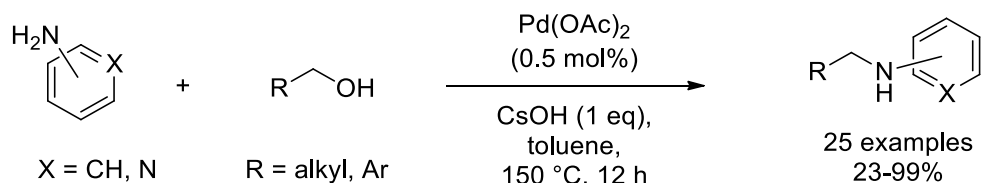


This process showed some drawbacks, even though copper acetate was a cheap and environmental friendly catalyst: it was active only with electron-poor aromatic and heteroaromatic amines and primary alcohols, such as benzyl alcohol and derivatives. When aliphatic alcohols were used, the yields were really poor (7-40%). Interestingly, halogens were not tolerated because the dehalogenation reaction occurred.

The same group also proposed another methodology using palladium(II) acetate to promote this reaction. However, substrates and conditions of reactions were similar to

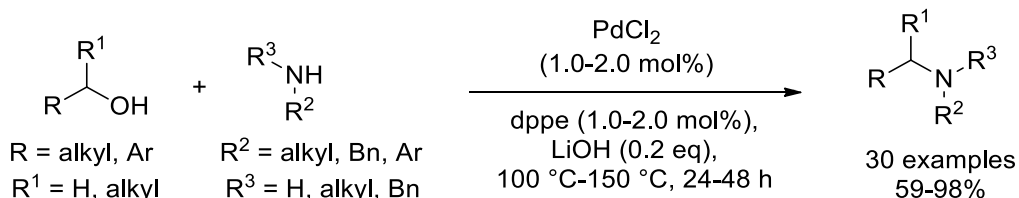
those showed in Scheme 16 with copper(II) acetate: best results were achieved with benzyl alcohol and derivatives, aromatic and heteroaromatic amines and 1 equivalent of base (Scheme 17).³⁹ The yields were moderate when aliphatic alcohols were used and the reaction did not work with secondary alcohols, such as 2-octanol. Additionally, starting with halogenated benzyl alcohols, the dehalogenation process occurred as a side reaction.

Scheme 17



Recently, Seayad and co-workers reported a new palladium-catalysed hydrogen borrowing process using palladium dichloride and an additive (dppe or Xantphos).⁴⁰ This methodology was more general than the previous one and aliphatic amines and alcohols were also well tolerated (Scheme 18). Increasing the temperature to 150 °C and the reaction time to 48 hours, secondary alcohols could also be tolerated and they afforded the corresponding products in good yields.

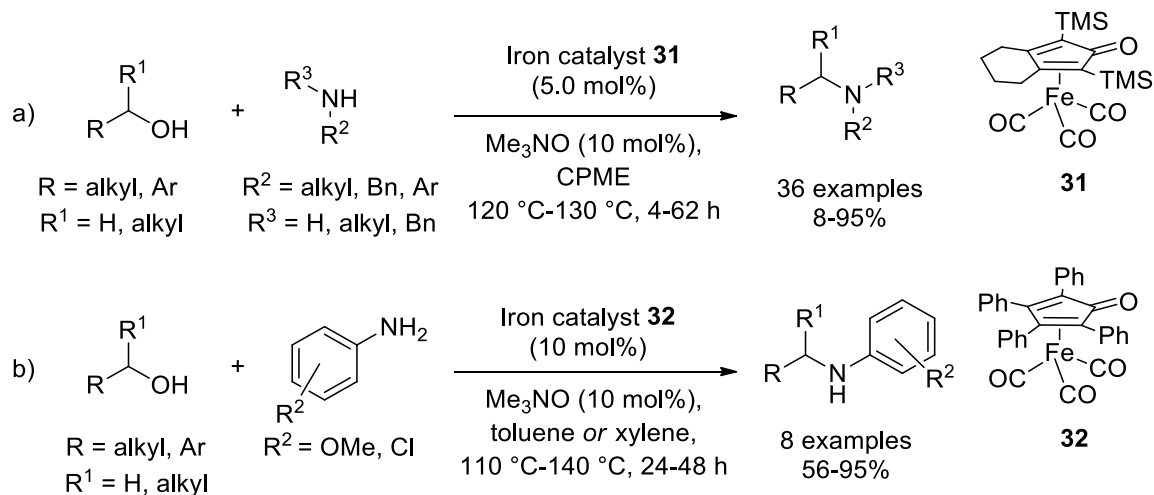
Scheme 18



Finally, the groups of Feringa⁴¹ and Wills⁴² independently reported the first two iron-catalysed *N*-alkylation of amines with alcohols mediated by hydrogen borrowing. The iron catalysts that these groups used were similar; however, the Knölker complex **31** used by Feringa *et al.* showed greater activity, higher yields and a broader substrate scope than the Schrauzer iron complex **32** used by Wills and co-workers (Scheme 19a and Scheme 19b respectively). Iron catalyst **31** generally worked with both aromatic and aliphatic amines, whereas complex **32** tolerated only derivatives of anilines. Unfortunately, in both the systems, amines bearing electron-withdrawing groups did not

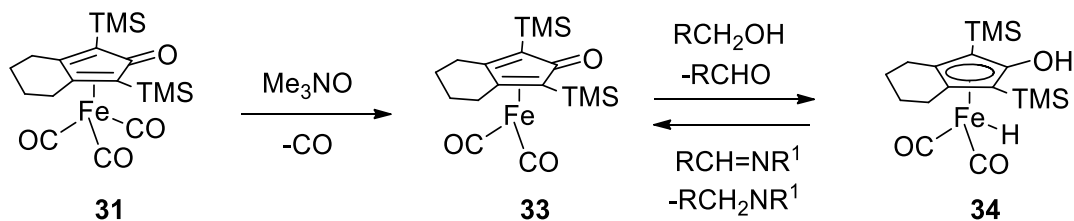
work and iodoaniline gave a poor yield. However, substrates bearing electron-rich groups afforded the corresponding products in excellent yields. Interestingly, the reaction between aniline and benzyl alcohol gave a better yield using the Schrauzer catalyst **32**.

Scheme 19



The mechanism for the activation of the two catalysts was similar; herein in Scheme 20 it is reported for complex **31**.

Scheme 20



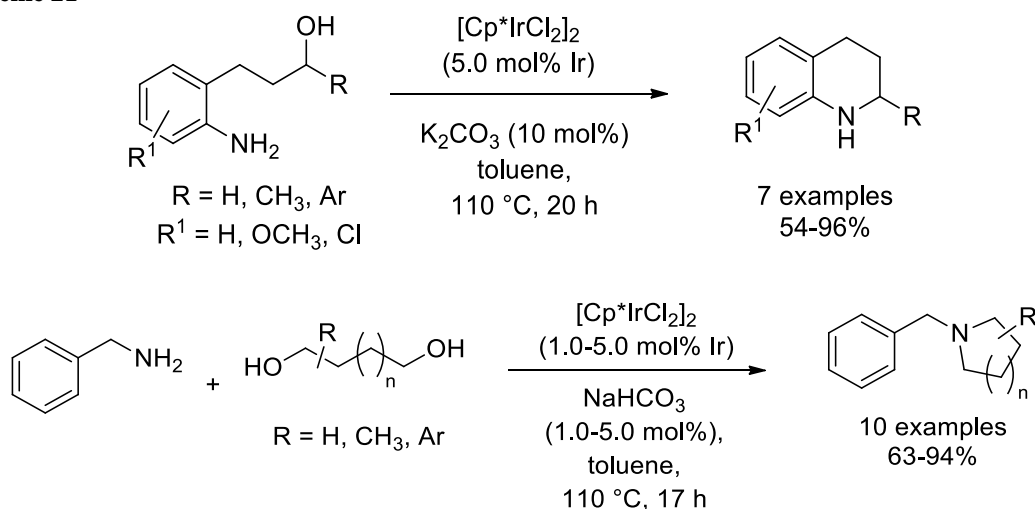
An oxidant (Me_3NO) was necessary to remove one CO from the air-stable complex **31** to form the active species **33**. The oxidation of the alcohol gave the formation of the reduced iron catalyst **34**, which could use the “borrowed” hydrogen to reduce the imine to the amine and reform the active species **33**.⁴¹

1.7 Formation of *N*-Heterocycles

Ruthenium and iridium catalysts were also effective in the synthesis of valuable *N*-heterocyclic compounds. Effectively, borrowing hydrogen was a very attractive method for the synthesis of *N*-heterocyclic compounds in one step, without generation of harmful by-products. Herein, the main chemical transformations to make *N*-heterocycles using borrowing hydrogen are reported.

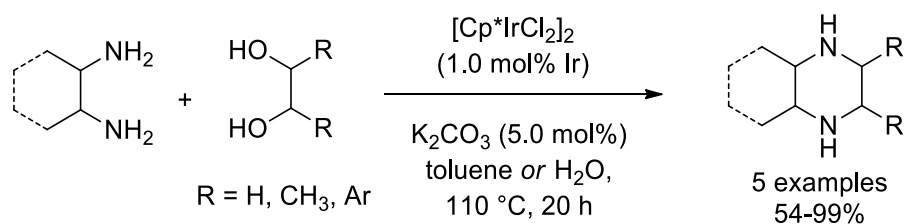
The $[\text{Cp}^*\text{IrCl}_2]_2/\text{K}_2\text{CO}_3$ system was found to be effective to catalyse intramolecular and intermolecular *N*-heterocyclization; some examples of this kind of reaction are shown in Scheme 21.^{19,43} Previous ruthenium-catalysed systems required high reaction temperatures ($> 150\text{ }^\circ\text{C}$) and applicable substrates were rather limited,^{1,6,44} whereas this iridium catalytic system had advantages in terms of reaction conditions, as well as in the versatility of the substrates.

Scheme 21



Using a similar catalytic system, Madsen and co-workers reported the synthesis of various piperazines, starting from a variety of diols and diamines (Scheme 22).⁴⁵

Scheme 22

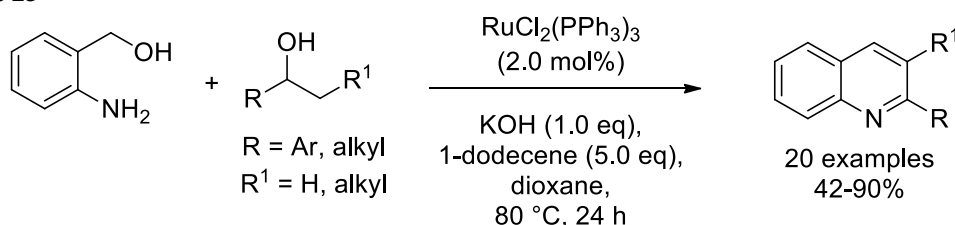


Several other groups have reported that other catalysts could promote this type of reaction in high yields, such as the groups of Bruneau,⁴⁶ Fujita²⁷ and Limbach.³³

N-Heteroaromatic compounds could also be synthesised by hydrogen borrowing and in the literature some examples were reported to prepare indoles, benzimidazoles, pyrroles and quinolines. The general proposed pathway was initiated by a borrowing hydrogen process, followed by a second oxidation, which gave the aromatic *N*-heterocycles.

Cho and co-workers reported the synthesis of quinolines using 2-aminobenzyl alcohol and a secondary alcohol. 1-Dodecene was the hydrogen acceptor, which would promote the initial oxidation of the alcohols (Scheme 23).⁴⁷

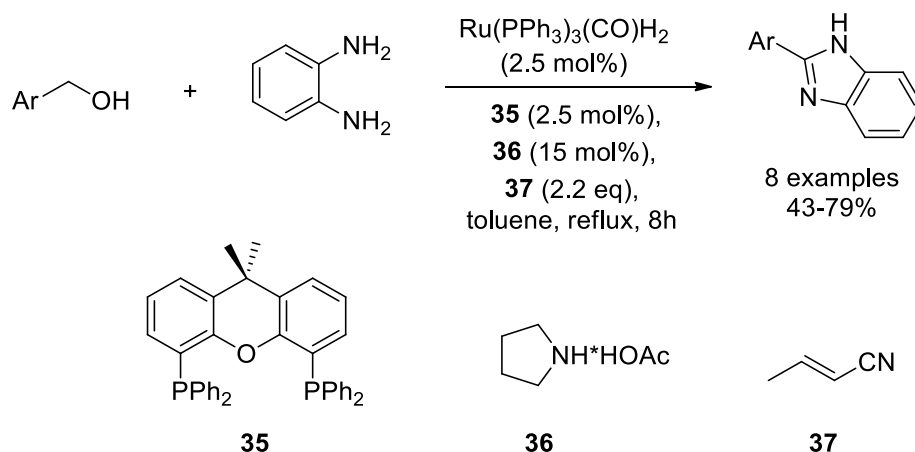
Scheme 23



A similar reaction was also reported by Ishii and co-workers, who reported that such quinolones could also be synthesised using $[\text{Ir}(\text{cod})\text{Cl}]_2$ and a phosphine ligand.⁴⁸

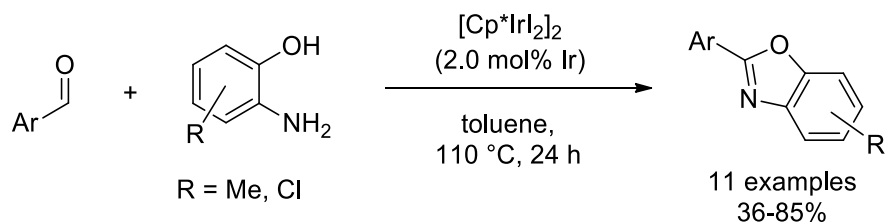
Recent work by the groups of Williams and Marsden employed $[\text{Ru}(\text{PPh}_3)(\text{CO})\text{H}_2]$ and Xantphos for the synthesis of benzimidazoles *via N*-alkylation. The hydrogen borrowing steps gave dihydrobenzimidazoles, which could then be oxidised to give the corresponding products. The addition of piperidinium acetate **36** may promote addition of *o*-aminoaniline to the intermediate aldehyde, forming the temporary iminium ion, whereas **37** acts as a proton acceptor (Scheme 24).⁴⁹

Scheme 24



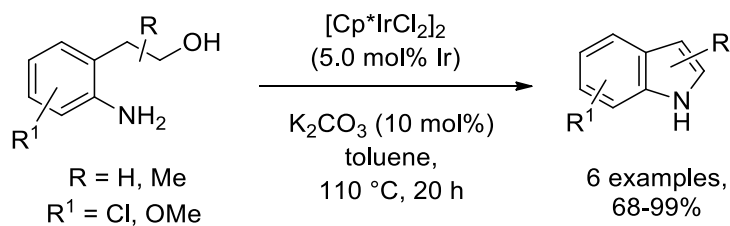
The same groups also reported a similar hydrogen borrowing process to make benzoxazoles, in a procedure catalysed by $[\text{Cp}^*\text{IrI}_2]_2$. Using this catalytic system, the presence of styrene as a sacrificial hydrogen acceptor was not necessary and good yields were also achieved in its absence. The authors suggested that the aromatisation step would be mediated by the loss of hydrogen from the intermediate dihydrobenzoxazole. Scheme 25 shows the general procedure for this process. Yields were generally good, although electron-deficient and aliphatic aldehydes gave the products only in moderate yields.

Scheme 25



Iridium dimer $[\text{Cp}^*\text{IrCl}_2]_2$ also promoted this type of reaction and several indoles were obtained in good yields (Scheme 26).⁵⁰

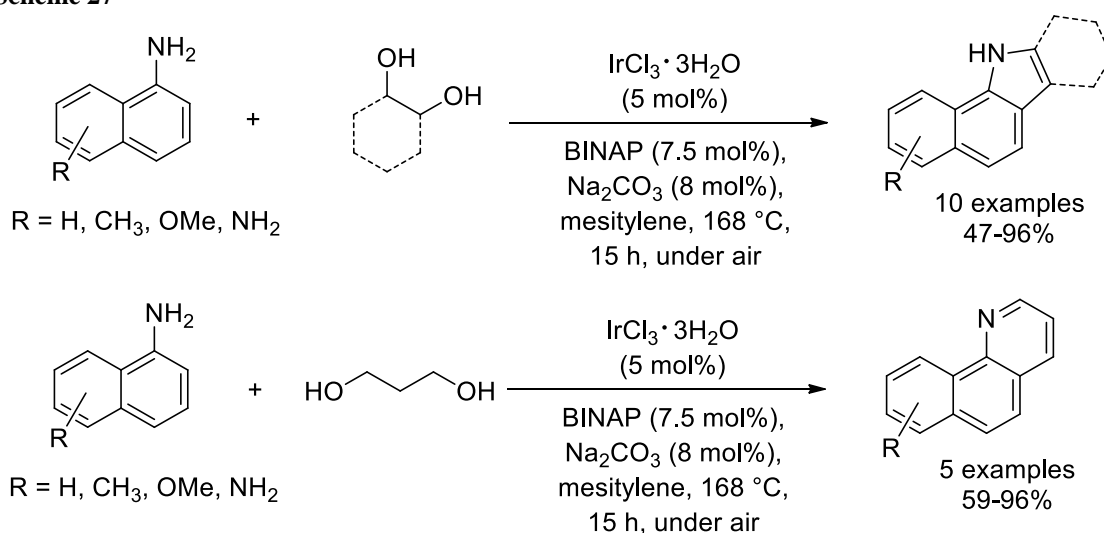
Scheme 26



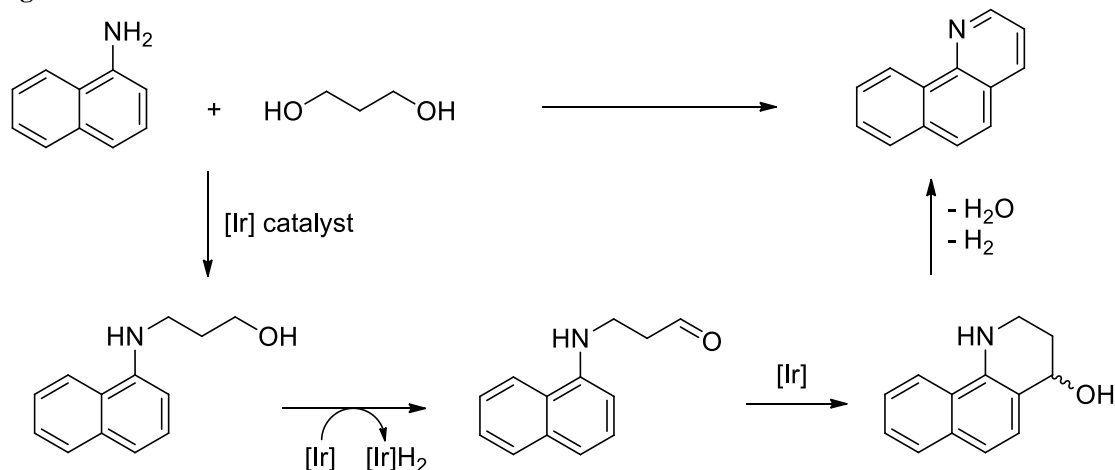
Interestingly, the authors observed that, increasing the length of the alcohol chain, the second oxidation step did not occur. Thus, tetrahydroquinolines were obtained in moderate to high yield, instead of quinolines or dihydroquinolines, as shown previously in Scheme 21.⁵⁰

Benzoquinolines and benzoindoles could be prepared in moderate to excellent yield using a catalyst generated *in situ* with a combination of nearly equimolar amounts of iridium trichloride and 2,2'-bis(diphenylphosphano)-1,1'-binaphthyl (BINAP) (Scheme 27). The reaction was faster in the presence of air and was not affected by substitution on the starting amine.⁵¹

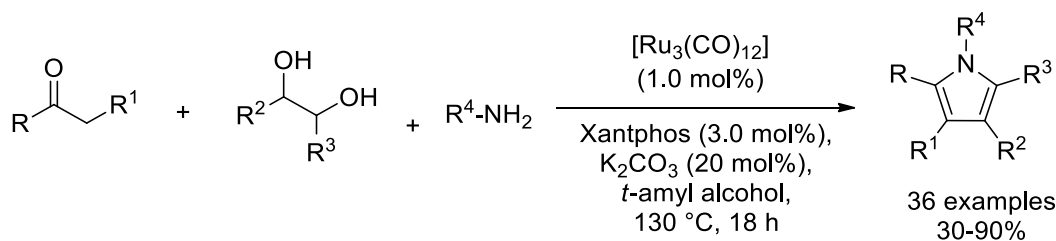
Scheme 27



A plausible mechanism for these reactions is reported in Figure 13, in which the iridium complex catalysed the direct intramolecular cyclisation between the aldehyde and the naphthalamine, followed by the aromatisation step.

Figure 13

Finally, during their study on the synthesis of quinolines catalysed by iridium complexes, Ishii and co-workers also found that [IrCl(cod)]₂ promoted the reaction between an aliphatic amino alcohol and a ketone to form a pyrrole.⁴⁸ Beller and co-workers developed this idea reporting a ruthenium-catalysed three-component synthesis of pyrroles, which afforded a broad range of multiply substituted heterocycles in moderate to high yield (Scheme 28). A broad range of substituents was tolerated, including electron-withdrawing and electron-donating groups on aromatic and aliphatic substituents.

Scheme 28

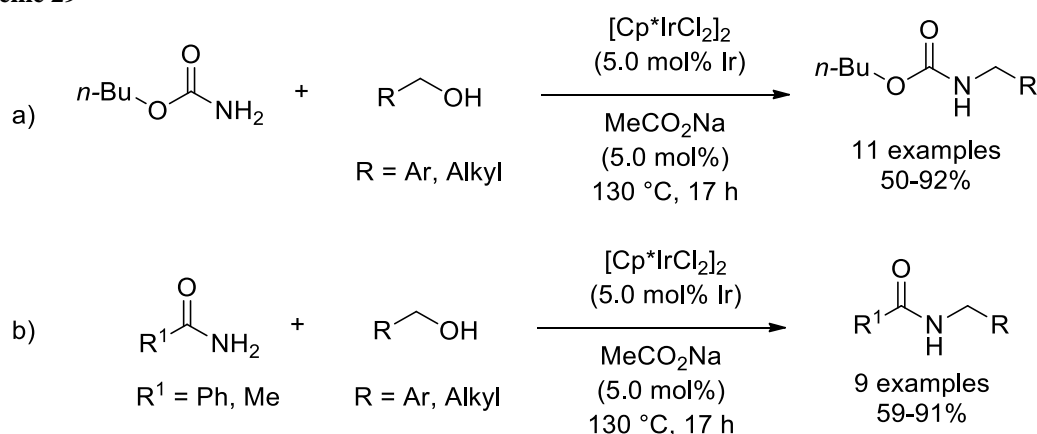
1.8 *N*-Alkylation of Amides, Carbamates and Sulfonamides with Alcohols

A few of the ruthenium and iridium complexes reported previously could also be used in the *N*-alkylation of amides, carbamates and sulphonamides with alcohols. The isolated yields were generally modest due to the poorer nucleophilicity and therefore, lower reactivity of the amide. This different reactivity of amides is due to the delocalisation of

the nitrogen's lone pair into the π system, which makes amides less nucleophilic than amines.

The iridium catalyst $[\text{Cp}^*\text{IrCl}_2]_2$ could also be used in the *N*-alkylation of carbamates and amides. The reaction of a carbamate with an excess amount of primary alcohol (4 equivalents) gave the carbamic derivatives in moderate to good yield (Scheme 29a). The presence of a base accelerated the reaction, with sodium acetate being the most effective and the optimal temperature was 130 °C. Using the same conditions, the *N*-alkylation of benzamide and acetamide was achieved in moderate to good yield (Scheme 29b).⁵²

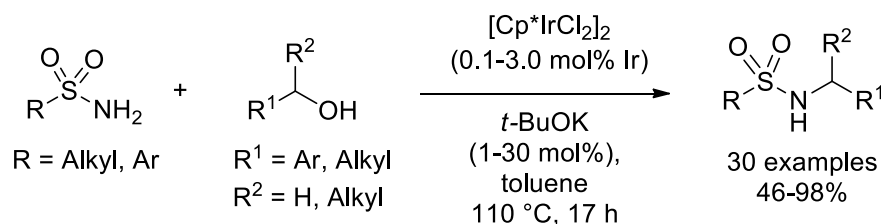
Scheme 29



Since either amides or carbamates were not good nucleophiles on the nitrogen, the catalyst loading used was higher and the yields lower than those obtained previously in the alkylation of amines. Besides, the substrate scope was not as broad and electron-withdrawing groups were not tolerated.

Fujita and co-workers demonstrated that the iridium complex $[\text{Cp}^*\text{IrCl}_2]_2$ in the presence of potassium *tert*-butoxide could alkylate sulphonamides, as shown in Scheme 30.⁵³ Since sulphonamides were more nucleophilic than amides, the yields were generally high and, indeed, more bulky secondary alcohols and both electron-withdrawing and electron-donating groups were tolerated.

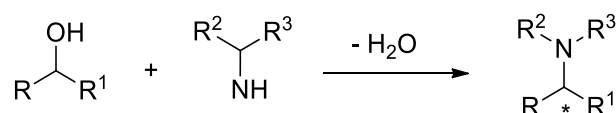
Scheme 30



1.9 N-Alkylation of Amines with Alcohols affording Chiral Compounds

Chiral amines are common moieties in pharmaceutical and agrochemical chemistry and several compounds are sold as a single enantiomer.^{54,55} Starting with a chiral catalyst or a chiral auxiliary, borrowing hydrogen could potentially be used to make enantioenriched amines. Effectively, starting with a secondary alcohol, a stereogenic centre can be formed, with the advantage of obtaining an enantioenriched molecule from a racemic alcohol (Scheme 31).

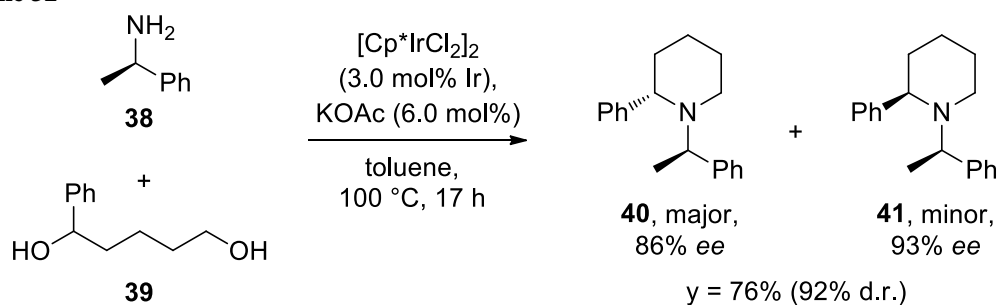
Scheme 31



Asymmetric hydrogen transfer was used with excellent results for the asymmetric reduction of ketones^{56,57} and imines.^{58,59} However, to the best of our knowledge, there are only a few examples in the literature of the asymmetric alkylation of amines with alcohols, reflecting the difficulty involved in the design of catalysts which could promote the asymmetric *N*-alkylation of amines with alcohols.

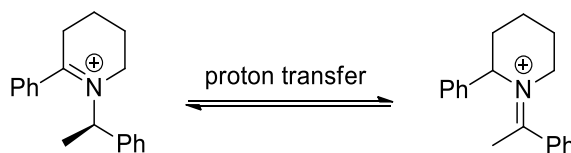
Fujita and co-workers reported the first asymmetric alkylation, taking advantage of using the chiral amine **38**, which acted as a chiral auxiliary. The reaction, exemplified by piperidines, is reported in Scheme 32.⁴³ The existing stereocentre determined the prevalent formation of the *trans* compound, **40**.

Scheme 32



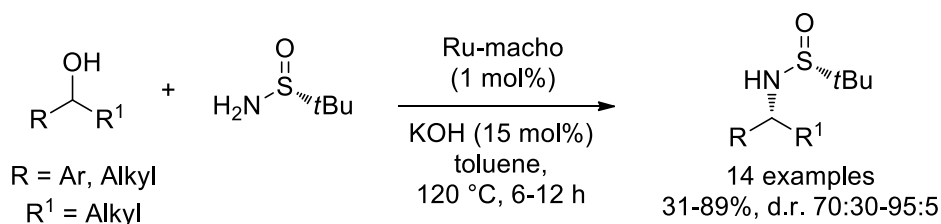
These workers noticed that a small amount of racemisation of the auxiliary also occurred during the reaction, which could be due to isomerisation of the imine or iminium intermediate, as shown in Scheme 33.⁴³

Scheme 33



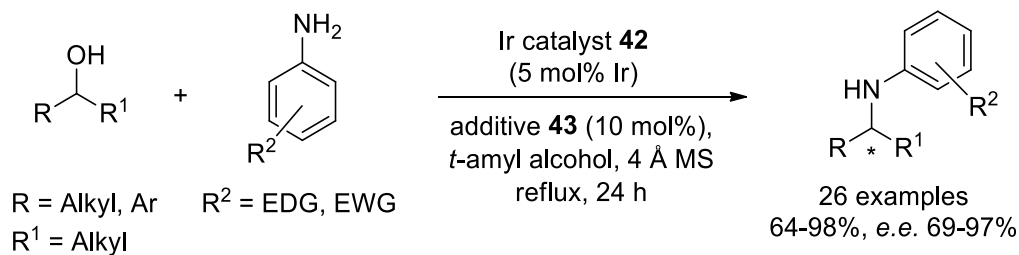
Developing a similar idea, Guan and co-workers obtained the alkylation of sulfinylamines in the reaction between a chiral sulfinylamine and alcohols in good to excellent diastereomeric excess, as shown in Scheme 34. The reaction worked better when one of the groups on the alcohol was aromatic and the other aliphatic because the hydrogenation of sulfinylimines proceeds with lowered diastereocontrol when the β -substituents are similar in size.⁶⁰

Scheme 34

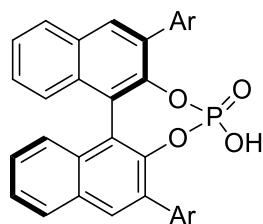


Recently, Zhao and co-workers have reported the first asymmetric synthesis of enantioenriched amines starting with a chiral catalyst.⁶¹ A screen of the conditions determined that the best results were obtained in a cooperative catalysis with the Noyori-type iridium catalyst **42** and the chiral phosphoric acid **43**. The matched/mismatched relationship between the iridium complex and the BINOL phosphoric acid was found to be significant to achieve good enantiomeric excesses and the combination of (*S,S*)-**42** and (*R*)-**43** gave the optimal results. The scope was quite general for the racemic alcohols and anilines (Scheme 35). Unfortunately, this catalytic system could not be applied with other amines because they afforded the corresponding compounds in low yield and poor enantiomeric excess.

Scheme 35

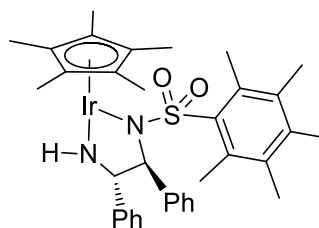


Additive:



43, Ar = (2,4,6-*i*-Pr) C_6H_2

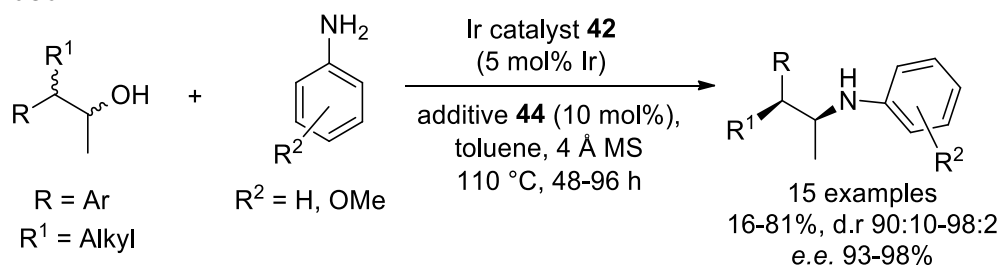
Catalyst:



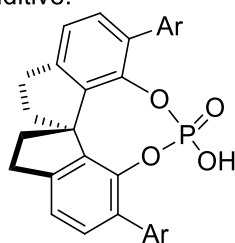
42, (S,S)

Finally, this group has further applied this methodology achieving the first dynamic kinetic asymmetric amination with alcohols. Starting with a mixture of four diastereoisomers, the authors managed to optimise the conditions to obtain the α -branched amines in excellent diastereoselectivity and enantioselectivity (Scheme 36).⁶²

Scheme 36

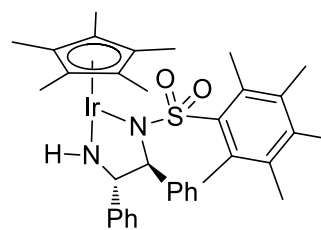


Additive:



44, Ar = (2,4,6-*i*-Pr) C_6H_2

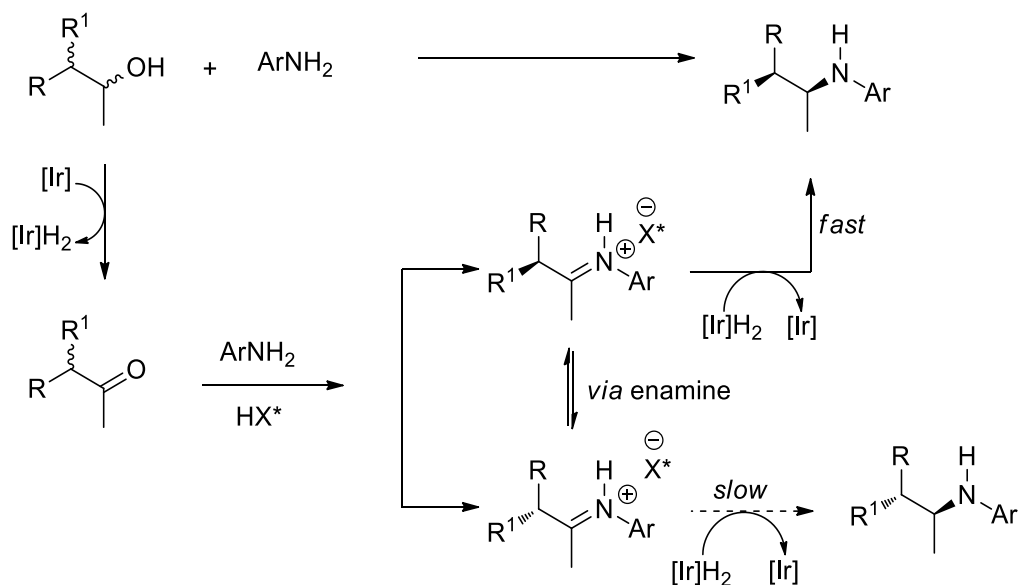
Catalyst:



42, (S,S)

The mechanism of the reaction is reported in Figure 14.

Figure 14



The first step was the oxidation of the alcohol to the ketone, which was followed by the condensation to the imine catalysed by the chiral phosphoric acid **44** (HX*). The two enantiomeric imines were in equilibrium *via* the enamine. One of the two enantiomers was hydrogenated faster than the other by the iridium catalyst, which led to product formation in excellent diastereoselectivity and enantioselectivity.⁶²

1.10 Project Aims

The work outlined above illustrates the potential for atom-efficient hydrogen borrowing processes which allow for the synthesis of amines and other C-N compounds starting with less reactive substrates than those traditionally used. Iridium and ruthenium complexes promote the *N*-alkylation by alcohols, generally with good results. The application of iridium catalysts is more recent than the use of ruthenium; nevertheless, several complexes have been synthesized and tested and the *N*-alkylation has often been achieved in high yields. This kind of reaction has great potential; however, this methodology suffers from a number of drawbacks, such as when a secondary alcohol is used as a substrate. In this case, the reaction is slow and the amount of catalyst has to be increased by up to 5 mol% Ir.²² Effectively, the *N*-alkylation of secondary alcohols is more difficult than that of primary alcohols because ketones are poorer electrophiles than aldehydes.⁶³

This project aims to develop new robust catalysts for the formation of pharmaceutically-relevant amines using the hydrogen borrowing methodology.

The development of new complexes will be focused on several aspects, such as:

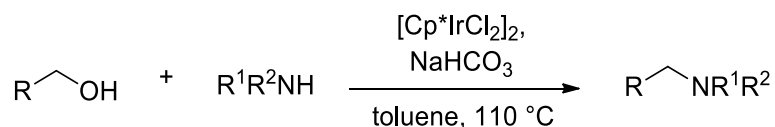
- the synthesis of more active catalysts, which could improve the catalyst loading and the reaction rate, particularly when the substrates have a great steric bulk;
- the synthesis of catalysts which are active not only in toluene, but also in a variety of more polar solvents;
- the development of new more efficient enantioselective methodologies to prepare chiral amines starting with racemic alcohols (Scheme 31).

Chapter 2. Initial Attempts to Study the Reaction Mechanism

2.1 Evaluation of the Active Iridium Catalyst: Amine-Coordination or Carbonate-Coordination

The work outlined in the introduction shows that the hydrogen borrowing process promoted by $[\text{Cp}^*\text{IrCl}_2]_2$ is a well-known methodology in the literature which has great potential.^{1,4,63} Recently, the first reported industrial optimisation using $[\text{Cp}^*\text{IrCl}_2]_2$ was also achieved in high yield and with a catalyst loading lower than 0.05 mol% iridium.²⁴ However, this process has some drawbacks, *e.g.* high catalyst loading, high concentration in non-polar solvents and slow reaction rates with bulky substrates,²² that could potentially be resolved if the mechanism of the reaction was completely understood. For instance, it is not clear what role the base plays in these reactions. Three different mechanisms have been proposed to explain the catalytic cycle of $[\text{Cp}^*\text{IrCl}_2]_2$, achieving completely different conclusions about the active coordination of the catalyst and the rate-determining step of the reaction.^{34,35,36} Our initial efforts were focused on understanding the reaction mechanism, particularly regarding the coordination of the active iridium species in the reaction. The knowledge of which molecules are coordinated to the metal would give us useful information to design a more active and robust iridium complex, bearing a more functional ligand than the Cp^* alone. Therefore, our first attempts were orientated towards understanding the role of the base in the catalytic cycle and to establish the rate-determining step in the reaction mechanism. Initially, the procedure described by Fujita and co-workers was tested (Scheme 37) to evaluate the reaction conditions, the reactivity of the iridium dimer $[\text{Cp}^*\text{IrCl}_2]_2$ and the reaction mechanism.²²

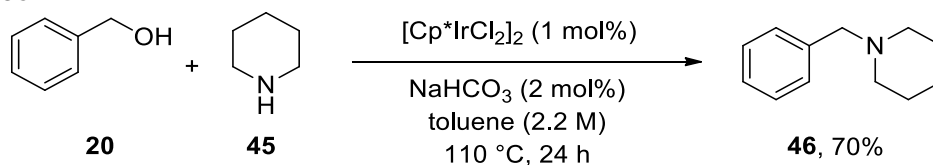
Scheme 37



Our first effort was to develop a reliable and consistent methodology to follow the kinetics by gas chromatography (GC). Hence, the reaction between 1 equivalent of benzyl alcohol

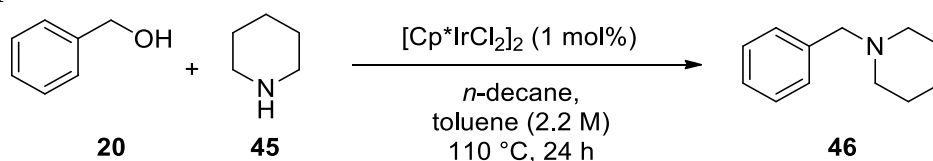
20 and 1 equivalent of piperidine **45** was chosen as a model reaction because it proceeded with high yield and no significant synthesis of by-products (Scheme 38).

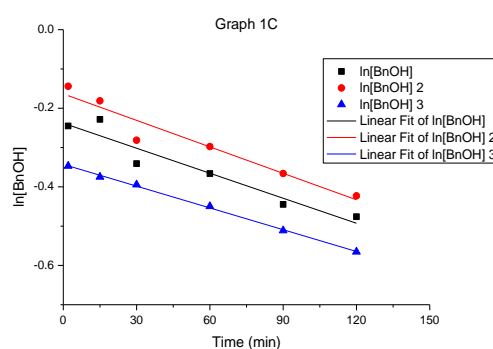
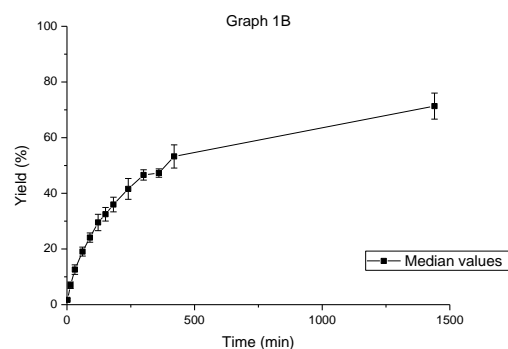
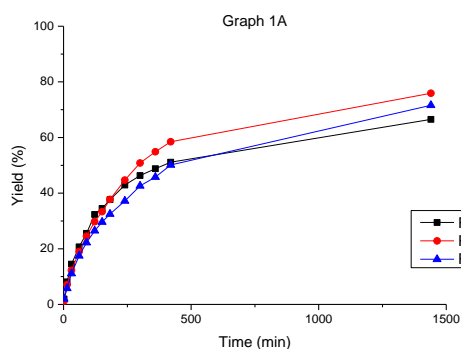
Scheme 38



n-Decane was chosen as internal standard, because it did not react under the reaction conditions and it gave a sharp and distinct peak in the GC chromatogram. To verify the reliability of the process and, therefore, to evaluate the error correlated to the methodology chosen, the reaction shown in Graph 1 has been carried out three times, maintaining constant concentration, but changing the amounts of starting materials. We sought to use a procedure in which we limited the human error, thus sodium bicarbonate, which was used in catalytic amount in the reaction shown in Scheme 38, was not added in the current experiment. Graph 1 shows the results from each these three experiments: Graph 1A shows the yield vs. time and Graph 1B the median values with the relevant error bars. The error increased slightly after 6 hours, when the reaction rate began to decrease. Nevertheless, errors were found to be very small in the first hours, confirming the consistency of this procedure. Additionally, conversions after 24 hours were also calculated by analysis of the $^1\text{H-NMR}$ spectra of the reaction mixtures (65-71% conversion) and they were comparable with those calculated by GC analysis. At the beginning of the reactions, we could approximate that the kinetics were in *pseudo*-first order with respect to benzyl alcohol. For this experiment, we analysed the kinetics achieved in the first 120 minutes of the reaction. Graph 1C shows the logarithms of the concentration of benzyl alcohol vs. time; the relevant equations gave an approximation of the rate constants.

Graph 1





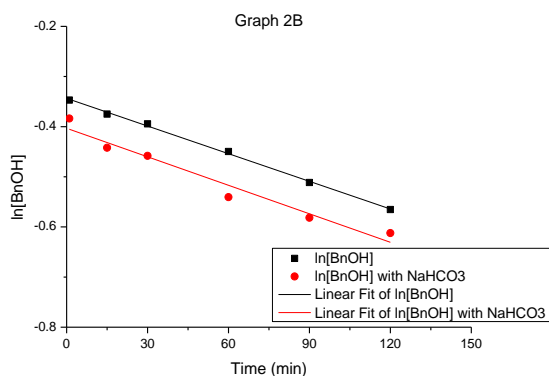
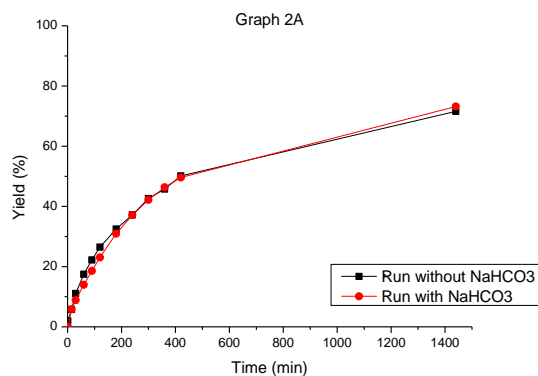
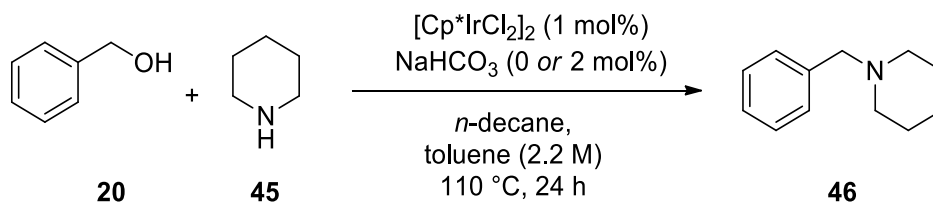
Equation	y = a + b*x		
Weight	No Weighting		
Residual Sum of Squares	0.00379	0.00348	5.62831E-5
Pearson's r	-0.96209	-0.9686	-0.99921
Adj. R-Square	0.90703	0.92273	0.99804
		Value	Standard Error
ln[BnOH]	Intercept	-0.23808	0.02026
ln[BnOH]	Slope	-0.00212	3.00697E-4
ln[BnOH] 2	Intercept	-0.16347	0.01942
ln[BnOH] 2	Slope	-0.00225	2.88274E-4
ln[BnOH] 3	Intercept	-0.3428	0.00247
ln[BnOH] 3	Slope	-0.00185	3.66405E-5

The slopes of the linear fits were found to have close values ($k = -0.0021 \pm 0.0002$), which confirmed the reliability of this procedure.

After developing a consistent methodology to analyse data, the effect of sodium hydrogen carbonate on the catalyst was studied. Three different iridium coordination modes, mainly based on computational studies, have been proposed in the literature to generate the active catalyst; one considering metal-carbonate coordination (Figure 10)³⁴, the second considering metal-amine coordination (Figure 11)³⁵ and the third considering both metal-amine coordination for the oxidation step and metal-carbonate coordination for the reduction step (Figure 12).³⁶

A reaction was carried out using the conditions reported above with an addition of 2 mol% of sodium hydrogen carbonate to compare the observed rate constants, as shown in Graph 2. “Run without NaHCO₃” and “ln[BnOH]” refer to the reaction carried out without any base (Graph 1), whereas “Run with NaHCO₃” and “ln[BnOH] with NaHCO₃” refer to the current experiment. Graph 2A shows the yield vs. time and Graph 2B shows the logarithm of the concentration of benzyl alcohol vs. time.

Graph 2



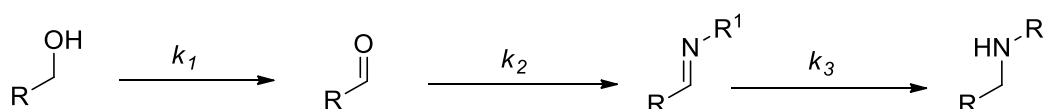
Equation	$y = a + b \cdot x$		
Weight	No Weightin		
Residual Sum of Squares	6.02057E-5	0.00153	
Pearson's r	-0.99916	-0.9804	
Adj. R-Square	0.9979	0.95162	
		Value	Standard Err
ln[BnOH]	Intercept	-0.3435	0.00254
ln[BnOH]	Slope	-0.0018	3.77118E-5
ln[BnOH] with N	Intercept	-0.4032	0.01281
ln[BnOH] with N	Slope	-0.0018	1.90106E-4

Even though a substoichiometric amount of base was reported in the literature to be fundamental to obtain higher yields,^{21,22,43} in our system the addition of sodium hydrogen carbonate did not change the activity of the dimer $[\text{Cp}^*\text{IrCl}_2]_2$. Both the conversion profiles and the rate constants show the same pathway, which suggests that, under these conditions, the preferred coordination mode is the amine-iridium coordination, instead of the carbonate-metal complex. Therefore, the catalyst could generate the active form in the absence of potassium carbonate or sodium hydrogen carbonate, supporting Madsen's proposal of amine-coordination.³⁵ Thus the following experiments were carried out in the absence of any base.

2.2 Determination of the Reaction Order: Amine

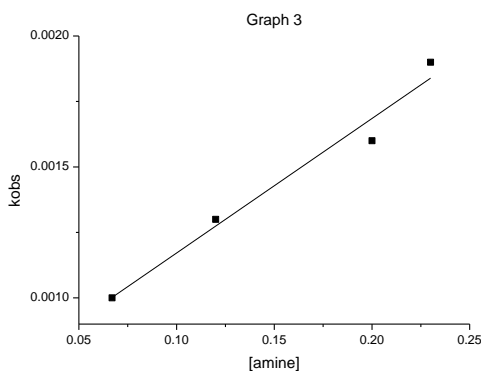
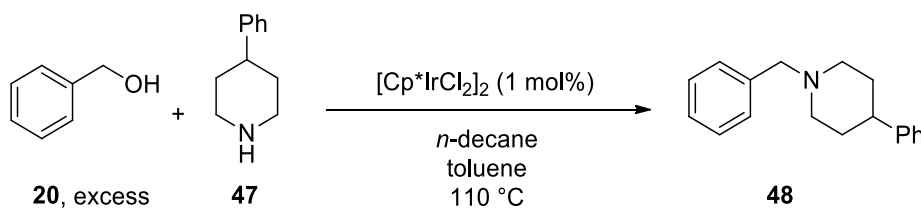
To establish if the rate-determining step was the oxidation of the alcohol (k_1), the formation of the imine (k_2) or the hydrogenation to amine (k_3) (Scheme 39), attempts were made to study the global reaction order, beginning with the evaluation of the reaction order in the amine.

Scheme 39



Several reactions were carried out in *pseudo*-first order conditions maintaining the alcohol in large excess, using respectively 10, 12, 15 and 20 equivalents of benzyl alcohol for 1 equivalent of 4-phenylpiperidine. Piperidine was changed to 4-phenylpiperidine to have a better separation and a sharper peak in the GC chromatogram. The observed rate constants, which were calculated plotting the logarithm of the amine concentration vs. time, were plotted versus the concentration of the amine, obtaining that the rate constant depended linearly with the concentration: the reaction is therefore first order with respect to the amine (Graph 3).

Graph 3

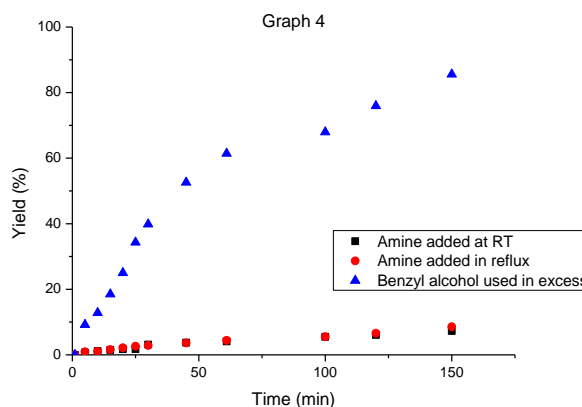
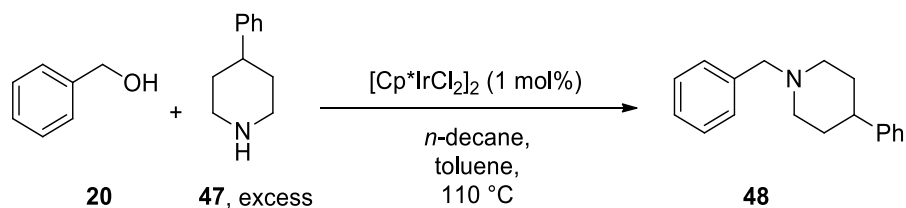


Equation	y = a + b*x		
Weight	No Weighting		
Residual Sum of Squares	1.16097E-8		
Pearson's r	0.98702		
Adj. R-Square	0.9613		
	Value	Standard Error	
kobs	Intercept	6.57713E-4	9.88079E-5
kobs	Slope	0.00514	5.91047E-4

2.3 Determination of the Reaction Order: Alcohol

To determine the reaction order with respect to the alcohol, our first attempt was to maintain the amine in large excess (10 equivalents of 4-phenylpiperidine for 1 equivalent of benzyl alcohol) to have *pseudo*-first order conditions respect to the alcohol. However, plotting the yield profile of **48** vs. time, we found that an excess of amine in the reaction inhibited the activity of the catalyst, obtaining **48** in less than 10% yield after 150 minutes. We also tried to add the amine when the reaction was already at reflux, instead of at room temperature, without achieving a better conversion. Graph 4 shows the results, comparing these two yield pathways with the one achieved in the previous section. Effectively, when benzyl alcohol was used in excess, product **48** was achieved in 80% yield after the same reaction time.

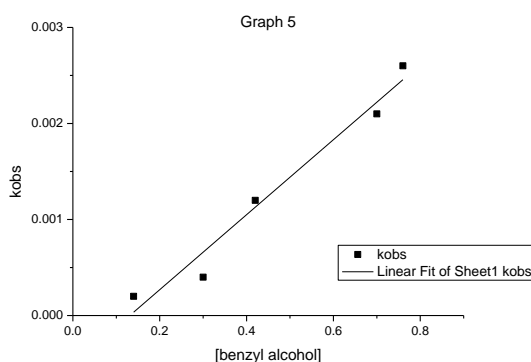
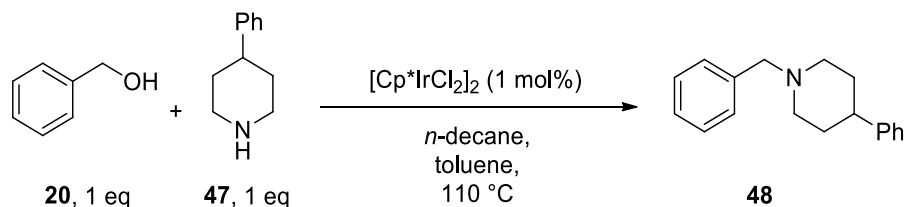
Graph 4



The excess of amine poisoned the catalyst, because it presumably generated a new iridium species which was very stable and, therefore, inactive. These results suggest that the amine-metal coordination is more favourable than the alcohol-metal coordination. Effectively, the reaction with an excess of benzyl alcohol gave a faster reaction rate than using the starting materials in a 1 : 1 *ratio*.

The results shown in Graph 4 could not be used to evaluate the reaction order with respect to the alcohol. We changed the approach and, using 1 equivalent of the amine and 1 equivalent of the alcohol, we analysed the data obtained between 0 and 5% yield to have *pseudo*-first order conditions with respect to the starting materials. For this reaction, we analysed the kinetics achieved in the first minutes. Several reactions have been carried out, changing the concentration of the benzyl alcohol. The relative observed rate constants have been calculated plotting the logarithm of the benzyl alcohol concentration vs. time. Graph 5 plots the observed rate constants vs. the concentration of the benzyl alcohol; the reaction is first order with respect to the alcohol, achieving a global second order reaction.

Graph 5



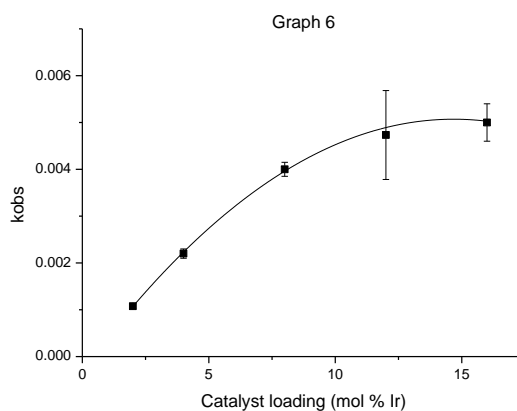
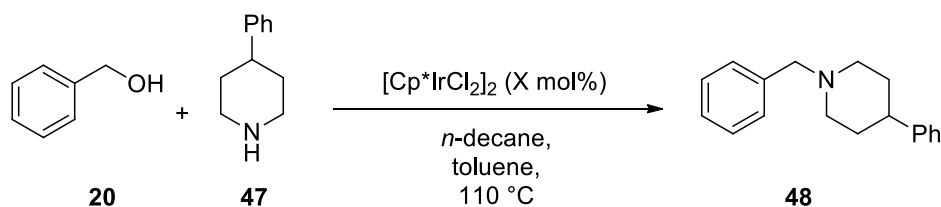
Equation		y = a + b*x	
Weight	No Weighting		
Residual Sum of Squares	1.3539E-7		
Pearson's r	0.98435		
Adj. R-Square	0.9586		
		Value	Standard Error
k_obs	Intercept	-5.11663E-4	2.09971E-4
k_obs	Slope	0.0039	4.03551E-4

Whilst we were working on this chemistry, Madsen and co-workers published their paper in which they affirmed this reaction is in first order with respect to the alcohol and to the amine, achieving a global second order reaction.³⁵ Our results suggest that, in the catalytic cycle, both the amine and the alcohol are involved in the rate-determining step, which confirms their conclusions.

2.4 Determination of the Reaction Order: Catalyst

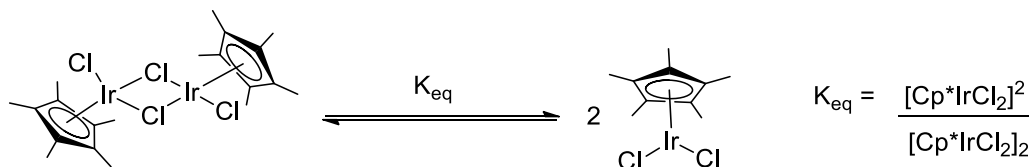
The last part of this preliminary study concerned the reaction order in the catalyst. Several reactions were carried out changing the amount of catalyst used, but maintaining a constant concentration of alcohol **20** and amine **47**. Again, we analysed the data obtained between 0 and 10% yield to have *pseudo*-first order conditions with respect to the starting materials. The observed rate constants have been calculated plotting the logarithm of the benzyl alcohol concentration vs. time. Graph 6 shows the observed rate constants vs. the catalyst loading.

Graph 6



The reaction rates did not show a linear pathway with an increasing amount of catalyst used. These results could be explained by considering the dimer-monomer equilibrium shown in Scheme 40. Recently, Madsen and co-workers have calculated computationally the energy related to the dimer-monomer equilibrium: when the reaction was at reflux in toluene (110 °C), a small amount of the active monomeric 16-electron complex was favoured by entropy, even if the dimer is the most stable complex.³⁵

Scheme 40



Our results suggest that the amount of the active species $[Cp^*IrCl_2]$ in the reaction does not increase linearly with the catalyst loading. Instead, its concentration in the reaction mixture is proportional to the square root of the concentration of $[Cp^*IrCl_2]_2$. The observed rate constants shown in Graph 6 depend on the amount of the $[Cp^*IrCl_2]$ in the reaction and therefore, since the two iridium species $[Cp^*IrCl_2]$ and $[Cp^*IrCl_2]_2$ deviate from linearity, the observed rate constants are not in linear dependence with the catalyst loading.

2.5 Conclusions

The results described above suggest that a monomeric complex could be potentially more active than the dimeric $[Cp^*IrCl_2]_2$, because it should not need pre-activation to generate the active monomeric 16-electron complex. Additionally, the active catalytic species does not contain a carbonate in its coordination sphere, but an amine. These observations suggest that an amine could be an interesting functional group to include in the design of new catalysts, since the amine-metal coordination is particularly favoured over the other possible ligands that could be considered, *e.g.* alcohol or carbonate. With the synthesis of more efficient catalysts which do not need the energy necessary to break the dimer in two monomers, it would be possible to decrease the high temperatures and the high catalyst loadings generally required in the hydrogen borrowing methodology.

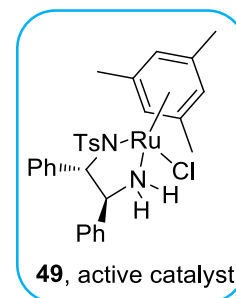
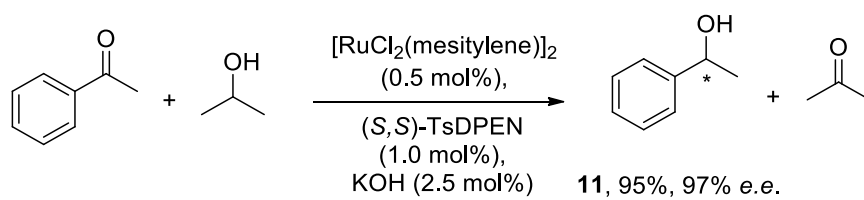
Chapter 3. Synthesis of New Complexes

3.1 Introduction

Our kinetic studies reported in the previous chapter showed that a monomeric complex could potentially be more active than the dimer $[\text{Cp}^*\text{IrCl}_2]_2$. We decided to focus on the development of complexes using two metals: rhodium and iridium. This choice was based on the knowledge that both rhodium and iridium complexes have been reported to catalyse hydrogen borrowing reactions.^{1,4} Besides, these two metals have several features in common: all the compounds of Rh(III) and Ir(III) are diamagnetic and low-spin and both metals have a great affinity for ammonia and amines. Both rhodium trichloride hydrate and iridium trichloride hydrate provide a convenient starting point for the preparation of complexes.⁶⁴ Furthermore, even if rhodium complexes generally show worse activities for hydrogen borrowing reactions than iridium catalysts, they are easier to synthesise, since the formation of iridium complexes is generally slow.⁶⁵ Therefore, the synthesis of the designed catalysts could be attempted starting with rhodium trichloride hydrate, followed by the optimisation of the methodology to make the corresponding iridium complexes.

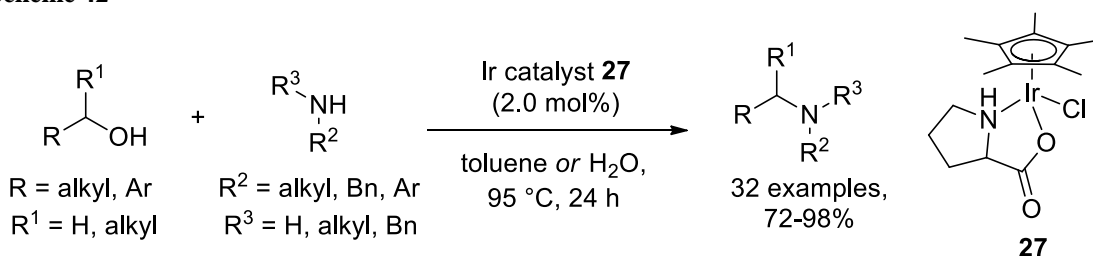
Since our previous results suggest that the active catalyst contains an amine in its coordination sphere, our aim was to prepare complexes which contained a coordinated amine as a ligand. The importance of the N-H functional group in organometallics is also well known in the literature and it often recurs in metal-catalysed reactions.⁶⁶ Effectively, the amine moieties can serve as coordination groups, hydrogen bonding donors, hydrogen bonding acceptors and proton sources and they are chemically stable and easily introduced to the ligands. The N-H functional group is largely used in symmetric and asymmetric hydrogen transfer. One of the first asymmetric examples was reported by Noyori in 1995 (Scheme 41).⁶⁷

Scheme 41



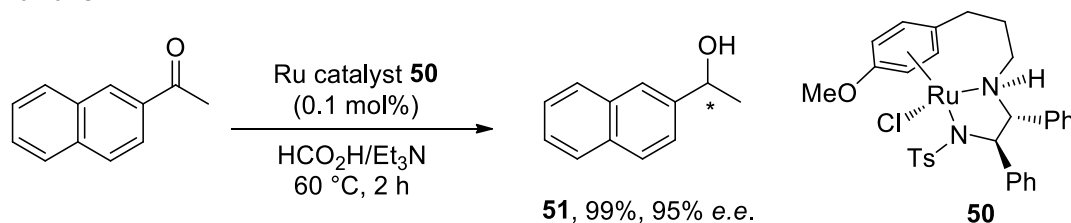
Two different families of ligands have been designed, both containing a coordinated amine. The first family has a bidentate ligand coordinated to the metal centre in a Noyori-type complex. Recently, Limbach and co-workers showed that similar complexes can be used efficaciously in the *N*-alkylation processes, as shown in Scheme 42.³³ A family of complexes was prepared containing aminoacidate ligands like **27**, which promoted the hydrogen borrowing reactions in good to excellent yields (72-98%).

Scheme 42



In the second family of complexes that could be designed, the aromatic ring was derived introducing a tethered chain which contained the amine group. Wills and co-workers have prepared a new family of ruthenium tethered catalysts, which have shown excellent activities in asymmetric transfer hydrogenation of ketones (Scheme 43).⁶⁸

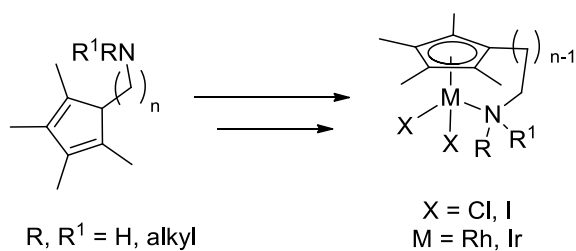
Scheme 43



The introduction of the tethered amine provided extra stability and a significant increase of the reaction rate related to the “untethered” Noyori-type catalyst.⁶⁹ This latter

modification is really interesting, because we could potentially prepare more active catalysts and increase the stability of the complexes simply introducing a tethered chain in the Cp* ring. Thus, a new family of monomers was designed, as shown in Figure 15; the general structure of the ligand contains a Cp* group which has been modified with a side chain bearing an amine group.

Figure 15



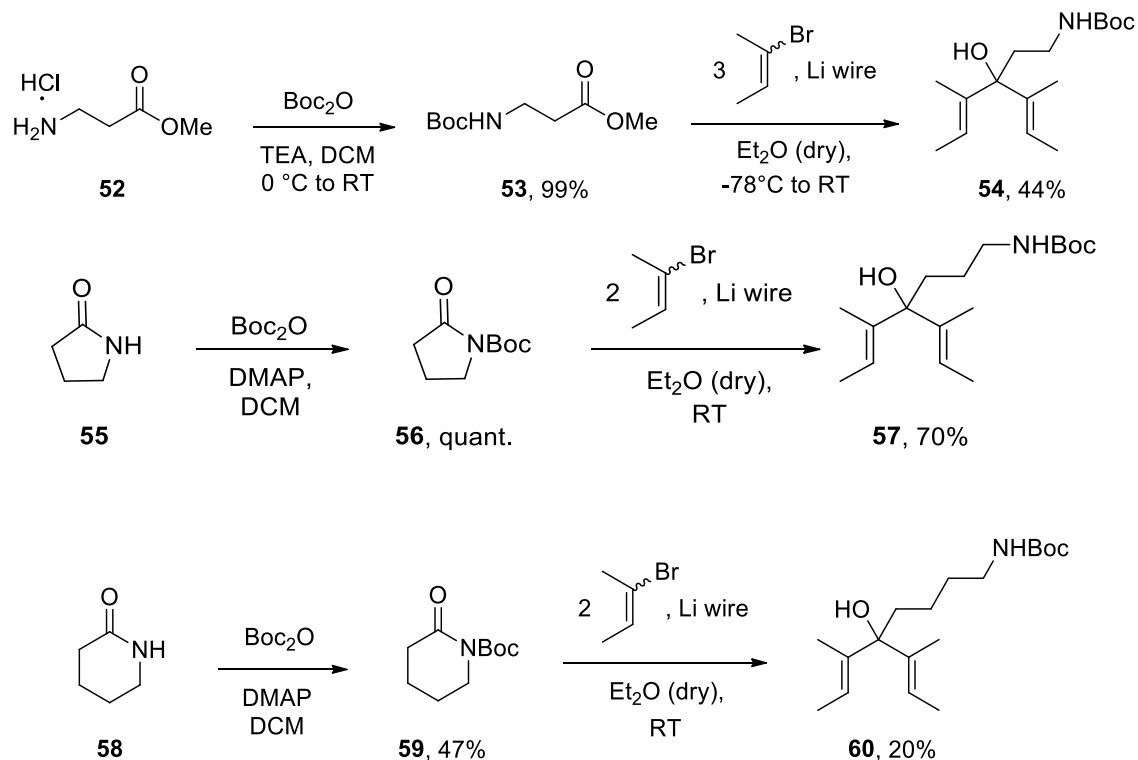
The designed structure represented above shows a great number of possible modifications, such as the length of the chain and the substituents on the nitrogen, which could permit us to compare the structure of the complexes vs. their activity in hydrogen borrowing processes. Since they are monomeric complexes, they should not need pre-activation from the dimer dissociation and the amine could act as an internal base. Additionally, the nitrogen in the amine could favour the monomeric structure, due to the great affinity between iridium or rhodium and nitrogen.

3.2 Synthesis of New Monomeric Rhodium(III) Catalysts

We started the synthesis of a series of ligands varying the length of the side chain to evaluate its role in the catalytic activity of the complex. Three different ligand precursors have been synthesised using similar procedures: the first one containing a $(CH_2)_2NHBoc$ unit (ligand **54**, Scheme 44), the second one containing a $(CH_2)_3NHBoc$ unit (ligand **57**, Scheme 44) and the third one containing a $(CH_2)_4NHBoc$ unit (ligand **60**, Scheme 44). These ligand precursors, which were obtained as a mixture of geometric isomers, have been prepared by double alkenylation of the *N*-Boc protected amine **53** or amides **56** and **59** with 2-lithium-2-butene. This procedure was used in the literature to synthesise the diene **57** in good yield, as reported by Ito *et al.*⁷⁰ Herein, it was efficaciously applied to synthesise dienes varying the length of the side chain. The organolithium reagent 2-lithium-2-butene was generated *in situ* by the reaction between lithium wire and

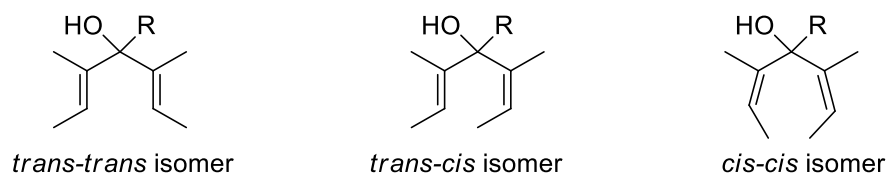
2-bromo-2-butene, used as a mixture of *cis* and *trans* isomers;⁷⁰ its *ratio* was not reported by the suppliers.

Scheme 44



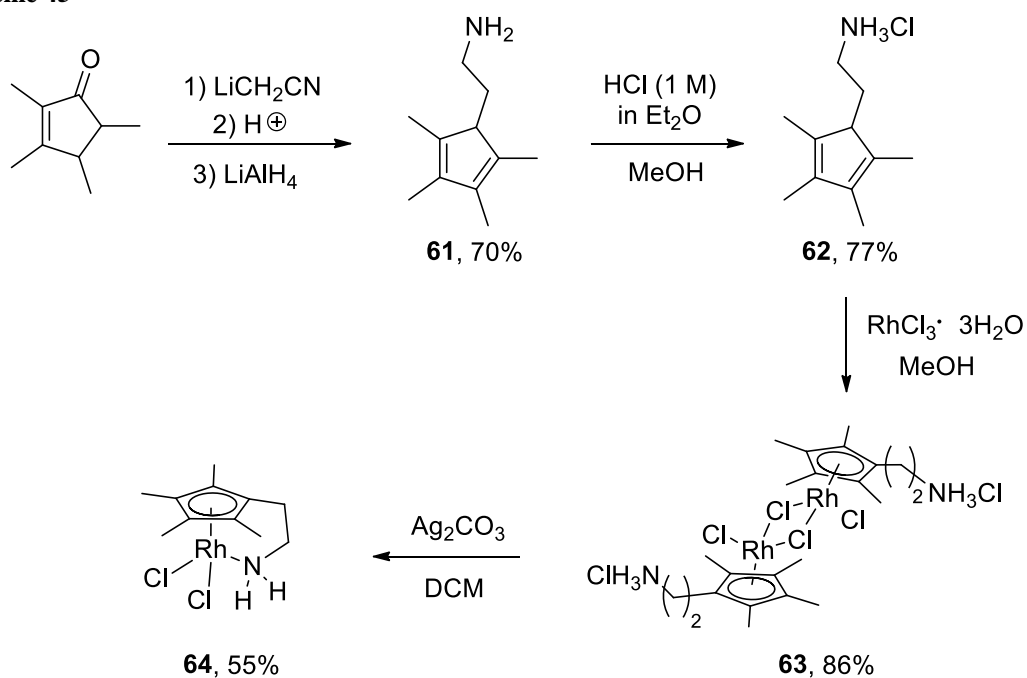
Three different isomers could be achieved, as shown in Figure 16: the *trans-trans* isomer, the *trans-cis* isomer and the *cis-cis* isomer. The dienes were generally purified by flash chromatography, isolating them in a mixture of 1 : 1 : 0 *ratio*.

Figure 16



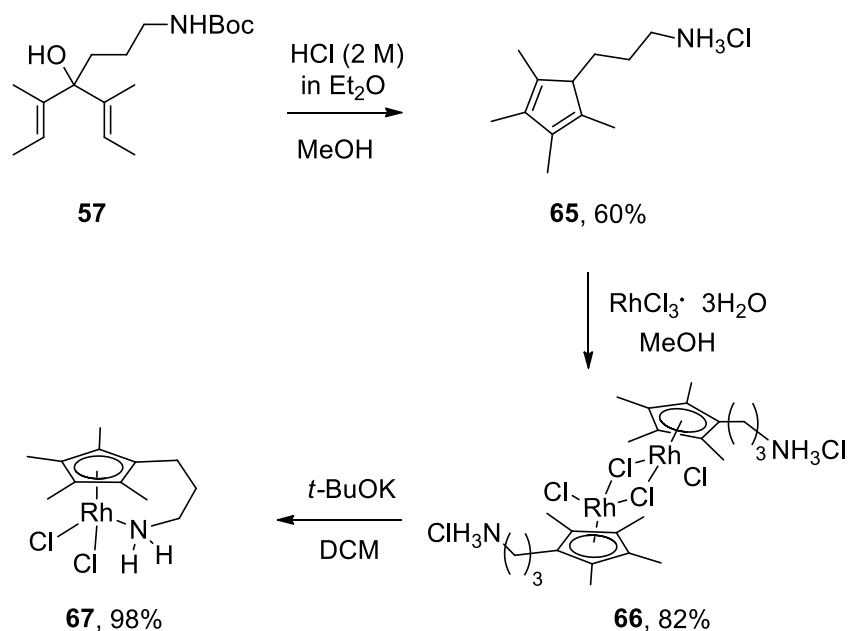
Two rhodium complexes containing a modified Cp* ligand bearing an amine in the side chain were already reported in the literature by Ito *et al.*⁷⁰ Complex **64** was synthesised in good yield starting from the ligand precursor **61**, which was prepared from tetramethylcyclopentenone in three steps, following a procedure reported by Teuben and co-workers⁷¹ (Scheme 45).

Scheme 45



Complex **67** was also reported in the literature by Ito *et al.* and it was synthesised from the ligand precursor **57** in three steps, as shown in Scheme 46.⁷⁰ Diene **57** was prepared using the same procedure reported in Scheme 44.

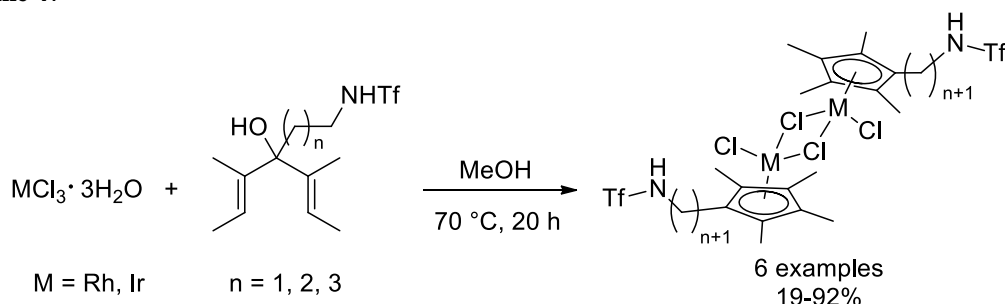
Scheme 46



Disappointingly, several attempts to synthesise the ligand precursor **65** failed in our hands. The NMR spectra of the crude reaction mixtures showed that the signals of diene **57** disappeared, but only a mixture of by-products was obtained.

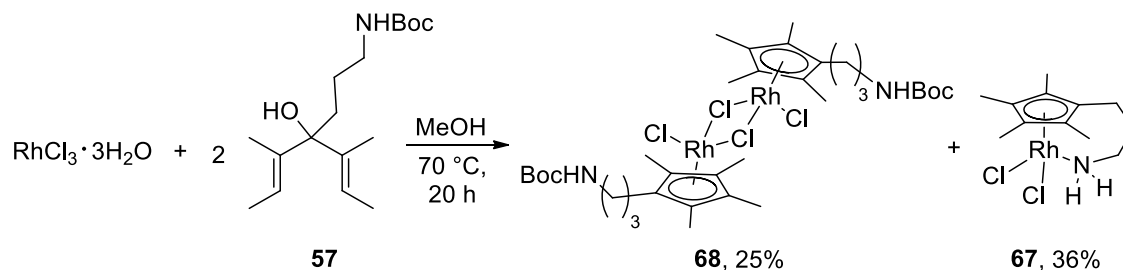
Therefore, we sought a different procedure to synthesise our complexes. Ito *et al.* reported in the literature that rhodium and iridium dimers could be synthesised *in situ* starting from modified dienes in moderate to excellent yields, as shown in Scheme 47.⁷²

Scheme 47



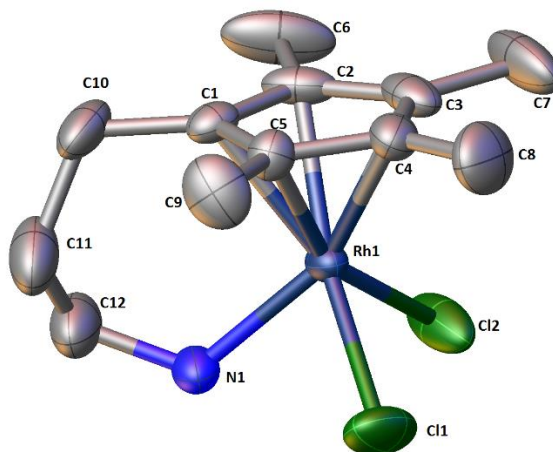
Following this general procedure, rhodium trichloride hydrate and diene **57** were dissolved in dry methanol and the mixture was heated at reflux overnight (Scheme 48). Unexpectedly, in addition to dimer **68** isolated in 25% yield and characterised by NMR spectroscopy and HRMS, a 36% yield of monomer **67** was purified by flash chromatography.

Scheme 48



The structure of compound **67** was confirmed by X-ray crystallography, after growing red diffraction-quality crystals by slow recrystallization from dichloromethane (Figure 17). The complex crystallised monoclinic, space group $P2_1/n$. The hydrogen atoms have been omitted for clarity. Displacement ellipsoids are at the 50% probability level.

Figure 17



Molecular structure of complex **67**

Table 1 reports the relevant bond lengths and angles for this complex.

Table 1

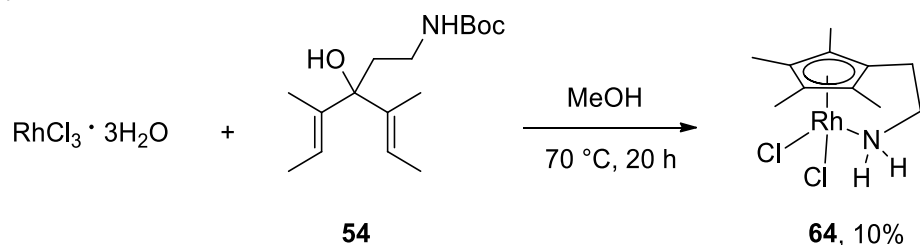
<i>Bond and Angle</i>	<i>Length (Å) and Angle (°)</i>
Range C _q (ring)-Rh1	2.142(3) to 2.196(3)
C1-Rh1	2.142(3)
Ring centroid-Rh1	1.781
N1-Rh1	2.139(3)
Cl1-Rh1	2.439(1)
Cl2-Rh1	2.441(1)
N1-Rh1-C1	94.54(10)

The maximum difference in the bond lengths between the carbons of the ring and the metal is 0.054 Å, with the bond between the carbon in the tethered chain (C1) and rhodium being the shortest (2.142(3) Å). The length between the ring centroid and the metal is 1.781 Å.

The yield for the synthesis of complex **67** reported in the literature was higher (Scheme 46); however, to the best of our knowledge, the development of a procedure to synthesise the Cp*-derived ligand *in situ* and, at the same time, deprotect the *N*-Boc amine to directly isolate monomeric complex **67** is new.

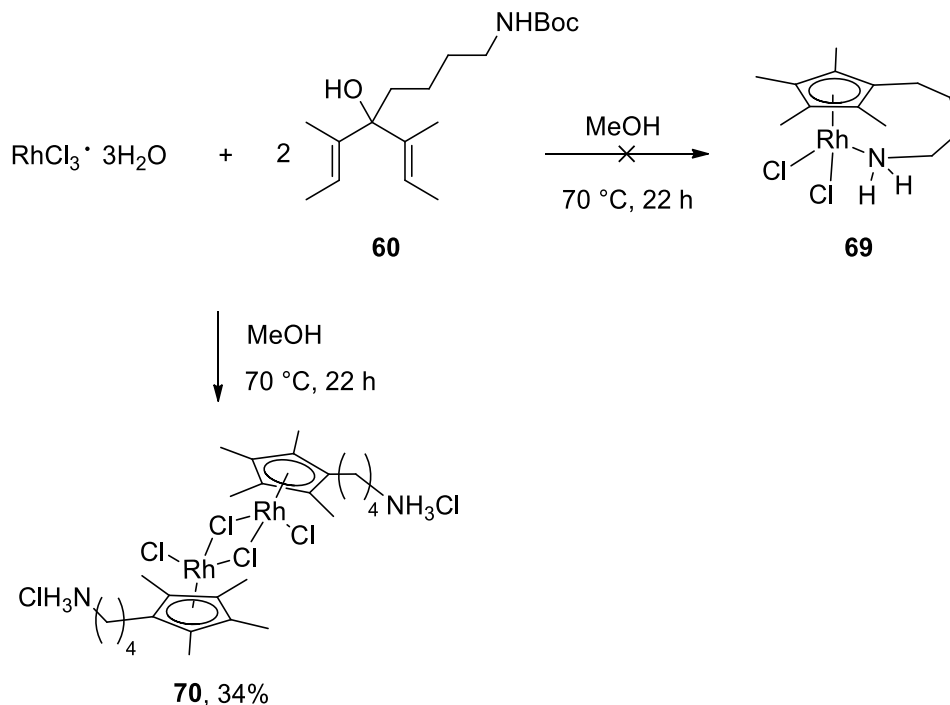
The same procedure described in Scheme 48 has been used to synthesise complexes **64** and **69**. Rhodium complex **64** was isolated after purification by flash chromatography in 10% yield (Scheme 49) and it was analysed by NMR spectroscopy and HRMS.

Scheme 49



When we attempted the same procedure starting with rhodium trichloride hydrate and the homologated diene **60** in dry methanol, we did not manage to directly isolate complex **69**, but instead we achieved a 34% yield of the dimer **70** (Scheme 50). Complex **70** was characterised by NMR spectroscopy, comparing the signals with similar dimers reported in the literature.⁷⁰

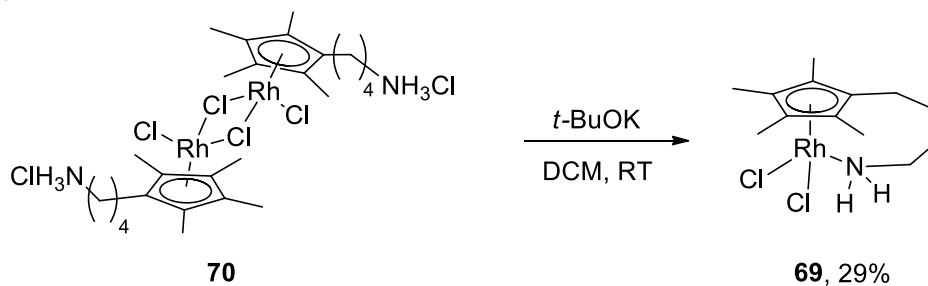
Scheme 50



The treatment of dimer **70** with 2 equivalents of potassium *tert*-butoxide in dry DCM gave complex **69** in modest yield (Scheme 51), which was not stable. The structure of the

complex was confirmed by $^1\text{H-NMR}$ and HRMS; however, upon the removal of the solvent decomposed **69** to give an insoluble orange by-product.

Scheme 51



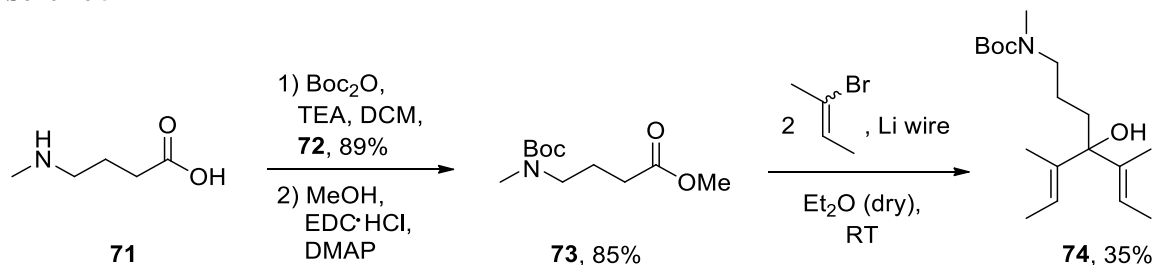
Among the dienes tried, **57** gave the highest yield in the synthesis of the corresponding rhodium complex. These results suggest that the length of three carbon chain would be optimal, because the complex **67** was isolated with the highest yield. The side chain of diene **54** is probably too short to give an easily formed monomer. Ito *et al.* reported that the conformational constraints of the cyclopentadienyl ligand is bigger in complex **64** than in **67**.⁷⁰ On the contrary, the chain in diene **60** is probably too lengthy to afford a stable monomer, **69**. Effectively, the dimer **70** was the only product isolated from the reaction shown in Scheme 50, which demonstrates that the *N*-Boc deprotection occurred, but a dimeric structure was more favoured than the monomeric one. The treatment of **70** with a strong base gave the monomer **69**, but it was unstable and it decomposed spontaneously to give an insoluble by-product. As a result of these considerations, the length of diene **57** (three carbon chain) was chosen for further modifications of the amine and the halide ligands.

3.3 Modification of Rhodium(III) Complex 67: Secondary Amine

The structure of catalyst **67** is interesting because it contains a primary amine in the side chain. The possibility to synthesise active catalysts with a secondary or a tertiary amine is intriguing because it would open the potential modifications of the catalysts, developing supported catalysts or introducing asymmetric centres for enantioselective alkylation.

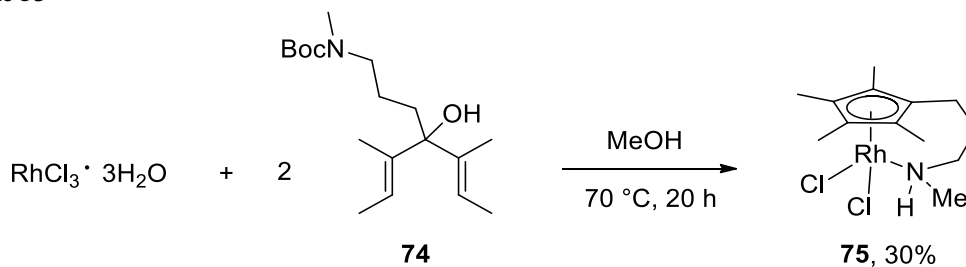
We synthesised a diene containing an *N*-Boc protected secondary amine as shown in Scheme 52, starting from the commercially available 4-(methylamino)butyric acid **71** in three steps.

Scheme 52



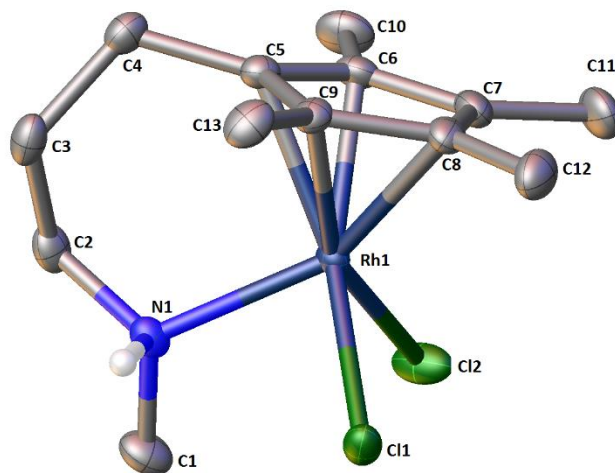
The procedure described in Scheme 48 has been applied here to synthesise monomer **75** starting from 2 equivalents of diene **74** and 1 equivalent of rhodium trichloride hydrate in methanol (Scheme 53).

Scheme 53



The structure of complex **75** has been confirmed by X-ray crystallography, after growing red diffraction-quality crystals by recrystallization from dichloromethane-hexane (*v/v* = 1/2) (Figure 18). The complex crystallised monoclinic, space group *P2₁/n*. The hydrogen atoms, except those on the protic amine, have been omitted for clarity. Displacement ellipsoids are at the 50% probability level.

Figure 18



Molecular structure of complex **75**

Table 2 reports the relevant bond lengths and angles for this complex.

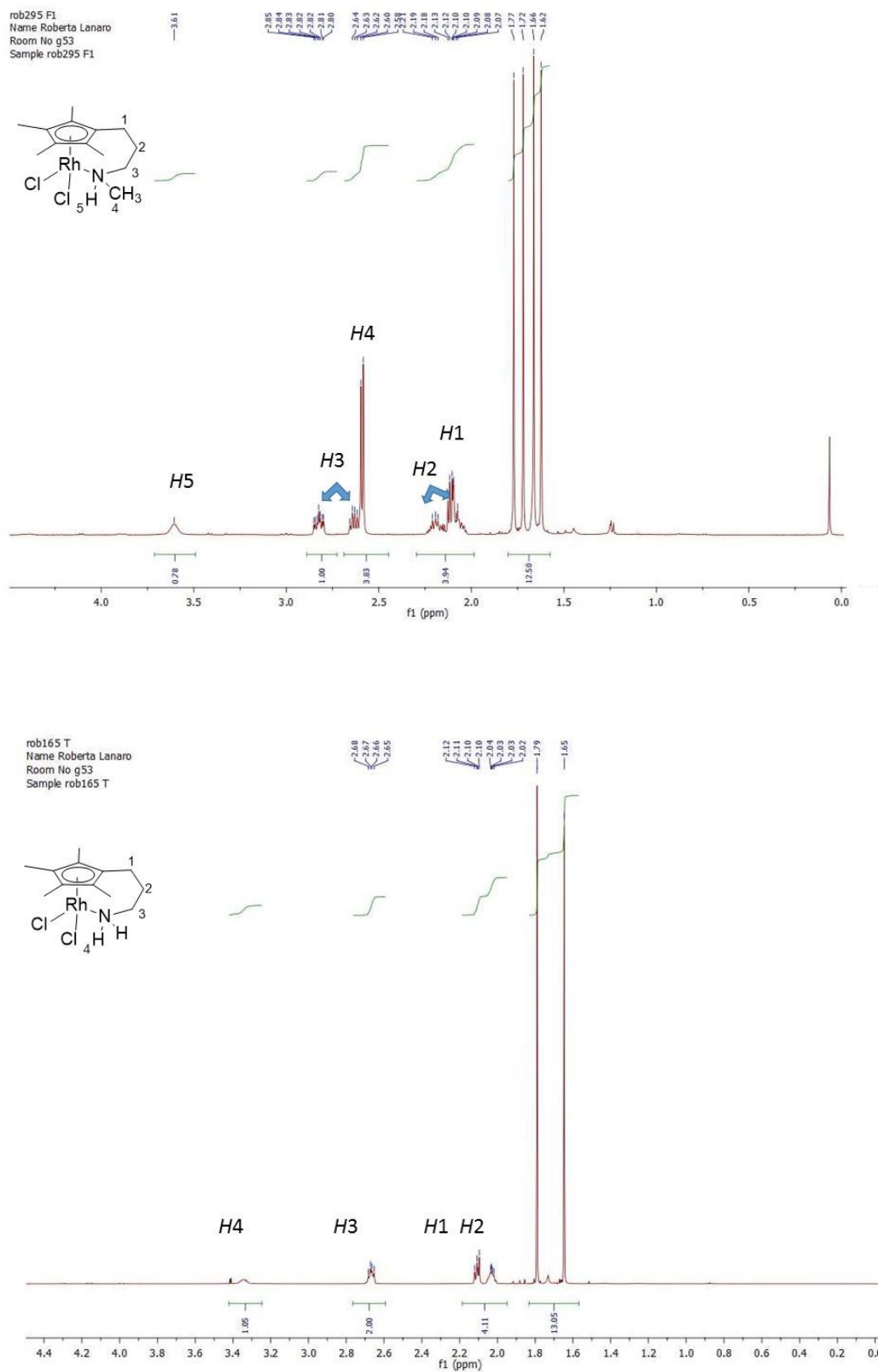
Table 2

<i>Bond and Angle</i>	<i>Length (Å) and Angle (°)</i>
Range C _q (ring)-Rh1	2.149(2) to 2.209(2)
C5-Rh1	2.161(2)
Ring centroid-Rh1	1.791
N1-Rh1	2.171(2)
Cl1-Rh1	2.454(5)
Cl2-Rh1	2.448(5)
N1-Rh1-C5	92.97(6)

The bond lengths and angles of complex **75** were compared with those of monomer **67**. The length of the C5-Rh bond and the length between the ring centroid and the metal are slightly greater in **75** than in **67** (respectively, 2.161(2) Å and 1.791 Å for **75** and 2.142(3) Å and 1.781 Å for **67**). The angle between N1-Rh-C5 is slightly more acute in **75** than in **67**. Additionally, the length of the nitrogen-rhodium bond is greater in complex **75** (2.171(2) Å) than in **67** (2.139(3) Å), suggesting that this bond is weaker with a secondary amine in the side chain.

The ¹H-NMR analyses of complex **75** showed that the protons of the side chain and of the methyl groups in the ring became diastereotopic, due to the asymmetric centre on the coordinated nitrogen. Figure 19 shows the ¹H-NMR spectra of complexes **75** and **67** for comparison.

Figure 19



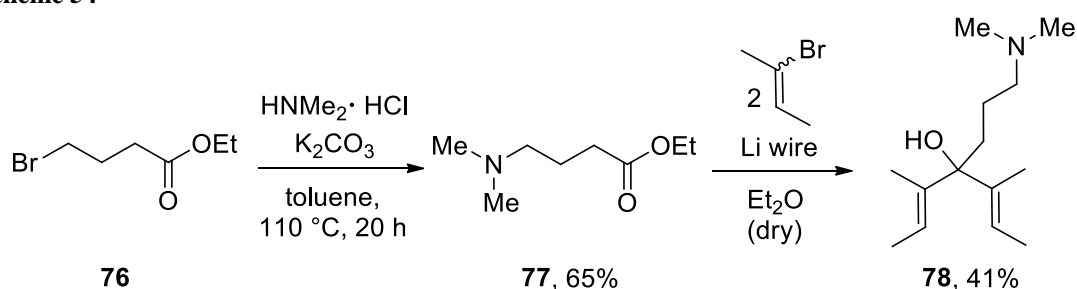
The ¹H-NMR spectra were recorded in deuterated chloroform using a 500 MHz Bruker spectrometer.

Firstly, the hydrogens of the two side chains were compared. The two hydrogens next to nitrogen (*H3* in the Figure) and the two next to them (*H2* in the Figure) in complex **75** are diastereotopic with four distinct signals for the four hydrogens. In comparison, the same four hydrogens in complex **67** (*H2* and *H3* in the Figure) occur in two homotopic pairs and only two signals are observed. The signals of the methyl groups in the Cp* were also compared. Complex **75** has four different signals, showing that the Cp*-derived ring is also diastereotopic, while **67** has only two signals. Finally, the methyl group attached to the nitrogen in complex **75** is a doublet in the spectrum, because it is coupled to the hydrogen on the coordinated amine.

3.4 Modification of Rhodium(III) Complex 67: Tertiary Amine

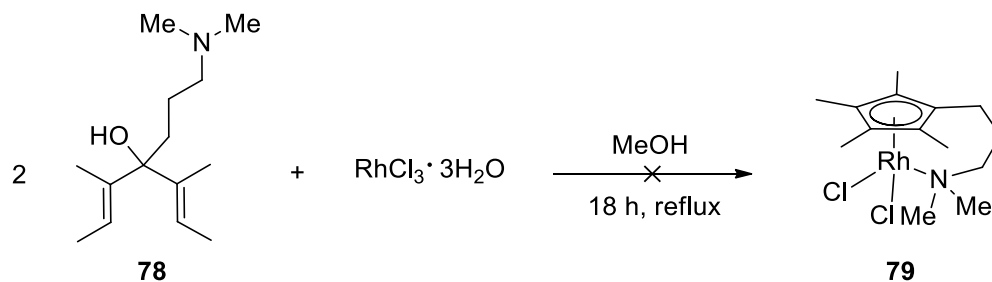
Some examples in which a tertiary amine is coordinated to the metal are reported in the literature; usually two methyl groups have been used as substituents on the amine.^{70,73} To conclude the screening of our family of amine-modified Cp* ligands, we synthesised diene **78** starting with a nucleophilic substitution between dimethylamine and ethyl 4-bromobutanoate **76** in toluene, followed by the double alkenylation of **77** by the organolithium generated *in situ* in the reaction between lithium wire and 2-bromo-2-butene, used as a mixture of *cis* and *trans* isomers (Scheme 54).

Scheme 54



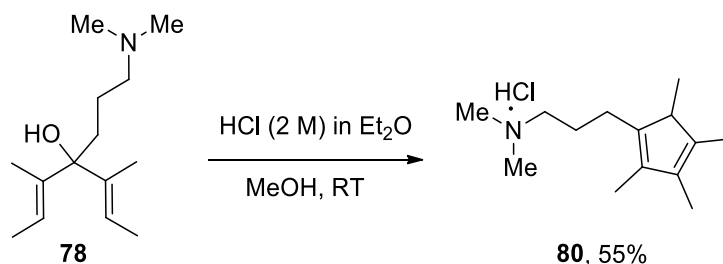
Unfortunately, the reaction between diene **78** and rhodium trichloride hydrate in methanol did not afford complex **79** (Scheme 55), suggesting that the *N*-Boc deprotection was a fundamental step for the synthesis of this family of monomers.

Scheme 55



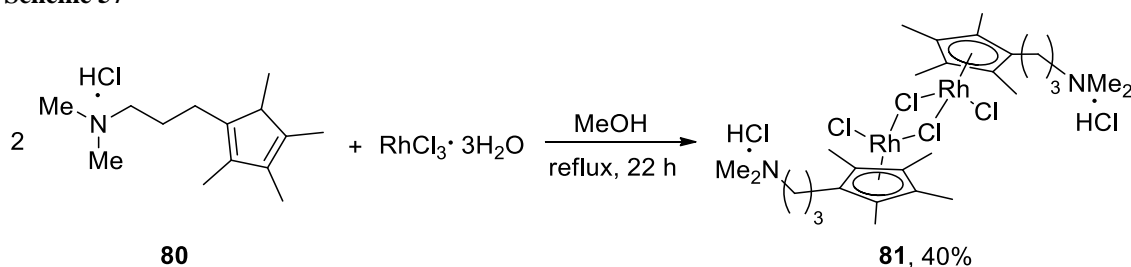
With the idea of synthesising rhodium(III) dimer **81** and then closing the structure to form the corresponding monomer **79**, we treated ligand **78** with 2.0 M hydrogen chloride in ether to give the hydrochloride salt **80** as an unresolved mixture of three isomers, following the general procedure reported by Ito and co-workers (Scheme 56).⁷⁰

Scheme 56



The reaction between rhodium trichloride hydrate and ligand precursor **80** in dry methanol gave rhodium(III) dimer **81** in 40% yield (Scheme 57).

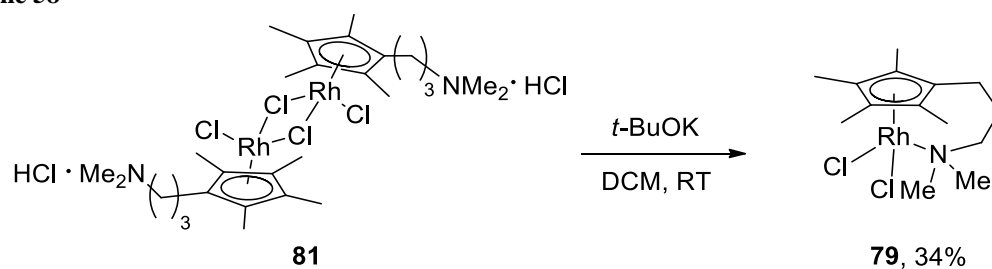
Scheme 57



This complex was characterised by NMR spectroscopy, comparing the signals with similar dimers reported in the literature⁷⁰ and by HRMS.

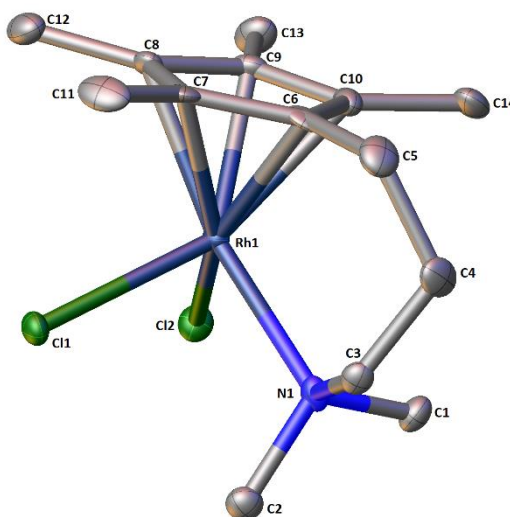
The rhodium dimer **81** was converted into the desired monomer **79** in moderate yield using 2 equivalents of potassium *tert*-butoxide in dichloromethane, as shown in Scheme 58.⁷⁰

Scheme 58



The structure has been confirmed by X-ray crystallography, after growing orange diffraction-quality block crystals from dichloromethane-hexane (v/v = 1/2) (Figure 20).

Figure 20



Molecular structure of complex **79**

The complex crystallised orthorhombic, space group $Pca2_1$. The hydrogen atoms have been omitted for clarity. Displacement ellipsoids are at the 50% probability level.

Table 3 reports the relevant bond lengths and angles for this complex. The characteristic bond lengths and angles of complex **79** were compared with those reported previously for **67** and **75**. The maximum difference in the bond lengths between the carbons in the ring and the rhodium is smaller than those previously observed (0.023 Å for **79** instead of 0.054 Å for **67** and 0.060 Å for **75**), suggesting that the presence of a tertiary amine gives an almost symmetry of coordination between the Cp*-derived ring and the metal. The length between the carbon in the tethered chain (C6) and rhodium is the shortest among the five carbon-rhodium bonds, like in complex **67**. Additionally, the bond length

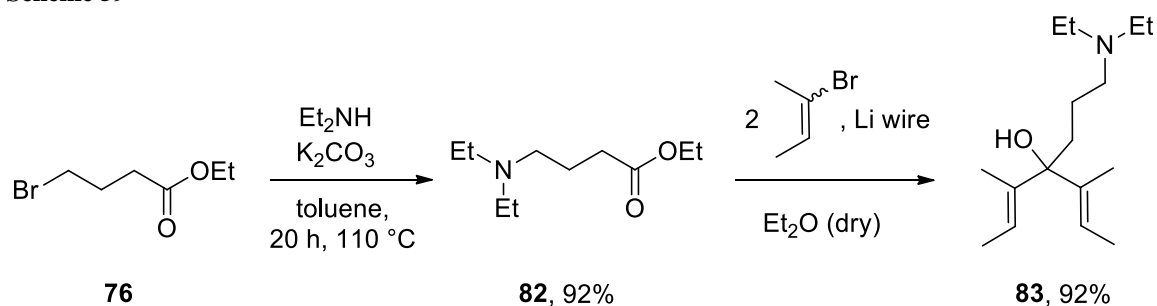
between nitrogen and rhodium is greater (2.196(4) Å for **79**, 2.171(2) Å for **75** and 2.139(3) Å for **67**), indicating that the weakest rhodium-nitrogen bond is the one with a tertiary amine in the side chain.

Table 3

<i>Bond and Angle</i>	<i>Length (Å) and Angle (°)</i>
Range C _q (ring)-Rh1	2.140(5) to 2.167(5)
C6-Rh1	2.140(5)
Ring centroid-Rh1	1.772
N1-Rh1	2.196(4)
Cl1-Rh1	2.417(2)
Cl2-Rh1	2.422(1)
N1-Rh1-C9	95.11(18)

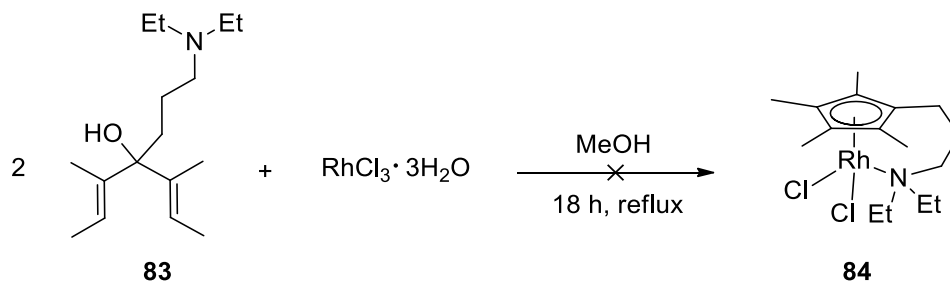
Finally, to analyse the effect of a bigger substituent on the tertiary amine coordinated to the metal, diene **83** was synthesised using a synthetic route which was similar to the one shown previously (Scheme 59).

Scheme 59



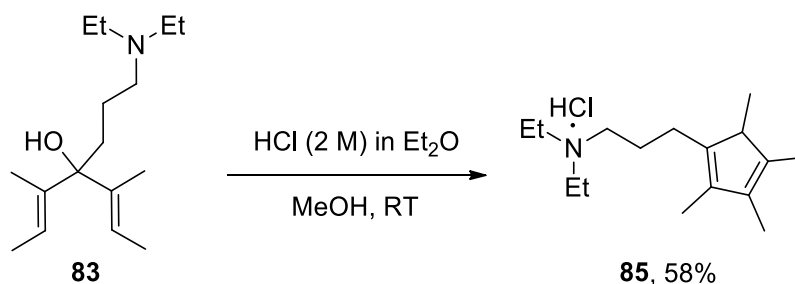
Similarly to what was observed previously in the synthesis of complex **79**, the reaction between diene **83** and rhodium trichloride hydrate did not afford complex **84** (Scheme 60).

Scheme 60



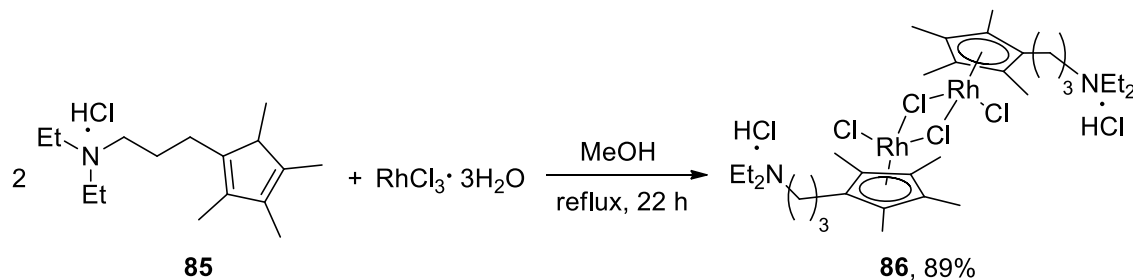
With the idea of synthesising rhodium(III) dimer **86** and then closing the structure to form the corresponding monomer **84**, ligand precursor **85** was synthesised (as an unresolved mixture of three isomers) following the general procedure reported by Ito and co-workers⁷⁰ (Scheme 61). This ligand was used in the following reaction without any other purification; a small amount was purified by flash chromatography for characterisation purposes, isolating the compound as a free amine.

Scheme 61



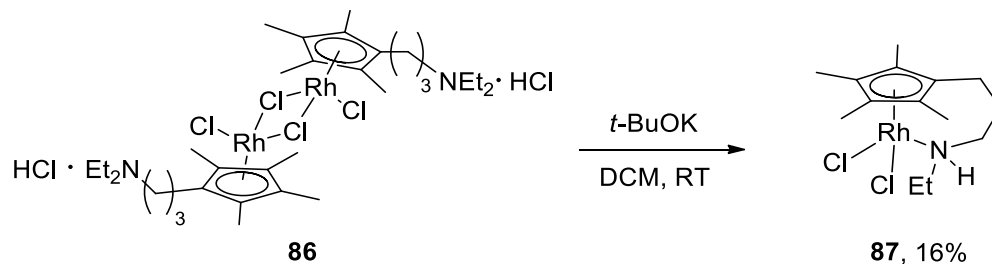
The reaction between rhodium trichloride hydrate and ligand **85** in dry methanol gave rhodium(III) dimer **86** in excellent yield, which was characterised by NMR spectroscopy, elemental analysis and HRMS (Scheme 62).

Scheme 62



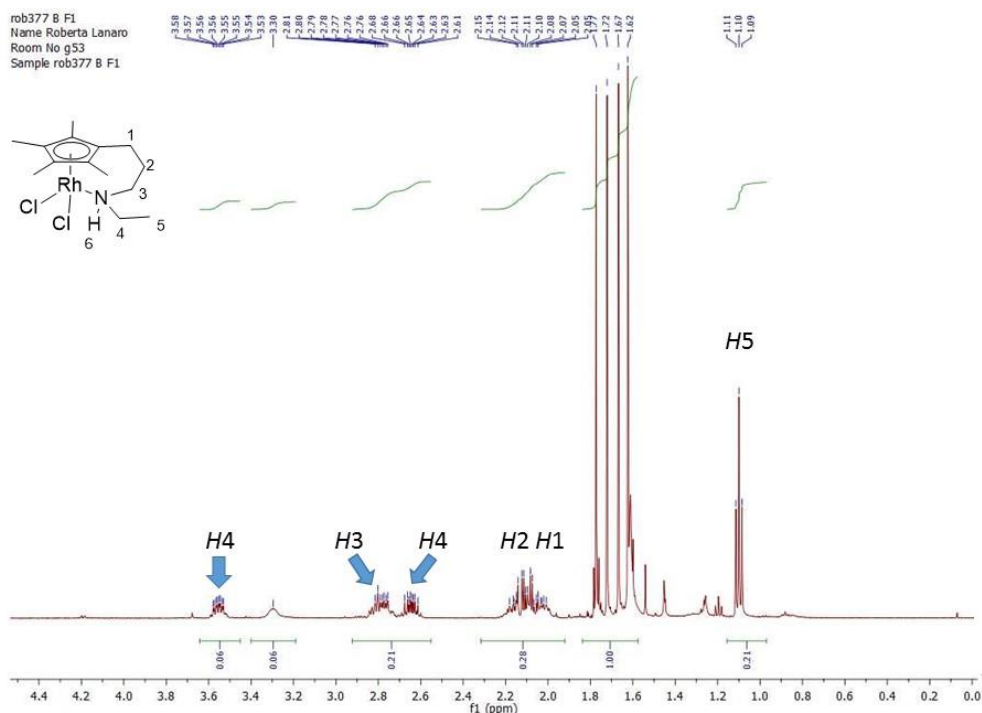
Two different procedures were attempted to synthesise monomeric complex **84**, the first one using potassium *tert*-butoxide as a base⁷⁰ and the second one using silver carbonate.⁷² Using the first procedure, instead of obtaining complex **84**, we found a small amount of the monomer **87** and unreacted starting material (Scheme 63).

Scheme 63



The formation of complex **87** was confirmed by NMR spectroscopy. Figure 21 shows the ¹H-NMR spectrum of monomer **87**.

Figure 21



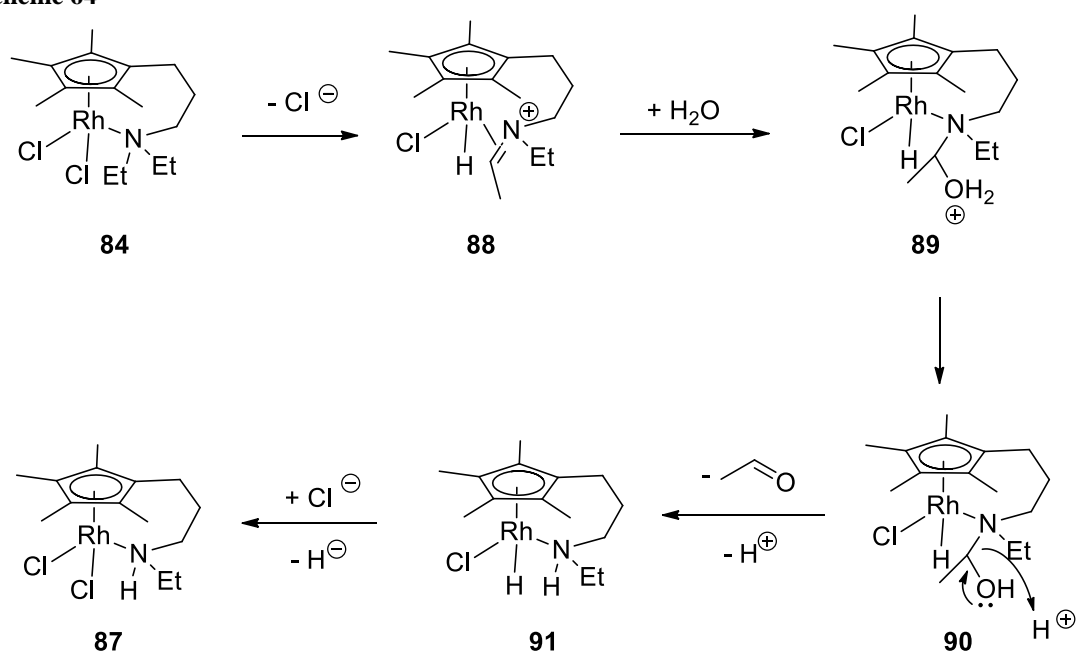
The ¹H-NMR spectrum was recorded in deuterated chloroform using a 500 MHz Bruker spectrometer.

The protons next to the nitrogen in the ethyl group (*H4* in the Figure) are diastereotopic and two signals are observed. The methyl groups in the Cp*-derived ring are also

diastereotopic and they appear as four different singlets. This diastereotopicity is due to the asymmetric centre on the coordinated nitrogen, similarly to complex **75**.

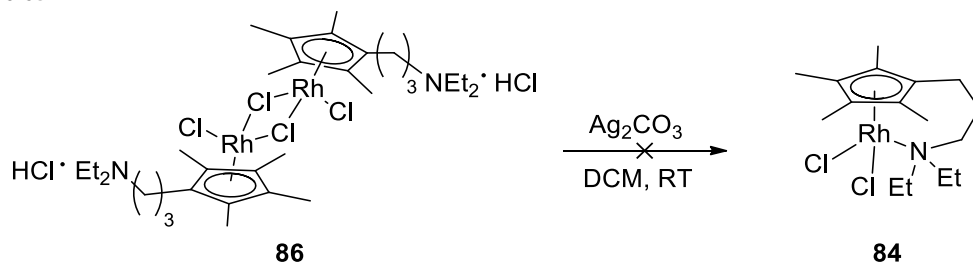
Since alkyl cations are not generally good leaving groups, the loss of the ethyl group to generate **87** was unexpected. The mechanism of this reaction was not certain, but our hypothesis is that the first step could be the formation of iminium ion **88** by dehydrogenation, followed by the formation of the hemiaminal **90** and its hydrolysis, which gave **87** (Scheme 64).

Scheme 64



Using the second procedure, we observed only unreacted starting material (Scheme 65).

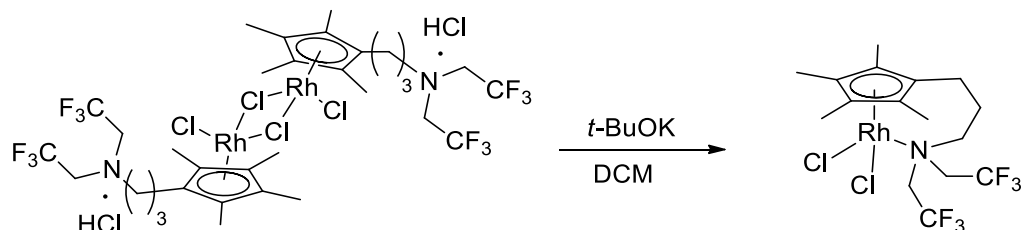
Scheme 65



Unfortunately, these unexpected results suggest that increasing the chain length of the substituents on the coordinated tertiary amine, the complex would be prone to lose one of the two groups on the nitrogen, generating a tethered chain which contains a secondary

amine. This side reaction could potentially be avoided by introducing two electron-withdrawing groups on the coordinated amine, which would disfavour the formation of the iminium ion, decreasing the rate of this hydrogen transfer side reaction (Scheme 66).

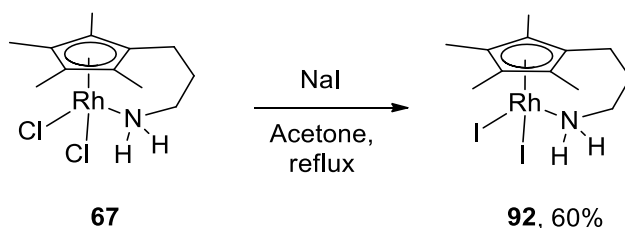
Scheme 66



3.5 Modification of Rhodium(III) Complex 67: Iodide as Halide ligand

After the modification of the length of the side chain and the substituents on the nitrogen of catalyst **67**, we decided to modify the halide ligand; treatment of **67** with sodium iodide in acetone gave the corresponding complex **92** in good yield *via* a salt metathesis reaction (Scheme 67). The complex was characterised by NMR spectroscopy, elemental analysis and HRMS.

Scheme 67

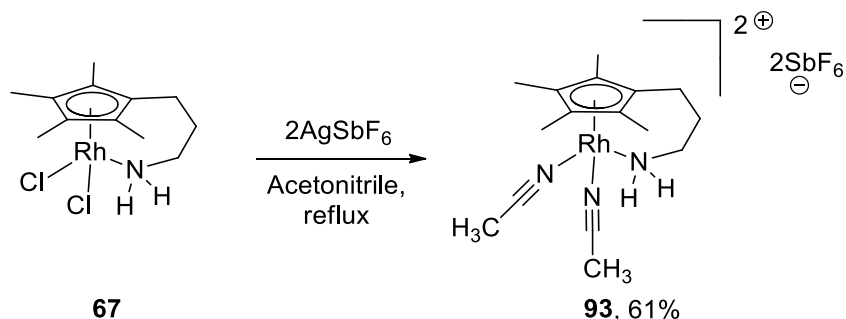


3.6 Modification of Rhodium(III) Complex 67: Dicationic Rhodium Monomer

To complete the possible modifications of complex **67**, the cationic version of compound **67** has been synthesised, treating the complex with 2 equivalents of silver

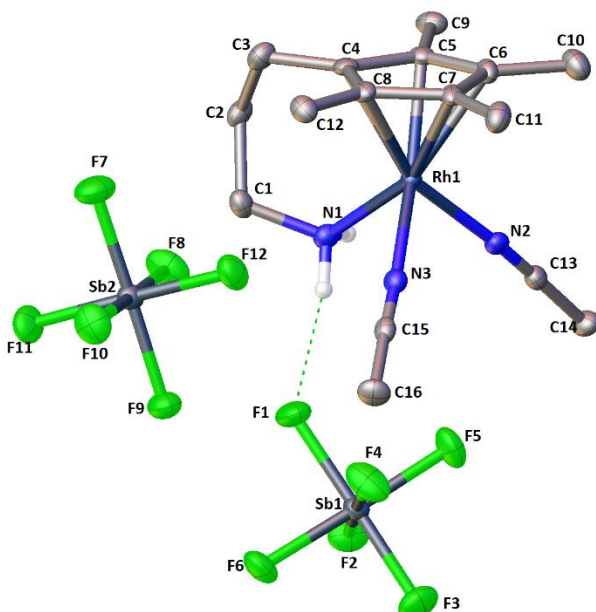
hexafluoroantimonate in acetonitrile. The cationic rhodium(III) complex **93** was isolated in 61% yield (Scheme 68).

Scheme 68



The monomer **93** was characterised by NMR spectroscopy, elemental analysis and HRMS. The structure has also been confirmed by X-ray crystallography, after growing diffraction-quality crystals as light orange prisms from slow evaporation of acetonitrile-diethyl ether ($v/v = 1/2$) (Figure 22). The complex crystallised monoclinic, space group $P2_1/n$. The hydrogen atoms, except those on the protic amine, have been omitted for clarity. Displacement ellipsoids are at the 50% probability level. Figure 22 shows the hydrogen bond between the proton on the coordinated amine and a fluorine atom of one hexafluoroantimonate ion.

Figure 22



Molecular structure of complex **93**

Table 4 reports the relevant bond lengths and angles for this complex.

Table 4

<i>Bond and Angle</i>	<i>Length (Å) and Angle (°)</i>
Range C _q (ring)-Rh1	2.129(4) to 2.182(4)
C4-Rh1	2.130(4)
Ring centroid-Rh1	1.764
N1-Rh1	2.134(3)
N2-Rh1	2.094(3)
N3-Rh1	2.121(3)
F1-N1	2.969(4)
N1-Rh1-C4	93.84(13)

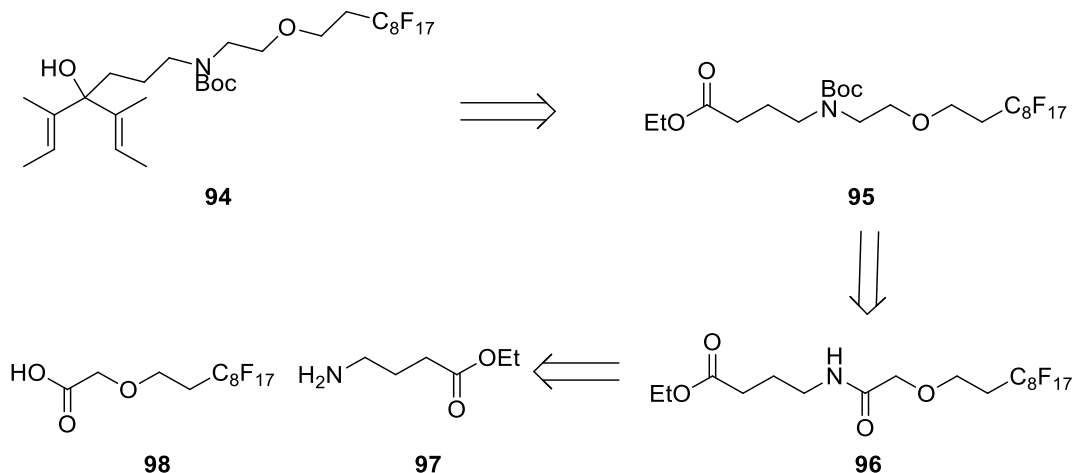
The characteristic bond lengths and angles of complex **93** were compared with those of neutral monomer **67**. The distance between the ring centroid and the metal is shorter in complex **93** than in **67** (respectively, 1.764 Å and 1.781 Å). The angle between N1-Rh-C4 in complex **93** is slightly more acute than the corresponding angle in **67** (93.84(13) for **93** and 94.54(10) for **67**). The distance from the nitrogen in the tethered chain and the metal is similar (2.134(3) Å and 2.139(3) Å), whereas the two nitrogens of the acetonitrile form a shorter bond with the rhodium than the two chlorides in complex **67** (2.121(3) Å and 2.094(3) Å instead of 2.439(1) Å and 2.441(1) Å). Since nitrogen is smaller than a chloride, it could get closer to the rhodium forming a stronger bond with the metal.

3.7 Modification of Rhodium(III) Complex 67: Synthesis of Monomer containing a Fluorous Tag

In the literature, some examples of immobilised fluorous tagged catalysts for enantioselective Diels-Alder reactions, asymmetric reduction of ketones and cross-coupling reactions are reported.^{74,75,76} These supported catalysts usually show comparable yields to the corresponding free catalysts and they can be easily recovered by fluorous solid-phase extraction⁷⁷ with good purity. After a screening of a few synthetic routes to synthesise a diene with a fluorous tag in the side chain, we developed the following retrosynthetic approach to synthesise ligand precursor **94** (Scheme 69). The

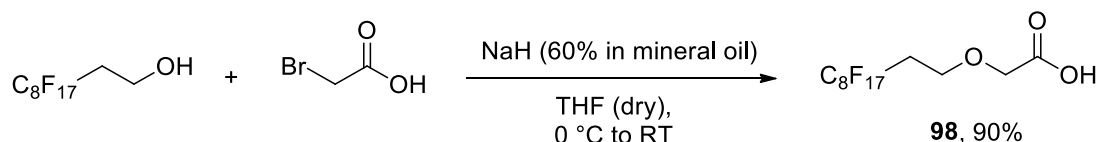
fluorous tag, which is separated from the active centre by a linker, was hypothesised to be inert in the catalytic cycle.⁷⁴

Scheme 69



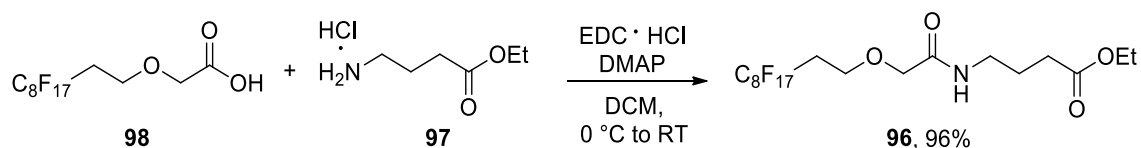
The diene **94** would be synthesised from the ester **95**, which could be synthesised from the reduction of amide **96**. This amide would be synthesised from the condensation between **97**, which is commercially available, and **98**, which could be made following the procedure reported in the literature by Smrcina *et al.*⁷⁸ Thus, the first step of this route was the synthesis of the linker, ether **98**, prepared in good yield from a reaction between bromoacetic acid and *1H,1H,2H,2H*-perfluorodecanol as shown in Scheme 70.

Scheme 70



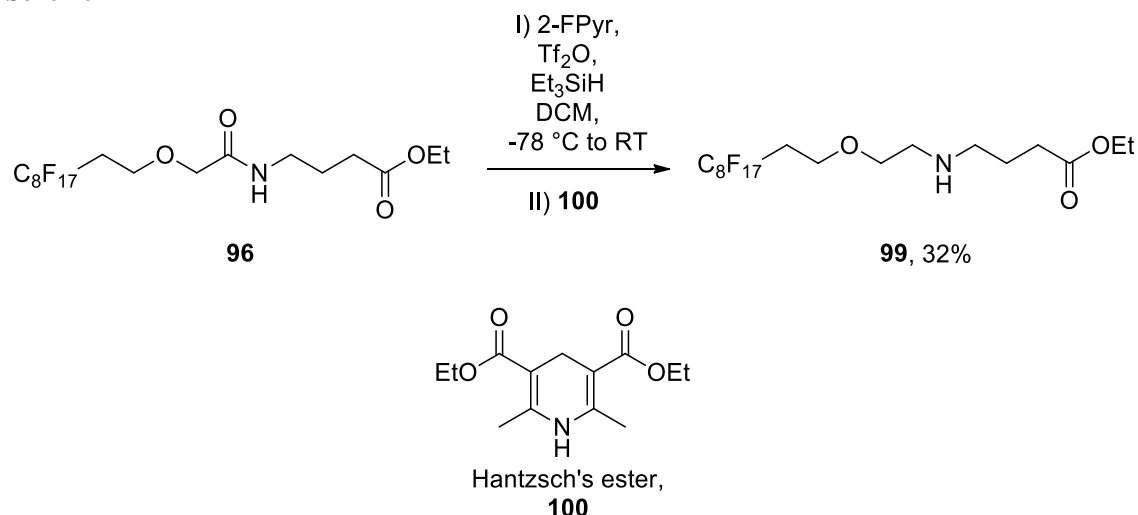
The next step was the synthesis of the amide **96**, which was obtained in excellent yield from the condensation between **98** and ethyl 4-aminobutanoate hydrochloride **97** (Scheme 71).

Scheme 71



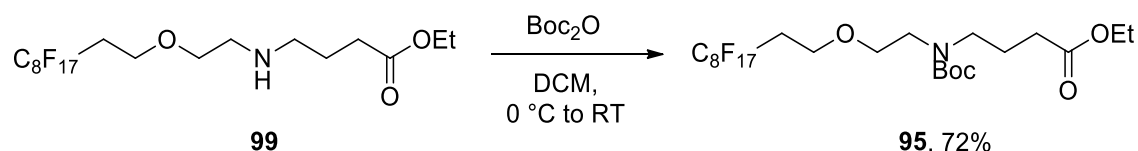
The reduction of the amide in the presence of the ester was more challenging. The first attempt was to use the borane·THF complex following the procedure for the selective reduction of amides reported by Brown *et al.*⁷⁹ Unfortunately, this procedure produced amine **99** in very moderate yield (9%). Depending on the equivalents of borane used (excess or stoichiometric), the main side products for this reaction were the fully reduced compound or the unreacted starting material. The next attempt was to follow the procedure reported by Charette and co-workers in which they selectively reduced secondary amides in the presence of esters.⁸⁰ The first step of their procedure was the reduction of the amide to the imine using trifluoromethanesulfonic anhydride and triethylsilane, followed by the *in situ* addition of Hantzsch's ester **100**, which gave the amine **99** in higher yield (Scheme 72).

Scheme 72



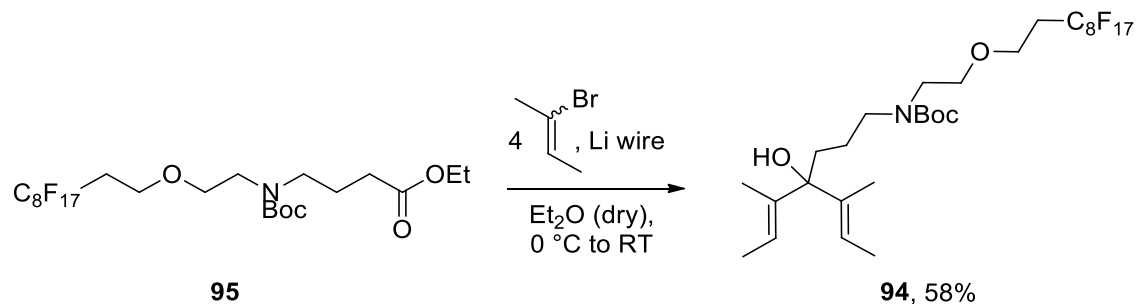
The amine was protected with a Boc group in 72% yield (Scheme 73).

Scheme 73



Finally, the diene **94** was synthesised by reacting the ester **95** with 4 equivalents of the organolithium generated *in situ* from the reaction between lithium wire and 2-bromo-2-butene (Scheme 74).

Scheme 74



For this substrate, the double alkenylation was less efficient, probably because ester **95** was less reactive than those used previously. Therefore, 4 equivalents of organolithium were necessary to afford the product, because only the unreacted starting material was observed when 2 equivalents were used.

The reaction between the diene **94** and rhodium trichloride hydrate gave the corresponding monomer **101** in moderate yield. This complex has been characterised by NMR spectroscopy and elemental analysis (Scheme 75).

Scheme 75

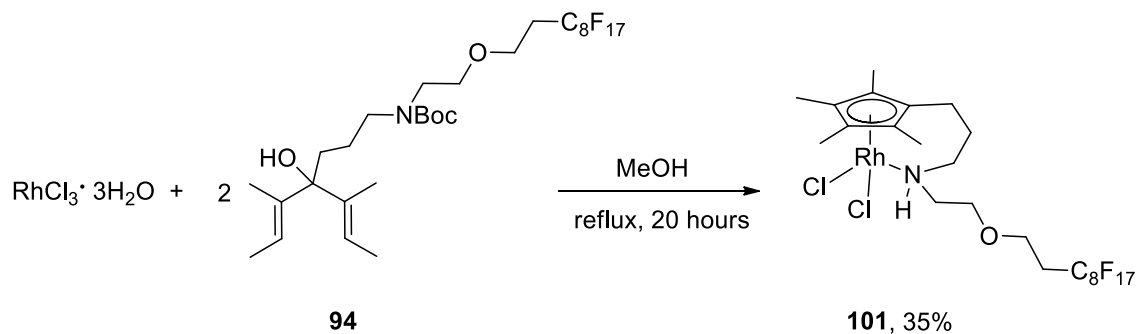
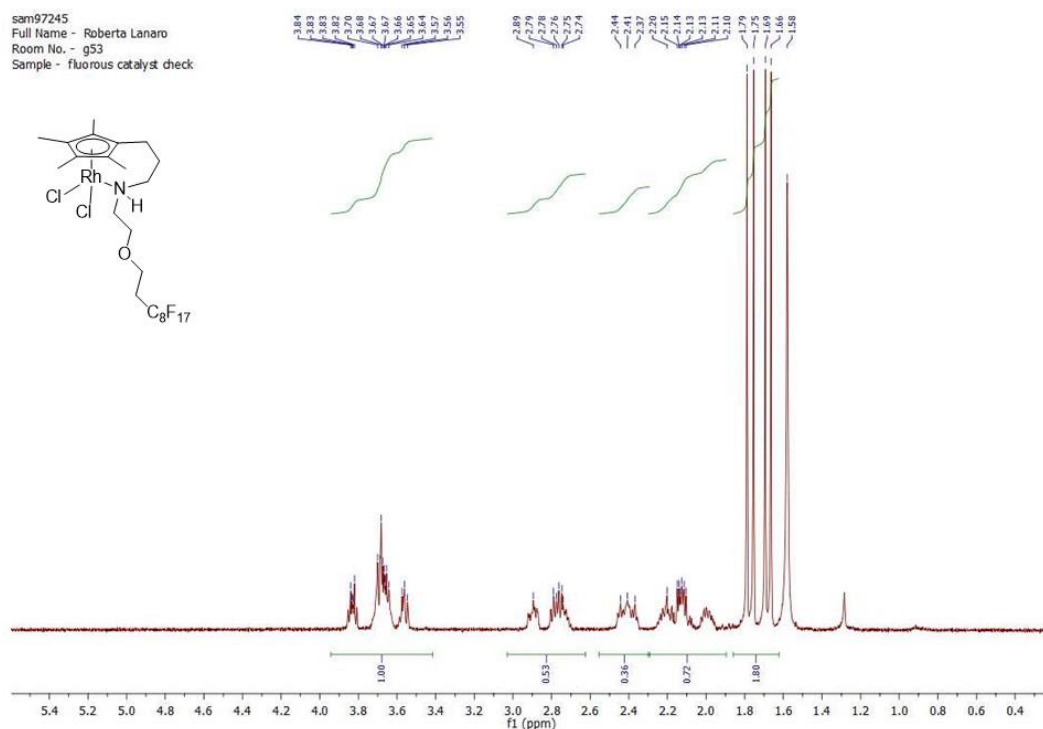


Figure 23 shows the ^1H -NMR spectrum of complex **101**. The protons in the side chain and next to the nitrogen are diastereotopic, as well as the methyl groups in the Cp*-derived ring, which appear as four different singlets. This diastereotopicity is due to the asymmetric centre on the coordinated nitrogen, similarly to complex **75**.

Figure 23

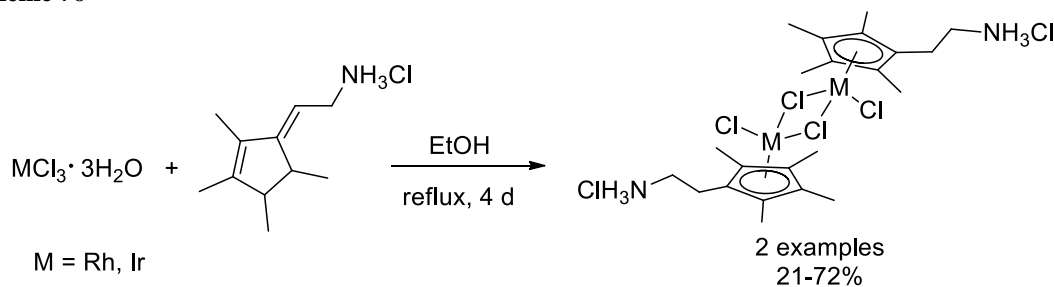


The ^1H -NMR spectrum was recorded in deuterated chloroform using a 500 MHz Bruker spectrometer.

3.8 Synthesis of New Monomeric Iridium(III) Complexes

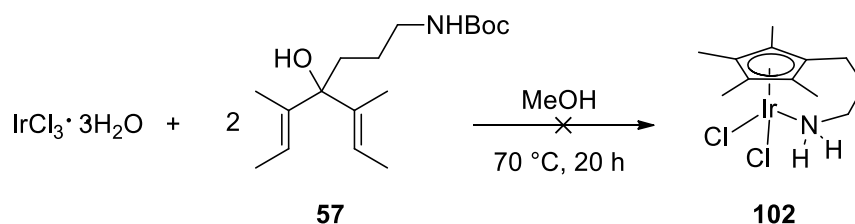
Despite rhodium and iridium complexes having several features in common (all of the compounds of Rh(III) and Ir(III) are diamagnetic and low-spin and both of them have a great affinity for ammonia and amines), rhodium complexes are easier to synthesise, since the formation of the corresponding iridium compounds is usually slow.⁶⁵ Eppinger and co-workers reported the synthesis of rhodium and iridium complexes with a functionalised Cp* bearing a pendant primary amine group (Scheme 76).⁸¹

Scheme 76



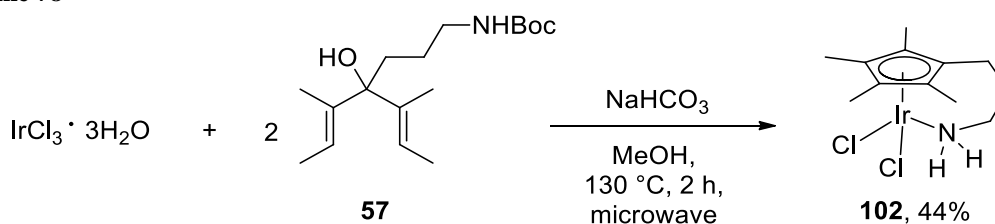
However, to the best of our knowledge, there are not examples in the literature of iridium complexes with a coordinated amine on the tethered chain of the cyclopentadienyl ligand. The first attempt to synthesise **102** using the procedure reported above for the rhodium complexes did not afford the desired iridium complex (Scheme 77), but a mixture of by-products.

Scheme 77



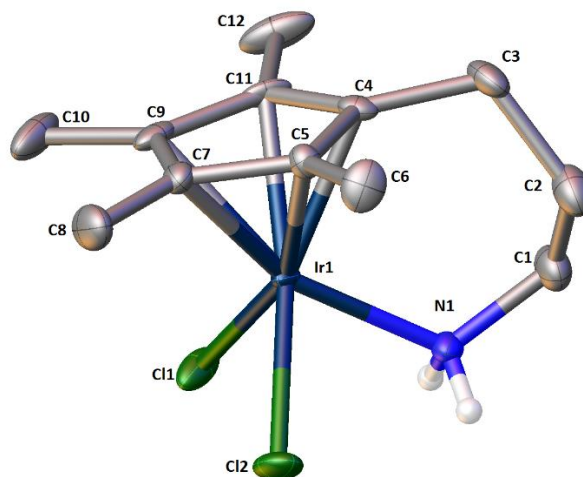
Changing the approach, iridium(III) complex **102** was synthesised in 44% yield by heating at $130\text{ }^\circ\text{C}$ in a microwave reactor containing 2 equivalents of diene **57** and 1 equivalent of iridium trichloride hydrate (Scheme 78).

Scheme 78



The structure of the complex has been confirmed by X-ray analysis, after growing orange diffraction-quality crystals by a slow recrystallization from dichloromethane-hexane ($v/v = 1/3$) (Figure 24). The complex crystallised monoclinic, space group $P2_1/n$. The hydrogen atoms, except those on the protic amine, have been omitted for clarity. Displacement ellipsoids are at the 50% probability level.

Figure 24



Molecular structure of complex **102**

Table 5 reports the relevant bond lengths and angles for this complex. The maximum difference in the bond lengths between the carbons of the Cp* and the metal is 0.054 Å, with the bond between the carbon in the tethered chain (C4) and iridium being the shortest. The length between the ring centroid and the metal is 1.775 Å.

Table 5

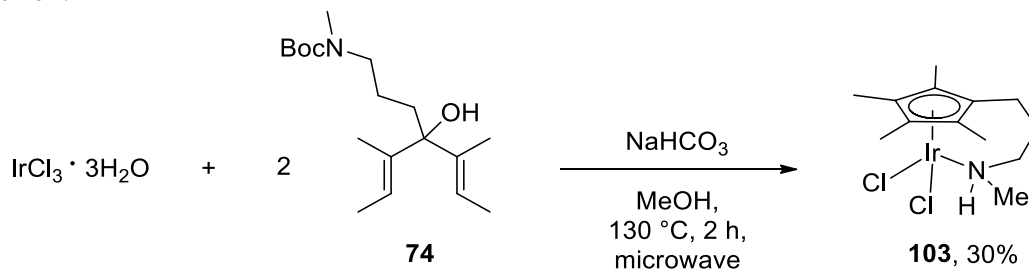
<i>Bond and Angle</i>	<i>Length (Å) and Angle (°)</i>
Range C _q (ring)-Ir1	2.141(3) to 2.195(4)
C4-Ir1	2.141(3)
Ring centroid-Ir1	1.775
N1-Ir1	2.138(3)
Cl1-Ir1	2.429(1)
Cl2-Ir1	2.440(9)
N1-Ir1-C4	95.50(11)

Unfortunately, reactions between the iridium trichloride hydrate and dienes **54** and **60** using the same microwave conditions did not afford the corresponding complexes, which confirms that the length of **57** gave the most easily formed rhodium and iridium complexes.

3.9 Modification of Iridium(III) Complex 102: Secondary Amine

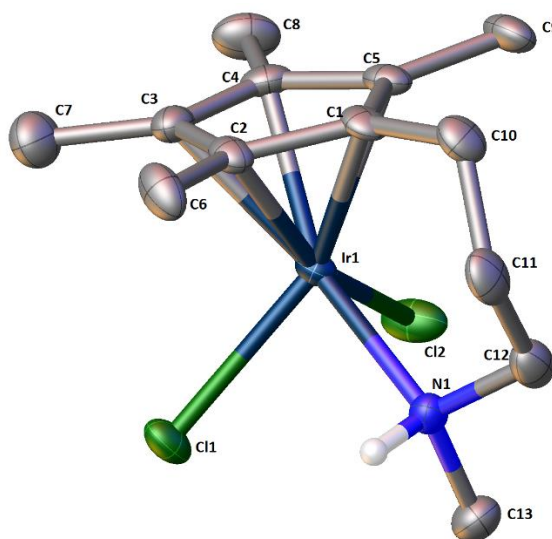
Using 2 equivalents of **74**, iridium(III) complex **103** bearing a secondary amine in the side chain could be synthesised in a microwave reactor (Scheme 79).

Scheme 79



The structure of this complex has been confirmed by X-ray crystallography, after growing yellow diffraction-quality crystals by slow recrystallization from dichloromethane (Figure 25). The complex crystallised monoclinic, space group $P2_1/c$. The hydrogen atoms, except those on the protic amine, have been omitted for clarity. Displacement ellipsoids are at the 50% probability level.

Figure 25



Molecular structure of complex **103**

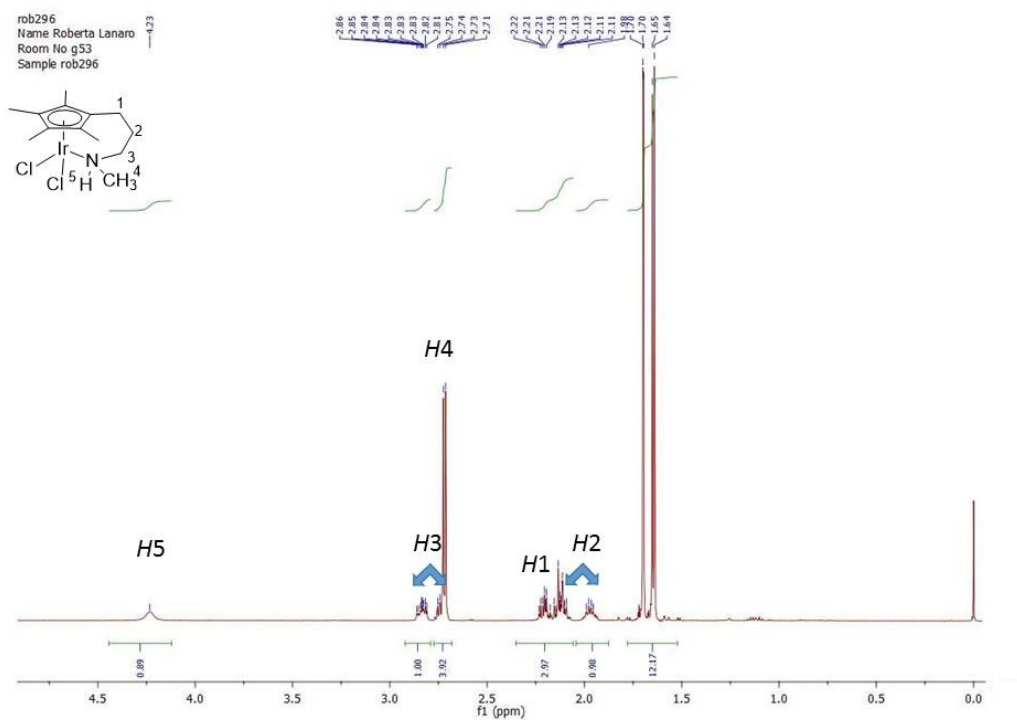
Table 6 reports the relevant bond lengths and angles for this complex.

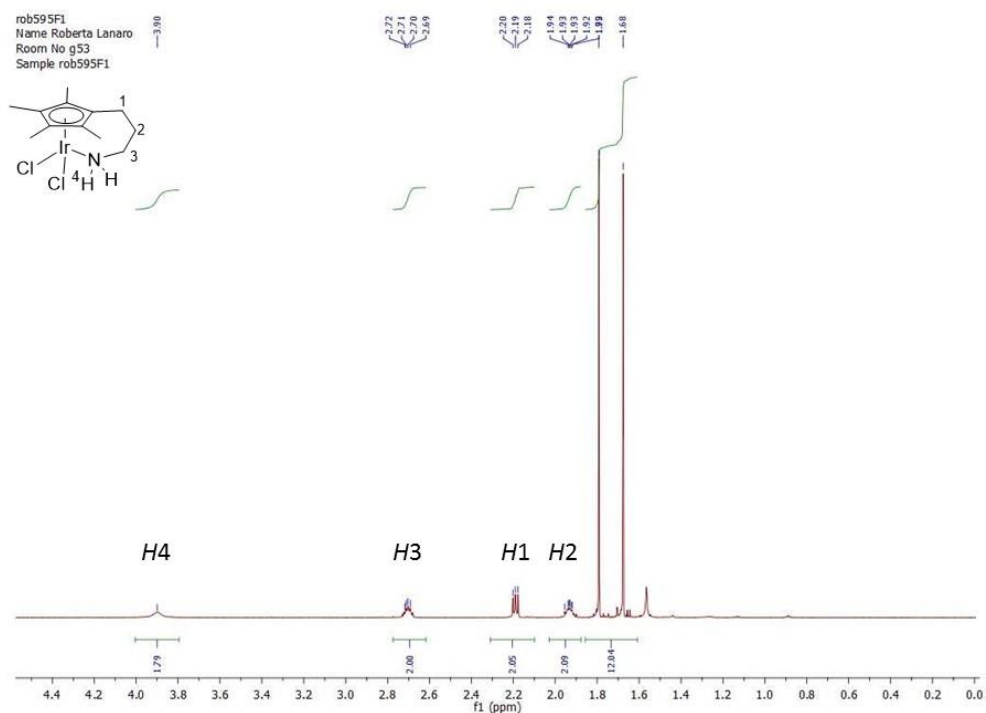
Table 6

Bond and Angle	Length (Å) and Angle (°)
Range C _q (ring)-Ir1	2.156(5) to 2.187(7)
C1-Ir1	2.162(5)
Ring centroid-Ir1	1.783
N1-Ir1	2.179(4)
Cl1-Ir1	2.445(1)
Cl2-Ir1	2.436(2)
N1-Ir1-C1	95.15(16)

The relevant lengths of bonds and the angles were compared with those reported in Table 5 for complex **102**. Monomer **103** possesses similar bond lengths and angles to **102**. The main difference is the length of the bond between the nitrogen and the metal, which is greater in **103** (respectively, 2.179(4) Å and 2.138(3) Å for **103** and **102**), similarly to what was observed previously with rhodium complexes **67** and **75**.

Figure 26 shows a comparison of the ¹H-NMR spectra of complexes **102** and **103**.

Figure 26



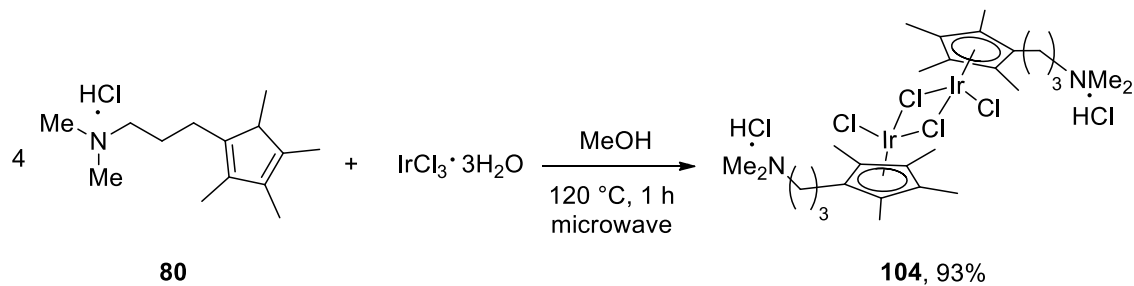
The ¹H-NMR spectra were recorded in deuterated chloroform using a 500 MHz Bruker spectrometer.

The protons of the side chain (*H1*, *H2* and *H3* in Figure 26) and of the methyl groups of the Cp*-derived ring in the complex **103** are diastereotopic, due to the asymmetric centre on the nitrogen, similarly to rhodium complex **75**. Again, the methyl group on the amine appears as a doublet, because it is coupled to the hydrogen on the coordinated amine.

3.10 Modification of Iridium(III) Complex 102: Tertiary Amine

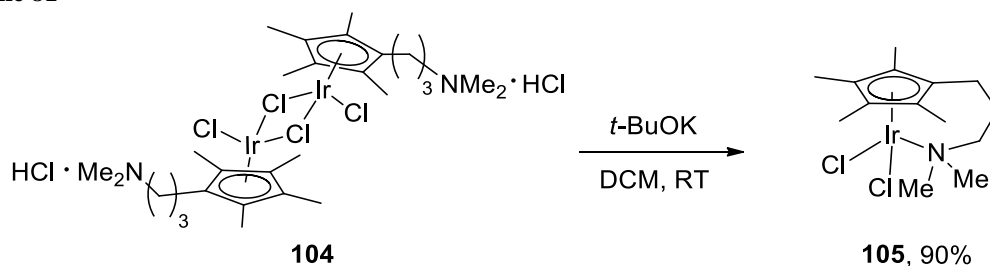
To complete the synthesis of modified iridium complexes bearing different substituents on the coordinated amine, the reaction between iridium trichloride hydrate and 4 equivalents of diene **80** in dry methanol gave iridium(III) dimer **104** in 93% yield (Scheme 80). In this case, the reaction with 2 equivalents of **80** did not afford the desired compound and only unreacted starting materials were observed by crude ¹H-NMR.

Scheme 80



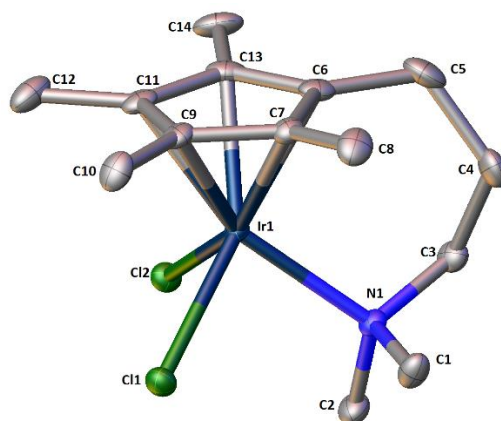
Dimer **104** was characterised by NMR spectroscopy, elemental analysis and HRMS. The same procedure reported above to synthesise the monomeric rhodium complex **79** was used here starting with the iridium dimer **104**; its treatment with 2 equivalents of potassium *tert*-butoxide in dichloromethane gave the desired monomer **105** in good yield, as shown in Scheme 81.

Scheme 81



The structure of **105** has been confirmed by X-ray crystallography, after growing orange diffraction-quality crystals by slow recrystallization from dichloromethane-hexane (*v/v* = 1/1) (Figure 27).

Figure 27



Molecular structure of complex **105**

The complex crystallised orthorhombic, space group $Pca2_1$. The hydrogen atoms have been omitted for clarity. Displacement ellipsoids are at the 50% probability level.

Table 7 reports the relevant bond lengths and angles for this complex. The lengths of bonds and the angles were compared with those reported in Table 5 and Table 6 for complexes **102** and **103**. Among these three monomers, **105** contains the longest bond length between the nitrogen and the metal (2.196(3) Å), suggesting that the coordination between the tertiary amine and the iridium is the weakest among the three. The length between the carbon in the tethered chain (C6) and iridium is the shortest among the five carbon-iridium bonds (2.142(3) Å), similarly to complex **102**. Comparable results have been observed among the corresponding three rhodium complexes **67**, **75** and **79**.

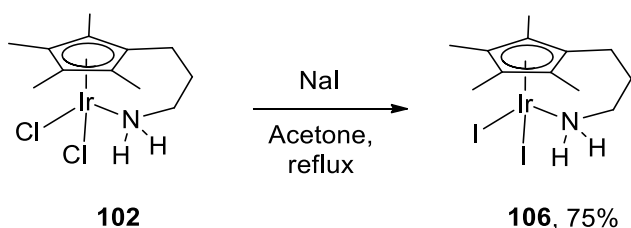
Table 7

<i>Bond and Angle</i>	<i>Length (Å) and Angle (°)</i>
Range C _q (ring)-Ir1	2.142(3) to 2.165(4)
C6-Ir1	2.142(3)
Ring centroid-Ir1	1.768
N1-Ir1	2.196(3)
Cl1-Ir1	2.409(1)
Cl2-Ir1	2.418(1)
N1-Ir1-C6	95.93(11)

3.11 Modification of Iridium(III) Complexes 102 and 105: Iodide as Halide Ligand

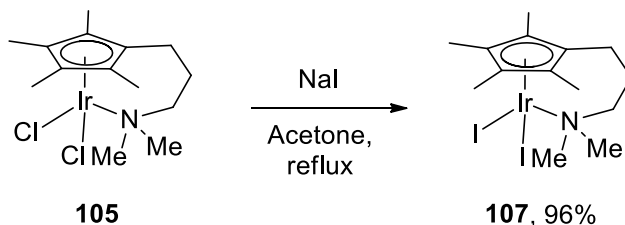
Following the procedure already presented above, the reaction between complex **102** and sodium iodide in acetone gave the corresponding diiodide iridium monomer **106** in good yield (Scheme 82). The complex was characterised by NMR spectroscopy, elemental analysis and HRMS.

Scheme 82



Following the same procedure, the halide ligands of complex **105** have been modified to achieve the corresponding diiodide iridium monomer **107** in 96% yield (Scheme 83).

Scheme 83



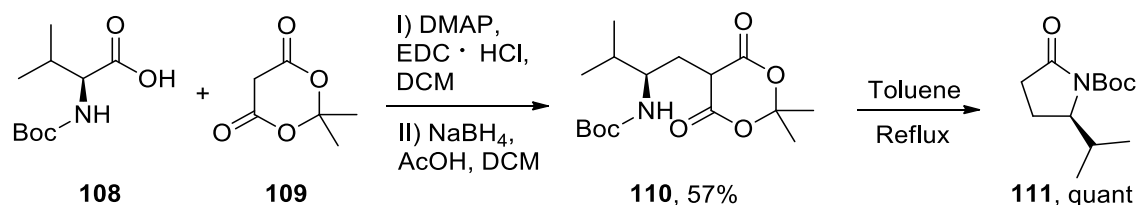
Complex **107** was characterised by NMR spectroscopy, elemental analysis and HRMS.

3.12 Modification of Iridium(III) Complex 102: Chiral Iridium Complexes

The work presented in this section (3.12) has been carried out in collaboration with Ashley Thompson, an MChem project student in our group. After the first synthesis of complex **113**, Ashley Thompson repeated and optimised the following synthetic route.

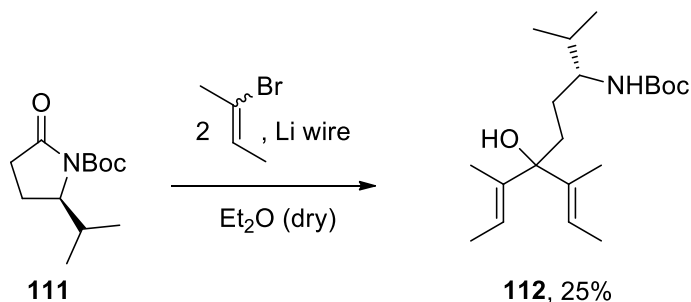
The structure of iridium complex **102** is interesting, because a chiral centre on the carbon next to the nitrogen could be easily inserted starting with enantiopure amino acids. Beginning with *N*-Boc-L-valine **108**, (*R*)-*N*-*t*-butoxycarbonyl-5-isopropyl-2-pyrrolidinone **111** has been synthesised following the procedure reported in the literature by Eissenstat *et al.*⁷⁸, as shown in Scheme 84.

Scheme 84



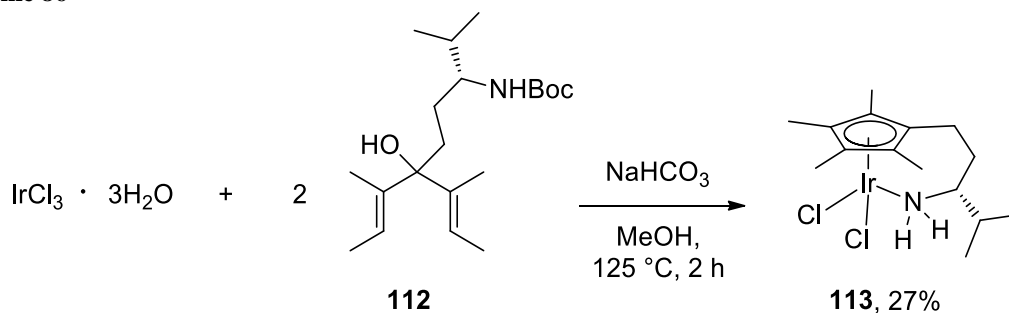
Diene **112** was synthesised with a double alkenylation of **111** with 2 equivalents of 2-lithium-2-butene generated *in situ* from the reaction between lithium wire and 2-bromo-2-butene (Scheme 85).

Scheme 85



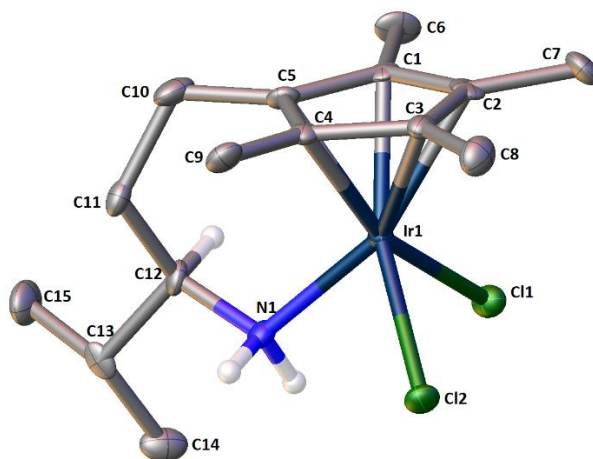
The reaction between 2 equivalents of diene **112** and iridium trichloride hydrate gave the corresponding iridium monomer **113** in 27% yield as shown in Scheme 86. This complex was characterised by NMR spectroscopy and elemental analysis.

Scheme 86



The structure has also been confirmed by X-ray crystallography, after growing yellow diffraction-quality prisms by slow recrystallization from dichloromethane-hexane (*v/v* = 1/3) (Figure 28). The complex crystallised orthorhombic, space group *Pca2*₁. The hydrogen atoms, except those on the protic amine and in the stereocentre, have been omitted for clarity. Displacement ellipsoids are at the 50% probability level.

Figure 28



Molecular structure of complex **113**

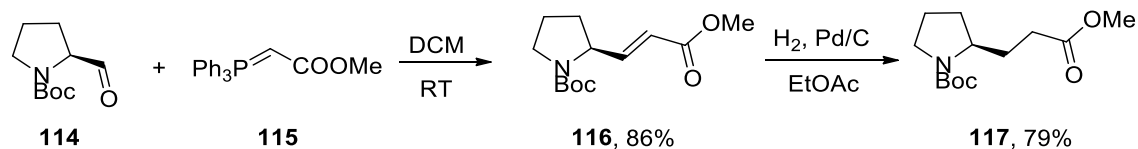
Table 8 reports the relevant bond lengths and angles for this complex.

Table 8

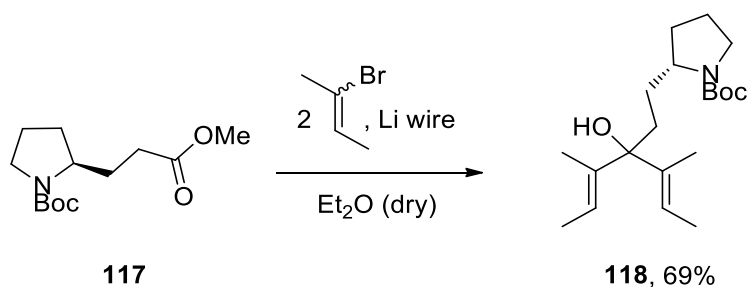
<i>Bond and Angle</i>	<i>Length (Å) and Angle (°)</i>
Range C _q (ring)-Ir1	2.117(6) to 2.175(7)
C5-Ir1	2.117(6)
Ring centroid-Ir1	1.761
N1-Ir1	2.119(5)
Cl1-Ir1	2.428(2)
Cl2-Ir1	2.406(2)
N1-Ir1-C5	94.6(2)

The lengths of the bonds and the angles were compared to those reported previously for complex **102**. Between these two complexes, **113** possessed the shortest bond length between the carbon in the tethered chain (C5) and the iridium (2.117(6) Å for **113** and 2.141(3) Å for **102**). The angle between N1-Ir-C5 in complex **113** was slightly more acute than the corresponding one in **102** (respectively, 94.6(2) and 95.50(11) for **113** and **102**).

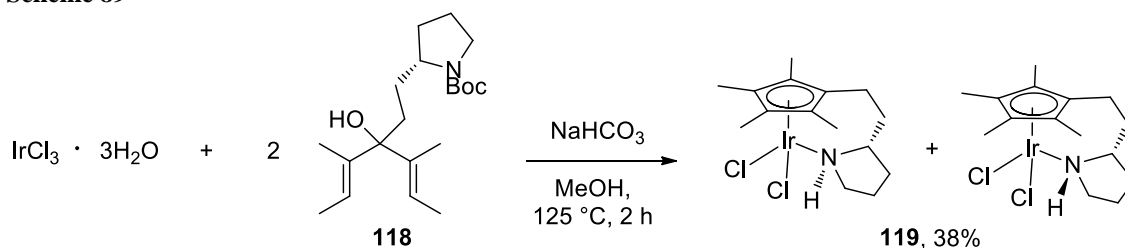
A similar complex was synthesised by Ashley Thompson, starting with the *N*-Boc-prolinal **114**. The first steps were a Wittig reaction to isolate the conjugate ester **116** in 86% yield and the hydrogenation of the double bond, which afforded **117** in 79% yield (Scheme 87), following the general procedure reported in the literature.⁸²

Scheme 87

Diene **118** was synthesised in 69% yield with a double alkenylation of **117** with 2 equivalents of 2-lithium-2-butene generated *in situ* from the reaction between lithium wire and 2-bromo-2-butene (Scheme 88).

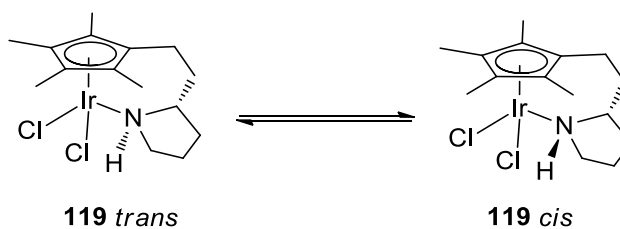
Scheme 88

Reaction between 2 equivalents of diene **118** and iridium trichloride hydrate gave the corresponding iridium monomer **119** in 38% yield (Scheme 89). This complex was isolated as a mixture of two diastereoisomers.

Scheme 89

A high temperature ^1H -NMR spectrum was run in deuterated acetonitrile to see if these two diastereoisomers could be interconverted in solution. Potentially, if one of the two was more stable than the other, it would be possible to isolate one pure diastereoisomer (Figure 29).

Figure 29

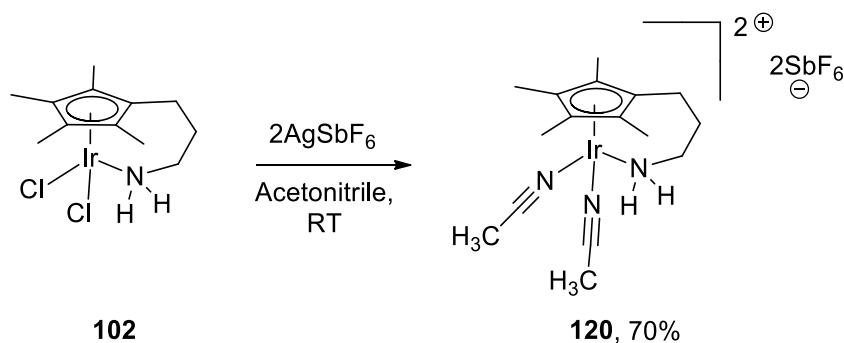


Disappointingly, the $^1\text{H-NMR}$ spectrum did not change, which suggests that the two diastereoisomers were not interconverting. Thus, complex **119** was used without any other purification as a mixture of two diastereoisomers.

3.13 Modification of Iridium(III) Complex 102: Dicationic Iridium Complexes

To complete the possible modifications of complex **102**, two dicationic monomers were synthesised. In the first example, the same procedure reported above to synthesise the dicationic monomeric rhodium complex **93** was used here, treating the complex **102** with 2 equivalents of silver hexafluoroantimonate in acetonitrile. The cationic iridium(III) complex **120** was isolated in 70% yield (Scheme 90).

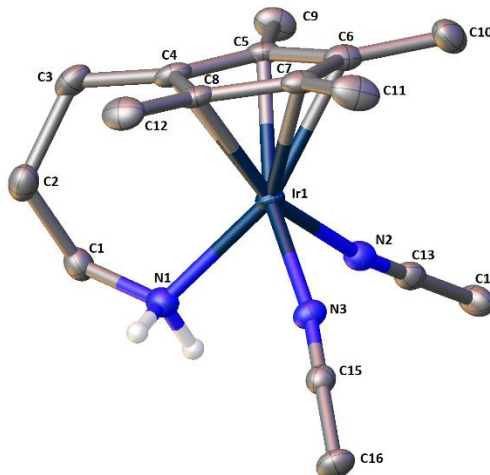
Scheme 90



Compound **120** was characterised by NMR spectroscopy, elemental analysis and HRMS. The structure has been also confirmed by X-ray crystallography, after growing diffraction-quality crystals as colourless plates from slow evaporation of acetonitrile-diethyl ether ($v/v = 1/4$) (Figure 30). The complex crystallised monoclinic, space group $P2_1/n$. The hydrogen atoms, except those on the protic amine, and the two

counterions have been omitted for clarity. Displacement ellipsoids are at the 50% probability level.

Figure 30



Molecular structure of complex **120**

Table 9 reports the relevant bond lengths and angles for this complex.

Table 9

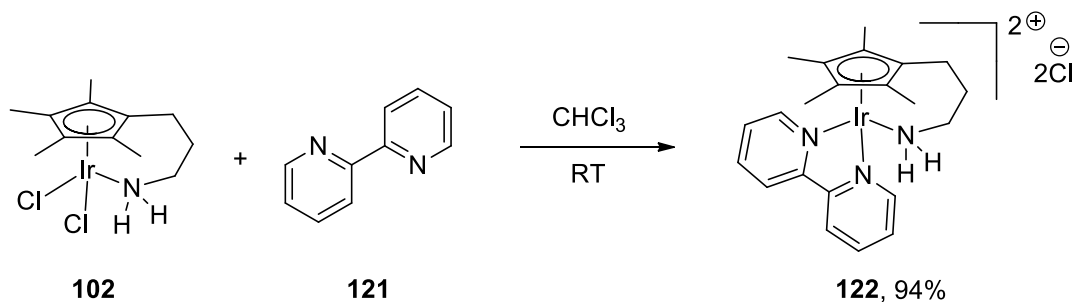
<i>Bond and Angle</i>	<i>Length (Å) and Angle (°)</i>
Range C _q (ring)-Ir1	2.137(4) to 2.181(3)
C4-Ir1	2.148(4)
Ring centroid-Ir1	1.773
N1-Ir1	2.131(3)
N2-Ir1	2.086(3)
N3-Ir1	2.068(3)
N1-Ir1-C4	94.47(13)

The relevant bond lengths and angles of complex **120** were compared with those of neutral monomer **102**. The distance between the nitrogen in the tethered chain and the metal is similar (2.131(3) Å and 2.138(3) Å), whereas the two nitrogens of the acetonitrile ligands form shorter bonds with the iridium than the two chlorides in complex **102** (2.086(3) Å and 2.068(3) Å for **120**, 2.429(1) Å and 2.440(9) Å for **102**). The angle between N1-Ir-C4 is more acute in this dicationic complex than in **102** (respectively,

94.47(13) and 95.50(11) for **120** and **102**). These results are similar to what was observed previously for the corresponding rhodium complexes **67** and **93**.

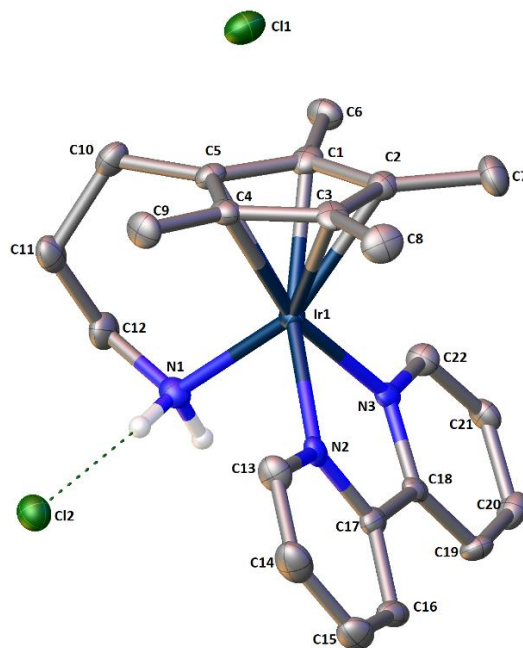
Finally, iridium monomer **102** was stirred with 1 equivalent of 2,2'-bipyridyl **121** to give the dicationic complex **122** in 94% yield (Scheme 91).

Scheme 91



The structure of this complex was characterised by NMR spectroscopy, HRMS and elemental analysis. This compound is slightly hygroscopic and the presence of water was observed both in the elemental analysis and in the crystal structure. Diffraction-quality crystals were grown as yellow prisms from a slow recrystallization in chloroform (Figure 31).

Figure 31



Molecular structure of complex **122**

The complex crystallised monoclinic, space group $P2_1/n$. The hydrogen atoms, except those on the protic amine, and the molecules of water have been omitted for clarity. Displacement ellipsoids are at the 50% probability level. The complex crystallised with 4 molecules of water in the asymmetric unit. Two chlorides were the corresponding counterions; one of them formed a hydrogen bond with the primary amine coordinated to the metal. Table 10 reports the relevant bond lengths and angles for this complex.

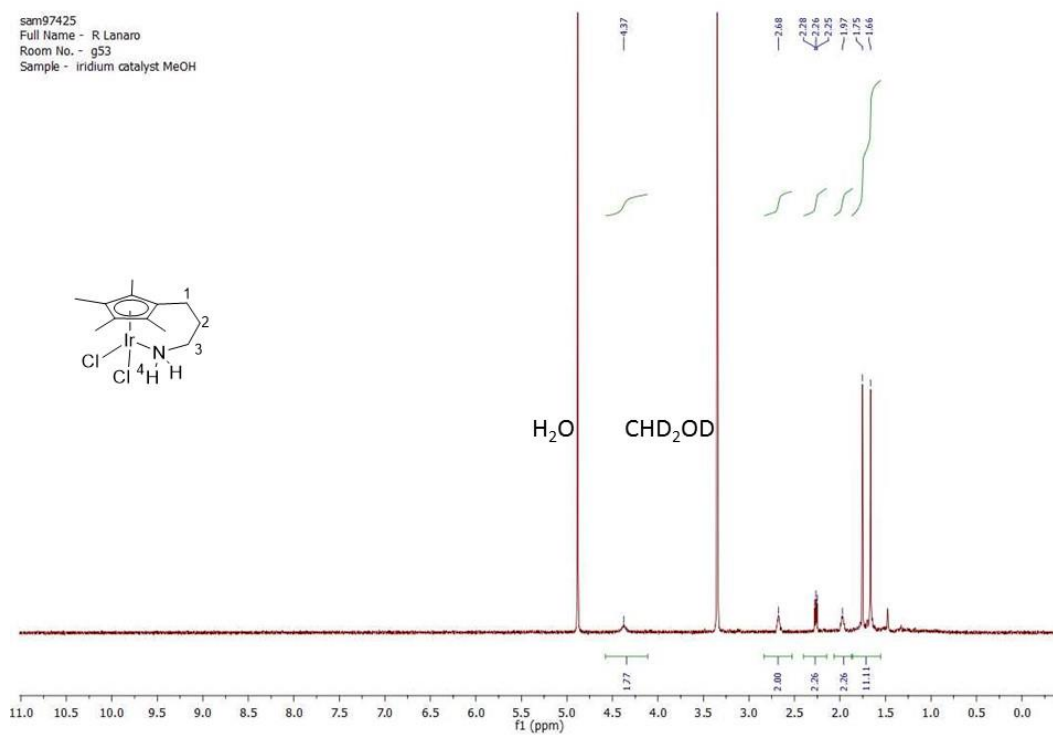
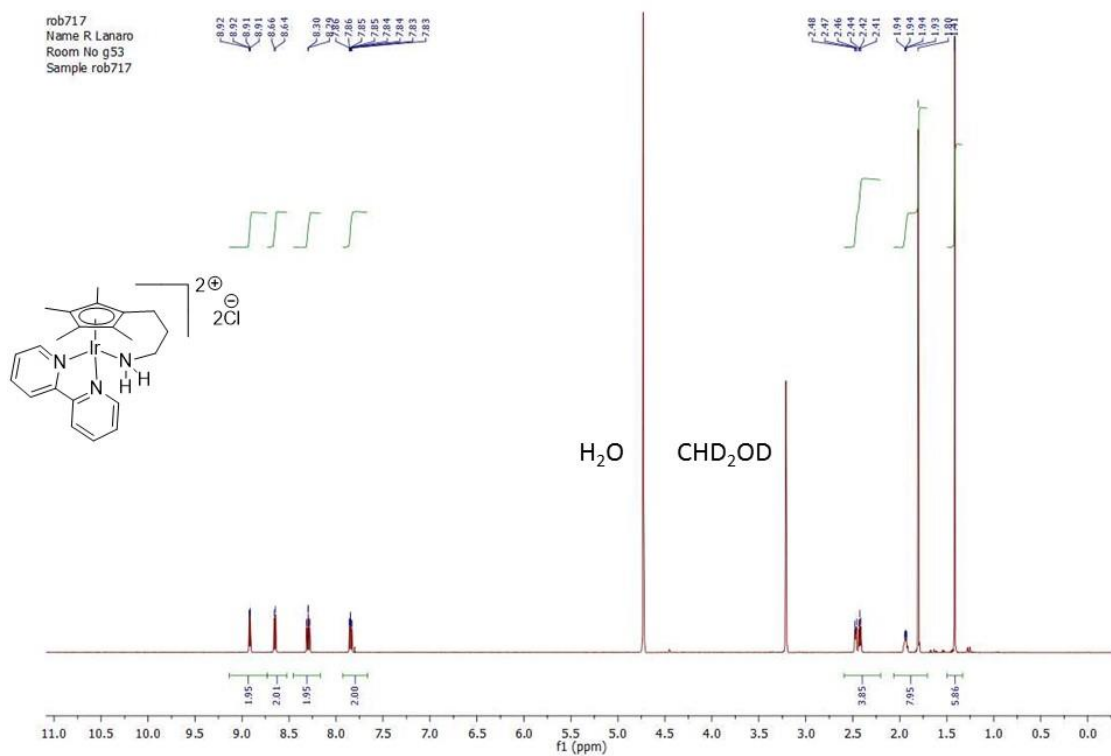
Table 10

<i>Bond and Angle</i>	<i>Length (Å) and Angle (°)</i>
Range C _q (ring)-Ir1	2.159(5) to 2.182(7)
C5-Ir1	2.169(5)
Ring centroid-Ir1	1.791
N1-Ir1	2.111(5)
N2-Ir1	2.082(4)
N3-Ir1	2.090(4)
N1-Cl2	3.214(5)
N1-Ir1-C5	93.24(18)

The lengths of bonds and the angles were compared with those reported in Table 5 for complex **102**. The three atoms of nitrogen in **122** are coordinated to the metal with shorter bonds than those observed in **102** between iridium and nitrogen and iridium and chlorides. The bond lengths between the carbon in the tethered chain (C5) and the metal, and between the ring centroid and the iridium, are greater in complex **122** than in **102** (respectively, 2.169(5) Å and 1.791 Å for **122**, 2.141(3) Å and 1.775 Å for **102**). The angle between N1-Ir-C5 is more acute in this dicationic complex than in **102** (93.24(18) and 95.50(11) for **122** and **102**). Comparing the angles of the two dicationic iridium complexes **120** and **122**, this monomer **122** has the most acute angle (93.24(18)).

To evaluate if complex **122** reconverted to the dichloride monomer **102** in solution, the ¹H-NMR spectra of complexes **122** and **102** in deuterated methanol were compared (Figure 32). The signals of the methyl groups in the Cp* and the protons in the tethered chain are significantly different in these two complexes, suggesting that **122** is stable when dissolved in methanol and it does not revert to the dichloride monomer **102**.

Figure 32



The ¹H-NMR spectra were recorded in deuterated methanol using a 500 MHz Bruker spectrometer.

3.14 Conclusions

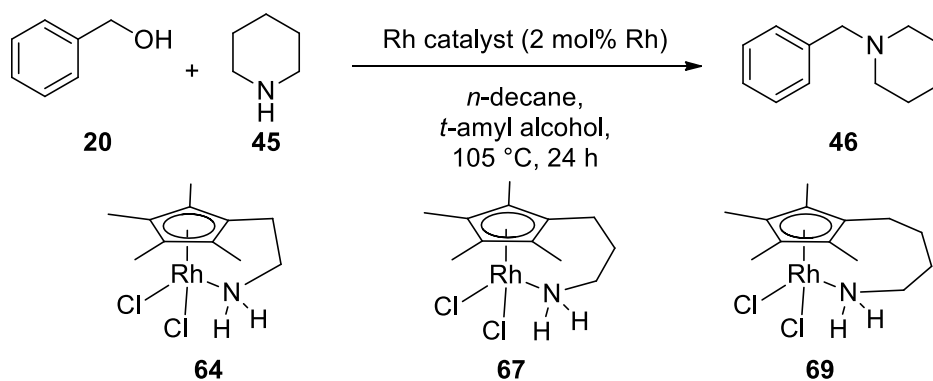
In conclusion, a new synthetic route to prepare *in situ* a new family of rhodium and iridium complexes has been developed. Nine rhodium monomeric complexes have been synthesised, of which seven have not been reported in the literature. The structure of four of these complexes was also confirmed by X-ray analysis. A family of nine new iridium complexes has also been prepared and six structures have been confirmed by X-ray analysis. The optimal length of the side chain for these monomers is that with three CH₂ units, which gave the highest yield in their syntheses. Complexes containing primary, secondary and tertiary amines have been synthesised with both rhodium and iridium metals. This family showed a great stability and, therefore, it has been possible to modify the halide ligands. The chlorides have been substituted with two iodides and dicationic complexes have been synthesised in good yields. The side chain in the catalysts has been modified in two different ways. The first modification was the introduction of a fluorous tag chain on the amine. These compounds could generally be recovered by fluorous solid-phase extraction.⁷⁷ The second modification was the introduction of a chiral centre in the side chain, starting from commercially available enantiopure amino acid derivatives. Two different chiral complexes have been synthesised, one containing a primary amine and the second one containing a secondary amine in the side chain. The catalytic activity of this family of rhodium and iridium complexes in hydrogen borrowing processes is reported in Chapters 4 and 5.

Chapter 4. Catalytic Activity of Rhodium and Iridium Complexes

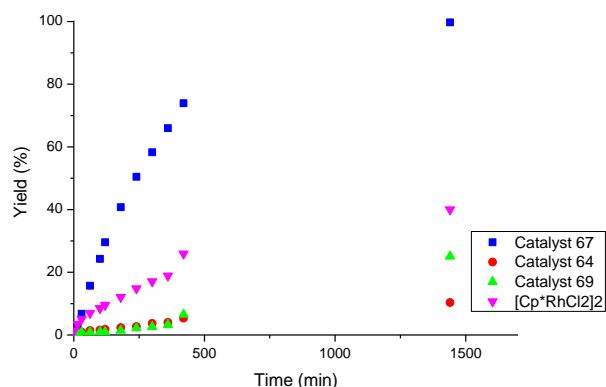
4.1 Activity of Rhodium Complexes with Respect to Length of Side Chain

After having synthesised the new family of complexes reported in the previous chapter, our next task was to test them in the hydrogen borrowing methodology. Our first aim was to investigate the effect of varying the length of the side chain in the catalyst activity. Using our standard reaction between benzyl alcohol and piperidine, with *n*-decane as an internal standard, 2 mol% of rhodium catalyst and *t*-amyl alcohol as solvent, the activities of complexes **64**, **67** and **69** were compared with that shown by the dimer $[\text{Cp}^*\text{RhCl}_2]_2$ (1 mol%, 2 mol% rhodium) (Graph 7).

Graph 7

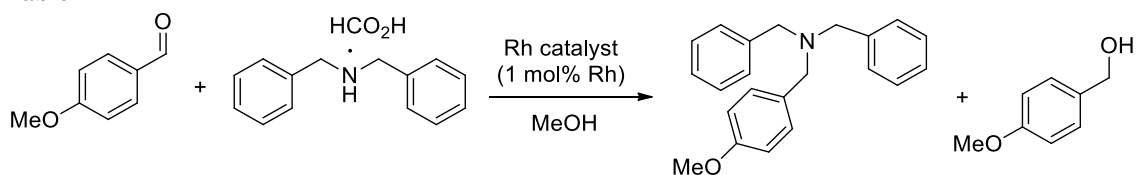


Graph 7



Pleasingly, catalyst **67** showed a faster reaction rate than the dimer $[\text{Cp}^*\text{RhCl}_2]_2$, achieving a 99% yield after 24 hours. Changing the length of the carbon chain did not help the activity of catalysts. Catalysts **64** and **69** were less active than the rhodium(III) dimer, achieving only a corresponding 10% and 25% yield after 24 hours. Therefore, the length of the side chain plays a relevant role in the activity of the catalysts, as well as in the synthesis of the complexes. A length of three CH_2 units in the side chain gave the optimal activity, whereas increasing or decreasing the number of carbons gave a less active complex. Besides, catalyst **67** showed a high level of activity which is not common for rhodium(III) complexes.^{1,4,63} These results are slightly discordant with those reported in the literature by Ito *et al.*⁷⁰ Effectively, the authors tested both complexes **64** and **67** in a transfer hydrogenation reaction between an aldehyde and an amine; the catalyst with the best selectivity for the formation of the alkylated amine was **64** (Table 11). On the contrary, catalyst **67** gave an almost 1 : 1 mixture of amine : alcohol.

Table 11



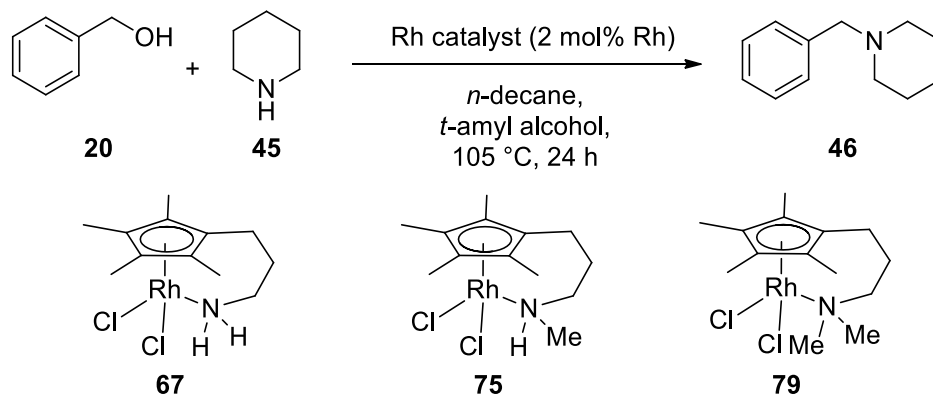
<i>Rh complex</i>	<i>Conversion (%)</i>	<i>amine : alcohol</i>
64	> 99%	96 : 4
67	> 99%	56 : 44

4.2 Activity of Rhodium Complexes with Respect to the Substitution on Tethered Amine

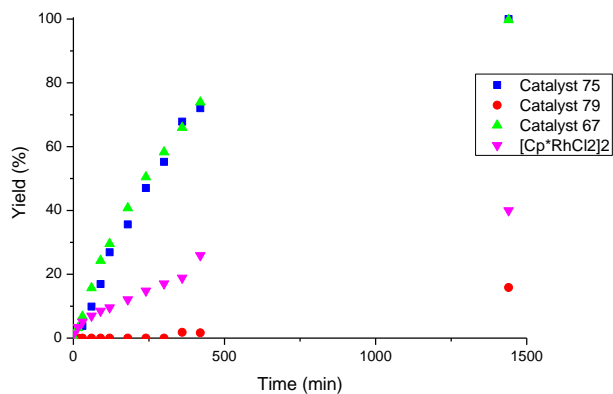
To evaluate the effect of having a substituent on the coordinated amine, the activities of complexes **75** and **79** were tested in our standard reaction between benzyl alcohol and piperidine and the results have been compared with the yield pathways achieved using complex **67** and rhodium dimer $[\text{Cp}^*\text{RhCl}_2]_2$ (Graph 8). The reaction profiles obtained using catalysts **67** and **75** were similar, suggesting that the presence of a secondary amine in the side chain did not influence the activity of the catalyst. However, a tertiary amine on the side chain gave a completely different reaction profile and a lower yield was

observed. Effectively, the activity of catalyst **79** was lower than both our catalysts **67** and **75** and the dimer $[\text{Cp}^*\text{RhCl}_2]_2$.

Graph 8



Graph 8



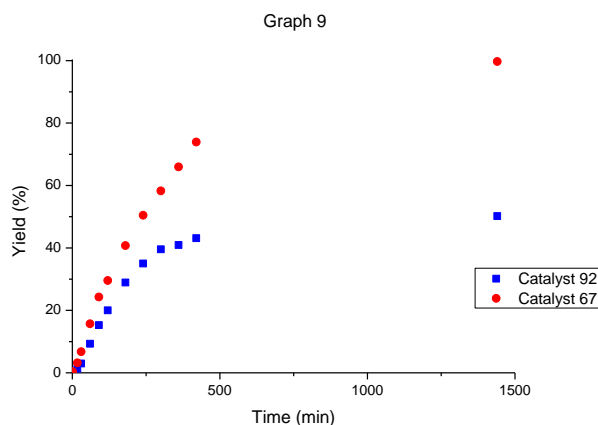
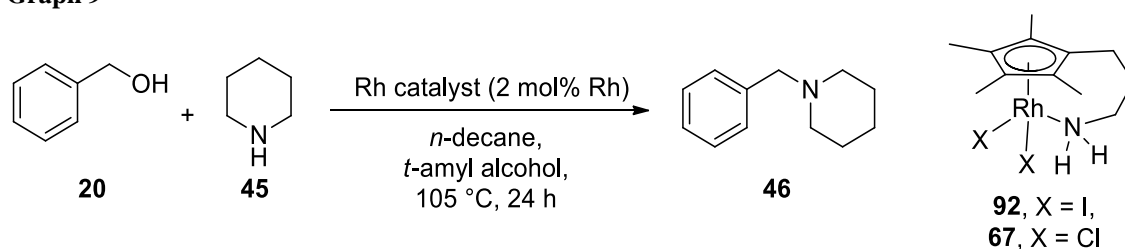
A semi-quantitative analysis of the initial rates of these catalysts gave an approximation of the observed rate constants. The observed rate constants were calculated plotting the logarithm of the benzyl alcohol vs. the time. The initial rates for catalysts **67** and **75** were similar (respectively, $k_{obs} = -0.0030$ for **67** and $k_{obs} = -0.0027$ for **75**) and both of them were three times as fast as the dimer $[\text{Cp}^*\text{RhCl}_2]_2$ ($k_{obs} = -0.0010$ for $[\text{Cp}^*\text{RhCl}_2]_2$). We considered these data as an approximation, because we extrapolated the rate constants plotting only the few collected data points which gave a yield between 0 and 15%.

These results suggest that the presence of at least one hydrogen in the side chain is necessary to achieve higher yields and faster reaction rates, confirming the importance of the N-H moiety in organometallic catalysis.⁶⁶

4.3 Activity of Rhodium Complexes with Respect to the Halide Ligands

Our next attempt was to evaluate the effect of the halogens on the metal. Thus, the activity of diiodide complex **92** has been tested in our standard reaction between benzyl alcohol and piperidine in *t*-amyl alcohol (Graph 9). These results have been compared with the reaction profile achieved using the catalyst **67**.

Graph 9

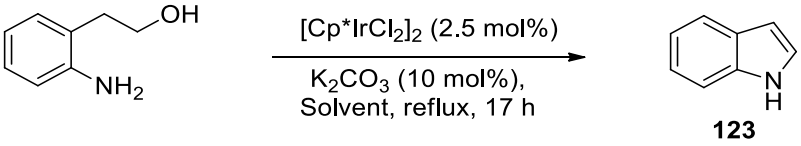


Graph 9 shows that, after 24 hours, the yield achieved using catalyst **67** is higher (99%) than the one obtained using the diiodide complex **92** (50%). Again, a semi-quantitative analysis of the initial rates of the two catalysts gave an approximation of the observed rate constants. The observed rate constants were calculated plotting the logarithm of the benzyl alcohol vs. the time. The initial rate for catalyst **67** was twice as fast as **92** (respectively, $k_{obs} = -0.0030$ for **67** and $k_{obs} = -0.0013$ for **92**). It was found that the best rhodium(III) catalyst in our new family was complex **67**, with a $(\text{CH}_2)_3\text{NH}_2$ unit in the side chain and chlorides as halide ligands, which has been used for further screening.

4.4 Solvent Tolerance and Catalyst Loading using Catalyst 67

After the determination of the most active rhodium(III) catalyst among this family, our next effort was to evaluate the activity of complex **67** in solvents other than *t*-amyl alcohol. One of the limitations of this methodology is that it is mainly carried out in non-polar solvent such as in toluene. When other organic solvents were tried, the yields dropped significantly, as reported in the literature by Fujita *et al.* (Table 12).⁵⁰

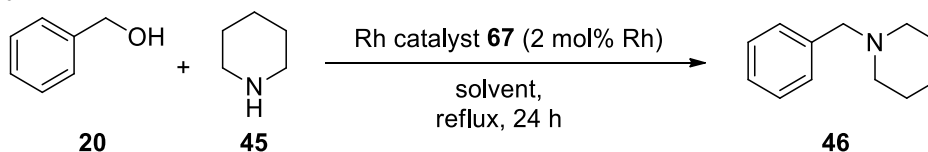
Table 12

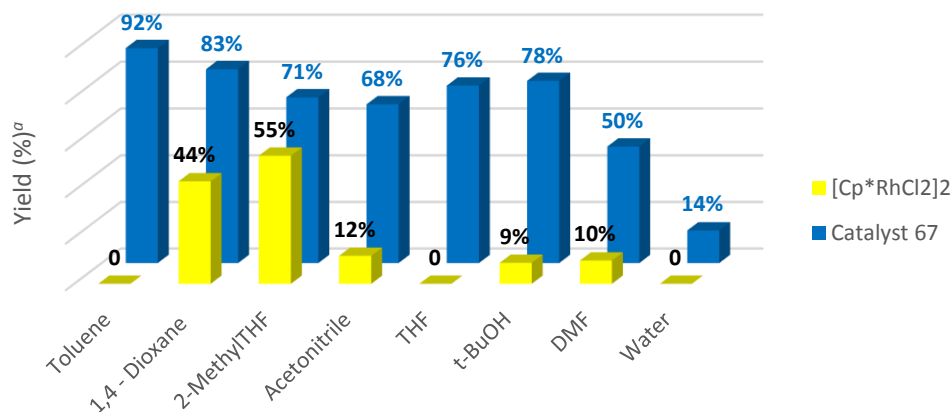


Entry	Solvent	Yield 123 (%)
1	Toluene	90
2	1,4-Dioxane	50
3	Acetonitrile	24

Since toluene is a non-polar solvent, polar substrates are usually not soluble in it. Some work has been done in this field. Williams and co-workers reported that the iridium dimer $[\text{Cp}^*\text{IrI}_2]_2$ (SCRAM) could promote the hydrogen borrowing processes in polar solvents, such as water and ionic liquids, as shown previously in Scheme 11.^{25,26} Limbach and co-workers developed and synthesised new half-sandwich complexes that showed a good activity both in water and in toluene (Scheme 14).³³ However, it would be useful to develop new systems that are working not only in toluene and water, but also in other organic solvents. Thus, catalyst **67** has been tested in several solvents and the conversions achieved have been compared to those obtained using the dimer $[\text{Cp}^*\text{RhCl}_2]_2$ (Graph 10).

Graph 10



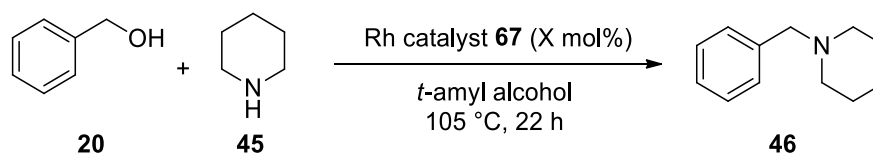


^a Conversion estimated by comparing the signal ratios of benzyl alcohol and *N*-benzylpiperidine in the crude ¹H-NMR spectrum.

Rhodium catalyst **67** showed great activity in a wide range of solvents. In all the entries, the conversions achieved were greater when catalyst **67** was used, which was particularly evident in the reactions carried out in THF and acetonitrile. Besides, the possibility to achieve good yields in non-polar solvents, such as toluene, and at the same time, in polar solvents, such as acetonitrile, *t*-amyl alcohol, *t*-butanol and DMF makes this catalyst really versatile and adaptable.

Using catalyst **67**, we analysed the catalyst loading for this reaction to evaluate the possibility of decreasing the amount of metal used, with economic and environmental advantages (Table 13). The results shown in this table suggest that the activity of the catalyst depended on the concentration of the reagents. Increasing the concentration, higher TONs were observed (entries 5 and 6) and good conversions (> 70%) could be achieved with a catalyst loading as low as 1 mol%.

Table 13



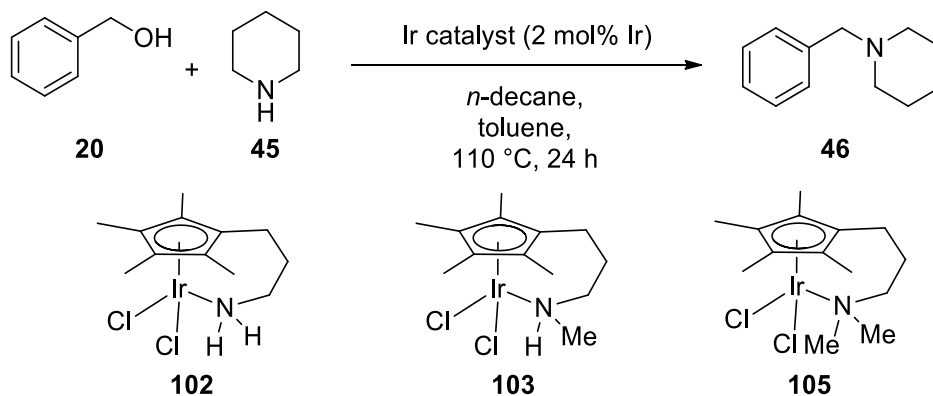
<i>Entry</i>	<i>[Alcohol]</i>	<i>X mol% Rh</i>	<i>Conversion (%)^a</i>	<i>TON</i>
1	0.8 M	2.0 mol%	55	27.5
2	1.4 M	2.0 mol%	90	45
3	1.4 M	1.5 mol%	85	63
4	1.4 M	1.0 mol%	61	61
5	2.2 M	1.0 mol%	70	70
6	3.3 M	1.0 mol%	73	73

^a Conversion estimated by comparing the signal ratios of benzyl alcohol and *N*-benzylpiperidine in the crude ¹H-NMR spectrum.

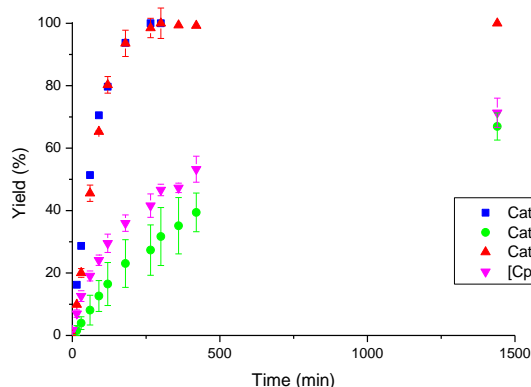
4.5 Activity of Iridium Complexes with Respect to the Substitution on Tethered Amine and with Respect to the Halide Ligands

Pleased with these good results, our next effort was to evaluate the activity of the corresponding iridium catalysts, particularly with respect to the substituents on the coordinated amine, to evaluate their behaviour in the reaction. Catalysts **102**, **103** and **105** were tested in the standard reaction between benzyl alcohol and piperidine in toluene and the results have been compared with those achieved with the dimer [Cp*IrCl₂]₂ (Graph 11). The graph reports the average yield of 2 or 3 experiments and error bars show the relative statistical errors. Graph 11 shows that our catalyst **102** is more active than the iridium dimer [Cp*IrCl₂]₂; the reaction using 2 mol% of complex **102** was effectively concluded after 5 hours, whereas with the dimer only a 72% yield was achieved after 24 hours. The presence of a secondary amine does not influence the activity of the catalyst, which agrees with the results achieved previously with rhodium(III) catalysts. Nevertheless, the presence of a tertiary amine in the side chain influences the activity of the monomer and the reaction profile obtained using complex **105** shows a pathway which is more similar to the one obtained with the dimer [Cp*IrCl₂]₂ than those achieved with catalysts **102** and **103**.

Graph 11



Graph 11

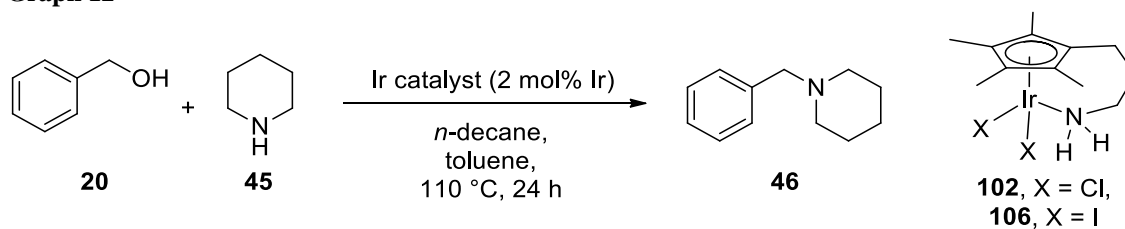


A semi-quantitative analysis of the initial rates of these catalysts gave an approximation of the observed rate constants. The observed rate constants were calculated plotting the logarithm of the benzyl alcohol vs. the time. The initial rates for catalysts **102** and **103** were similar (respectively, $k_{obs} = -0.0098$ for **102** and $k_{obs} = -0.0088$ for **103**) and both on them were four times as fast as the dimer $[\text{Cp}^*\text{IrCl}_2]_2$ and **105** ($k_{obs} = -0.0021$ for $[\text{Cp}^*\text{IrCl}_2]_2$ and $k_{obs} = -0.0024$ for **105**). We considered these data as an approximation, because we extrapolated the rate constants plotting only the few collected data points which gave a yield between 0 and 15%.

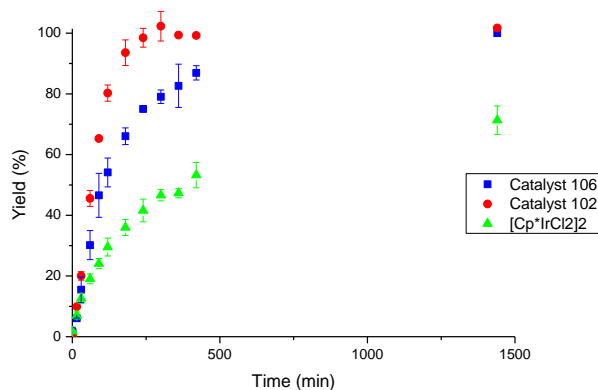
It was found that the presence of one hydrogen on the amine is necessary to achieve high yields and fast reaction rates, similarly to the results observed with the corresponding rhodium complexes and suggesting a common mechanism impart of the substituents.

Finally, activities of complexes **106**, **102** and $[\text{Cp}^*\text{IrCl}_2]_2$ were compared (Graph 12). This graph reports the average yield of 2 or 3 experiments and error bars are referred to the relative statistical errors. Both catalysts **102** and **106** promoted the hydrogen borrowing reactions better than the dimer $[\text{Cp}^*\text{IrCl}_2]_2$ and, between them, the best one in toluene was complex **102** with chlorides as halide ligands.

Graph 12



Graph 12

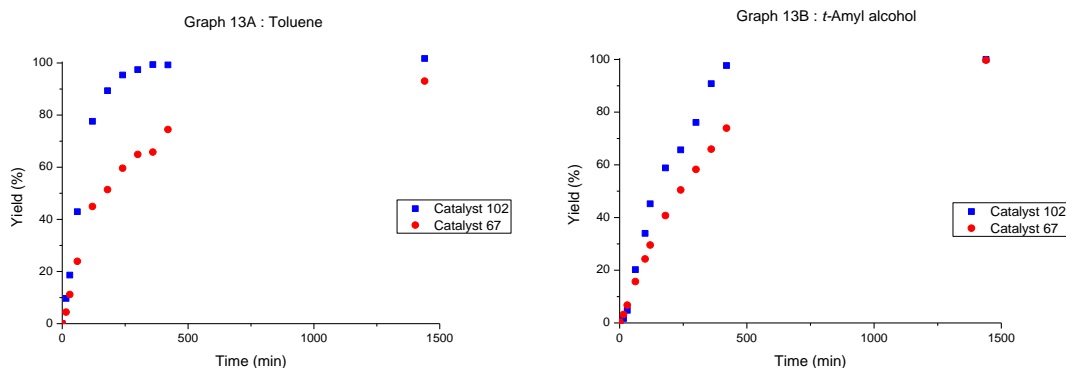
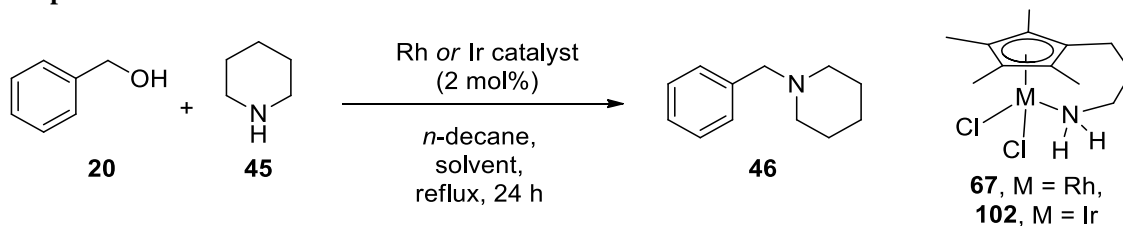


Again, a semi-quantitative analysis of the initial rates of these three catalysts gave an approximation of the observed rate constants. The observed rate constants were calculated plotting the logarithm of the benzyl alcohol vs. the time. The initial rate for catalyst **102** was twice as fast as **106** (respectively, $k_{obs} = -0.0098$ for **102** and $k_{obs} = -0.0053$ for **106**). These results agree with those observed using the corresponding rhodium catalysts.

4.6 Comparison between Catalysts 67 and 102

To determine if the most active catalyst was the rhodium complex **67** or the iridium complex **102**, they have been tested in the reaction between benzyl alcohol and piperidine using the same solvent system, as shown in Graph 13. Graph 13A reports the results using toluene as solvent, while Graph 13B reports the results using *t*-amyl alcohol.

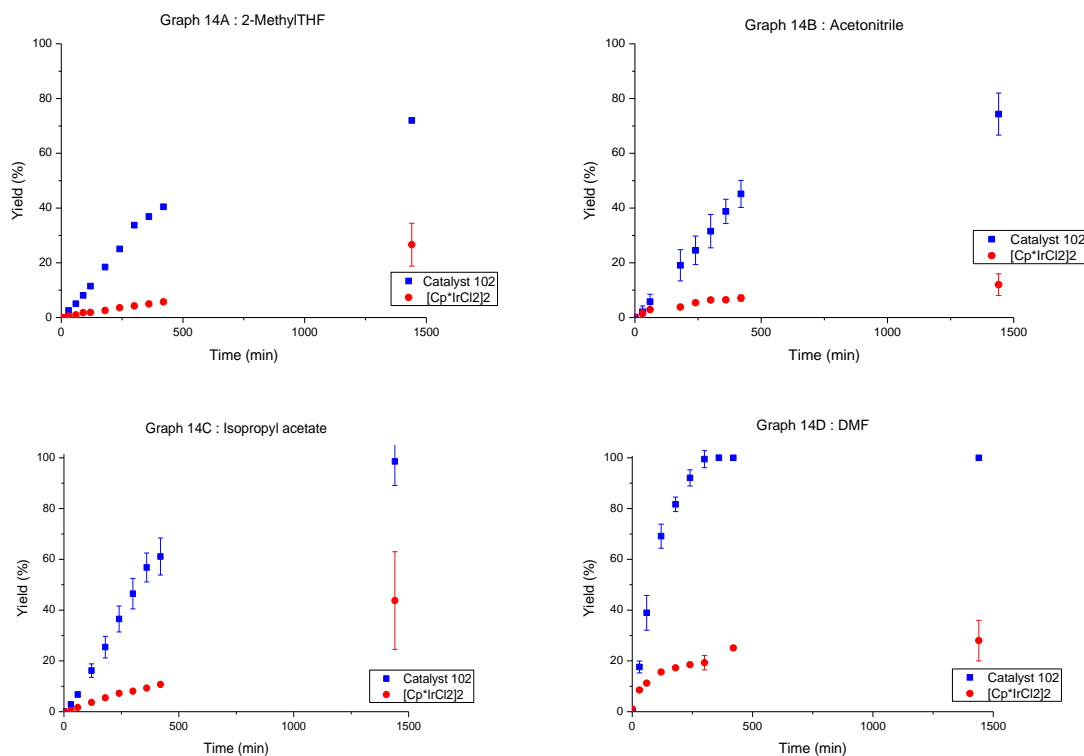
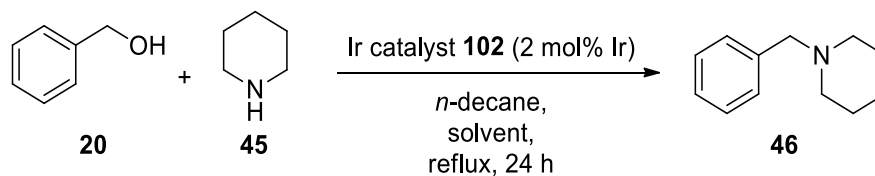
Graph 13



Again, a semi-quantitative analysis of the initial rates of these two catalysts gave an approximation of the observed rate constants. The observed rate constants were calculated plotting the logarithm of the benzyl alcohol vs. the time. The initial rates for catalyst **102** was faster than **67** both in toluene and *t*-amyl alcohol (respectively, $k_{obs} = -0.0098$ for **102** and $k_{obs} = -0.0070$ for **67** in toluene and $k_{obs} = -0.0044$ for **102** and $k_{obs} = -0.0023$ for **67** in *t*-amyl alcohol). Therefore, complex **102** was chosen for further screening.

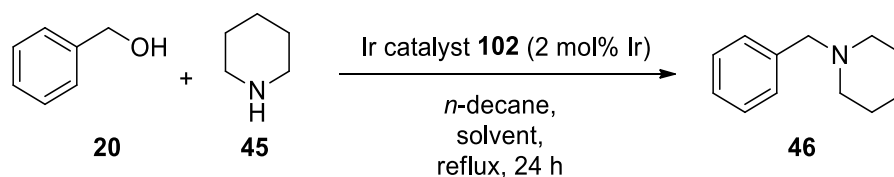
4.7 Solvent Tolerance and Catalyst Loading using Catalyst 102

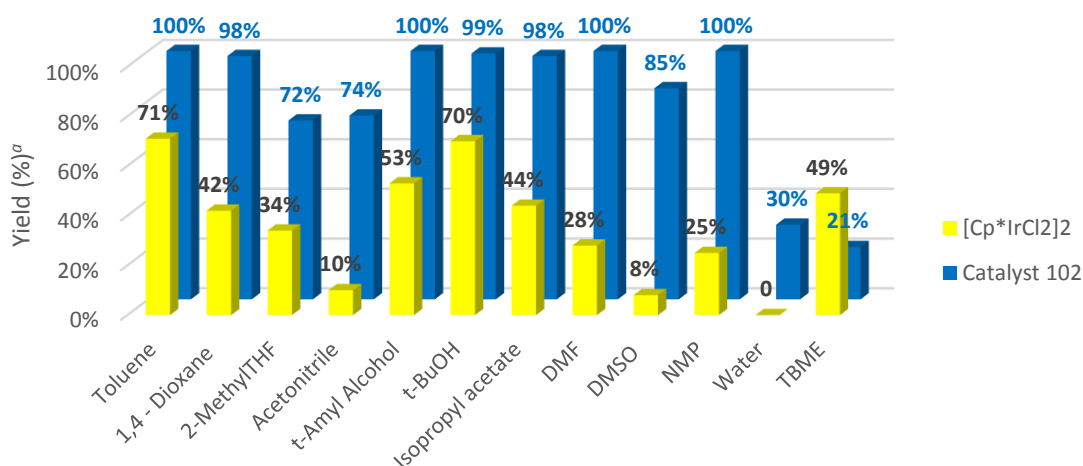
Pleased with these results, our next attempt was to evaluate if the good activity shown previously by catalyst **67** in a broad range of solvents was also maintained in complex **102**. Thus, monomer **102** was tested in a variety of solvents, using our standard reaction between benzyl alcohol and piperidine. Graph 14 reports four experiments carried out in four different solvents, comparing the yield profiles with those obtained using $[\text{Cp}^*\text{IrCl}_2]_2$ as catalyst.

Graph 14

In all these four experiments, catalyst **102** showed a better activity than $[Cp^*IrCl_2]_2$ with good yields (> 70%) after 24 hours. For instance, our monomer **102** in acetonitrile afforded product **46** in 70% yield, whereas the dimer gave only a 10% yield after the same reaction time (Graph 14B). Besides, iridium catalyst **102** was active in solvents widely used in industry, such as 2-methylTHF and isopropyl acetate (Graph 14A and Graph 14C) and, also, in very polar solvents, like DMF (Graph 14D).

In Graph 15, the yields obtained after 24 hours for a broader range of solvents are reported, including those already shown in Graph 14.

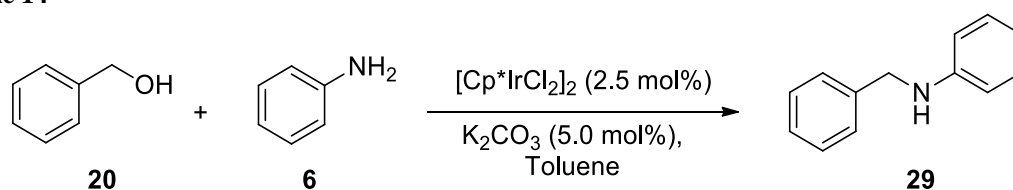
Graph 15



^a Yield calculated by comparing the areas of *n*-decane and *N*-benzylpiperidine in the GC chromatogram.

Since *n*-decane was not soluble in DMSO, the yields for this solvent were calculated by ¹H-NMR spectroscopy using 1,3,5-trimethoxybenzene as internal standard. Interestingly, catalyst **102** promoted the reaction with good yields in both non-polar, *e.g.* toluene, and very polar solvents, such as DMF, DMSO and NMP. TBME was the only example in which the dimer [Cp*IrCl₂]₂ gave a higher yield than complex **102**. For all the other examples, catalyst **102** was more active than [Cp*IrCl₂]₂ in a broad range of solvents, showing a wide tolerance. Additionally, good yields were also achieved at 85 °C, when 2-methylTHF, acetonitrile and *t*-butanol were used. This is an interesting result because it suggested that the reaction could also work at lower temperatures than those generally used. A few attempts to decrease the reaction temperature in these processes have been reported in the literature. For instance, Fujita *et al.* described that the reaction between benzyl alcohol and aniline, which gave complete conversion at 110 °C, also proceeded at 90 °C, but a longer reaction time (40 hours) was required in order to obtain a satisfactory yield (Table 14).²¹

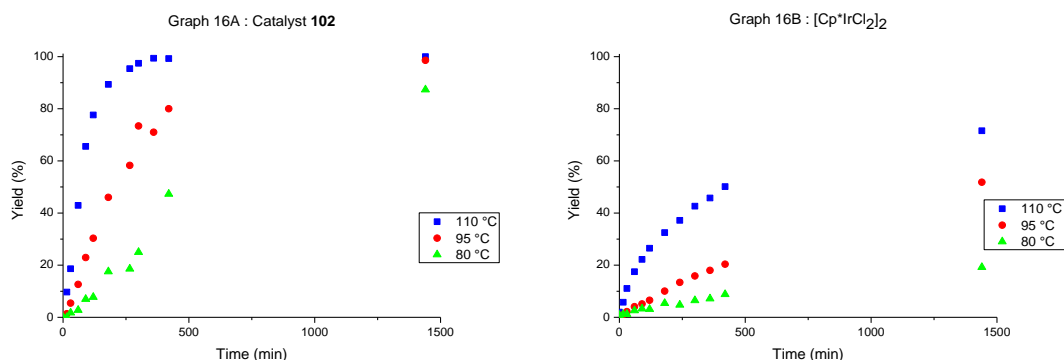
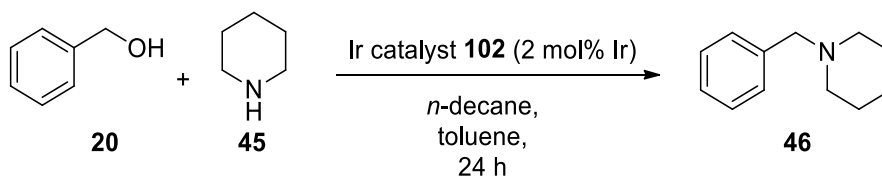
Table 14



<i>Entry</i>	<i>Temperature</i>	<i>Reaction time</i>	<i>Yield 29 (%)</i>
1	110 °C	17 h	100
2	90 °C	17 h	52
3	90 °C	40 h	81

Since running the reaction at lower temperatures than the boiling points of solvents would be beneficial for industry, our next effort was to run the standard reaction between benzyl alcohol, piperidine and 2 mol% of iridium in toluene at temperatures lower than 110 °C, as shown in Graph 16. Graph 16A and Graph 16B show the yield profiles achieved using respectively catalyst **102** and the dimer [Cp*IrCl₂]₂.

Graph 16

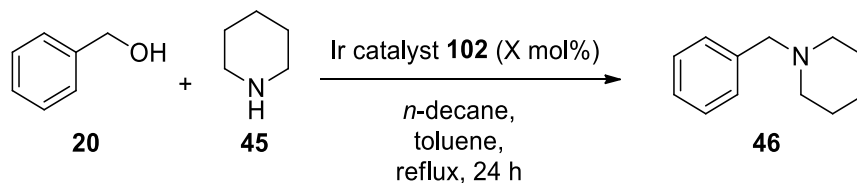


Using our complex **102**, the reaction at 95 °C was complete after 24 hours and a 90% GC yield was observed after the same reaction time running the reaction at 80 °C, as shown in Graph 16A. Comparing the results with Graph 16B, it was possible to observe that the monomer **102** was definitely more active than the dimer also at lower temperature. For instance, at 80 °C, the dimer afforded the product **46** in 20% yield after 24 hours, showing that catalyst **102** could promote the amine alkylation under milder more energy efficient conditions than those traditionally used.

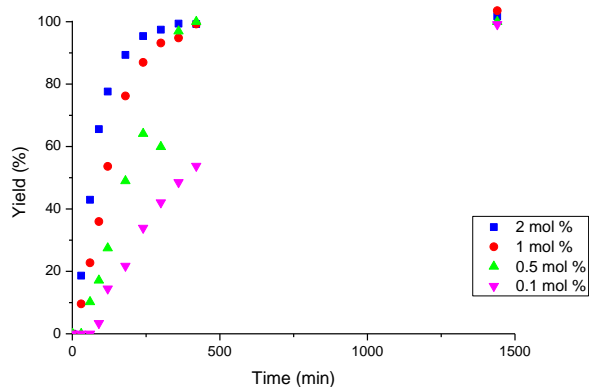
In all the examples reported above, the catalyst loading was 2 mol% of iridium. However, decreasing the amount of metal used in the reaction would have economic and environmental advantages. Thus, we carried out a few experiments in which the catalyst

loading of **102** has been decreased as low as 0.1 mol% of iridium (Graph 17). A complete conversion after 24 hours was observed in all the experiments.

Graph 17



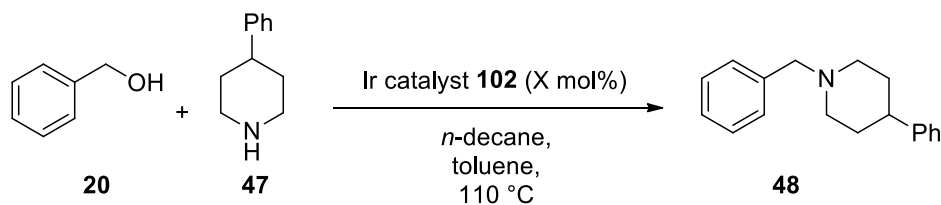
Graph 17



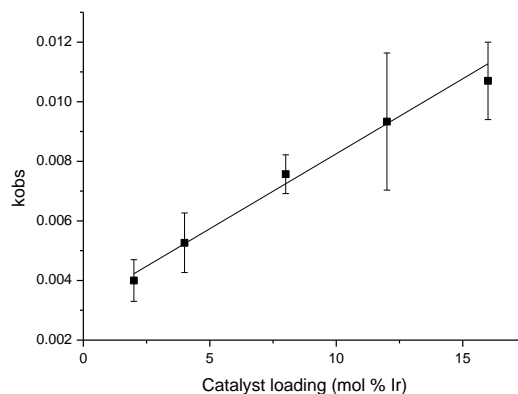
The reaction profile of the experiment carried out using 0.1 mol% of catalyst suggests the presence of an induction period for the first 30 minutes, in which the catalyst did not show any activity; effectively, we found the presence of the product in the GC samples only after 60 minutes. These results suggest that the rate of the addition of amine could influence the activity of the catalyst, in particular when the catalyst loading is as low as 0.1 mol% of iridium.

To compare the effect of the catalyst loading using our complex **102** with the results achieved with dimer $[\text{Cp}^*\text{IrCl}_2]_2$ in Section 2.4, several reactions were carried out maintaining the same conditions used previously. Using 1 equivalent of the amine and 1 equivalent of the alcohol, we analysed the data obtained between 0 and 10% yield to have an approximation of *pseudo*-first order conditions with respect to the starting materials. The observed rate constants have been calculated plotting the logarithm of the benzyl alcohol vs. the time. Graph 18 plots the observed rate constants vs. the catalyst loading.

Graph 18



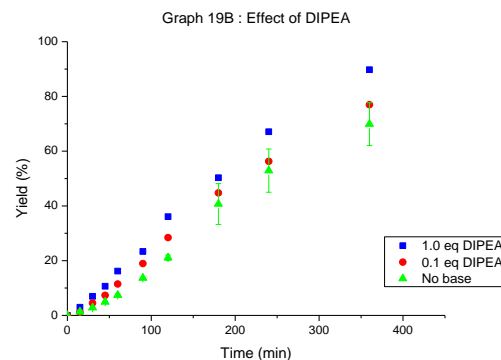
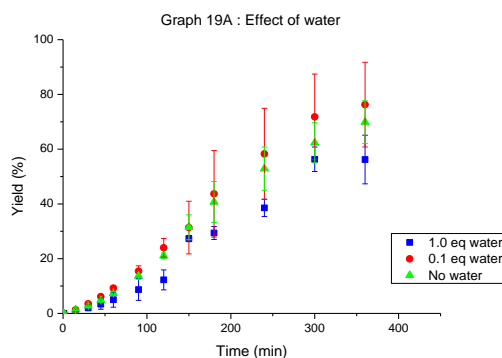
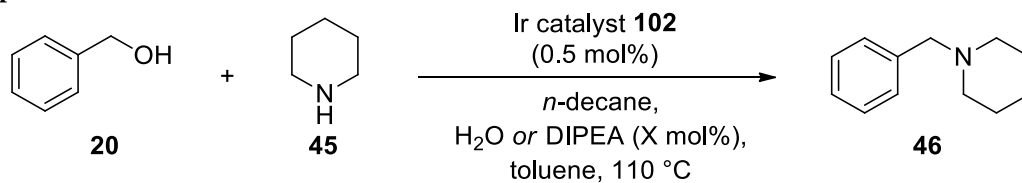
Graph 18



A linear dependence between the rate constant and the catalyst loading was observed, suggesting that the reaction rate is now first order in complex **102**. The monomer **102** did not need the dissociation energy to generate the active catalyst, which instead was necessary for the iridium dimer $[\text{Cp}^*\text{IrCl}_2]_2$, as shown previously in Section 2.4. Therefore, the observed rate constants of the reaction depended linearly with the catalyst loading of **102**.

4.8 Effects of Water, Bases and Acids in the Catalytic System

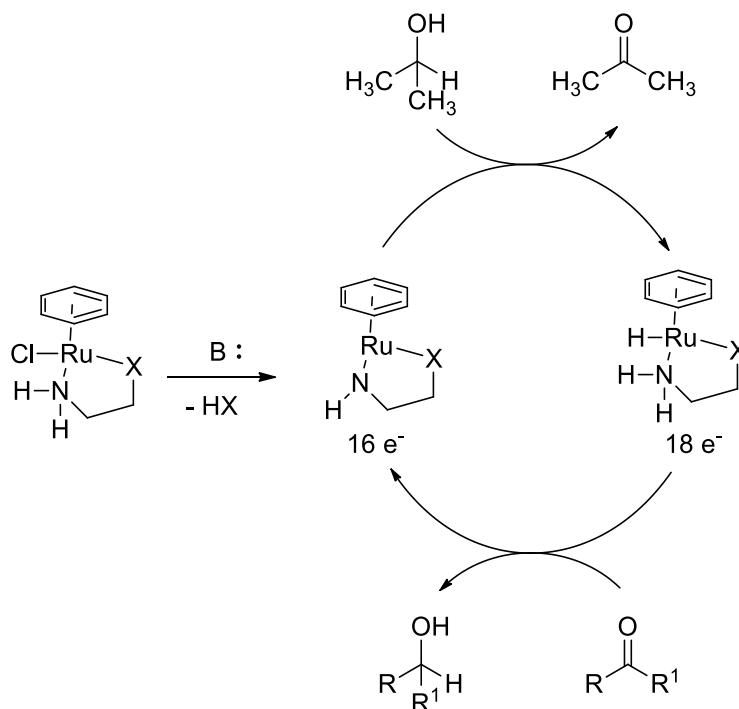
To evaluate if the activity of catalyst **102** could be improved by the presence of an additive, such as water, a base or an acid, and, at the same time, to study the pH tolerance of our family of complexes, several reactions were carried out adding different equivalents of water, diisopropylethylamine and acetic acid. Graph 19A and Graph 19B show respectively the effect of water and diisopropylethylamine in the reaction. The reactions were monitored for 6 hours using the Amigo automated sampling reactor.

Graph 19

The addition of water in the reaction did not massively change the activity of the iridium catalyst. It was found that the addition of 1 equivalent of water, which is the by-product of the reaction, did not poison complex **102**. Therefore, drying agents (*e.g.* molecular sieves) were not necessary to drive the reaction equilibrium to the right. Additionally, the effect of a weak base, such as diisopropylethylamine, was moderate, either using substoichiometric or stoichiometric amount of base in respect to the piperidine. The highest conversion after 6 hours was achieved on adding one equivalent of base, suggesting that it could positively help the catalytic activity of **102**.

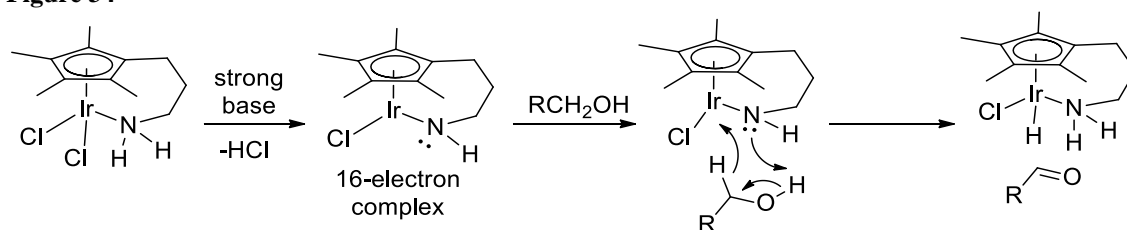
Noyori and co-workers showed that strong bases like potassium hydroxide or potassium *tert*-butoxide were necessary to generate the active catalyst. A representative example has been previously reported in Scheme 41.⁶⁷ The mechanism to generate the active ruthenium complex has been reported in the literature (Figure 33).⁵⁶ A strong base was necessary for the generation of the 16-electron complex from the precatalyst by a Dcb elimination of hydrochloric acid.

Figure 33



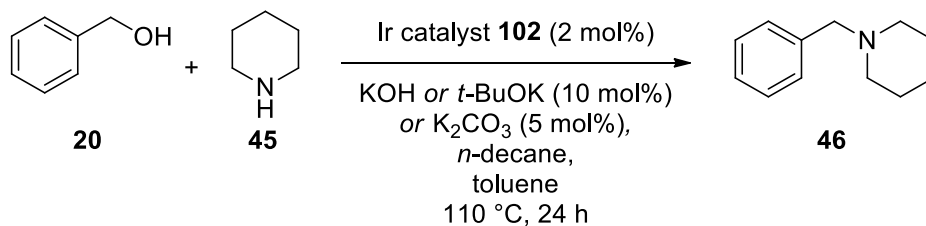
Therefore, the activity of our complexes could be potentially improved by deprotonation of the coordinated amine, which would give a reactive 16-electron complex which would promptly dehydrogenate the alcohol (Figure 34).

Figure 34

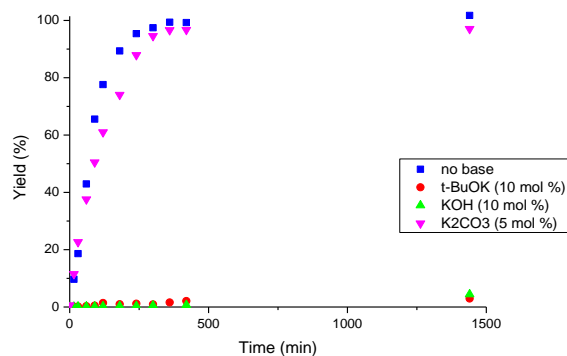


Thus, the standard reaction between benzyl alcohol and piperidine was carried out in the presence of a substoichiometric amount of potassium hydroxide or *tert*-butoxide. Graph 20 reports the yield of the two experiments vs. the time, comparing the yield profiles with two other reactions, one carried out without any base and the second carried out with a substoichiometric amount of potassium carbonate.

Graph 20



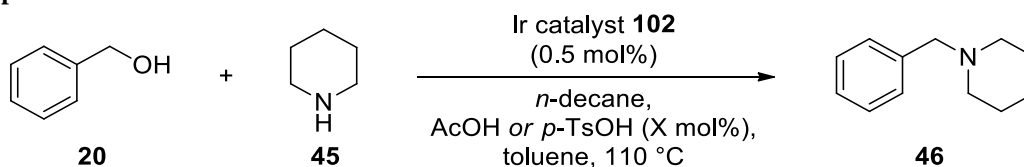
Graph 20

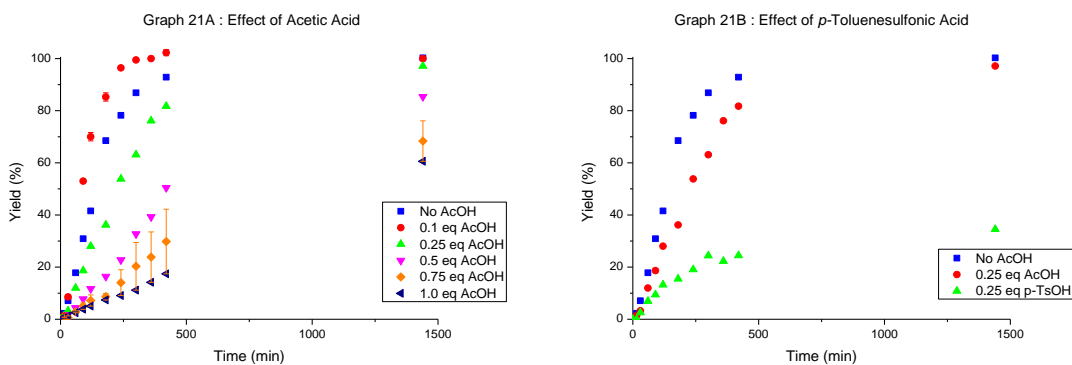


Unfortunately, both the reactions with potassium hydroxide and *tert*-butoxide gave very poor yields, whereas a weaker base such as potassium carbonate gave a complete conversion after 24 hours. These results suggest that a strong base, instead of activating the complex, formed a species which is inactive in borrowing hydrogen. Additionally, a closer comparison of this last run and the reaction carried out without base showed that the latter had a faster reaction rate.

Furthermore, the effect of acids was studied. Several reactions were carried out adding different equivalents of acetic acid (Graph 21A). Graph 21B shows the effects of the substoichiometric addition of two different acids, acetic acid and *p*-toluenesulfonic acid.

Graph 21

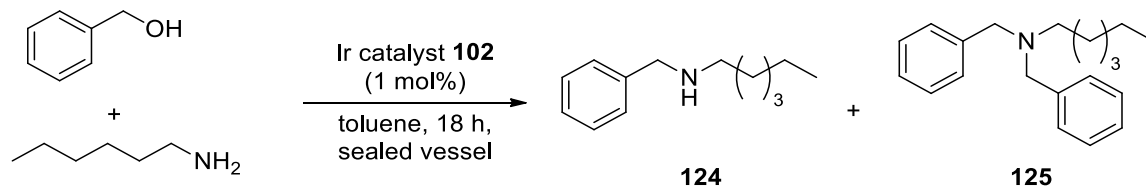




Interestingly, it was found that the addition of 10 mol% of a weak acid, such as acetic acid, slightly improved the activity of catalyst **102**, which could be useful in scaling-up processes. This substoichiometric amount of acid was paramount to increase the reaction rate. However, increasing the amount of acetic acid in the reaction, the activity of complex **102** decreased. An addition of 25 mol% of acid gave a slower reaction rate than the one obtained when no acid was present. When 1 equivalent of acetic acid was added, the GC yield of product **46** was slightly more than 50% after 24 hours, whereas the reaction carried out with 10 mol% of acid gave complete conversion after the same time. It was also found that the pK_a of the acid used was fundamental. When a substoichiometric amount of strong acid was used, in this case 25 mol% of *p*-toluenesulfonic acid, the reaction rate dropped significantly, giving less than 30% GC yield after 24 hours (Graph 21B). The presence of acid in the reaction could protonate either the piperidine or the coordinated amine in complex **102**. In the first case, the protonated amine would become non-nucleophilic and, therefore, less reactive. In the second case, the complex would change structure, because the protonated amine could not remain coordinated to the metal, causing the dropping of reaction rate.

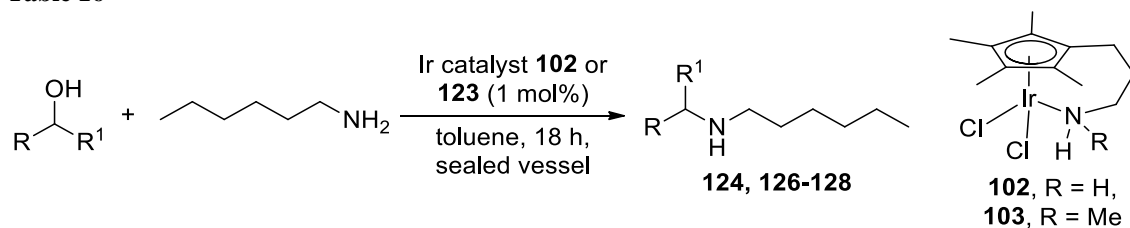
4.9 Substrate Scope using Catalyst **102**: Secondary and Tertiary Amines

With an efficient family of catalysts in hand, we sought to extend the substrate scope using our best state-of-the-art iridium complex, **102**. Preliminary investigations commenced with the development and the optimisation of procedures to obtain a good selectivity for the synthesis of secondary and tertiary amines. Firstly, we focused on the optimisation of the procedure to synthesise selectively secondary amines (Table 15).

Table 15

Entry	Amine equivalents	Temperature	Ratio 124 : 125	Conversion 124 (%)
1	1	110 °C	0:100	-
2	2	110 °C	67:33	64
3	2	130 °C	100:0	100

It was found that using catalyst **102** only a tertiary amine was observed when 1 equivalent of primary amine and 1 equivalent of primary alcohol were used; the amine was alkylated twice by two molecules of alcohol (entry 1). Reacting 2 equivalents of amine and 1 equivalent of alcohol at 110 °C, a mixture of secondary and tertiary amines was isolated (entry 2). Fortunately, a good selectivity for the synthesis of the secondary amine **124** was achieved when the reactions were carried out using 2 equivalents of amine and 1 equivalent of alcohol at 130 °C (entry 3). With these optimised conditions in hand, the scope was next explored using primary and secondary alcohols (Table 16).

Table 16

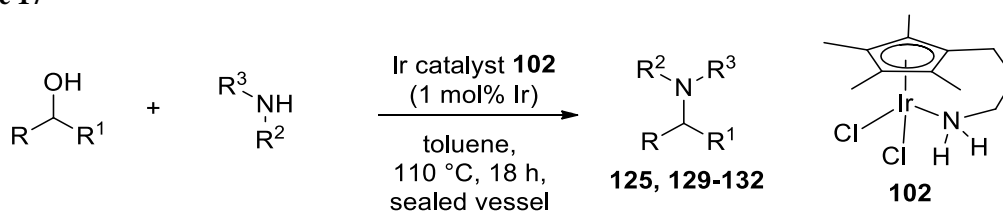
Entry	Alcohol	Catalyst	Temperature	Isolated Yield (%)
1 ^a	R = Ph, R ¹ = H	102	130 °C	124 , 99
2	R = Ph, R ¹ = H	103	110 °C	124 , 91
3 ^a	R = (CH ₂) ₆ CH ₃ , R ¹ = H	102	130 °C	126 , 81
4	R = (CH ₂) ₆ CH ₃ , R ¹ = H	103	110 °C	126 , 84
5 ^b	R, R ¹ = (CH ₂) ₅	102	110 °C	127 , 80
6 ^b	R = Ph, R ¹ = CH ₃	102	130 °C	128 , 70

^a 2 equivalents of amine were used; ^b 2 mol% of iridium were used.

The optimised procedure for the synthesis of secondary amines also afforded the product **126** in high yield (entry 3). In entries 5 and 6, two secondary alcohols have been used as substrates and, in both the entries, the amount of complex **102** has been increased to 2 mol% of iridium in order to achieve a good yield. Interestingly, starting with these two secondary alcohols, only the mono-alkylated secondary amines were observed in the crude NMR spectra, even though 1 equivalent of amine and 1 equivalent of alcohol were used. These results suggested that increasing the steric bulk of the product disfavoured its approach to the catalyst for a further alkylation. The same effect was also observed increasing the steric bulk on the amine in the tethered chain of the catalyst. Using the iridium monomer **103** instead of the catalyst **102**, we obtained a complete selectivity for the monoalkylated product using only one equivalent of primary amine and one equivalent of primary alcohol at 110 °C (entries 2 and 4) with yields comparable to those reported in entries 1 and 3. The methyl group on the coordinated amine was probably bulky enough to disfavour the approach of the secondary amine near the active site of the catalyst.

The next attempt was to optimise the reaction conditions to obtain a variety of tertiary amines. Table 17 reported the results, starting with primary and secondary alcohols and with primary and secondary amines.

Table 17



Entry	Alcohol	Amine	Isolated Yield (%)
1 ^a	R = Ph, R ¹ = H	R ² = (CH ₂) ₅ CH ₃ , R ³ = H	125 , 84
2 ^a	R = (CH ₂) ₆ CH ₃ , R ¹ = H	R ² = (CH ₂) ₅ CH ₃ , R ³ = H	129 , 68
3	R = (CH ₂) ₆ CH ₃ , R ¹ = H	R ² , R ³ = (CH ₂) ₅	130 , 96
4	R, R ¹ = (CH ₂) ₅	R ² , R ³ = (CH ₂) ₅	131 , 77
5 ^{b,c}	R = Ph, R ¹ = CH ₃	R ² , R ³ = (CH ₂) ₅	132 , 72

^a 2 equivalents of alcohol were used; ^b 2 mol% of iridium were used; ^c reaction performed at 130 °C.

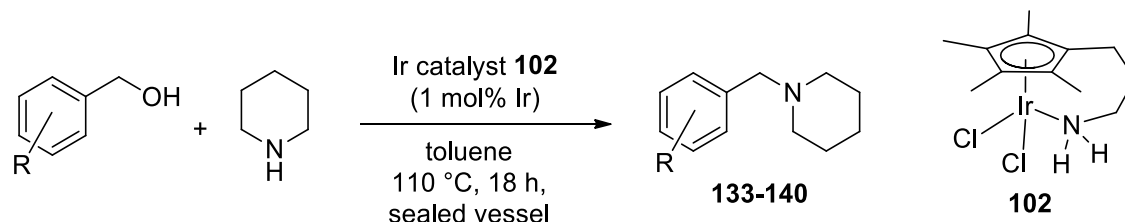
Entries 1 and 2 were performed using 2 equivalents of a primary alcohol to obtain a second alkylation of the amine. The reaction between piperidine and *n*-octanol gave the corresponding tertiary amine in excellent yield (entry 3). In entries 4 and 5, the reactions

were carried out between a secondary alcohol and a secondary amine isolating the final products in good yields. In both the entries, the amount of complex **102** has been increased to 2 mol% of iridium in order to isolate the products in better yields.

4.10 Substrate Scope using Catalyst **102**: Functional Groups

The scope was next investigated with respect to the functional groups that can be tolerated using our family of catalysts. First efforts explored the functional groups tolerated by the complexes on the benzene ring of benzylic alcohol. The results are summarised in Table 18.

Table 18



Entry	R	Isolated Yield (%)
1	4-Br-	133 , 99
2	3-Br-	134 , 94
3	2-Br-	135 , 99
4	4-NO ₂ -	136 , 80
5	4-MeO-	137 , 90
6	4-NH ₂ CO-	138 , 56 (71) ^a
7	4-CN-	139 , 82
8	4-HO-	140 , 62

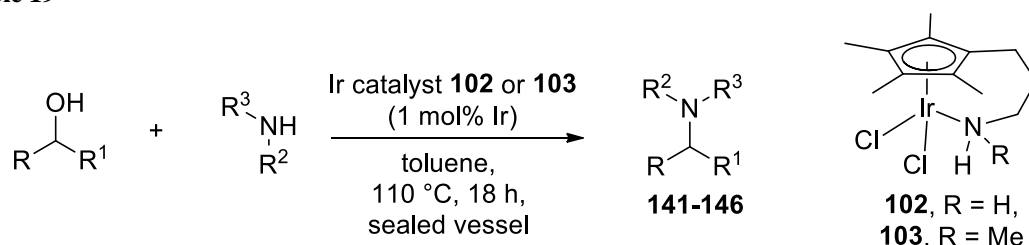
^aIn brackets, the yield obtained using *t*-amyl alcohol as solvent.

We demonstrated that, using complex **102**, the group tolerance was broad, which included halogens (entries 1-3), nitro and nitrile groups (entries 4 and 7), methoxy and phenoxy groups (entries 5 and 8) and also primary amides (entry 6). In this last case, a 56% yield was achieved using toluene as solvent, possibly due to a poor solubility of the starting material amide. However, we managed to increase the yield up to 71% by changing the solvent to *t*-amyl alcohol. Additionally, benzyl alcohols with substituents in the *para*,

meta and *ortho* positions were well tolerated, as shown in entries 1, 2 and 3. Pleasingly, even though nitro and nitrile groups reacted slowly in many catalytic systems, as reported for instance by Williams and co-workers¹⁵ and by Fujita *et al.*,²² these two functional groups were well tolerated in our system and products **136** and **139** were isolated in high yields. Besides, nitroarenes could be reduced to the corresponding anilines in hydrogen borrowing processes, as reported by the groups of Deng^{83,84} and Peris.⁸⁵ On the contrary, using our complex **102**, the formation of by-products in this reaction was not significant and the isolated yield was high.

We also explored the functional group tolerance on the amines, for which Table 19 summarises the results obtained.

Table 19



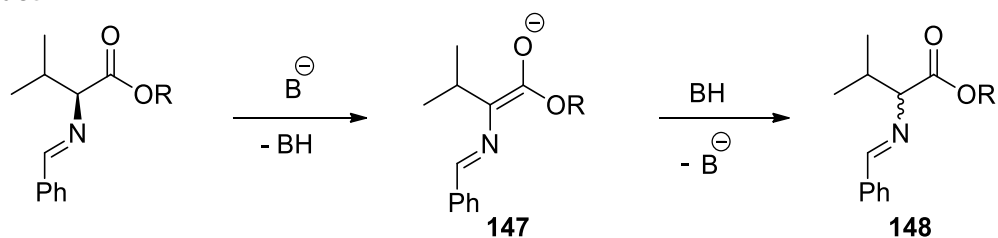
Entry	Alcohol	Amine	Catalyst	Isolated Yield (%)
1 ^{a,b,c}	R = (CH ₂) ₆ CH ₃ , R ¹ = H	R ² = Bn, R ³ = H	102	141 , 85
2 ^{a,b,c}	R = (CH ₂) ₆ CH ₃ , R ¹ = H	R ² = 4-ClC ₆ H ₄ CH ₂ , R ³ = H	102	142 , 74
3	R = (CH ₂) ₆ CH ₃ , R ¹ = H	R ² = CH(Ph)(CH ₃), R ³ = H	102	143 , 67
4	R = Ph, R ¹ = H	R ² , R ³ = ((2-CH ₃)CH ₂) ₅	102	144 , 96
5 ^{b,d}	R = Ph, R ¹ = H	R ² = CH(CH ₃) ₂ CH(COOMe), R ³ = H, hydrochloride	102	145 , 72 (<i>e.e.</i> 76%)
6 ^b	R = Ph, R ¹ = H	R ² = CH(CH ₃) ₂ CH(COObn), R ³ = H	102	146 , 63 (<i>e.e.</i> 91%)
7 ^b	R = Ph, R ¹ = H	R ² = CH(CH ₃) ₂ CH(COObn), R ³ = H	103	146 , 44 (<i>e.e.</i> 98%)

^a 2 equivalents of amine were used; ^b 2 mol% of Iridium were used; ^c reaction performed at 130 °C;

^d 1 equivalent of NaHCO₃ was used.

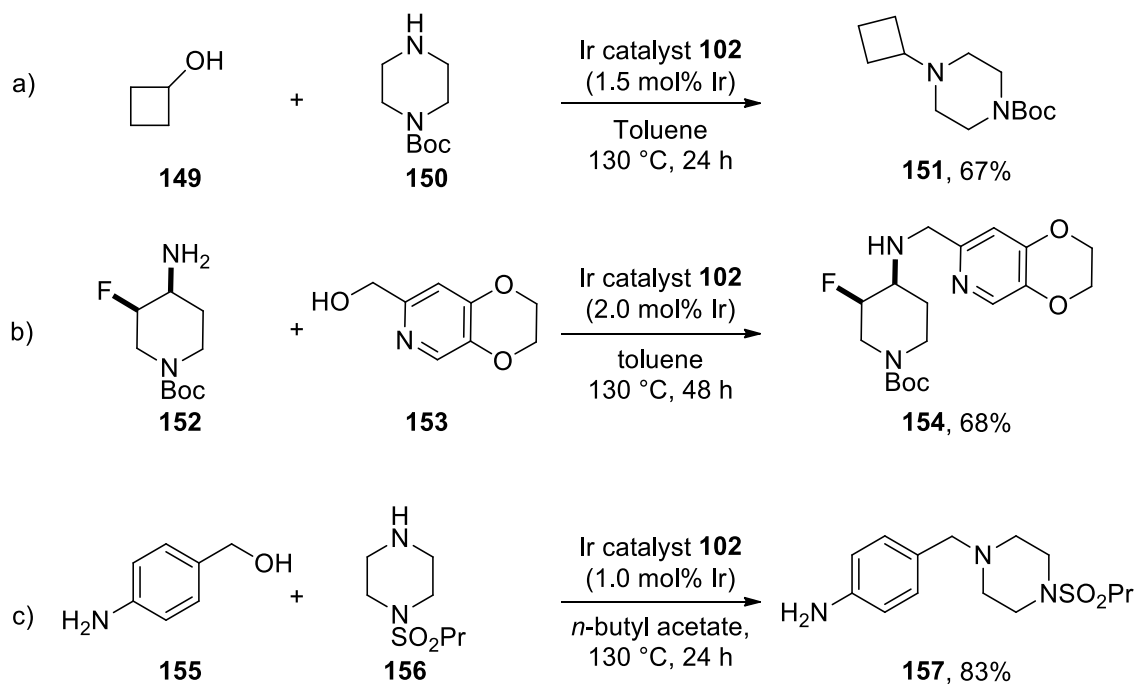
Three different benzylamines gave the corresponding products in good yields (entries 1-3). Two equivalents of amine were used in entries 1 and 2 to obtain a good selectivity for the monoalkylated product. Amines branching a substituent in the α -position were also tolerated (entries 3 and 4). Starting with the amino acid esters, a branched functionalised substituent in the α -position was introduced. We were able to use the methyl ester of L-valine which gave the alkylated product in 72% yield (entry 5). However, a small amount of racemisation occurred and the product **145** was isolated with 76% *e.e.* Starting with the benzyl ester of L-valine, product **146** was obtained in a slightly lower yield (63%), but the enantiomeric excess was higher (91% *e.e.*) (entry 6). Using catalyst **103**, product **146** was isolated in lower yield (44%), but the side reaction of racemisation did not occur and the enantiomeric excess at the end of the reaction was comparable to the optical purity of the starting material (entry 7). Our hypothesis was that the racemisation process could occur during the formation of the imine. The presence of an EWG in the β -position made the proton in the α -position more acidic and prone to form the corresponding enolate **147**, as shown in Figure 35. Effectively, the racemisation was higher when 1 equivalent of sodium hydrogen carbonate was added (entry 5). The formation of the enolate would lose the stereogenic information, affording a small amount of the racemic amine **148**.

Figure 35



To demonstrate the possible applications of this methodology using our catalysts, the synthesis of some actual pharmaceutical intermediates developed by AstraZeneca was attempted using complex **102**. For each reaction, several solvents were screened, which included toluene, 1,4-dioxane, acetonitrile, *n*-butyl acetate, 2-methylTHF and *t*-amyl alcohol. Scheme 92 reported the best optimised conditions for the synthesis of three pharmaceutical intermediates.

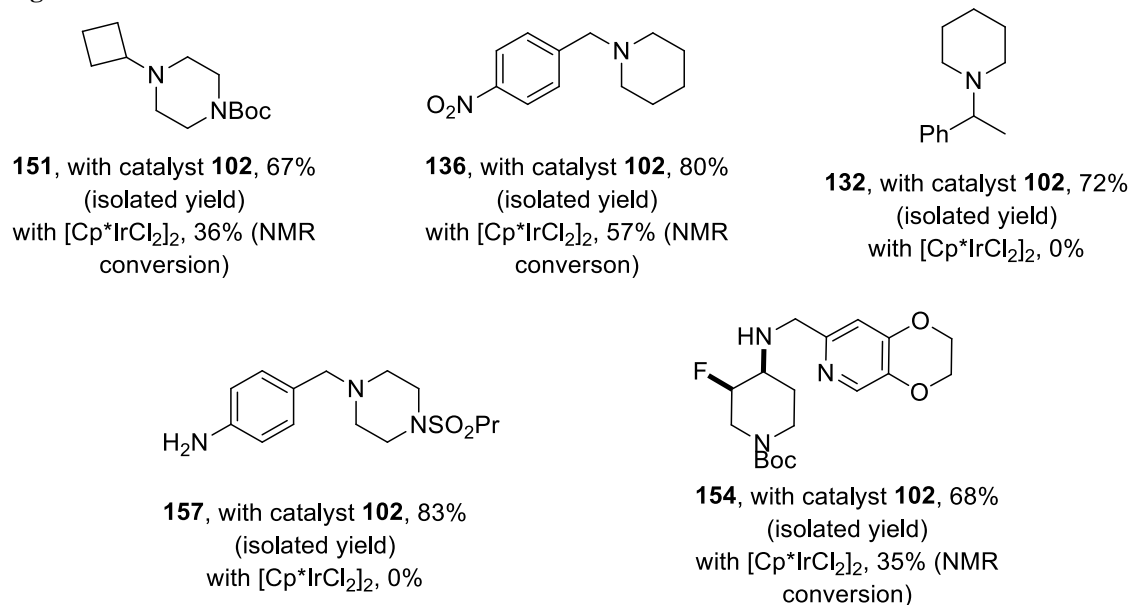
Scheme 92



In the first example (a), the optimised conditions afforded the product **151** from the reaction between cyclobutanol **149** and *N*-Boc-piperazine **150** in 67% yield using 1.5 mol% of iridium in toluene. In the second example (b), product **154** was isolated in 68% yield from a reaction between **152** and **153** which were obtained and used without any other purification from the AstraZeneca Process R&D Site in Macclesfield. In order to obtain this intermediate in satisfactory yield, the catalyst loading was increased to 2 mol% of iridium and the reaction time was longer (48 hours, instead of 24). In the last example (c), the reaction between 4-aminobenzyl alcohol **155** and piperazine *N*-propylsulfonamide **156** gave the product **157** in 83% yield using 1 mol% of catalyst **102**. Interestingly, it was found that, for this substrate, the best solvent was *n*-butyl acetate instead of toluene. These reactions showed that other functional groups were tolerated, such as carbamates, sulfonamides, anilines and heteroaromatics.

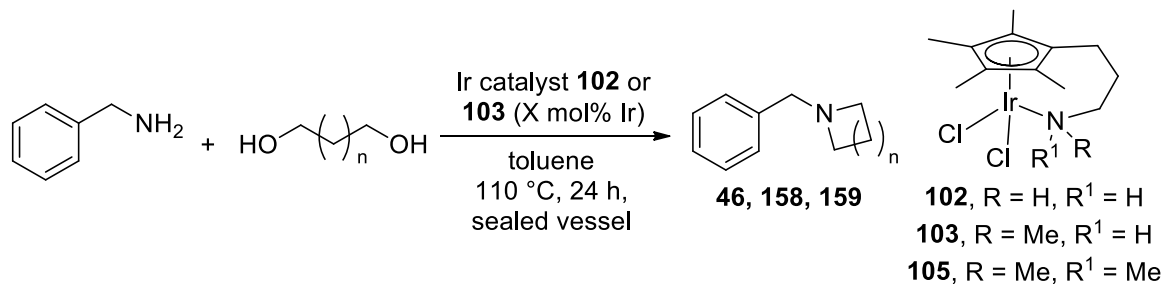
To demonstrate that catalyst **102** was more active than the dimer $[\text{Cp}^*\text{IrCl}_2]_2$, we repeated a few of the experiments reported above using $[\text{Cp}^*\text{IrCl}_2]_2$ instead of **102**, using the same conditions for each reaction, *e.g.* the same reaction time and catalyst loading. The results are shown in Figure 36. In all the examples, a higher yield was obtained using catalyst **102** than using the dimer, which confirmed that iridium complex **102** promoted the hydrogen borrowing processes better than $[\text{Cp}^*\text{IrCl}_2]_2$.

Figure 36



As described in the introduction, hydrogen borrowing methodology can be used to generate *N*-heterocycles from the reaction of a primary amine with 1,*n*-diols. Thus, the scope was then investigated with respect to the use of diols and benzylamine to synthesise *N*-heterocycles (Table 20). Reactions between benzylamine and three different diols (1,4-butanediol, 1,5-pentanediol and 1,6-hexanediol) were explored. Both iridium complexes **102** and **103** were tested for these reactions. The corresponding products were obtained in moderate yields using both catalyst **102** and **103**. For these reactions the best catalyst was the iridium complex **103**, which could be used at lower temperature (110 °C instead of 130 °C) and lower catalyst loading (1.0 mol% instead of 2.0 mol%). Additionally, it gave a better yield for two substrates (entries 6 and 8). To complete the screening, two other iridium catalysts were tested in the reaction between the 1,5-pentanediol and benzylamine: our complex **105** and the dimer $[\text{Cp}^*\text{IrCl}_2]_2$. Both of them afforded product **46** in lower yields than those achieved with **103** (entries 6, 9 and 10). Again, these results support the importance of the N-H moiety in the catalyst, because the catalyst **105**, which contains a coordinated tertiary amine in the side chain, gave the lowest yield.

Table 20

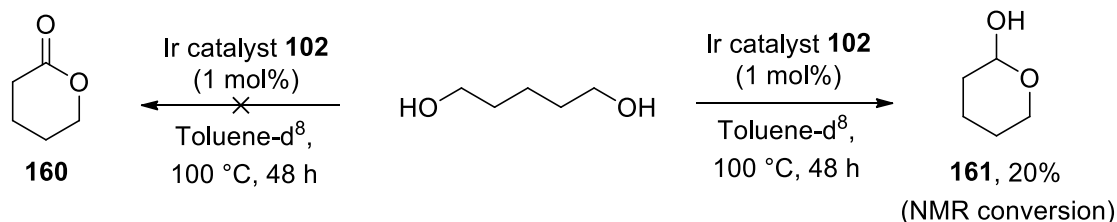


Entry	<i>n</i> =	Catalyst	Catalyst loading	Isolated Yield (%)
1	2	102	2.0 mol% Ir	158 , 50 ^b
2 ^a	2	102	2.0 mol% Ir	158 , 69
3	2	103	1.0 mol% Ir	158 , 50
4 ^a	3	102	2.0 mol% Ir	46 , 26
5 ^a	3	103	2.0 mol% Ir	46 , 47 ^b
6	3	103	1.0 mol% Ir	46 , 64
7 ^a	4	102	2.0 mol% Ir	159 , 28
8	4	103	1.0 mol% Ir	159 , 45
9	3	105	2.0 mol% Ir	46 , 15
10 ^a	3	[Cp*IrCl ₂] ₂	2.0 mol% Ir	46 , 38

^a Reaction performed at 130 °C; ^b NMR conversion.

One of the reason for these low yields could be the formation of the lactone in a self-condensation of the diol. Thus, 1,5-pentanediol and iridium catalyst **102** were heated at 100 °C for two days in deuterated toluene to see if the corresponding lactone was observed. NMR analysis of the crude (¹H-, ¹³C- and HMQC NMRs) did not show any signals that could come from the lactone **160**, but the corresponding hemiacetal **161** was obtained in 20% NMR conversion (Scheme 93).

Scheme 93



The oxidation of diols to lactones is a well-known reaction; however, the low conversion obtained with **102** suggests that our catalyst did not release easily H₂ which would have

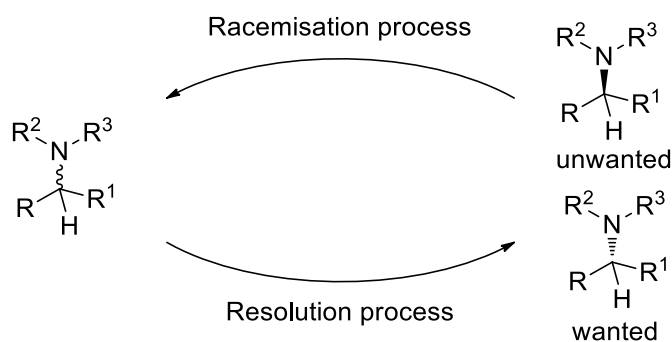
led to the formation of the lactone **160**. This lack of reactivity in the oxidation of diols to lactones could be an advantage with respect to using other iridium catalysts.²⁰

4.11 Substrate Scope: Racemisation

The small amount of racemisation that occurred in the reactions between the L-valine methyl or benzyl ester and benzyl alcohol using catalyst **102** (entries 5 and 6, Table 19) suggests that this class of compounds may be active as racemisation catalysts.

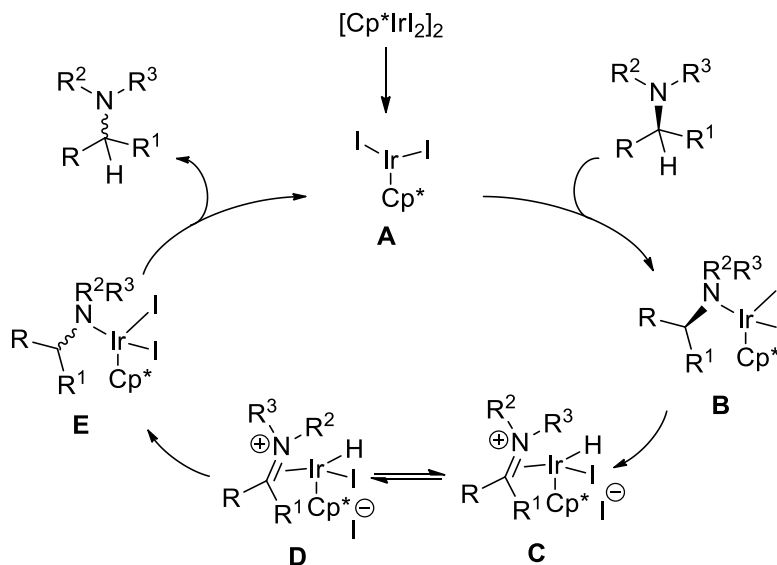
A variety of resolution strategies are reported in the literature to separate two enantiomers, which include diastereomeric crystallisations, enzymatic resolutions or chiral chromatography. Diastereomeric crystallisations are usually robust and simple to operate, but with the disadvantage of low yields (max. 50%).⁸⁶ Blacker and co-workers reported that the iridium dimer $[\text{Cp}^*\text{IrI}_2]_2$ (SCRAM) could be an efficient catalyst for the racemisation of primary, secondary and tertiary amines.⁸⁷ Effectively, if the unwanted enantiomer undergoes a racemisation reaction, the yield and the productivity of these processes will improve (Figure 37).⁸⁶

Figure 37



Amine racemisation processes can be promoted by hydrogen borrowing and the group of Professor John Blacker has made a great effort to develop and improve this methodology. One of the catalysts that can be used for these reactions is SCRAM, $[\text{Cp}^*\text{IrI}_2]_2$; Figure 38 reports the proposed mechanism for amine racemisation using this catalyst.⁸⁶

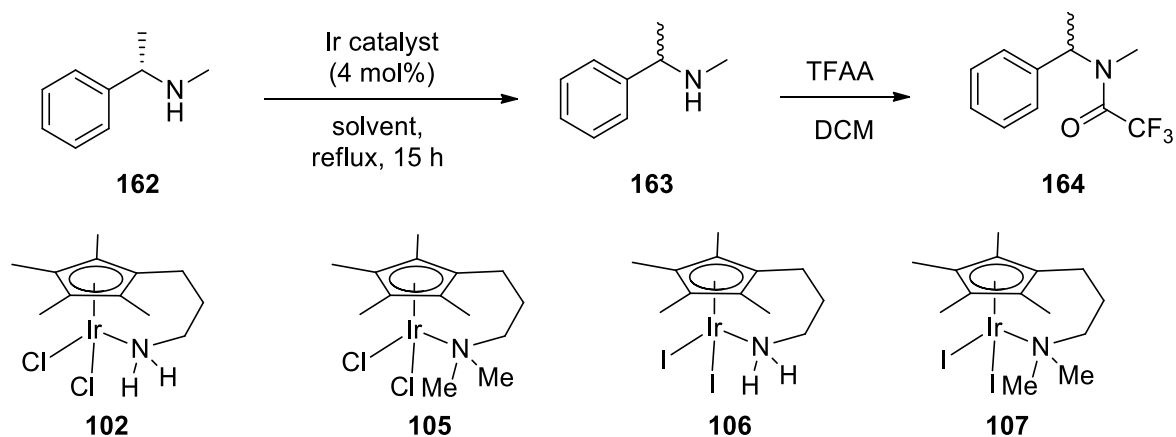
Figure 38



The first step of the mechanism is the dissociation of the dimer to give a 16-electron complex **A**, which can coordinate the amine to generate species **B**. The iridium catalyst dehydrogenates the amine to form the corresponding iminium (**C**). The following hydrogenation step gives the racemic amine because the catalyst cannot distinguish the two enantiotopic faces of the iminium ion (**C** and **D**). The final step is the dissociation of the amine to regenerate the active monomer **A**.

Our aim was to test our complexes in the amine racemisation processes to evaluate their activity. To compare the results with those achieved previously with the SCRAM catalyst, we chose the reaction shown in Table 21, which was previously optimised by Dr. Jessica Breen in the group of Professor John Blacker. (*S*)-(-)-*N*, α -Dimethylbenzylamine **162** was heated at reflux with 4 mol% of catalyst. To analyse the enantiomeric excess at the end of the reaction by chiral GC, compound **163** was treated with 2 equivalents of trifluoroacetic anhydride, which afforded **164**. A few of our catalysts have been tested as shown in Table 21.

Table 21



Entry	Solvent	Temperature	Catalyst	<i>e.e.</i> (%)
1	Toluene	110 °C	102	99%
2	EtOAc	80 °C	102	99%
3	Toluene	110 °C	105	99%
4	EtOAc	80 °C	105	99%
5	Toluene	110 °C	106	99%
6	EtOAc	80 °C	106	99%
7	Toluene	110 °C	107	25%
8	EtOAc	80 °C	107	18%
9	Toluene	110 °C	[Cp*IrI ₂] ₂	0%
10	EtOAc	80 °C	[Cp*IrI ₂] ₂	0%

Using SCRAM, the racemisation occurred completely and a 0% *e.e.* was observed in both toluene and ethyl acetate (entries 9 and 10). Four other different complexes have been tested in both solvents. Iridium catalysts **102** and **106** bearing a primary amine on the tethered chain were found to be inactive in this reaction (entries 1 to 4), as well as complex **105** which contains a tertiary amine (entries 5 and 6). We were pleased to observe that the corresponding diiodide catalyst **107** with a tertiary amine on the tethered chain afforded compound **164** with enantiomeric excess as low as 25% in toluene and 18% in ethyl acetate. Interestingly, the catalyst containing a primary amine in the side chain, which was our best catalyst in the alkylation of amine, was not active in this reaction. On the contrary, the catalyst bearing a tertiary amine was the most active among our family, suggesting that the reaction mechanism for these two complexes is different. The role of the halide ligands was also important. The dichloride complex **105** did not racemise the amine **162**, whereas diiodide catalyst **107**, which contains exactly the same tethered chain,

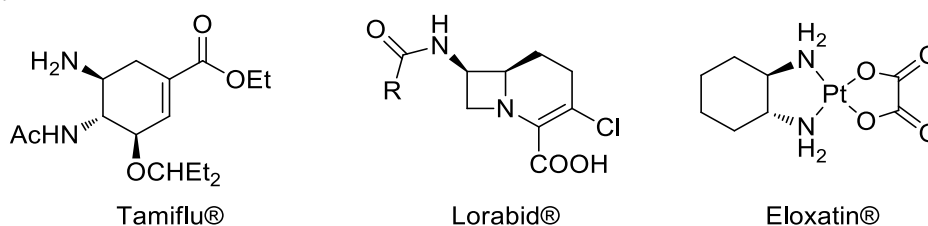
afforded the compounds with the lowest *e.e.* among our monomers. The importance of the halide ligands in the amine racemisation processes has already been reported in the literature, for instance by Blacker *et al.*⁸⁶ Interestingly, catalyst **107** in entries 7 and 8 could be recovered in quantitative yield after the racemisation reactions by precipitation from hexane. Analysis by NMR spectroscopy showed a good purity of the recovered complex, meaning that it could potentially be recycled.

Unfortunately, the dimer $[\text{Cp}^*\text{IrI}_2]_2$ was more active than our best catalyst **107** and, using the same condition, SCRAM catalyst gave a complete racemisation of the amine. The proposed mechanism for the amine racemisation using SCRAM suggests that the amine **162** coordinates the iridium in the presence of two iodide ligands (species **B**, Figure 38). Therefore, the amine on the tethered chain must dissociate to generate an active site on the complex allowing the coordination of the amine **162**. A comparison of the X-ray structures of **102** and **105** shows that the nitrogen-iridium bond was shorter and, therefore, stronger in complex **102** than in **105**. Thus, we could assume that the dissociation of the coordinated amine would also be faster in **107** than in **106**, which supported the difference of reactivity observed in Table 21.

4.12 Substrate Scope using Catalyst 102: Amino alcohols

Diamine moieties are present in several biologically active compounds.⁸⁸ Figure 39 reports three examples of drugs containing a diamine in their structure.

Figure 39

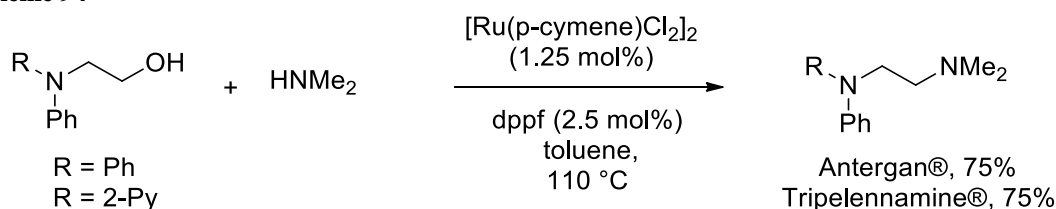


Tamiflu® is a powerful antiviral used to prevent and treat influenza A and influenza B,⁸⁹ which has been considered as a front line defence against the avian flu.⁸⁸ Lorabid® is a cephalosporin with antibacterial activity⁹⁰ and Eloxatin® is a 1,2-diaminoplatinum complex which has shown high anticancer activity.⁹¹ Thus, the possibility of using amino alcohols as starting materials was considered. The final products would contain two

nitrogens in the β position to each other that could be functionalised orthogonally. Additionally, since the amine racemisation reactions with catalyst **102** did not occur easily, it would be potentially possible to obtain enantiopure compounds starting with chiral amino alcohols.

First of all, we sought in the literature to verify that this type of alcohol has not been used in hydrogen borrowing before. To the best of our knowledge, only three examples have been reported in which amino alcohols have been used in the hydrogen borrowing methodology. In the first paper, Williams and co-workers utilised two different amino alcohols to synthesise two pharmaceutical compounds in high yield using a ruthenium catalyst and dppf as additive (Scheme 94).¹⁵

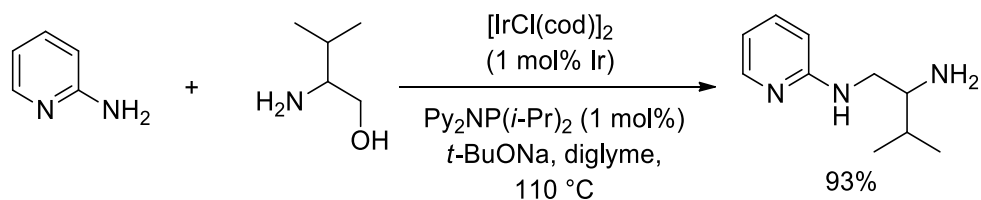
Scheme 94



However, the substrate scope was limited and other protecting groups on the amine were not reported in this paper.

In the second example, Kempe and co-workers reported that an iridium(I) catalyst generated *in situ* by mixing $[\text{IrCl}(\text{cod})]_2$ and a P,N ligand could promote the *N*-alkylation of aromatic and heteroaromatic amines with amino alcohols. This methodology also showed some limitations, because the reaction did not work when secondary alcohols or aliphatic amines were used (Scheme 95).⁹²

Scheme 95

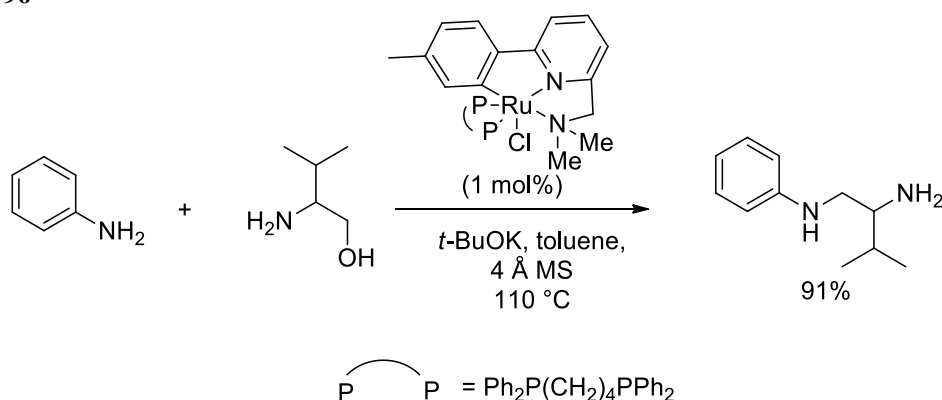


The authors also observed that the reaction proceeded faster when 2-aminopyridine was used, for which they managed to add only 1 mol% of iridium. However, when they used 3-aminopyridine and 4-aminopyridine, the yields decreased, even if they increased

respectively the amount of iridium to 2 mol% and 4 mol%. Finally, when they used anilines, they achieved good yields (63-86%) only by increasing the amount of iridium to 5 mol%. Interestingly, they also reported that, even starting with chiral β -amino alcohols, only racemic products were obtained.

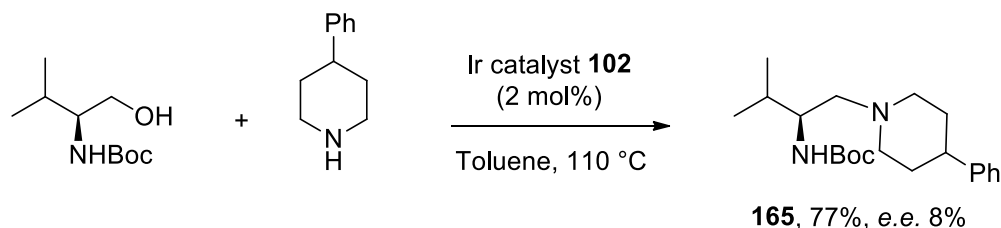
In the last paper, a similar catalyst has been reported to promote this reaction; in this case, a ruthenium pincer complex was found to be an active catalyst for the alkylation of aromatic amines with amino alcohols (Scheme 96).⁹³ Again for this methodology, the authors reported similar substrate limitations to those described in the previous example.

Scheme 96



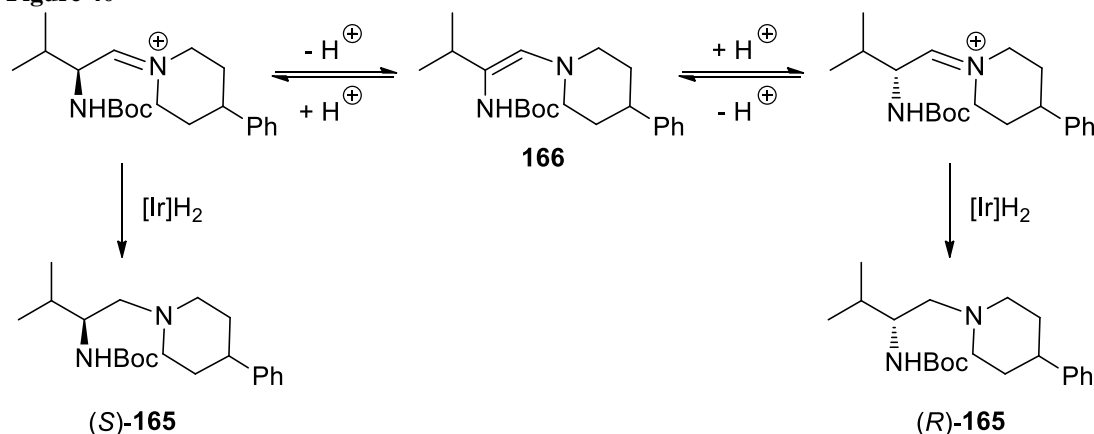
These few examples reported in the literature showed many limitations for the substrate scope and for the functional groups that could be tolerated. For instance, to the best of our knowledge, there were no examples in which aliphatic amines were used with readily synthetically accessible *N*-protected amino alcohols. Our first effort was to test our catalyst **102** in a simple reaction between *N*-Boc-L-valinol and 4-phenylpiperidine using 2 mol% of iridium (Scheme 97). We were pleased to observe that a 77% isolated yield of product **165** was achieved using this unoptimised procedure.

Scheme 97



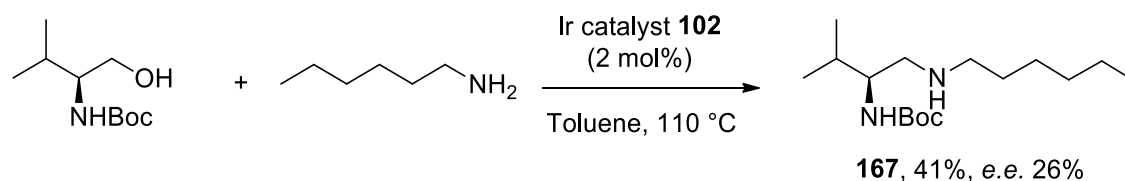
Disappointingly, chiral HPLC analysis showed that an almost complete racemisation occurred in the reaction (8% *e.e.*). Decreasing the temperature from 110 °C to 95 °C gave only a slightly better *e.e.* (13%). The racemisation probably occurred when the iminium ion was formed, which could easily give the enamine **166**, losing the stereogenic information. The following hydrogenation step gave the racemic product **165**, as shown in Figure 40.

Figure 40



Since the migration of the double bond to form the enamine from the imine is usually slower than from an iminium ion, our next attempt was to use a primary amine. The reaction between *N*-Boc-L-valinol and *n*-hexylamine was carried out using 2 mol% of catalyst **102** (Scheme 98).

Scheme 98

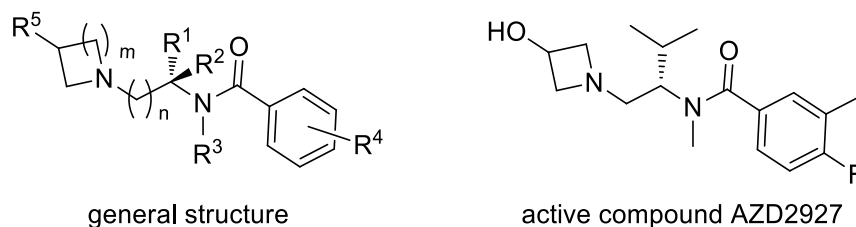


Disappointingly, product **167** was isolated in 41% yield and the observed enantiomeric excess, even if better than the previous example, was poor, at only 26%. However, to the best of our knowledge, this is the first example in which primary and secondary amines were alkylated with *N*-Boc-protected amino alcohols obtaining the corresponding products in good yield.

Our last effort was to investigate the use of azetidines as starting materials. Recently, AstraZeneca has patented a family of compounds, which were found to be active in the

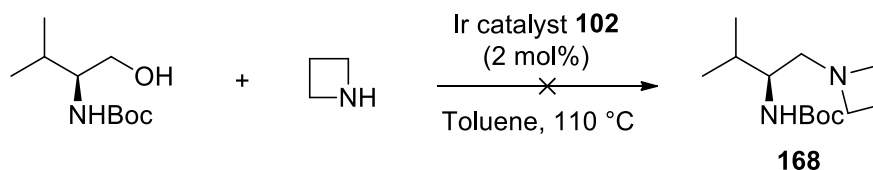
treatment of atrial fibrillation.⁹⁴ These substrates could potentially be made by hydrogen borrowing. Figure 41 shows the general structure of this family and the most active molecule.

Figure 41



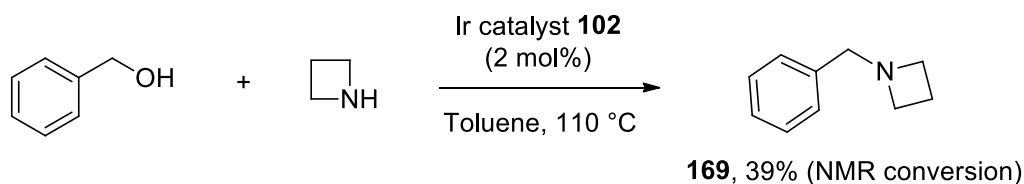
With the idea to synthesise the active compound AZD2927 after the optimisation of the reaction conditions, a reaction between azetidine and *N*-Boc-L-valinol was carried out. Disappointingly, it did not afford the product **168**, but only the signals of the amino alcohol were observed in the crude NMR spectrum (Scheme 99).

Scheme 99



Azetidines are four member ring cycles, which may be reluctant to form the corresponding iminium ion because they would form an sp^2 nitrogen on a very small and rigid ring. Thus, our next effort was to investigate the suitability of the azetidine with our methodology. A simpler reaction between benzyl alcohol and azetidine was carried out using 2 mol% of catalyst **102**. Even though the compound **169** was obtained with a 39% NMR conversion, we did not manage to purify it by flash chromatography (Scheme 100).

Scheme 100



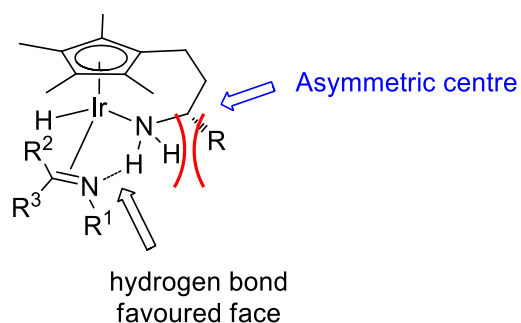
Since the boiling point of the azetidine is 61 °C, our next attempt was to decrease the reaction temperature to avoid the possible evaporation of the reagent. Unfortunately, even if the reaction was run at 80 °C, product **169** was obtained only with a 10% NMR conversion, suggesting that azetidines were not good substrates for our catalysts.

4.13 Synthesis of Chiral Amines using Iridium Catalysts **113** and **119**

The work presented in this section has been carried out by Ashley Thompson, an MChem project student in our group.

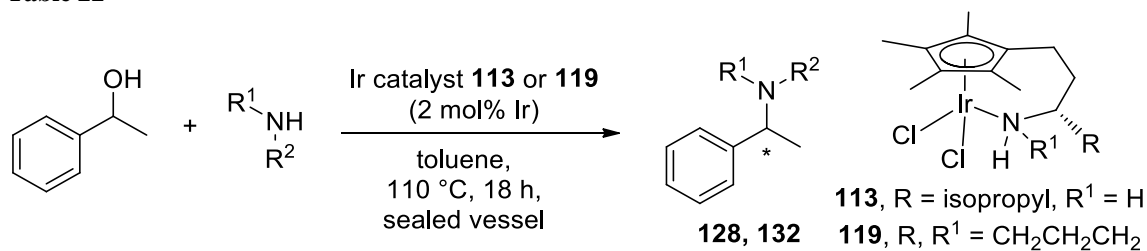
Two chiral iridium complexes, **113** and **119**, have been synthesised and characterised starting from enantiopure amino acid derivatives. Our aim was to block one of the two faces of the imine, so the hydrogenation would prefer the less bulky face to give an enantiomerically enriched product, as shown in Figure 42.

Figure 42



The two catalysts were tested in two different reactions, between 1-phenylethanol and two different amines: *n*-hexylamine and piperidine. Table 22 reports the results achieved.

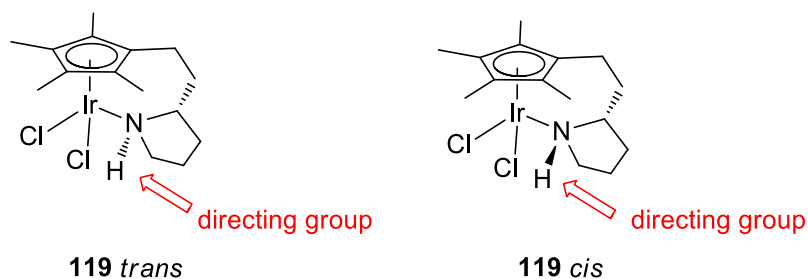
Table 22



Entry	Amine	Catalyst	Isolated Yield (%)	e.e. (%)
1	<i>n</i> -Hexylamine	113	128 , 54	6%
2	<i>n</i> -Hexylamine	119	128 , 36	<2%
3	Piperidine	113	132 , 61	10%
4	Piperidine	119	132 , 23	<2%

Unfortunately, the enantiomeric excesses achieved using these two catalysts were very poor. The best results were achieved using complex **113** which contains an isopropyl group in the side chain (entries 1 and 3), whereas catalyst **119** gave almost racemic compounds (entries 2 and 4). Complex **119** was formed as a non-interconverting ~ 1 : 1 mixture of two diastereoisomers and it may be that the effect of the N-H moiety was more important than the role of the stereocentre (Figure 43).

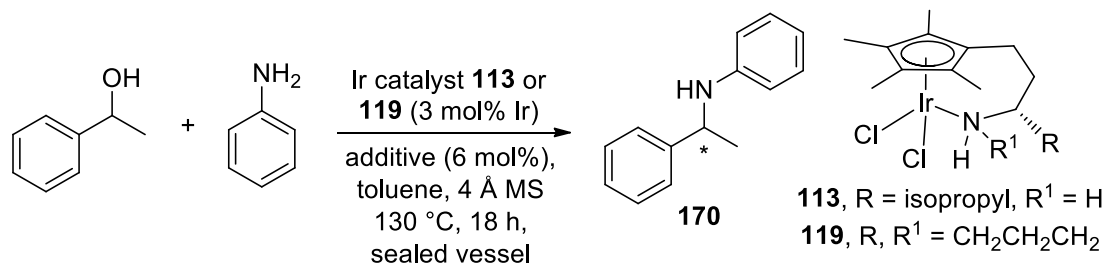
Figure 43



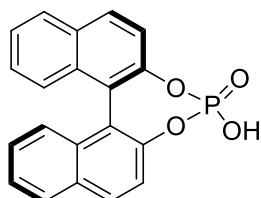
Thus, we sought to confirm our hypothesis trying to separate the two diastereoisomers but unfortunately, it was found that they could not be separated by flash chromatography and they showed only one peak in the LC-MS. Besides, a high temperature ¹H-NMR spectrum in deuterated acetonitrile showed that both diastereoisomers were not interconverting.

Additionally, our chiral catalysts were tried in a reaction between 1-phenylethanol and aniline, with a chiral BINOL phosphoric acid added as an additive, following a similar methodology reported in the literature (Table 23).⁶¹

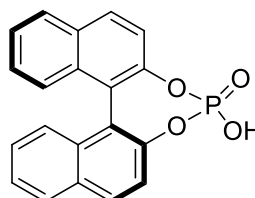
Table 23



Additives:



(*R*)-BINOL phosphoric acid



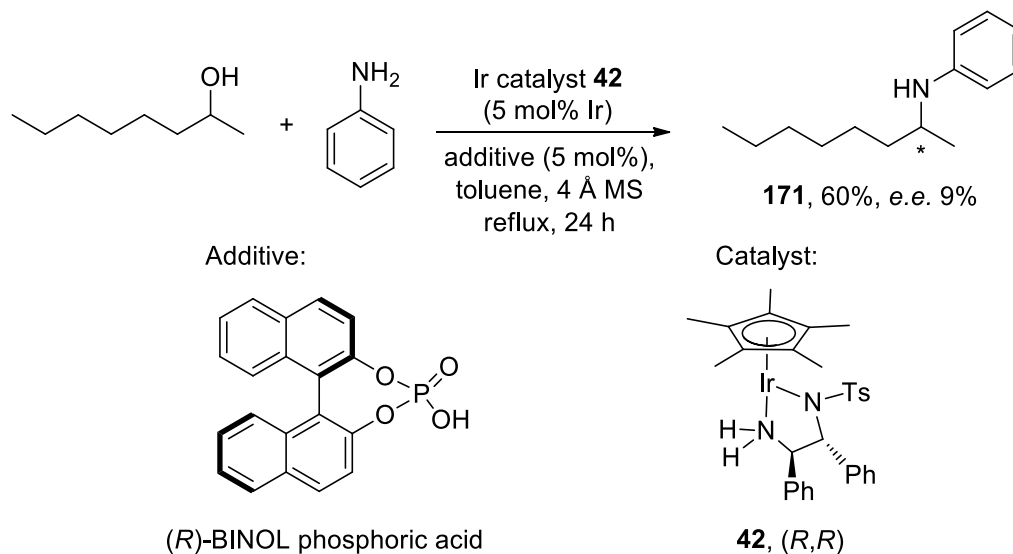
(*S*)-BINOL phosphoric acid

Entry	Additive	Catalyst	Isolated Yield (%)	<i>e.e.</i> (%) ^a
1	(<i>R</i>)-BINOL phosphoric acid	113	170 , 41	+7%
2	(<i>R</i>)-BINOL phosphoric acid	119	170 , 36	-2%
3	(<i>S</i>)-BINOL phosphoric acid	113	170 , 46	+3%
4	(<i>S</i>)-BINOL phosphoric acid	119	170 , 38	-4%

^aThe sign of the enantiomeric excess is relative.

Both (*R*) and (*S*) enantiomers of the chiral phosphoric acid were tried to evaluate the match/mismatch with our complexes. The best catalyst was again **113**, which gave the highest *e.e.* (+7%) matched with the (*R*)-BINOL phosphoric acid. The sign of the enantiomeric excess is relative, because the absolute (*R*) or (*S*) configuration of the product is unknown and currently under investigation. Interestingly, complex **113** afforded the product **170** with a small preference for the formation of the same enantiomer, even though it was matched with both (*R*) and (*S*) enantiomers of the chiral phosphoric acid (entries 1 and 3). Unexpectedly, our catalyst **119** gave a better *e.e.* matched with the (*S*)-BINOL phosphoric acid, showing a small preference for the formation of the other enantiomer (-4%). Pleasingly, the best enantiomeric excess obtained with our complex **113** (entry 1) was comparable to the one reported in the literature (Scheme 101), which suggests that higher yields and *e.e.s* could be achieved with further improvements.⁶¹

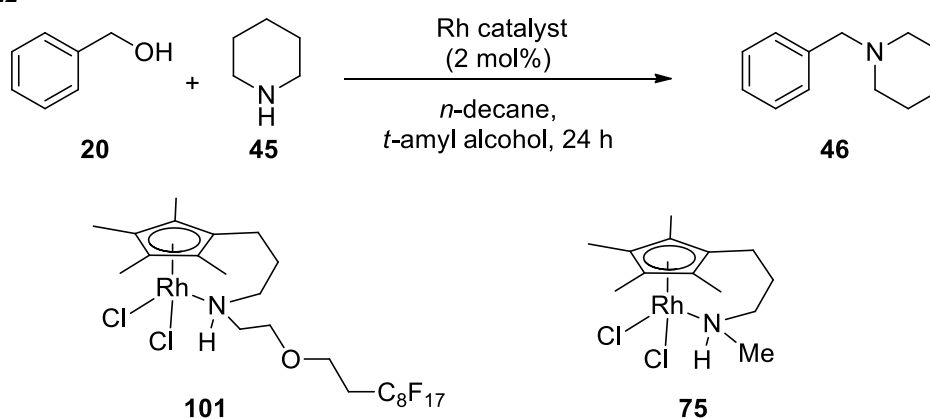
Scheme 101

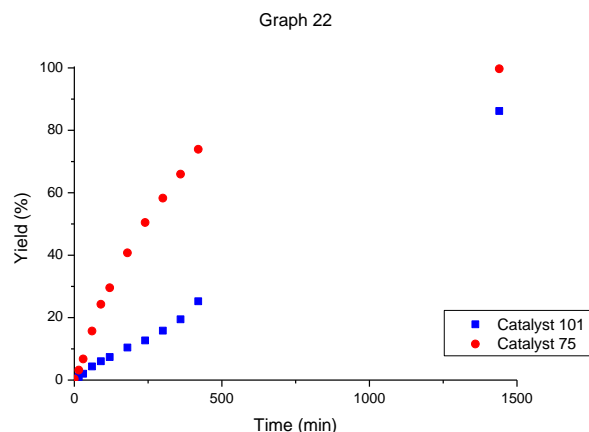


4.14 Activity of Rhodium Catalyst **101** and Attempts to Recycle

Rhodium catalyst **101** contains a fluororous tag on the tethered chain. Fluororous tagged compounds can generally be recovered by fluororous solid-phase extraction^{77,95} with good purity. Firstly, the activities of rhodium catalyst **101** and rhodium catalyst **75** were compared in order to evaluate the effect of the fluororous tag on the activity of the catalyst. Thus, catalyst **101** was used in our standard reaction between benzyl alcohol and piperidine in *t*-amyl alcohol (Graph 22).

Graph 22



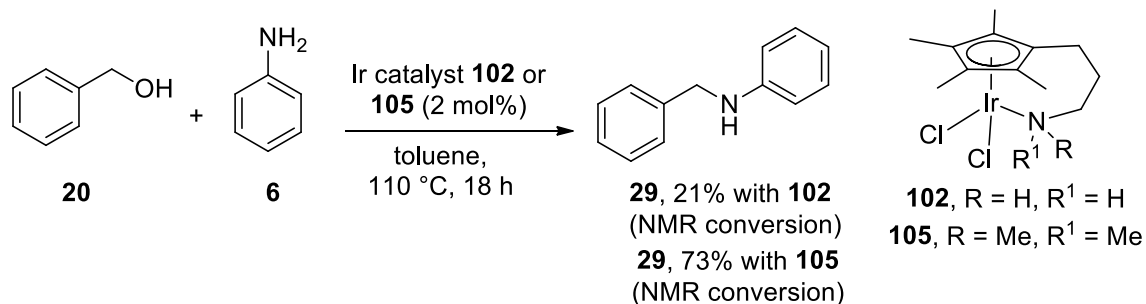


The catalyst bearing the fluororous tagged ligand **101** is less active than the previous monomer **75**; however, an almost 90% yield was achieved after 24 hours. Unfortunately, at the end of the reaction, we did not manage to separate the organic compounds from the fluororous tagged complex using a fluororous solid phase extraction (F-SPE). This unsuccessful separation could be due to the instability of the catalyst on the F-SPE cartridge or its decomposition in the reaction. The latter hypothesis was less probable, because the cleavage of the fluororous tagged chain would form a complex similar to **75** and it would not explain the slower activity of **101**. Thus, a small amount of pure catalyst **101** was purified with this cartridge to check its stability. Unexpectedly, we could not isolate the pure complex either in the non-fluororous fraction or the fluororous one, suggesting that the catalyst was not stable on the F-SPE cartridge. These results were quite surprising, because this catalyst was originally purified by silica gel flash chromatography. Our next attempt was to separate the fluororous tagged complex from the organic mixture using a liquid-liquid separation.⁹⁵ Unfortunately, complex **101** was not soluble either in perfluoro(butyltetrahydrofuran) (FC-75) or in perfluorohexane (FC-72). These results suggest that the design of catalysts containing a fluororous tag or other supported functional groups needs to be reconsidered in order to make more stable complexes. An alternative idea could be the introduction of a supported functional group linked directly on the Cp* ring, which gave good results in the recycle of the immobilised [Cp*IrCl₂]₂.⁹⁶

4.15 Mechanistic studies

Our last effort was to understand the mechanism of the reaction catalysed by our new class of complexes. One main consideration was that the presence of a N-H moiety on the catalyst was necessary to achieve fast reaction rates and higher yields. Complex **105** bearing a coordinated tertiary amine was not as active as catalysts **102** and **103**, meaning that the N-H functional group was involved in the catalytic cycle. The reaction between benzyl alcohol and aniline, which usually gave excellent yields in hydrogen borrowing,^{22,30,33} afforded the product in only moderate NMR conversion using catalyst **102** (Scheme 102), which was consistent with the selectivity for aliphatic amines over anilines shown previously in Scheme 92(c). Interestingly, the same reaction carried out using complex **105** gave product **29** in a better conversion (73%), suggesting again that the mechanism of these two catalysts was different.

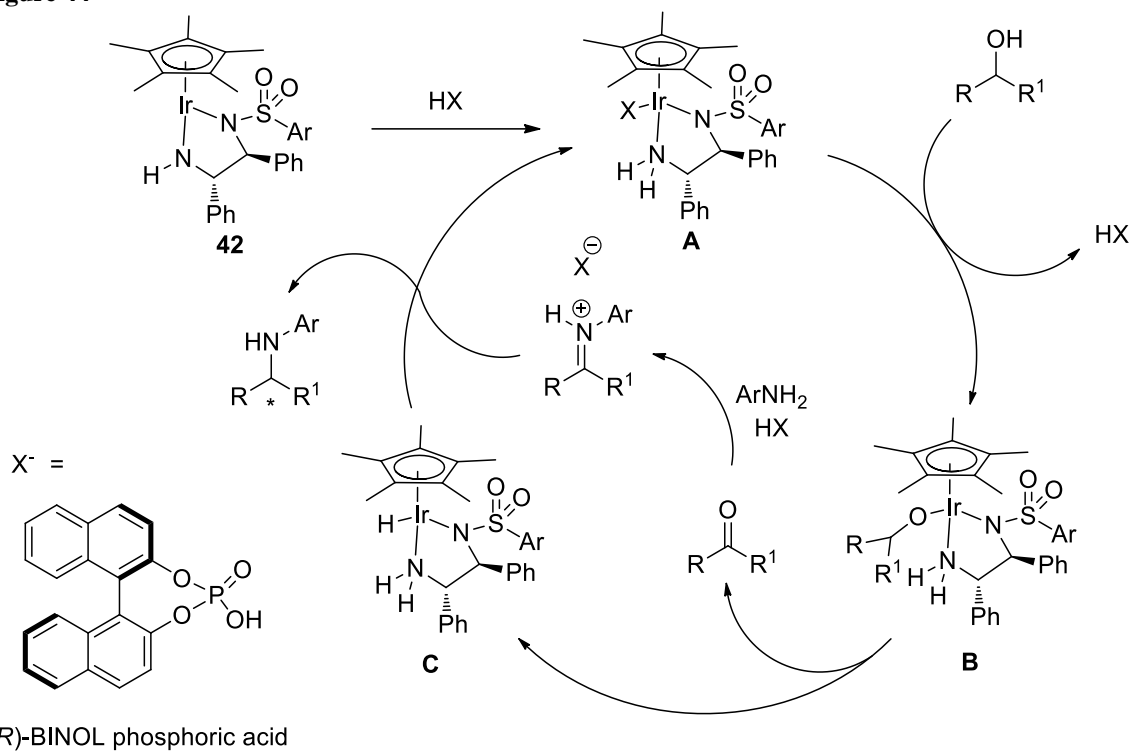
Scheme 102



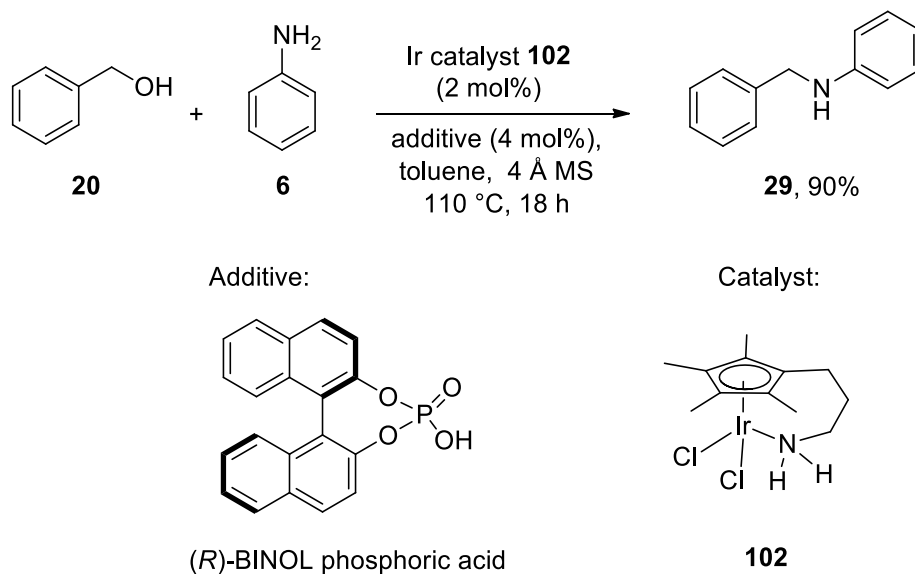
Fujita *et al.* proposed that the mechanism for the imine formation in the [Cp*IrCl₂]₂ catalytic cycle, reported previously in Figure 8, was metal-templated.²² These results supported our hypothesis that complex **105** behaved similarly to the dimer. On the contrary, our assumption was that the formation of the imine using complex **102** was not metal-templated and the aniline was not nucleophilic enough to give the corresponding imine. Zhao and co-workers have proposed an alternative mechanism for the enantioselective amination of alcohols in a cooperative catalysis by iridium and chiral phosphoric acid (Figure 44).⁶¹ The catalytic cycle proposed is an extension of the mechanism proposed by Noyori *et al.*⁵⁶ The first step was the formation of the species **A**, which was supported by NMR studies. They then hypothesised that the next step was the formation of the iridium-alkoxide species **B**, followed by the alcohol oxidation to give the iridium hydride intermediate **C**, which was again observed by NMR spectroscopy.

The formation of the imine was not metal-templated, but it was promoted by the chiral phosphoric acid, which also activates the imine as the iminium ion before the reduction. The formation of the iminium ion phosphoric acid salt was also reported independently by the groups of Xiao⁹⁷ and MacMillan.⁹⁸

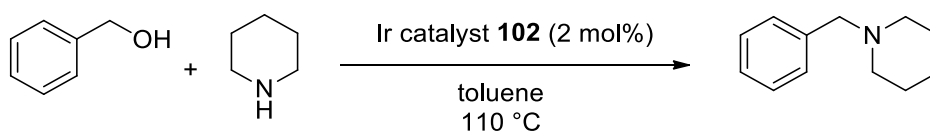
Figure 44

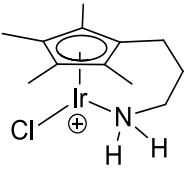
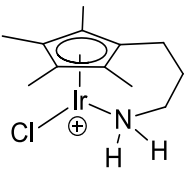
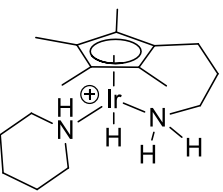
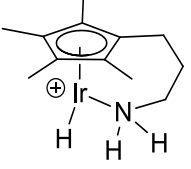
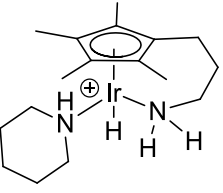
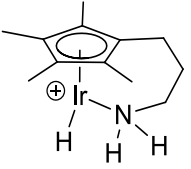


Thus, to confirm that our catalysts behaved with a similar mechanism, we added a substoichiometric amount of phosphoric acid in the reaction between benzyl alcohol and aniline. Pleasingly, compound **29** was isolated in 90% yield (Scheme 103), supporting the hypothesis that the mechanism proposed in Figure 44 could be similar to our catalytic cycle.

Scheme 103

Our next effort was to seek intermediates in the catalytic cycle. We thought that mass spectral analyses of the crude mixtures could be helpful in understanding which complexes were formed in the reaction. Additionally, the accurate mass instrument was sensitive enough to detect the mass of the complex, even if it was present in only small amounts. Table 24 shows the iridium-containing intermediates found. In entry 2, catalyst **102** was mixed with the benzyl alcohol; the mass observed was the same one achieved with the catalyst alone (entry 1), suggesting that the alcohol did not strongly coordinate to the iridium. The addition of the piperidine made two new species both in the presence and absence of benzyl alcohol (entries 3 and 4).

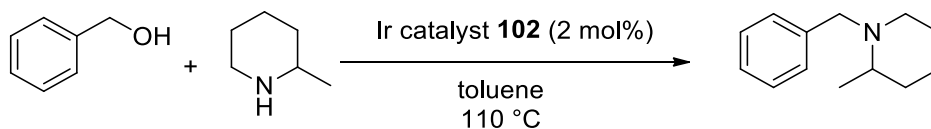
Table 24

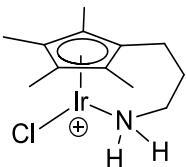
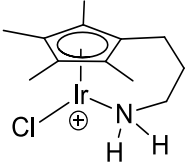
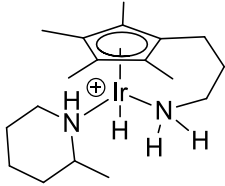
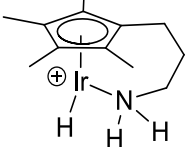
<i>Entry</i>	<i>Reagents</i>	<i>Intermediates</i>	<i>Mass</i>
1	Catalyst alone		Found: 406.0901; Calculated for C ₁₂ H ₂₀ ³⁵ Cl ¹⁹³ IrN: 406.0900.
2	Catalyst + benzyl alcohol		Found: 406.0911; Calculated for C ₁₂ H ₂₀ ³⁵ Cl ¹⁹³ IrN: 406.0900.
3	Catalyst + piperidine		Found: 457.2190; Calculated for C ₁₇ H ₃₂ ¹⁹³ IrN ₂ : 457.2190.
			Found: 372.1296; Calculated for C ₁₂ H ₂₁ ¹⁹³ IrN: 372.1298.
4 ^a	Catalyst + piperidine + benzyl alcohol		Found: 457.2201; Calculated for C ₁₇ H ₃₂ ¹⁹³ IrN ₂ : 457.2190.
			Found: 372.1302; Calculated for C ₁₂ H ₂₁ ¹⁹³ IrN: 372.1298.

^a Sample collected after 5 minutes at 110 °C.

To confirm that one of the intermediates had an amine coordinated to the iridium, the reaction was repeated with 2-methylpiperidine (Table 25).

Table 25

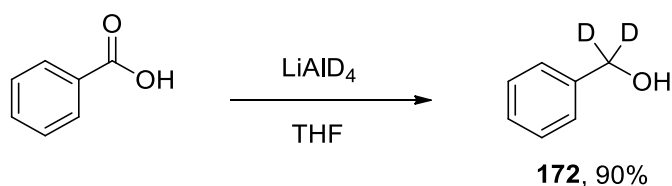


Entry	Reagents	Intermediates	Mass
1	Catalyst alone		Found: 406.0901; Calculated for $C_{12}H_{20}^{35}Cl^{193}IrN$: 406.0900.
2	Catalyst + benzyl alcohol		Found: 406.0899; Calculated for $C_{12}H_{20}^{35}Cl^{193}IrN$: 406.0900.
3 ^a	Catalyst + 2-methyl piperidine + benzyl alcohol		Found: 471.2357; Calculated for $C_{18}H_{34}^{193}IrN_2$: 471.2346.
			Found: 372.1294; Calculated for $C_{12}H_{21}^{193}IrN$: 372.1298.

^a Sample collected after 5 minutes at 110 °C.

Similar results of those reported before were found in this experiment. The alcohol-iridium coordination was again not observed (entry 2). The addition of the 2-methylpiperidine made the corresponding two iridium species observed before, which supports the hypothesis that one of the intermediates contains an amine-iridium coordination (entries 3 and 4). Interestingly, it was found that, after the addition of the amine, the iridium species contained a hydride in its coordination sphere, which could come partially from the oxidation of the alcohol to the corresponding aldehyde. Thus, we sought to analyse the incorporation of deuterium in the complex. The required deuterated benzyl alcohol was synthesised by the reduction of benzoic acid with $LiAlD_4$ in THF which gave $[1',1'-^2H_2]$ benzyl alcohol **172** in 90% yield (99% D), following the procedure reported in the literature (Scheme 104).⁹⁹

Scheme 104



The reaction between [1',1'-²H₂] benzyl alcohol and piperidine was carried out and the results were reported in Table 26, in comparison with the entry 2 in Table 24 and the simulated pattern for the non-deuterated compound. In brackets, the intensity of the peaks is reported.

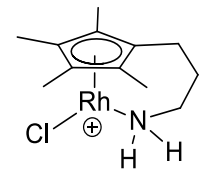
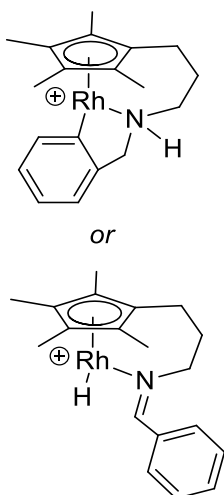
Table 26

<i>Intermediates</i>	<i>Mass (current experiment)</i>	<i>Entry 3, Table 24</i>	<i>Simulated pattern</i>
	455.2158 (59%); 456.2205 (21%); 457.2190 (100%); 458.2231 (38%).	455.2153 (58%); 456.2181 (12%); 457.2190 (100%); 458.2217 (16%).	455.2166 (58%); 456.2198 (11%); 457.2190 (100%); 458.2221 (19%).
	370.1269 (61%); 371.1317 (18%); 372.1293 (100%); 373.1243 (28%).	370.1270 (56%); 371.1300 (7%); 372.1296 (100%); 373.1325 (14%).	370.1274 (58%); 371.1307 (8%); 372.1298 (100%); 373.1330 (13%).

Pleasingly, the coordination of deuterium is evident in both the two iridium species because the peaks which would correspond to the deuterated complex increased in intensity in the current experiment. It was found that the hydride came partially from the oxidation of the alcohol to the corresponding aldehyde; however, the hydrides that were coordinated to the metal came mainly from other sources. Our hypothesis was that the hydrides could come from the oxidation of the piperidine to the corresponding iminium species or to the enamine, which mechanism has already been observed in the literature, *e.g.* by the groups of Bruneau⁴⁶ and Beller.¹⁰⁰

Interestingly, when the rhodium complex **67** was used and analysed by accurate mass, the corresponding rhodium species to those observed for iridium were not found. Instead, the mass of a different intermediate was assigned (Table 27).

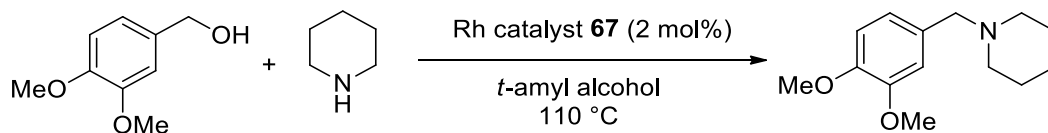
Table 27

Entry	Reagents	Intermediates	Mass
1	Catalyst + benzyl alcohol		Found: 316.0335; Calculated for $C_{12}H_{20}^{35}ClNRh$: 316.0334.
2 ^a	Catalyst + piperidine + benzyl alcohol		Found: 370.1041; Calculated for $C_{19}H_{25}NRh$: 316.0334.

^a Sample collected after 60 minutes at 110 °C.

Again, evidence of alcohol-rhodium coordination were not found (entry 1). The structure of the intermediate in entry 2 was not certain and two hypotheses were made; however, in both the cases it seems that a molecule of alcohol reacted with the coordinated amine on the rhodium to form an imine or a rhodacycle. The following attempt was to seek evidence of the formation of one of these two rhodium species by NMR spectroscopy. Thus, benzyl alcohol and piperidine were heated at reflux with a stoichiometric amount of rhodium complex **67** in deuterated DMSO. Unfortunately, even if the signals of the complex changed, we did not manage to identify which compounds were coordinated on the metal. Our last effort was to change the alcohol to see if the mass of the intermediate would change, confirming the presence of the benzyl group attached to the amine (Table 28).

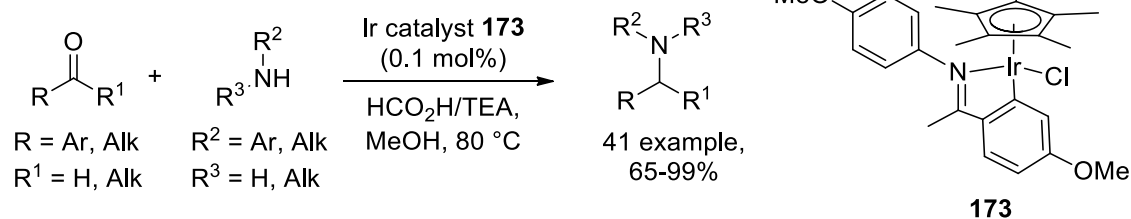
Table 28



<i>Entry</i>	<i>Reagents</i>	<i>Intermediates</i>	<i>Mass</i>
1	Catalyst + piperidine + 3,4-dimethoxy benzyl alcohol		Found: 428.1091; Calculated for C ₂₁ H ₂₇ NO ₂ Rh: 428.1091.
2	Catalyst + piperidine + 3,4-dimethoxy benzyl alcohol		Found: 430.1251; Calculated for C ₂₁ H ₂₇ NO ₂ Rh: 430.1248.

Starting with 3,4-dimethoxybenzyl alcohol, the mass of the intermediates changed, confirming that the benzyl group coming from the alcohol is attached to the coordinated amine (entry 2). Interestingly, in this experiment, also the mass corresponding to the intermediate shown in entry 1 was detected, which supported the hypothesis that a rhodacycle could be the active catalyst. Xiao and co-workers reported that a similar iridium complex, **173**, was found to catalyse the transfer hydrogenation reaction between an aldehyde or a ketone and an amine (Scheme 105).¹⁰¹

Scheme 105

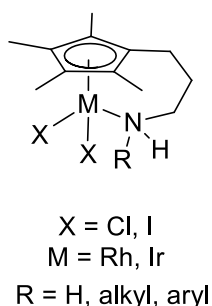


This complex **173** is similar to the structure proposed in entry 1, Table 28, which supports the hypothesis that a rhodacycle could be the active catalyst in our system.

4.16 Conclusions

Our two classes of rhodium and iridium complexes have shown to be active in hydrogen borrowing. Several modifications on the ligand have been tested in catalytic reactions, including the length of the side chain, the substituents on the coordinated amine and the effect of the halide ligands. Both the activities of rhodium and iridium complexes were not influenced by the presence of a secondary amine in the side chain, but the length of the side chain was fundamental to the catalyst activity, with an optimal length of three CH₂ units (Figure 45). A tertiary amine on the side chain decreases the activity of this family of catalysts, both for the rhodium and for the iridium. The halogens that complete the coordination of the complex also influence the activity of the catalysts; however, both the dichloride and diiodide monomers were more active than the corresponding rhodium and iridium dimers, affording the product with higher yield and faster reaction rates.

Figure 45

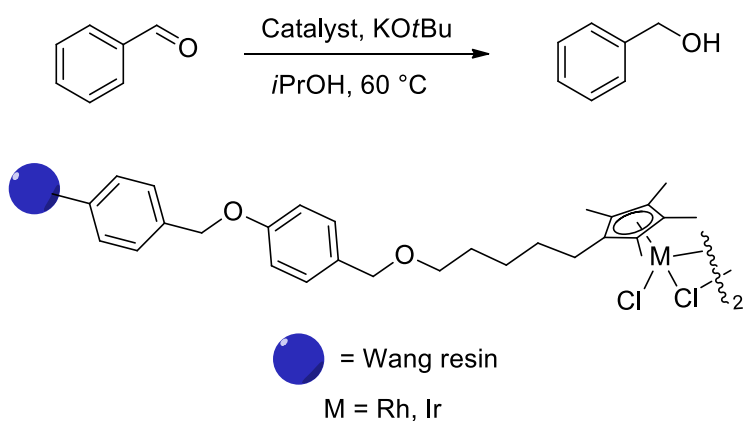


Among rhodium and iridium complexes, iridium(III) catalysts **102** and **103** showed the best activities in the hydrogen borrowing methodology. The solvent and functional group

tolerances using these catalysts were wide. Iridium monomer **102** promoted the reaction both in non-polar and polar solvents, such as toluene, *t*-amyl alcohol, isopropyl acetate, 2-methylTHF, DMF, DMSO and acetonitrile in good yield (>70%). Catalyst loading could be decreased as low as 0.1 mol% Ir, achieving quantitative yield after 24 hours. More than 20 substrates containing aryl, heteroaryl and alkyl groups were prepared in 62-99% yields using the iridium catalyst **102**; among them, primary and secondary alcohols and primary and secondary amines have been used. Furthermore, a broad range of functional groups were tolerated, such as halides, nitriles, ethers, esters, amides, sulfonamides and carbamates. Finally, amino alcohols can also be tolerated obtaining the alkylated products in good yields. A study of the mechanism was begun to seek evidence of the role of the N-H moiety in this reaction and to determine the active intermediates in the catalytic cycle.

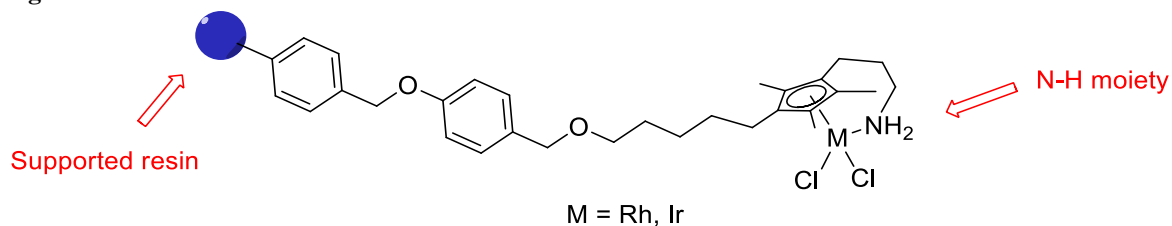
A complex containing a fluororous-tagged ligand on the side chain was tested in our methodology with the idea of recycling the catalyst. Unfortunately, our attempts to recover the complex at the end of the reaction were in vain. However, McGowan and co-workers have shown that the introduction of a Wang resin linked directly on the Cp* ring maintained activity in the complex in hydrogen borrowing processes and gave good results in the recycle of the immobilised $[\text{Cp}^*\text{IrCl}_2]_2$ up to 26 runs (Scheme 106).⁹⁶

Scheme 106



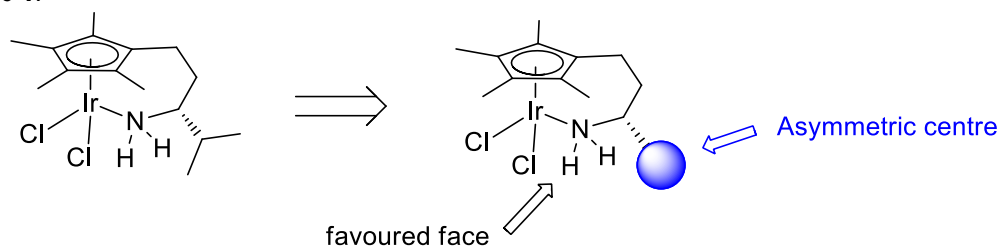
A possible future improvement would be the synthesis of similar complexes containing a supported group on the Cp* ring and bearing an amine on the side chain, as shown in Figure 46.

Figure 46



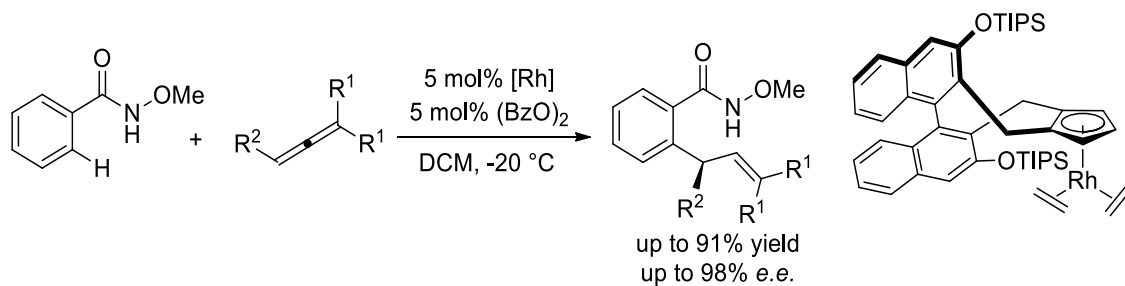
Finally, our last modification was the introduction of a stereocentre in the side chain starting from enantiopure amino acids. The best results were obtained when the iridium catalyst **113**, which contained an isopropyl group on the side chain, was used. Unfortunately, the enantiomeric excess was poor. Two main modifications could improve the enantioselectivity in these processes. The first one would modify the isopropyl group in complex **113** with a bulkier group as shown in Figure 47. In this way, the combined effect of the bulky group and the directing effect of the N-H moiety would favour the formation of one enantiomer with higher *e.e.*

Figure 47



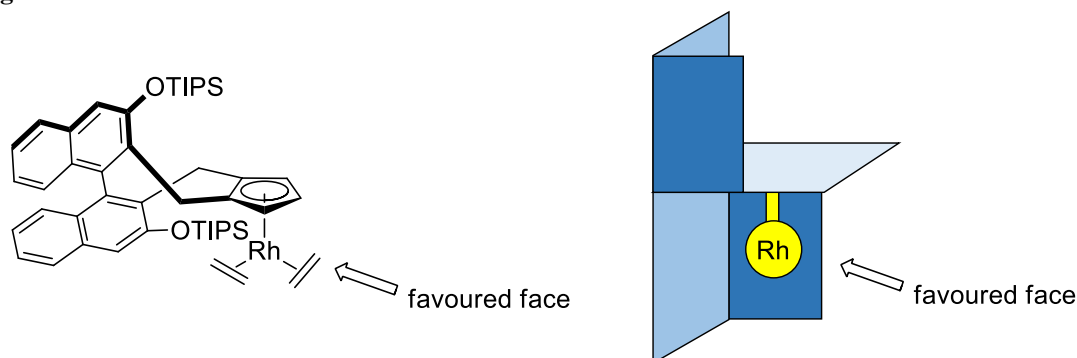
The second possible modification would introduce the asymmetry in the Cp* ligand. Recently, similar modifications of the cyclopentadienyl ligand were reported by the groups of Cramer¹⁰² and Rovis¹⁰³, who then used these new complexes in C-H activation with excellent enantioselectivity. Scheme 107 reports an example of an asymmetric methodology developed by Cramer and co-workers using the second-generation of their chiral catalysts.¹⁰⁴

Scheme 107



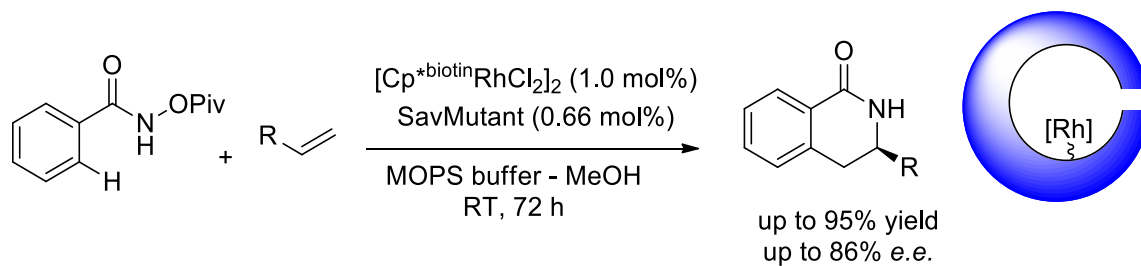
Conceptually, they synthesised a complex with a chiral ligand that blocked one of the faces of the metal. Therefore, to minimise the steric interaction, the coordination between the metal and the reactants was favoured on the more accessible face. The chirality of the ligand was finally transferred to the substrates, which generated the enantioselectivity (Figure 48).¹⁰⁴

Figure 48



Using a different strategy, Rovis and co-workers achieved asymmetric C-H activation docking the biotinylated rhodium(III) complex, [Cp*^{biotin}RhCl₂]₂ to the mutant of the protein streptavidin (SavMutant) (Scheme 108).¹⁰³

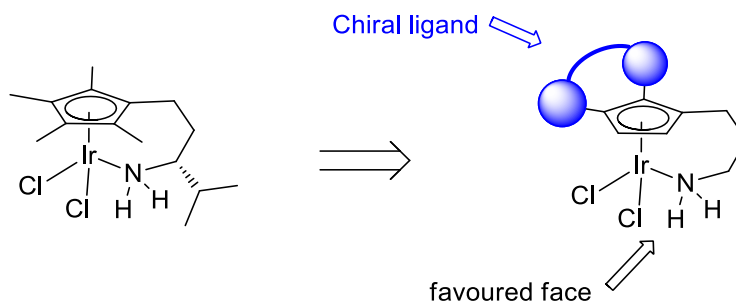
Scheme 108



The enantiomeric excess in the substrate came from the chiral environment of the protein streptavidin in a second coordination sphere.¹⁰⁵

As results of these considerations, a second family of chiral catalysts could be synthesised introducing the chirality *via* a cyclopentadienyl ligand modification (Figure 49).

Figure 49

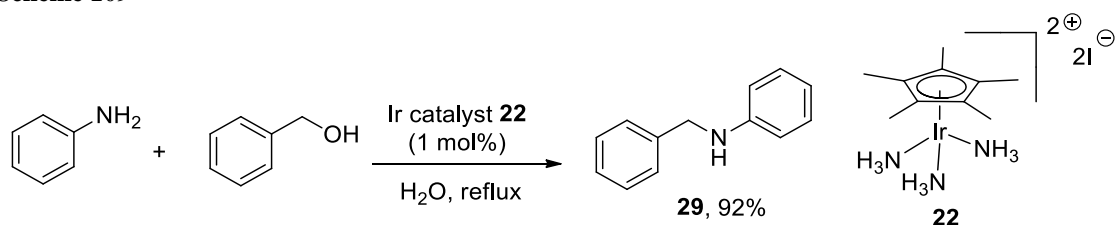


Chapter 5. Improved Catalytic Activity using Dicationic Rhodium and Iridium Complexes

5.1 Activity of Dicationic Rhodium Complex 93

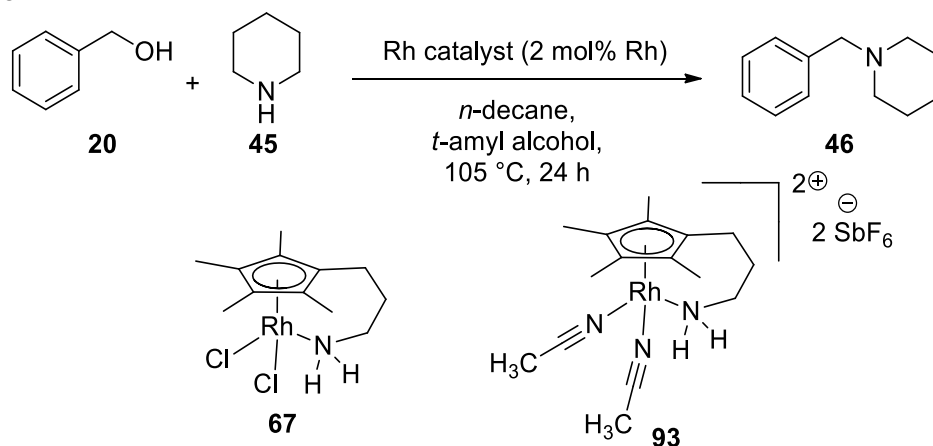
Recently, Fujita *et al.* have demonstrated that dicationic iridium catalysts could be used in hydrogen borrowing and their complex **22** has shown an improved activity in water (Scheme 109).²⁷

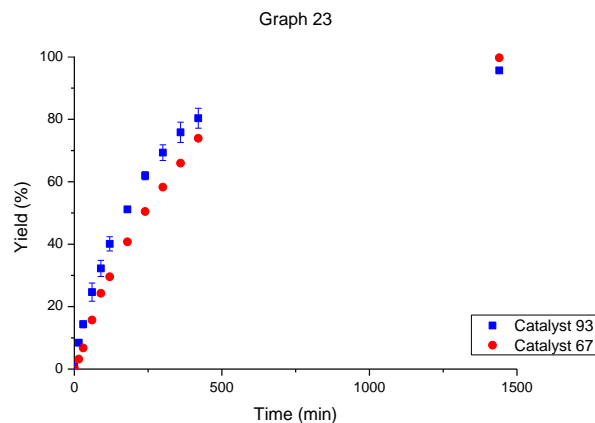
Scheme 109



Attempting to further increase the reaction rate in our processes, we designed the corresponding dicationic versions of our complexes, completing the coordination on the metal with two labile molecules of acetonitrile. Dicationic rhodium catalyst **93** was tested in the standard reaction between benzyl alcohol and piperidine using 2 mol% of rhodium in *t*-amyl alcohol and the yield profile has been compared with the one obtained with our previous rhodium monomer **67** (Graph 23).

Graph 23



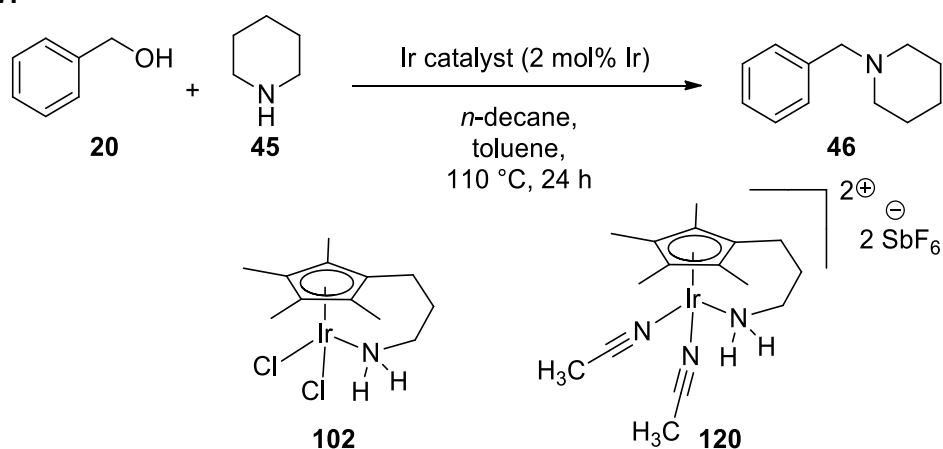


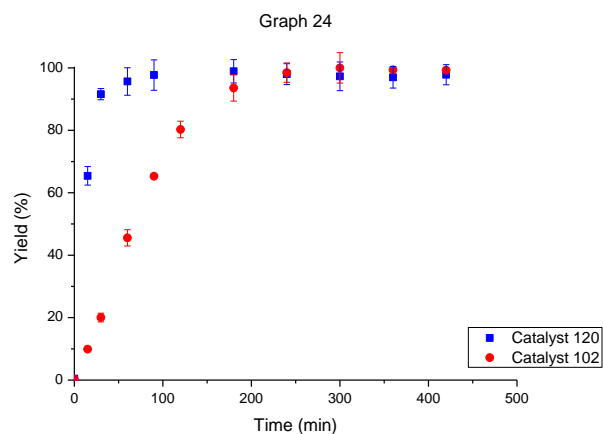
This graph reports the average yield of 2 or 3 experiments and error bars are referred to the relative statistical errors. Disappointingly, the new cationic catalyst **93** was only slightly faster than **67** and the yield profiles obtained with **93** and **67** were similar.

5.2 Activity of Dicationic Iridium Complexes **120** and **122**

Our next effort was to evaluate the activity of the corresponding dicationic iridium catalyst **120**. Thus, a reaction between benzyl alcohol and piperidine in toluene using 2 mol% of **120** was carried out. Graph 24 shows the yield profiles obtained with our complexes **102** and **120**. This graph reports the average yield of 2 or 3 experiments and error bars are referred to the relative statistical errors.

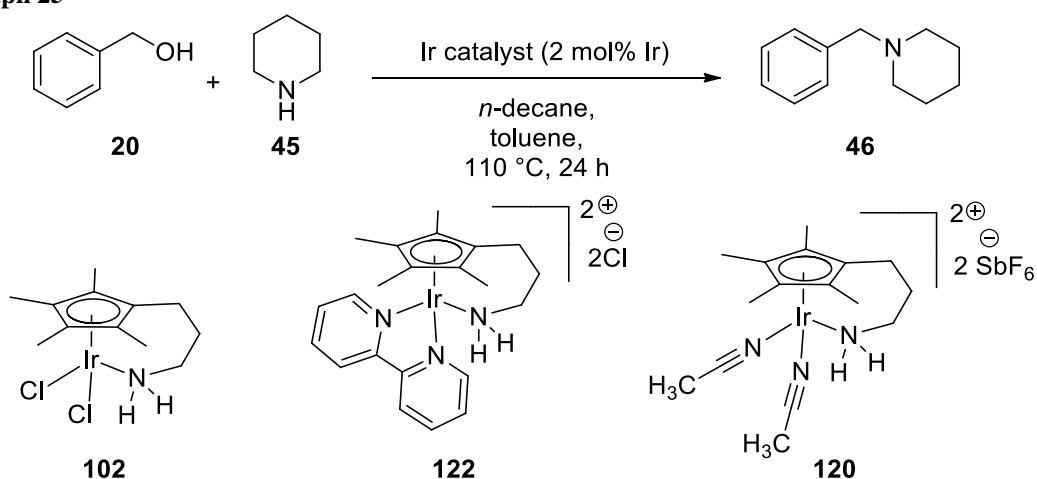
Graph 24

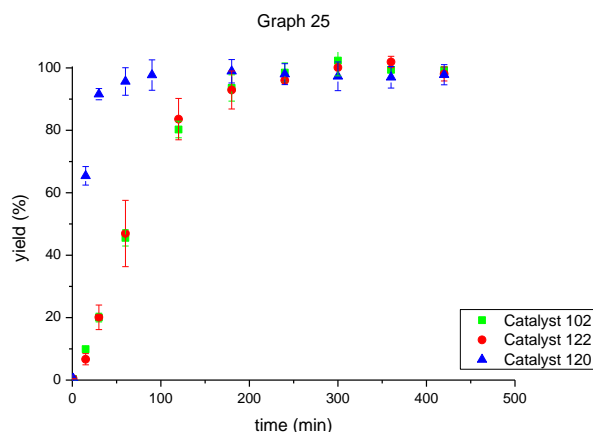




Pleasingly, this time the cationic iridium catalyst **120** definitely showed a faster reaction rate than the corresponding dichloride monomer **102** and product **46** was achieved with complete conversion after only 1 hour. This was a great improvement from our previous catalysts and, obviously, from the dimer $[\text{Cp}^*\text{IrCl}_2]_2$. Our next effort was to study the role of the acetonitrile in the improved activity of the complex. Thus, a different dicationic iridium complex **122** was tested in our standard reaction between benzyl alcohol and piperidine; in this case, the two coordinated chlorides were substituted with a molecule of 2,2'-bipyridine. Graph 25 reports the results obtained comparing the yield profile with those achieved with **120** and **102**.

Graph 25

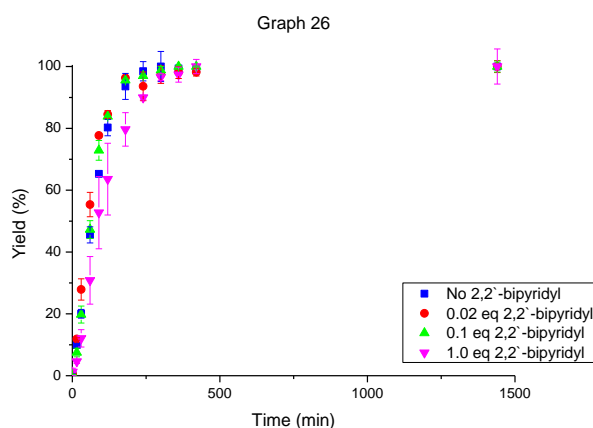
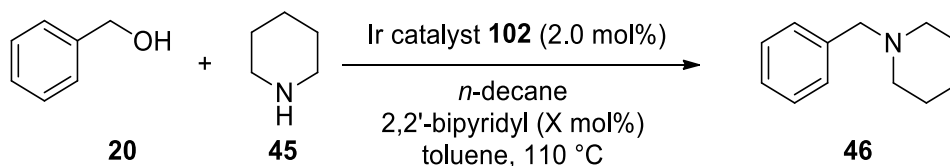




Catalysts **102** and **122** showed a similar activity, suggesting that they converged on a similar intermediate. On the contrary, catalyst **120** gave the fastest reaction rate among the three complexes.

If the coordination between 2,2'-bipyridine **121** and **102** was very strong, starting materials with a similar structure of **121** could potentially poison the catalyst. Thus, to study the effect of the 2,2'-bipyridine **121** in the reaction system, several reactions were carried out adding different aliquots of **121** (Graph 26).

Graph 26



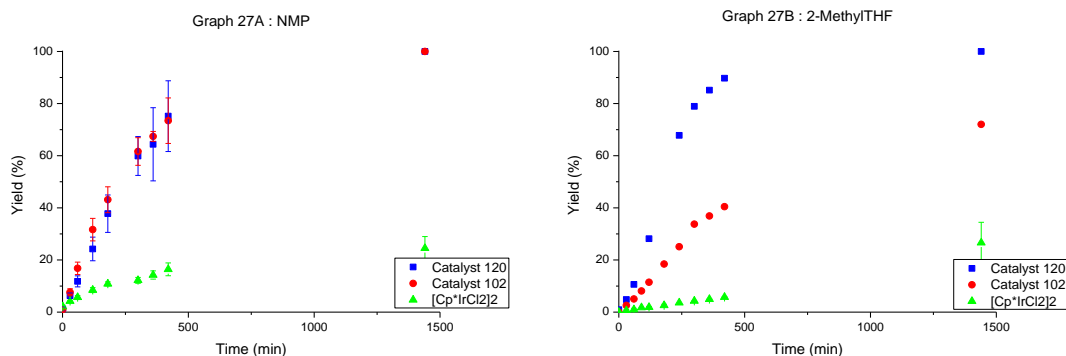
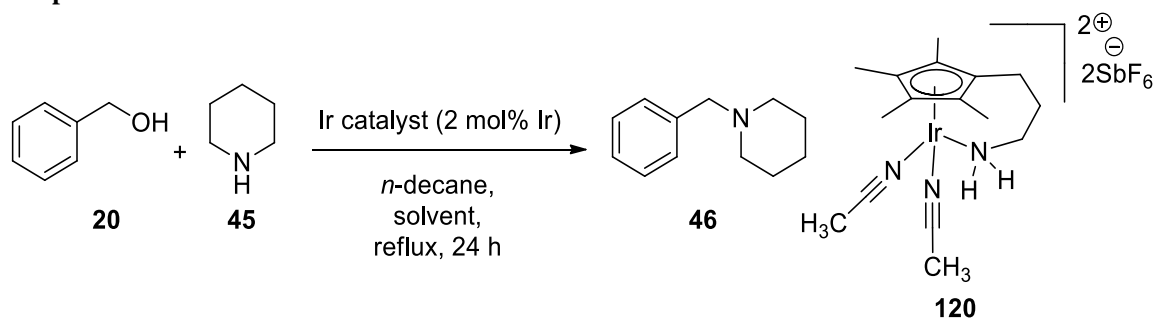
The addition of substoichiometric amounts of 2,2'-bipyridine **121** (0.02 and 0.1 equivalents) did not poison the complex; the reaction rates were similar to the reaction

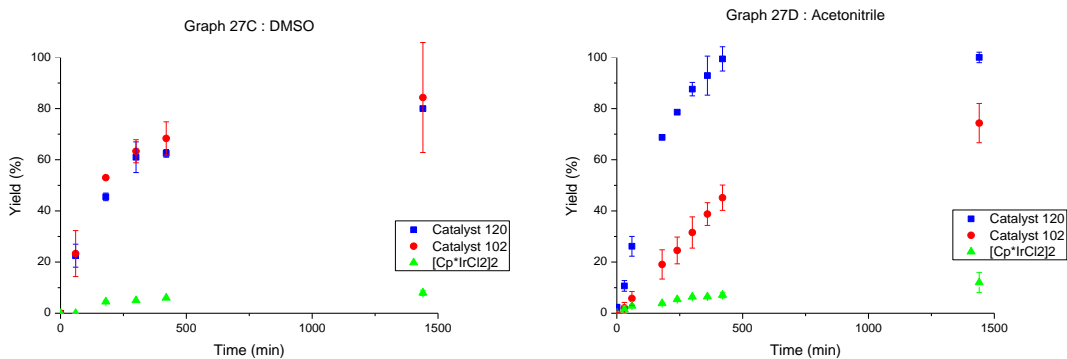
profile obtained carrying out the reaction in the absence of **121**. Interestingly, increasing the amount of 2,2'-bipyridine to 1 equivalent did not significantly change the yield and the reaction rate was only slightly slower. These results suggest that the coordination between the bipyridine and our catalyst is reversible and does not completely poison the activity of **102**. Among our three dicationic complexes, the most active was the iridium catalyst **120**, which was chosen for further screening.

5.3 Screening of Solvents and Catalyst Loading

In developing new cationic complexes, we sought to improve the solvent tolerance of our family of catalysts, particularly increasing their activity in solvents that previously did not give complete conversion of product **46**, such as 2-methylTHF, acetonitrile and water. Thus, a solvent screen was carried out, using our standard reaction between benzyl alcohol and piperidine. Graph 27 reports four experiments carried out in four different solvents, comparing the yield profiles with those obtained previously using our monomer **102** and the dimer $[\text{Cp}^*\text{IrCl}_2]_2$.

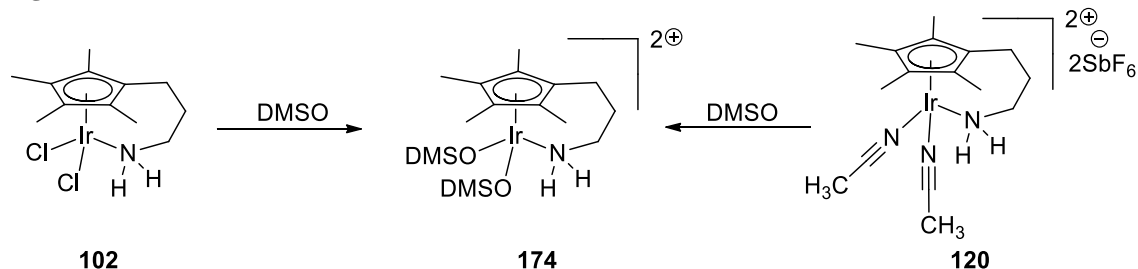
Graph 27





Pleasingly, in moderately polar solvents like 2-methylTHF and acetonitrile, the new catalyst was more active than **102** and it afforded product **46** with complete conversion after 24 hours (Graph 27B and Graph 27D). Surprisingly, the reaction profiles observed using catalyst **120** in very polar solvents, like DMSO and NMP, were similar to those achieved previously with complex **102** (Graph 27A and Graph 27C). Our hypothesis was that the two catalysts converged on a similar intermediate, as shown in an explicative example with DMSO in Figure 50.

Figure 50

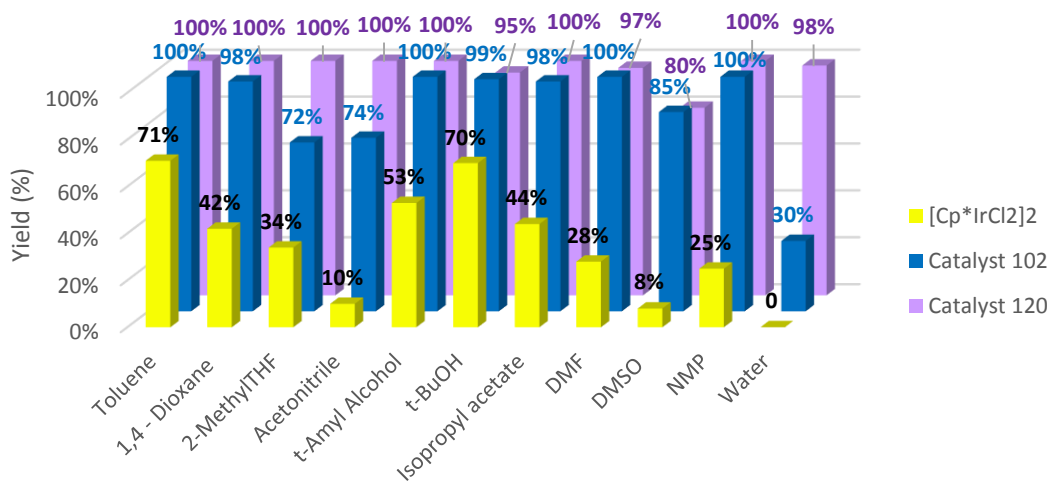
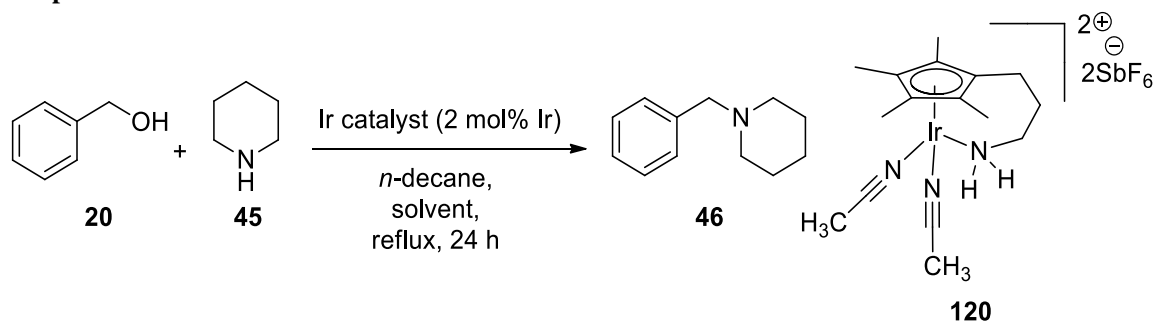


Thus, to confirm our hypothesis, an NMR study was carried out to evaluate the stability of our two complexes. Complexes **102** and **120** were dissolved in deuterated DMF and DMSO and heated at 100 °C for 24 hours. ¹H-NMR spectra were recorded after this time; unfortunately, the crude spectra showed the same signals of the starting complexes, suggesting that neither DMSO or DMF were coordinated to the iridium.

To complete the screen, our catalyst **120** was tested in a broader range of solvents. Graph 28 reports the yields obtained after 24 hours in comparison with those previously shown in Graph 15. Generally, at the end of 24 hours the yields achieved using our two complexes **102** and **120** were similar and both of them were definitely more active than the dimer [Cp*IrCl₂]₂. The main difference between our two complexes regards the

activities in acetonitrile, 2-methylTHF and, especially, water. In water, a 98% NMR conversion was observed using the dicationic complex, whereas with **102** *N*-benzylpiperidine **46** was achieved in only 30% NMR conversion.

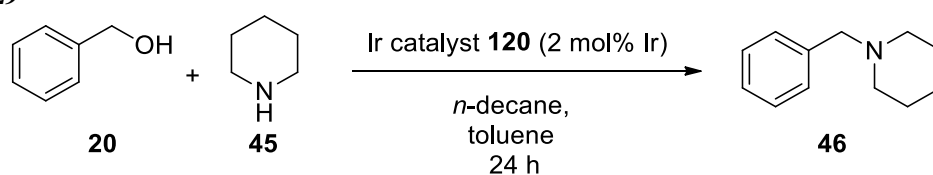
Graph 28



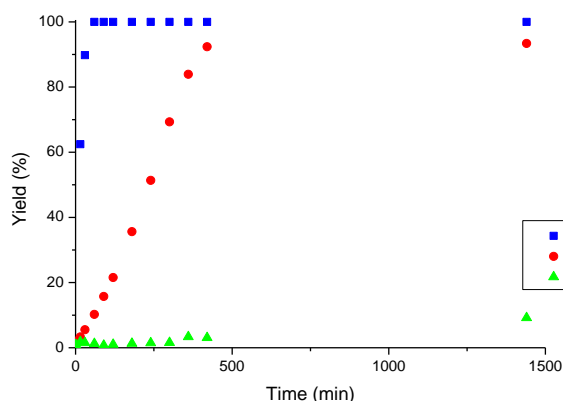
^a Yield calculated by comparing the areas of *n*-decane and *N*-benzylpiperidine in the GC spectrum.

Again, excellent yields were also achieved at 85 °C, when 2-methylTHF, acetonitrile and *t*-butanol were used. Thus, the next effort was to run the standard reaction between benzyl alcohol, piperidine and 2 mol% of iridium in toluene at different temperature, as shown in Graph 29.

Graph 29



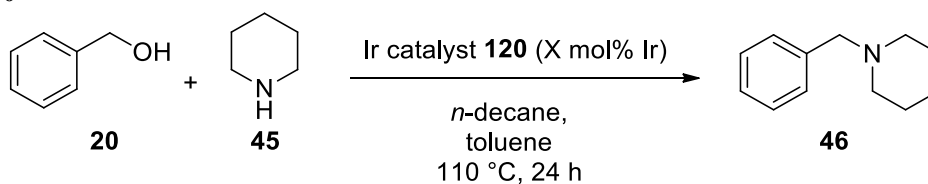
Graph 29



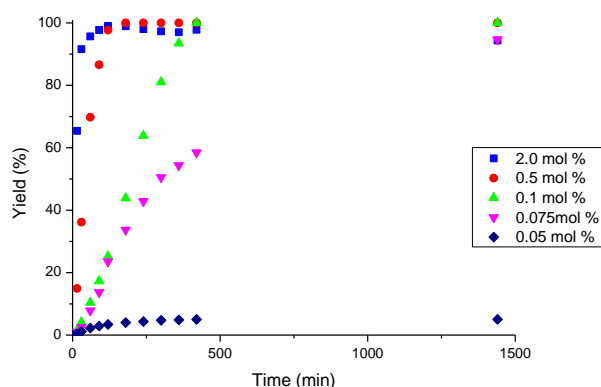
The reaction profile at 80 °C shows that the reaction was almost complete after 7 hours (GC yield > 90%), improving the results achieved previously with complex **102** (Graph 16). Unfortunately, when we decreased the temperature to 50 °C, the reaction did not work and less than 10% GC yield was achieved after the same reaction time. It was found that the active intermediate of catalyst **120** could only be formed by heating the reaction at a temperature between 50 °C and 80 °C. Our hypothesis is that the catalyst needs some energy to break the acetonitrile-iridium bonds to generate the active species.

In all the examples reported above, the catalyst loading was 2 mol% of iridium. To evaluate the possibility of decreasing the amount of iridium used in the reaction, we carried out a few experiments in toluene in which the catalyst loading of **120** has been decreased as low as 0.05 mol% (Graph 30). Excellent yields were achieved with a catalyst loading as low as 0.075 mol% of iridium. Disappointingly, when the amount of metal was decreased further to 0.05 mol%, product **46** was obtained in very poor yield, showing also a slow reaction rate. However, the reaction profile achieved using 0.1 mol% of **120** compared with the one obtained with 0.1 mol% of **102** (previously reported in Graph 17) confirmed that the cationic iridium catalyst **120** was more active than the neutral complex **102**. Comparing the yields observed after 7 hours, indeed we had complete conversion using the new monomer **120**, whereas, using **102**, we obtained **46** in less than 60% yield.

Graph 30

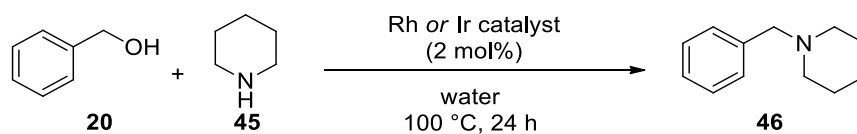


Graph 30



5.4 Activity in Water of Rhodium and Iridium Catalysts and Substrate Scope

Nowadays, catalysis in or on water is widely studied from an environmental perspective because water is a green, non-toxic and cheap solvent.¹⁰⁶ Furthermore, a wide number of pharmaceutical intermediates are polar substrates which are soluble in water. In the literature, only few examples are reported in which the hydrogen borrowing methodology can be carried out in or on water.^{25,26,27,33} In this context, the development of water-tolerant catalysts has become an active area of research.²⁷ In Graph 28 we reported that our dicationic iridium catalyst **120** showed good activity also in water and product **46** was achieved with a 98% conversion. Our next effort was to test a few of our previous catalysts to confirm that complex **120** was the best of our family in this medium. Table 29 reports the conversions obtained in water using some of our rhodium and iridium complexes. Among our neutral catalysts, rhodium catalysts **67** and **92** (entries 4 and 5) did not work as well as the corresponding iridium complexes **102** and **106** (entries 1 and 2). Between the iridium catalysts **102** and **106**, the best one was **106** (87% conversion after 24 hours, entry 2). Iodide catalysts usually promote *N*-alkylation processes in water better than the corresponding chloride complexes and our results confirm the trend present in the literature.^{25,27} Between our dicationic catalysts **120** and **93** (entries 3 and 6), iridium complex **120** afforded product **46** in higher yield (98% conversion after 24 hours, entry 3). It was found that **120** gave product **46** with the highest conversion and, therefore, it was our best catalyst not only in toluene, but also in water.

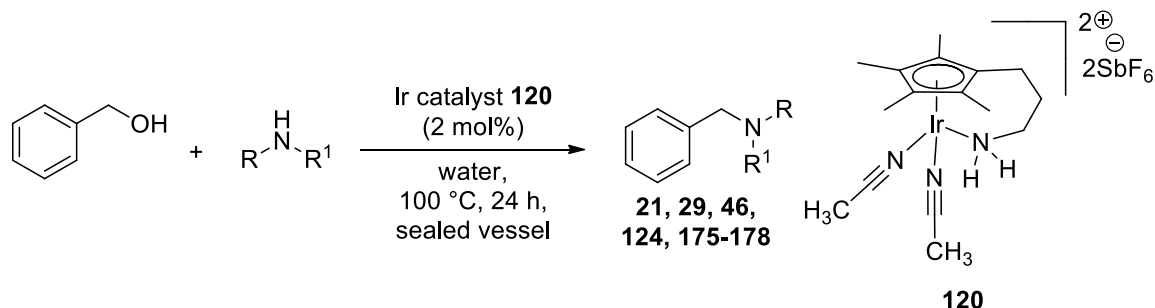
Table 29

Entry	Catalyst	Conversion (%) ^a
1	Iridium Catalyst 102	30
2	Iridium Catalyst 106	87
3	Iridium Catalyst 120	98
4	Rhodium Catalyst 67	14
5	Rhodium Catalyst 92	18
6	Rhodium Catalyst 93	13

^a Conversion estimated by comparing the signal ratios of benzyl alcohol and *N*-benzylpiperidine in the crude ¹H-NMR spectrum.

Interestingly, our best iridium catalysts **106** and **120** were not soluble in water and the complexes dissolved completely only after the addition of the starting materials, suggesting that these catalysts promoted the reaction on water, instead of in water. This was an interesting result because catalysis on water has the advantage of an easy product purification, which is carried out simply by phase separation or filtration.¹⁰⁷

Having developed a good catalyst, **120**, which could promote hydrogen borrowing on water, we sought to extend the substrate scope using this complex. Firstly, we focused on the screening of amines, which is reported in Table 30. The yields are compared with those reported previously in the literature by the groups of Fujita,²⁷ Limbach³³ and Williams.^{25,26}

Table 30

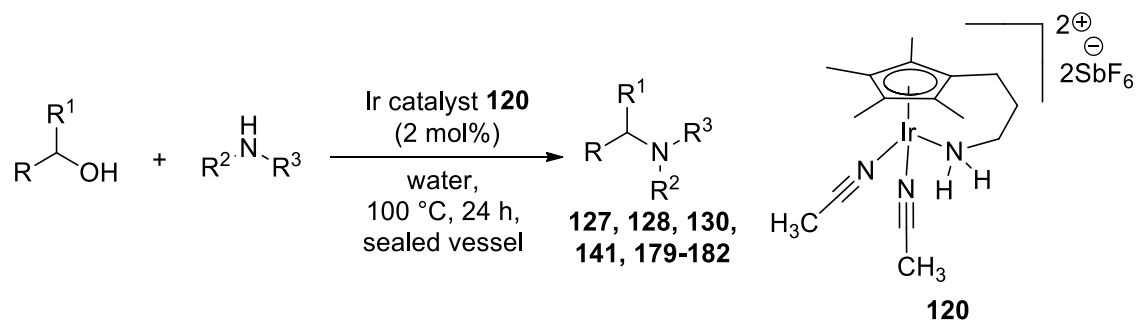
Entry	Amine	Isolated yield (%)	Fujita's yield (%) ²⁷	Limbach's yield (%) ³³	Williams' yield (%) ^{25,26}
1 ^a	R = -(CH ₂) ₅ CH ₃ , R ¹ = H	124, 74 ^b	82	-	-
2	R = -CH(Ph)(CH ₃), R ¹ = H	175, 48	-	-	98
3	R = Bn, R ¹ = H	176, 60	91	-	-
4	R = Ph, R ¹ = H	29, 79	92	95	-
5	R = -CH(CH ₂) ₅ , R ¹ = H	177, 85	-	-	-
6	R, R ¹ = (CH ₂) ₅	46, 82	-	-	-
7	R, R ¹ = (CH ₂) ₂ O(CH ₂) ₂	21, 82	-	-	54
8	R = Ph, R ¹ = CH ₃	178, 0	-	-	-

^a 1 mol% of iridium was used; ^b 9% yield of tertiary amine **125** was also isolated.

Generally, primary amines, such as *n*-hexylamine (entry 1), 1-phenylethylamine and benzylamine (entries 2 and 3), were well tolerated. Surprisingly, aniline was tolerated as well and *N*-benzylaniline **29** was isolated in good yield (79%, entry 4), whereas, carrying out the same reaction on water using our previous catalyst **102**, **29** was obtained only in 21% NMR conversion. These results suggest that the dicationic complex **120** shows an improved hydrogen-bonding ability than **102**. Three secondary amines were also tried. Piperidine and morpholine afforded the corresponding products **46** and **21** in good yield (entries 6 and 7), while, unfortunately, *N*-methylaniline did not work and only the signals of the starting materials were observed in the crude NMR spectrum (entry 8). Comparing our results with those reported in the literature, it was found that catalyst **120** afforded one product with the highest yield (entry 7) and gave comparable results in entries 1 and 4. However, it afforded two compounds in lower yield (entries 2 and 3).

The scope was next investigated for the alcohols; Table 31 reports the results achieved in the reactions between a broad range of alcohols and amines. The yields are compared with those described previously in the literature by the group of Limbach,³³ which reported the highest yields for the following compounds.

Table 31



Entry	Alcohol	Amine	Isolated Yield (%)	Limbach's yield (%) ³³
1 ^a	R = -(CH ₂) ₆ CH ₃ , R ¹ = H	R ² = Ph, R ³ = H	179 , 33 ^b	97
2	R = -(CH ₂) ₆ CH ₃ , R ¹ = H	R ² , R ³ = (CH ₂) ₅	130 , 31 ^b	-
3 ^a	R = -(CH ₂) ₆ CH ₃ , R ¹ = H	R ² = -CH(CH ₂) ₅ , R ³ = H	180 , 71	27
4	R = -(CH ₂) ₆ CH ₃ , R ¹ = H	R ² = -C(CH ₃) ₃ , R ³ = H	181 , 20 ^b	<10
5	R = -(CH ₂) ₆ CH ₃ , R ¹ = H	R ² = Bn, R ³ = H	141 , 34 ^b	92
6	R = Ph, R ¹ = CH ₃	R ² = Ph, R ³ = H	182 , 0	-
7 ^{a,c}	R = Ph, R ¹ = CH ₃	R ² = -(CH ₂) ₅ CH ₃ , R ³ = H	128 , 39	-
8	R, R ¹ = (CH ₂) ₅	R ² = -(CH ₂) ₅ CH ₃ , R ³ = H	127 , 24 ^b	84

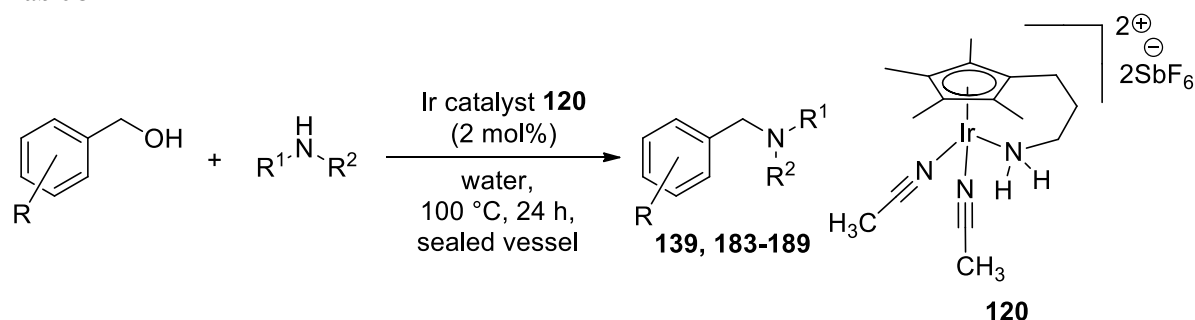
^a 1.5 equivalents of alcohol were used; ^b conversion estimated by comparing the signal ratios in the crude ¹H-NMR spectrum; ^c 3 mol% of iridium were used.

Disappointingly, it was found that alcohols other than the benzyl alcohol were not as active. For instance, conversions obtained in the reactions between *n*-octanol and a variety of amines were generally poor (entries 1-5). Increasing the amount of alcohol to 1.5 equivalents, we managed to isolate product **180** in 71% yield (entry 3). Two secondary alcohols were also tested: 1-phenylethanol and cyclohexanol. Unfortunately, the reaction between 1-phenylethanol and aniline did not work and only the signals of the unreacted starting materials were observed in the crude NMR spectrum (entry 6). In order to obtain product **128** in decent yield (39%, entry 7), the catalyst loading was increased to 3 mol% of iridium and the amount of alcohol to 1.5 equivalents. The reaction between

cyclohexanol and *n*-hexylamine afforded the corresponding product **127** in poor conversion (24%, entry 8). Comparing our results with those reported in the literature by Limbach and co-workers,³³ it was found that catalyst **120** afforded one product in significantly higher yield (entry 3). Unfortunately, our complex afforded another three products in lower yield (entries 1, 5 and 8).

Finally, we sought to expand the substrate scope with respect to the functional groups that could be tolerated using catalyst **120**. Table 32 reports the results achieved in the reaction between a variety of benzyl alcohols and amines.

Table 32



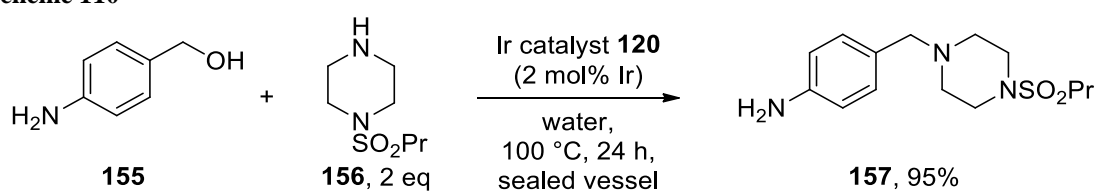
Entry	R	Amine	Isolated Yield (%)
1 ^a	4-NH ₂ -	R ² , R ³ = (CH ₂) ₅	183 , 86
2	3,4-Dimethoxy-	R ² , R ³ = (CH ₂) ₅	184 , 75
3	4-CN-	R ² , R ³ = (CH ₂) ₅	139 , 35 ^b
4	4-NO ₂ -	R ² = Ph, R ³ = H	185 , 54
5	2-Br-	R ² = Ph, R ³ = H	186 , 45
6	H	R ² = 3-ClC ₆ H ₄ , R ³ = H	187 , 60
7	H	R ² = 3-MeOC ₆ H ₄ , R ³ = H	188 , 45
8	H	R ² = 4-MeC ₆ H ₄ , R ³ = H	189 , 69

^a 2 equivalents of amine were added; ^b conversion estimated by comparing the signal ratios in the crude ¹H-NMR spectrum.

Catalyst **120** showed a good tolerance of functional groups, even if not as broad as the one observed using complex **102**. Benzyl alcohols bearing electron-donating groups afforded the corresponding products in good yield (entries 1 and 2). In entry 2, two equivalents of piperidine were added in order to avoid the alkylation of the aniline with another molecule of alcohol. Disappointingly, 4-cyanobenzyl alcohol and 4-nitrobenzyl alcohol were not particularly reactive using catalyst **120** and the final yields were moderate (entries 3 and 4). A substituent in the *ortho* position on the benzyl alcohol gave again a moderate yield (entry 5). Pleasingly, three different anilines gave the

corresponding products from moderate to good yields (entries 6-8). Among the substituents, it was found that halogens, amines, ethers and nitro groups were tolerated. To conclude the substrate scope, we sought to use our methodology to demonstrate its potential application in synthesis. Thus, the reaction between 1 equivalent of 4-aminobenzyl alcohol **155** and 2 equivalents of piperazine *N*-propylsulfonamide **156** gave the drug intermediate **157** in excellent yield (Scheme 110). Again, two equivalents of amine were used in order to avoid the alkylation of the aniline with another molecule of alcohol.

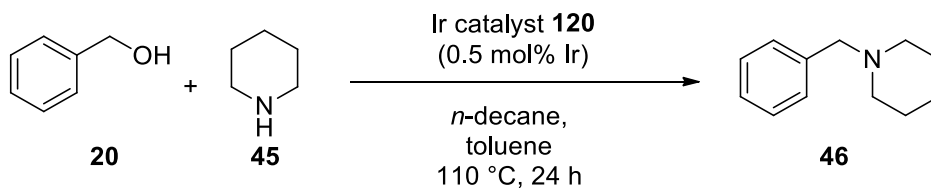
Scheme 110



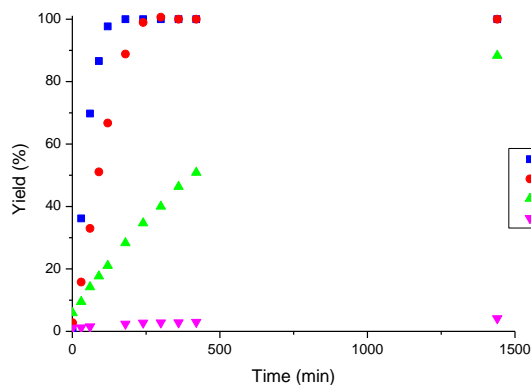
Interestingly, complex **120** was not soluble in water and it dissolved completely only after the addition of the starting materials. Two different phases were often observed throughout our substrate scope, supporting our hypothesis that the catalyst worked on water, instead of in water.

5.5 Catalyst recovery

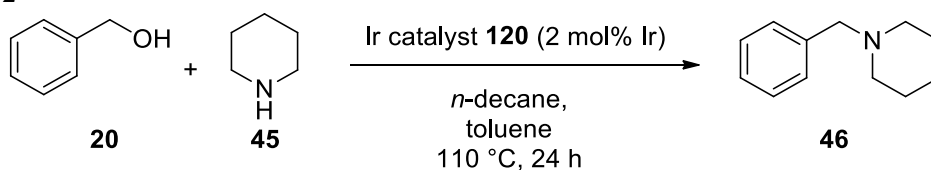
During our kinetic experiments, we observed that an iridium-containing species started to precipitate at the end of the reaction. That was interesting because it would be possible to reuse the precipitate in another reaction to determine if the catalyst was still active after the first run. Thus, a reaction between benzyl alcohol and piperidine using 0.5 mol% of iridium in toluene was carried out. At the end of the reaction, the addition of Et₂O favoured the precipitation of the complex, which was then recovered and recycled in a new reaction between benzyl alcohol and piperidine. The catalyst was recovered three times; Graph 31 shows the results for these four runs.

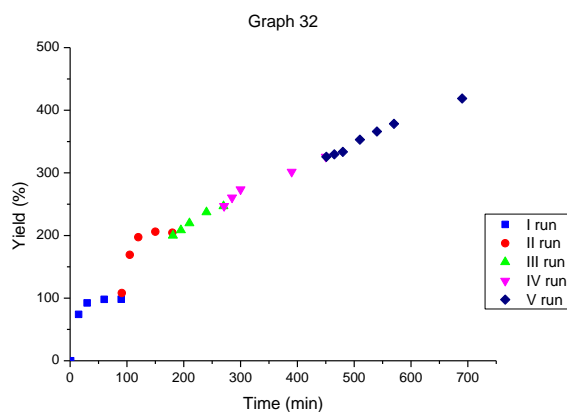
Graph 31

Graph 31



The yield profile of the second run showed that the catalyst was still active, even if the reaction rate was slightly slower than the one observed in the first run, which could derive from a loss of material during the precipitation process. Unfortunately, recycling and reusing the catalyst for the second time showed a definitely slower reaction rate and the fourth run showed that the recovered precipitate was inactive. This could be due to either a loss of material during the precipitation process or the formation of an inactive complex in the reaction. Thus, our next attempt was to study the stability of complex **120**. Instead of isolating the catalyst at the end of the reaction, we added another aliquot of benzyl alcohol and another aliquot of piperidine maintaining the reaction at reflux. We repeated this process four times to compare the rate of product formation (Graph 32). Disappointingly, the third run was already slower than the first two runs, suggesting that an inactive catalyst was formed in the reaction or the complex decomposed after few hours at reflux.

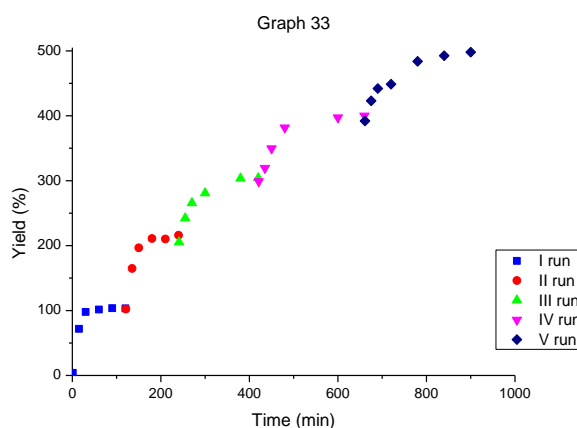
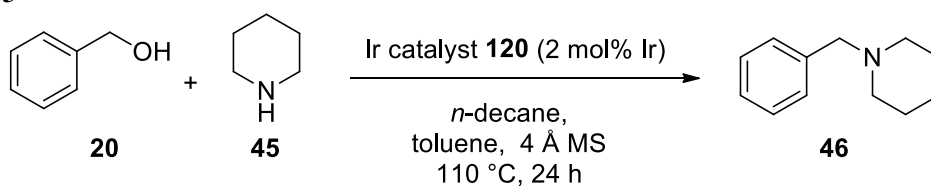
Graph 32



Our next attempt was to determine if the catalyst became inactive because it was poisoned by one of the two products of the reaction, *N*-benzylpiperidine or water.

We began studying the effect of the water. The same reaction between benzyl alcohol and piperidine was carried out again, but this time molecular sieves were added in order to absorb the water that was formed. Again, aliquots of benzyl alcohol and piperidine were added another four times maintaining the reaction at reflux (Graph 33).

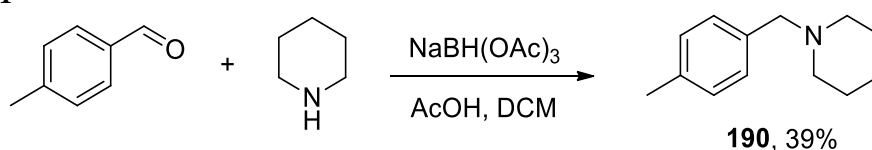
Graph 33



With the increase of the number of runs, the observed reaction rates decreased slightly and in the last run a complete conversion was only achieved after 4 hours. Nevertheless, in the presence of molecular sieves, it was possible to obtain a complete conversion for

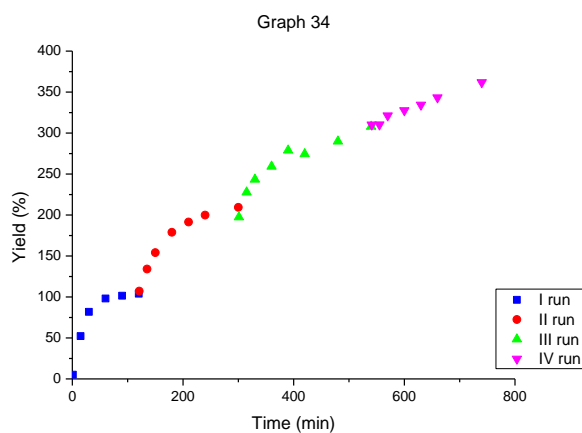
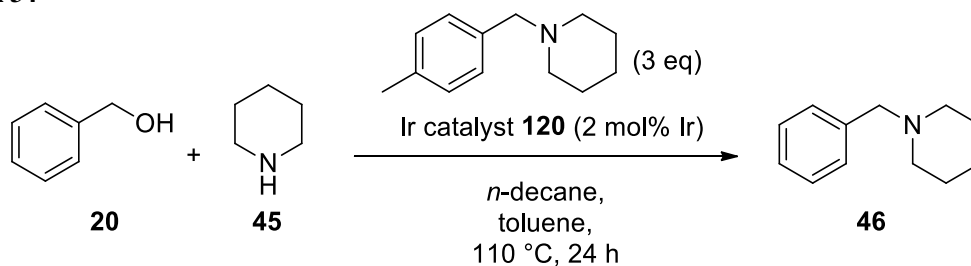
up to five times in a reasonable reaction time (< 4 hours), while, in their absence, the reaction rate was definitely slower from the third addition of reagents. Our final effort was to study the stability of the catalyst in the presence of *N*-benzylpiperidine. We sought to create the same conditions in which catalyst **120** would be at the fourth run to check if the presence of three equivalents of product **46** would slow down its activity. Our aim was to add an amine which would behave similarly to our product **46**, but its GC signal did not overlap with any other peaks. Thus, 1-(4-methyl)benzylpiperidine **190** was synthesised in moderate yield by reductive amination, as shown in Scheme 111.

Scheme 111



Three equivalents of compound **190** were added to our standard reaction between benzyl alcohol and piperidine. Again, aliquots of benzyl alcohol and piperidine were added another three times maintaining the reaction at reflux (Graph 34).

Graph 34

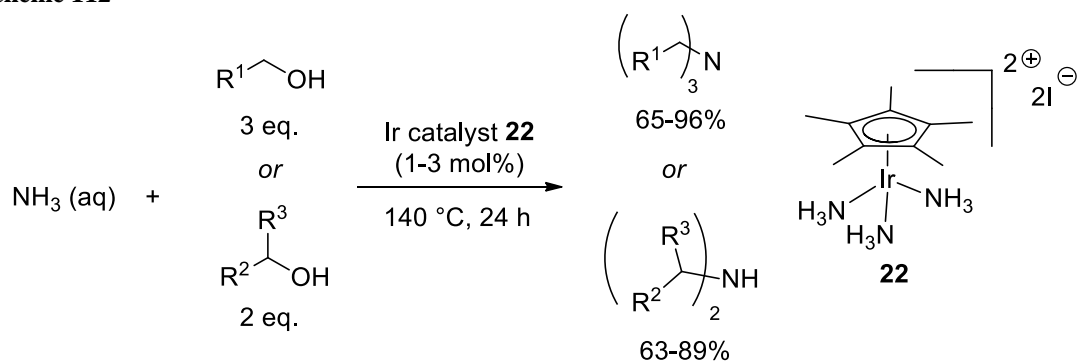


Interestingly, in the first run, a complete conversion was achieved after one hour, which was comparable to the yield profile shown previously in Graph 24. The reaction rate started to decrease significantly in the third run when a complete conversion was only observed after four hours. These results suggest that the tertiary amine does not poison the catalyst, whereas the presence of water seems to reduce the activity faster, which is surprising since the catalyst has shown to promote the hydrogen borrowing methodology on water. An NMR study was carried out to evaluate the stability of catalyst **120** in the presence of a large excess of water. Complex **120** was dissolved in deuterated acetonitrile and 100 equivalents of D₂O were added at regular intervals six times maintaining the solution at reflux between the additions. ¹H-NMR spectra were recorded before any addition. Disappointingly, the signals of the complex did not change after the additions of D₂O, suggesting that the presence of water alone did not explain the decrease in the activity of complex **120**, showing that the mechanism is more complicated than we expected.

5.6 Conclusion

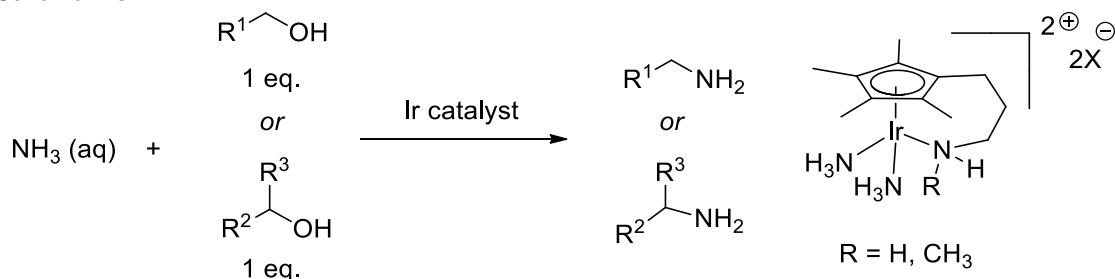
In conclusion, we have synthesised an improved dicationic iridium catalyst, which gave us faster reaction rates than those obtained previously. The catalyst loading was decreased as low as 0.075 mol% obtaining excellent yields for the reaction between benzyl alcohol and piperidine. Dicationic iridium complex **120** showed great activity also in water and ten substrates were achieved in good isolated yields (> 69%). The great activity shown by monomer **120** in the hydrogen borrowing processes suggests that this new family of catalysts bearing an amine on the side chain can be improved further. A possible modification would be the synthesis of new complexes containing more labile ligands than the acetonitrile and the application of these catalysts in new methodologies. For instance, Fujita and co-workers have shown that their water-soluble iridium catalyst **22** could be used not only in the *N*-alkylation of amines, as shown previously in Scheme 109, but also in the multialkylation of aqueous ammonia (Scheme 112).¹⁰⁸

Scheme 112



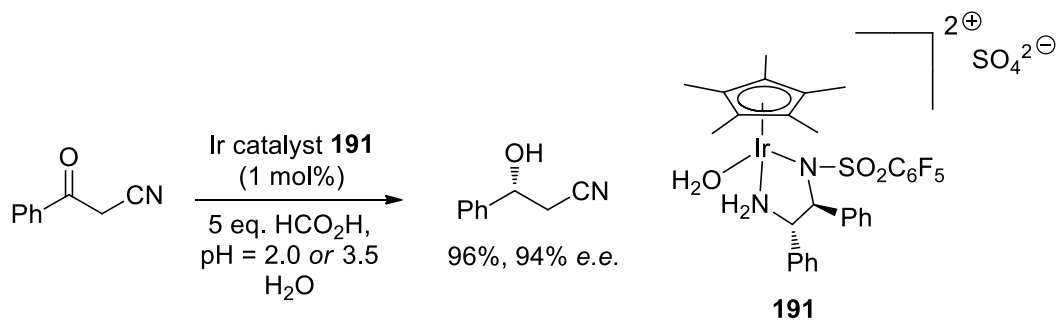
This transformation is quite interesting because the utilisation of ammonia as a nitrogen source is usually unsatisfactory in hydrogen borrowing processes.¹⁰⁸ Catalyst **22** promoted this transformation in high yield; however, the conditions used were quite harsh and the reactions could not be stopped to achieve the monoalkylated amines, but, instead, only secondary and tertiary amines were obtained. Thus, it would be interesting to make a new version of our catalysts changing the acetonitriles with two molecules of ammonia. The tethered chain can potentially be bulky enough to disfavour the approach of the primary amine on the coordination sphere of the catalyst, obtaining a better selectivity for the monoalkylated products (Scheme 113).

Scheme 113



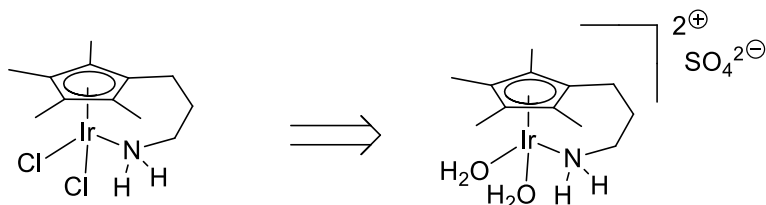
Carreira and co-workers showed that the aqueous complex **191** was active in the asymmetric transfer hydrogenation of α -cyano and α -nitro-acetophenones with a pH tolerance between 2.0 and 3.5 (Scheme 114).¹⁰⁹

Scheme 114



Thus, it would be interesting to make a corresponding aqueous complex starting with our monomer **102** trying to improve the functional group tolerance shown by our dicationic catalyst **120** on water (Figure 51).

Figure 51



Indeed, the functional groups that could be tolerated by complex **120** were not very broad and cyano and nitro groups did not work particularly well, as shown previously in Table 32. Potentially, the corresponding aqueous iridium complexes could be more active in water, improving the yield and the functional group tolerance.

Chapter 6. Experimental

6.1 General Considerations

Instrumentation

Proton (^1H) and carbon (^{13}C) magnetic resonance spectra were recorded using a Bruker DPX 300, a Bruker DRX 500 or a Bruker Advance 500 spectrometer using an internal deuterium lock. ^1H -NMR chemical shifts (δ) are quoted in ppm downfield of tetramethylsilane and coupling constant (J) are quoted in Hz. ^{13}C -NMR spectra were recorded with broadband proton decoupling at 125 MHz.

Assignments were made on the basis of chemical shift and coupling data, using ^1H - ^{13}C HMQC, DEPT, HMBC and nOe experiments where necessary. Infra-red spectra were recorded on a Perkin Elmer Spectrum One FT-IR spectrometer, with absorption reported in wavenumbers (cm^{-1}). High-resolution electrospray mass spectra (ESI-MS) were obtained on a Bruker MicroTOF-Q or Bruker MaXis Impact spectrometer in positive or negative mode. X-Ray crystal structures were recorded by Dr. Helena Shepherd or Dr. Christopher Pask on an Agilent SuperNova single crystal X-ray diffractometer, fitted with an Atlas area detector and a kappa-geometry 4-circle goniometer. The elemental analyses were recorded by Ian Blakeley or Tanja Marinko-Covell on a Carlo Erba 1108 Elemental Analyser. Melting points were determined using a Griffin D5 variable temperature apparatus and are uncorrected. Unless otherwise specified, gas chromatographic spectra were recorded on an Agilent machine fitted with a Capillary Column HP-5 (5% phenylmethylsiloxane) HP 19091J-413 (30 mm x 320 μm x 0.25 μm), with the following methods:

- Method 1 : 1 μL injection volume, inlet temperature: 250 $^\circ\text{C}$, inlet pressure: 10.00 psi, temperature column: 60 $^\circ\text{C}$ - hold time: 3 min, from 60 $^\circ\text{C}$ to 200 $^\circ\text{C}$ with 20 $^\circ\text{C}/\text{min}$ ramp, 200 $^\circ\text{C}$ - hold time: 3 min, detector temperature: 300 $^\circ\text{C}$, $\text{H}_2:\text{Air}:\text{N}_2$ 30:300:10 ml/min; $t_{n\text{-decane}} = 3.1$ min, $t_{\text{benzyl alcohol}} = 3.7$ min, $t_{N\text{-benzylpiperidine}} = 7.3$ min.

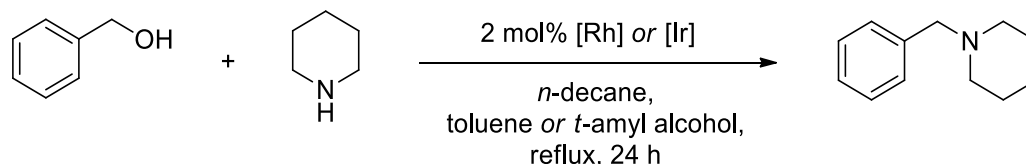
- Method 2 : 1 μ L injection volume, inlet temperature: 300 °C, inlet pressure: 10.00 psi, temperature column: 60 °C - hold time: 3 min, from 60 °C to 200 °C with 20 °C/min ramp, 200 °C - hold time: 20 min, detector temperature: 300 °C, H₂:Air:N₂ 30:300:10 ml/min; $t_{n\text{-decane}}$ = 3.0 min, $t_{\text{benzyl alcohol}}$ = 3.7 min, $t_{4\text{-phenylpiperidine}}$ = 7.6 min, $t_{N\text{-benzyl-4-phenylpiperidine}}$ = 12.2 min.

Experimental Procedures

All reactions were carried out under an inert atmosphere of nitrogen using oven-dried glassware, unless stated. Toluene, methanol, diethyl ether, acetonitrile, DCM, chloroform and THF were dried prior to use using a Pure Solv MD solvent purification system (SPS). All other solvents and reagents were obtained from commercial sources and used without purification. Molecular weights of rhodium trichloride hydrate and iridium trichloride hydrate were considered on anhydrous basis and, therefore, the yields for the synthesis of the complexes starting with these two reagents were underestimated. Flash column chromatography was conducted using Fischer Matrix silica gel (35-70 μ m) or Alfa Aesar activated aluminium oxide basic (Brockmann I) or pre-packed Combiflash silica cartridges running using Combiflash Rf machine. Thin layer chromatography was conducted using pre-coated silica plates (Merck silica Kieselgel 60F₂₅₄) or using pre-coated alumina plates (Merck alumina Kieselgel 150F₂₅₄). Spots were visualized using UV fluorescence (λ_{max} = 254 nm) and chemical staining with potassium permanganate. Petrol refers to light petroleum (b.p. 40-60 °C).

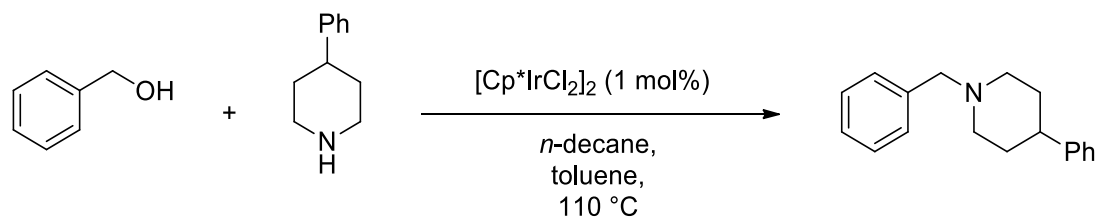
6.2 General Procedures

Example of a general procedure A: GC Monitoring reactions



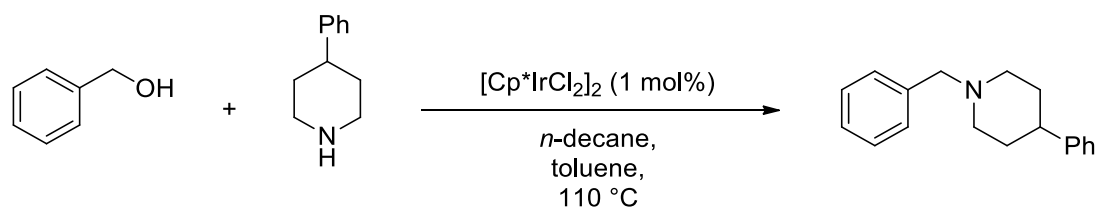
All the experiments analysed by GC have been carried out using the following procedure, unless otherwise specified. To a stirred suspension of the corresponding rhodium *or* iridium complex (2 mol% [Rh] *or* 2 mol% [Ir]) in toluene *or t*-amyl alcohol (1.5 ml) under nitrogen were added benzyl alcohol (1.88 mmol, 1.0 eq) and *n*-decane (0.94 mmol, 0.5 eq), maintaining a constant concentration (2.2 M). The solution was heated at reflux, piperidine (1.88 mmol, 1.0 eq) was added and aliquots of the reaction mixture (30 μ l) were collected at regular intervals (0 min, 15 min, 30 min, 60 min, 90 min, 120 min, 180 min, 240 min, 300 min, 360 min, 420 min, 1440 min), diluted with MeCN (2 ml) and analysed by GC using method 1.

General procedure B: Section 2.2



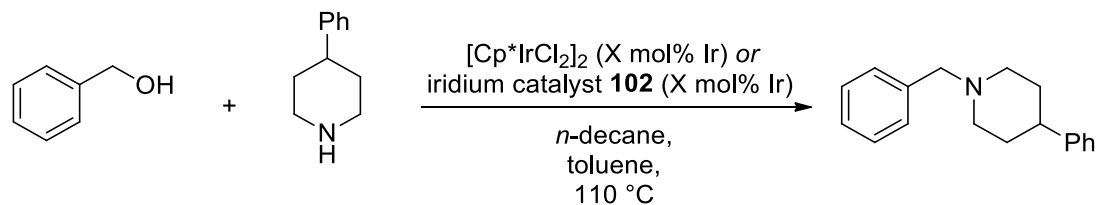
All the experiments in Section 2.2 have been carried out using benzyl alcohol in excess (respectively 10, 12, 15 and 20 equivalents), *n*-decane (0.5 equivalent) and catalyst (1 mol% [Cp*IrCl₂]₂) in toluene (respectively, 3.8 ml, 5.5 ml, 5.5 ml and 5.5 ml). The solution was heated at 110 °C and 4-phenylpiperidine (1.0 equivalent, respectively, 1.0 mmol, 1.25 mmol, 0.84 mmol, 0.62 mmol) was added. Aliquots of the reaction mixture (30 μ l) were collected at regular intervals for 150 minutes, diluted with MeCN (2 ml) and analysed by GC, using method 2. The observed rate constants used in Graph 3 were calculated plotting the logarithm of the concentration of the amine vs. time.

General procedure C: Section 2.3



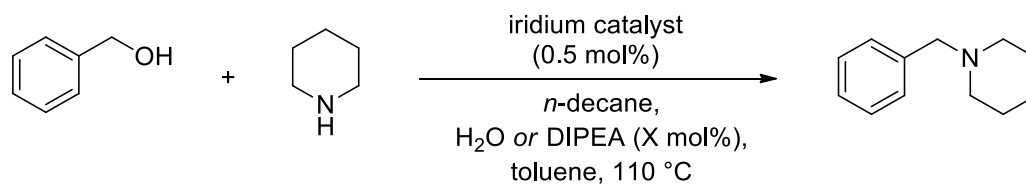
All the experiments in Section 2.3 have been carried out using benzyl alcohol (1.0 equivalent), *n*-decane (0.5 equivalent) and catalyst (1 mol% [Cp*IrCl₂]₂) in toluene. The solution was heated at 110 °C and 4-phenylpiperidine was added (1.0 equivalent), with an amine concentration of 0.12 M, 0.2 M, 0.07 M and 0.25 M. Aliquots of the reaction mixture (30 μl) were collected at regular intervals for 150 minutes, diluted with MeCN (2 ml) and analysed by GC using method 2. The observed rate constants used in Graph 5 were calculated plotting the logarithm of the concentration of the alcohol vs. time in *pseudo*-first order condition.

General procedure D: Sections 2.4 and 4.7



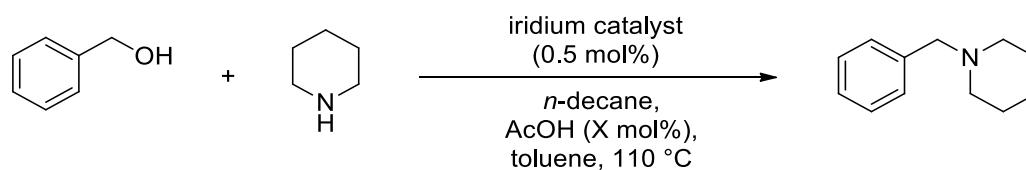
The experiments in Section 2.4 and 4.7 have been carried out using benzyl alcohol (1.88 mmol, 1.0 equivalent), *n*-decane (0.94 mmol, 0.5 equivalent) and catalyst (iridium catalyst **102** or [Cp*IrCl₂]₂, iridium catalyst loading: 2 mol%, 4 mol%, 8 mol%, 12 mol%, 16 mol%) in toluene (1.5 ml). The solution was heated at 110 °C and 4-phenylpiperidine was added (1.88 mmol, 1.0 equivalent). Aliquots of the reaction mixture (30 μl) were collected at regular intervals for the first 2 hours, diluted with MeCN (2 ml) and analysed by GC using method 2. The observed rate constants used in Graph 6 and in Graph 18 have been calculated plotting the logarithm of the benzyl alcohol vs. the time in *pseudo*-first order condition.

General procedure E: GC Monitoring reactions using automatic sampling Amigo



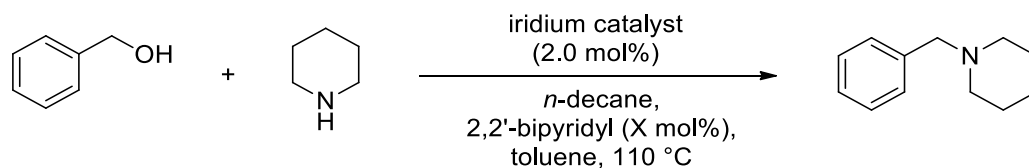
To a stirred suspension of iridium complex **102** (18.8 μ mol, 0.5 mol%) in toluene (3.0 ml) under nitrogen were added benzyl alcohol (3.76 mmol, 1.0 equivalent), *n*-decane as internal standard (1.88 mmol, 0.5 equivalent) and water (0.1 *or* 1.0 equivalents) *or* diisopropylethylamine (0.1 *or* 1.0 equivalents). The solution was heated at 110 °C, piperidine (1.88 mmol, 1.0 equivalent) was added and aliquots of the reaction mixture (30 μ l) were automatically collected at regular intervals (1 min, 15 min, 30 min, 45 min, 60 min, 90 min, 120 min, 180 min, 240 min, 300 min, 360 min). The yield of the product was determined by GC using a Rxi-5Sil MS column (20 mm x 180 μ m x 0.36 μ m, temperature of injection: 235 °C, 1 μ l injection volume, temperature column: 40 °C - hold time: 2 min, from 40 °C to 100 °C with 30 °C/min ramp, from 100 °C to 240 °C with 45 °C/min ramp, detector temperature: 300 °C, H₂:Air:N₂ 30:300:30 ml/min; $t_{n\text{-decane}} = 7.4$ min, $t_{\text{benzyl alcohol}} = 7.6$ min, $t_{N\text{-benzylpiperidine}} = 9.0$ min).

General procedure F: Section 4.8



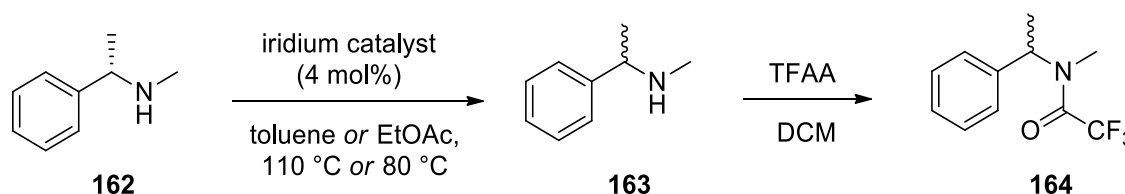
To a stirred suspension of iridium complex **102** (9.4 μ mol, 0.5 mol%) in toluene (1.5 ml) under nitrogen were added benzyl alcohol (1.88 mmol, 1.0 equivalent), *n*-decane as internal standard (0.94 mmol, 0.5 equivalent) and acetic acid (respectively, 0.1, 0.25, 0.5, 0.75, 1.0 equivalents). The solution was heated at 110 °C, piperidine (1.88 mmol, 1.0 equivalent) was added and aliquots of the reaction mixture (30 μ l) were collected at regular intervals (1 min, 15 min, 30 min, 60 min, 90 min, 120 min, 180 min, 240 min, 300 min, 360 min, 420 min, 1440 min), diluted with MeCN (2 ml) and analysed by GC, using method 1.

General procedure G: Section 5.2



To a stirred suspension of iridium complex **102** (37.6 μmol , 2.0 mol%) in toluene (1.5 ml) under nitrogen were added benzyl alcohol (1.88 mmol, 1.0 equivalent), *n*-decane as internal standard (0.94 mmol, 0.5 equivalent) and 2,2'-bipyridyl (respectively, 0.02, 0.1, 1.0 equivalents). The solution was heated at 110 °C, piperidine (1.88 mmol, 1.0 equivalent) was added and aliquots of the reaction mixture (30 μl) were collected at regular intervals (1 min, 15 min, 30 min, 60 min, 90 min, 120 min, 180 min, 240 min, 300 min, 360 min, 420 min, 1440 min), diluted with MeCN (2 ml) and analysed by GC, using method 1.

General procedure H: Racemisation



All the experiments of racemisation have been carried out as follows. To a stirred suspension of iridium catalyst (4 mol% [Ir]) in toluene (10 ml) *or* EtOAc (10 ml) was added (S)-(-)-N,α-dimethylbenzylamine (54 μl , 0.4 mmol). The resulting solution was heated at 110 °C *or* 80 °C for 20 hours, cooled at RT and the solvent was removed under reduced pressure. The residue was dissolved in hexane, filtered to remove the catalyst and the solvent was evaporated under reduced pressure. Amine **163** was dissolved in DCM (5.0 ml) and trifluoroacetic anhydride (0.8 mmol) was added. The solution was stirred for 90 minutes and the solvent was removed under reduced pressure. The *e.e.* of the product was determined by GC using a CP-ChiraSil-Dex column (25 mm x 250 μm x 0.25 μm , 1 μl injection volume, inlet temperature: 300 °C, inlet pressure: 15.00 psi, temperature column: 40 °C - hold time: 30 minutes, H₂ flow: 3.5ml/min, H₂ pressure: 15.00 psi, detector temperature: 300 °C, H₂:Air:N₂ 30:300:10 ml/min; $t_{(S)\text{-enantiomer}}$ = 11.7 min, $t_{(R)\text{-enantiomer}}$ = 13.4 min).

General procedure I: Synthesis of substrates 46, 124-146, 158, 159, 165 and 167

To a stirred suspension of iridium complex **102** (4.4 mg, 0.01 mmol) in toluene (0.5 ml) under nitrogen were added the corresponding alcohol (1.0 mmol) and the corresponding amine (1.0 mmol). The resulting solution was heated at 110 °C for 18 hours in a sealed vessel. The solvent was removed under reduced pressure and purification by filtration or by flash chromatography gave **46, 124-146, 158, 159, 165** and **167**.

General procedure J: Synthesis of substrates 46, 124, 126, 146, 158 and 159

To a stirred suspension of iridium complex **103** (4.6 mg, 0.01 mmol) in toluene (0.5 ml) under nitrogen were added the corresponding alcohol (1.0 mmol) and the corresponding amine (1.0 mmol). The resulting solution was heated at 110 °C for 18 hours in a sealed vessel. The solvent was removed under reduced pressure and purification by flash chromatography gave **46, 124, 126, 146, 158** and **159**.

General procedure K: Synthesis of substrates 151, 154 and 157

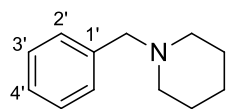
To a stirred suspension of iridium complex **102** (8.8 mg, 0.02 mmol) in toluene (1.0 ml) or *n*-butylacetate (1.0 ml) under nitrogen were added the corresponding alcohol (2.0 mmol) and the corresponding amine (2.0 mmol). The resulting solution was heated at 110 °C for 24 hours. The solvent was removed under reduced pressure and purification by flash chromatography using the automatic purification system (Combiflash) gave **151, 154** and **157**.

General procedure L: Synthesis of substrates 21, 29, 46, 124, 128, 157, 175-177, 180 and 183-189

To a stirred suspension of iridium complex **120** (18.5 mg, 0.02 mmol) in water (0.1 ml) under nitrogen were added the corresponding alcohol (1.0 mmol) and the corresponding amine (1.0 mmol). The resulting mixture was heated at 100 °C for 24 hours in a sealed vessel. The solvent was removed under reduced pressure and purification by flash chromatography gave **21, 29, 46, 124, 128, 157, 175-177, 180** and **183-189**.

6.3 Experimental Procedures

1-Benzylpiperidine (**46**)



To a stirred suspension of $[\text{Cp}^*\text{IrCl}_2]_2$ (15 mg, 0.019 mmol) and NaHCO_3 (3 mg, 0.04 mmol) in toluene (1.0 ml) were added benzyl alcohol (196 μl , 1.89 mmol) and piperidine (190 μl , 1.89 mmol). The resulting suspension was heated at 110 °C for 22 hours. The solvent was removed under reduced pressure to give a crude material which was purified by flash chromatography (Al_2O_3 pH 9.5 \pm 0.5, eluting with hexane-EtOAc (80:20)), affording **46** as a pale yellow oil (227 mg, 1.30 mmol, 70%).

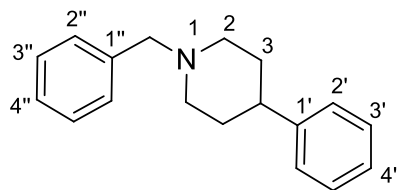
Following general procedure I, **46** was prepared from 1,5-pentanediol (105 μl , 1.00 mmol) and benzylamine (110 μl , 1.00 mmol) using 2 mol% of iridium complex **102** (8.8 mg, 0.020 mmol) at 130 °C. Purification by flash chromatography (Al_2O_3 pH 9.5 \pm 0.5, eluting with hexane-EtOAc (95:5 to 85:15)) gave **46** as a colourless oil (46 mg, 0.26 mmol, 26%).

Following general procedure J, **46** was prepared from 1,5-pentanediol (105 μl , 1.00 mmol) and benzylamine (110 μl , 1.00 mmol). Purification by flash chromatography (Al_2O_3 pH 9.5 \pm 0.5, eluting with hexane-EtOAc (95:5 to 80:20)) gave **46** as a colourless oil (112 mg, 0.640 mmol, 64 %).

Following general procedure L, **46** was prepared from benzyl alcohol (103 μl , 1.00 mmol) and piperidine (100 μl , 1.00 mmol). Purification by flash chromatography (Al_2O_3 pH 9.5 \pm 0.5, eluting with hexane-EtOAc (85:15 to 70:30)) gave **46** as a colourless oil (143 mg, 0.817 mmol, 82%).

R_f = 0.89 (Basic aluminium oxide, hexane-EtOAc 90:10); ^1H NMR (500 MHz, CDCl_3 , δ/ppm): 7.29-7.21 (4H, m, 4ArH), 7.17-7.14 (1H, m, H-4'), 3.39 (2H, s, ArCH₂), 2.30 (4H, br s, 2H-2), 1.52-1.47 (4H, m, 2H-3), 1.35 (2H, br s, H-4); ^{13}C NMR (125 MHz, CDCl_3 , δ/ppm): 138.2 (C-1'), 129.3 (Ar), 128.1 (Ar), 126.9 (Ar), 63.8 (ArCH₂), 54.4 (C-2), 25.9 (C-3), 24.3 (C-4); IR (ν_{max} , neat, cm^{-1}): 2932, 2852, 2792, 2754, 1467, 1346, 1153, 1113, 1066; HRMS (ESI+) m/z : Calculated for $\text{C}_{12}\text{H}_{18}\text{N}$ ($\text{M}+\text{H}^+$): 176.1434, found: 176.1427. Spectroscopic data consistent with literature values.¹¹⁰

1-Benzyl-4-phenylpiperidine (**48**)

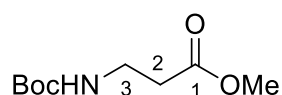


To a stirred suspension of $[\text{Cp}^*\text{IrCl}_2]_2$ (15 mg, 0.019 mmol) in toluene (1.0 ml) were added benzyl alcohol (207 μl , 2.00 mmol) and 4-phenylpiperidine (322 mg, 2.00 mmol). The resulting suspension was heated at 110 $^\circ\text{C}$ for 22 hours. The solvent was removed under reduced pressure to give a crude material which was purified by flash chromatography (SiO_2 , eluting with hexane-EtOAc (90:10)), affording **48** as a pale yellow oil (362 mg, 1.44 mmol, 72%).

$R_f = 0.31$ (hexane-EtOAc 80:20); $^1\text{H NMR}$ (500 MHz, CDCl_3 , δ/ppm): 7.40-7.20 (10H, m, 10ArH), 3.59 (2H, s, ArCH₂), 3.07-3.04 (2H, m, H-2), 2.53 (1H, quin, $J = 7.5$ Hz, H-4), 2.15-2.08 (2H, m, H-2), 1.87-1.83 (4H, m, 2H-3); $^{13}\text{C NMR}$ (125 MHz, CDCl_3 , δ/ppm): 146.6 (C-1' or C-1''), 138.5 (C-1' or C-1''), 129.3 (Ar), 128.4 (Ar), 128.2 (Ar), 127.0 (Ar), 126.9 (Ar), 126.1 (Ar), 63.5 (ArCH₂), 54.3 (C-2), 42.8 (C-4), 33.5 (C-3); HRMS (ESI+) m/z : Calculated for $\text{C}_{18}\text{H}_{22}\text{N}$ ($\text{M}+\text{H}^+$): 252.1747, found: 252.1743.

Preparation of rhodium and iridium complexes

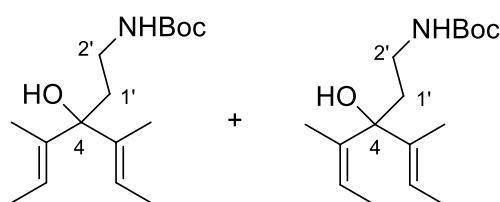
Methyl *N*-Boc-4-aminopropanoate (**53**)¹¹¹



To a stirred solution of β -alanine methyl ester hydrochloride **52** (1.80 g, 13.0 mmol) in DCM (20 ml) at 0 °C was added triethylamine (3.6 ml, 26 mmol) and, dropwise, a solution of di-*tert*-butyl dicarbonate (2.80 g, 13.0 mmol) in DCM (20 ml). The mixture was stirred at RT for 18 hours, the solvent was removed under reduced pressure and the residue was dissolved in EtOAc (40 ml), washed with 0.4 M aqueous HCl (40 ml), 5% aqueous NaHCO₃ (40 ml) and brine (40 ml). The organic phase was dried with Na₂SO₄ and the solvent was removed under reduced pressure to afford **53** as a colourless oil (2.60 g, 12.9 mmol, 99%).

R_f = 0.46 (hexane-EtOAc 70:30); ¹H NMR (500 MHz, CDCl₃, δ /ppm): 5.01 (1H, br s, NH), 3.70 (3H, s, OCH₃), 3.40 (2H, q, J = 6.0 Hz, H-3), 2.53 (2H, t, J = 6.0 Hz, H-2), 1.44 (9H, s, C(CH₃)₃); ¹³C NMR (125 MHz, CDCl₃, δ /ppm): 172.9 (C-1), 155.9 (C(O)N), 79.6 (C(CH₃)₃), 51.7 (OCH₃), 36.1 (C-3), 34.5 (C-2), 28.4 (C(CH₃)₃); HRMS (ESI+) m/z : Calculated for C₉H₁₇NNaO₄ (M+Na⁺): 226.1050, found: 226.1057. Spectroscopic data consistent with literature values.¹¹¹

N-Boc-4-(2'-Aminoethyl)-3,5-dimethyl-hepta-2,5-dien-4-ol (**54**)

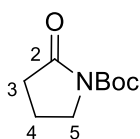


Lithium wire (516 mg, 74.0 mmol) was washed with hexane, cut into small pieces and suspended in Et₂O (15 ml). 2-Bromo-2-butene (1.8 ml, 18 mmol, mixture of *cis* and *trans* isomers) was added in one portion to the mixture and stirred until the reaction started, observed by the reflux of the solvent; another aliquot of 2-bromo-2-butene (2.0 ml, 20 mmol) in Et₂O (10 ml) was added dropwise to maintain a gentle reflux. The suspension was stirred for 2 hours at RT and then cooled to -78 °C. A solution of *N*-Boc- β -alanine methyl ester **53** (2.40 g, 12.0 mmol) in Et₂O (10 ml) was added dropwise, the mixture was warmed to RT, stirred overnight and quenched with careful addition of saturated aqueous NH₄Cl (60 ml). The phases were separated and the product was extracted with Et₂O (2 \times 30 ml). The combined organic

extracts were dried with Na₂SO₄ and the solvent was removed under reduced pressure. Purification by flash chromatography (SiO₂, eluting with hexane-EtOAc (95:5)) gave **54** as a colourless oil as a 1 : 1 mixture of *trans-trans* and *cis-trans* isomers which was used without any other purification (1.50 g, 5.30 mmol, 44%).

R_f = 0.30 (hexane-EtOAc 80:20); ¹H NMR (500 MHz, CDCl₃, δ/ppm): 5.65-5.59 (2H, m, 2CH for the *trans-trans* isomer), 5.44-5.34 (2H, m, 2CH for the *trans-cis* isomer), 5.18-5.10 (2H, m, 2NH), 3.30-3.22 (4H, m, 2H-2'), 1.95-1.86 (4H, m, 2H-1'), 1.77 (6H, s, 2CH₃), 1.69-1.60 (18H, m, 6CH₃), 1.44 (18H, s, 2C(CH₃)₃); ¹³C NMR (125 MHz, CDCl₃, δ/ppm): 156.1 (C(O)), 139.7 (C_qCH₃), 139.0 (C_qCH₃), 137.7 (C_qCH₃), 123.1 (CH for the *trans-cis* isomer), 118.6 (CH for the *trans-trans* isomer), 80.7 (C(CH₃)₃), 79.8 (C-4), 78.9 (C-4), 39.1 (C-1'), 36.7 (C-2'), 28.4 (C(CH₃)₃), 23.3 (CH₃), 22.7 (CH₃), 14.7 (CH₃), 14.4 (CH₃), 13.2 (CH₃), 12.5 (CH₃); IR (ν_{max}, neat, cm⁻¹): 3387 (N-H and O-H), 2976, 2933, 1696 (C=O), 1509, 1452, 1366, 1279, 1250, 1173; HRMS (ESI+) *m/z*: Calculated for C₁₆H₂₉NNaO₃ (M+Na⁺): 306.2040, found: 306.2034.

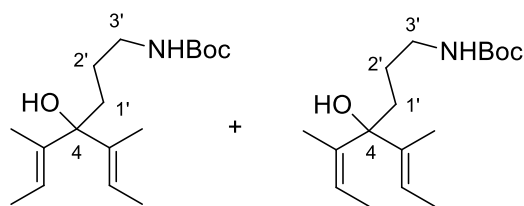
N-Boc-2-Pyrrolidinone (**56**)



Prepared by a slightly modified version of the reported method of Yoshitomi *et al.*¹¹² as follows. To a stirred solution of DMAP (8.50 g, 70.0 mmol) and di-*tert*-butyl dicarbonate (9.00 g, 42.0 mmol) in DCM (20 ml) was added *via* cannula a solution of 2-pyrrolidinone **55** (3.00 g, 35.0 mmol) in DCM (30 ml). The resulting solution was stirred for 21 hours. The solvent was removed under reduced pressure, the residue was dissolved in EtOAc (30 ml) and water (30 ml) and the phases were separated. The product was extracted with EtOAc (2 × 30 ml) and the combined organic phases were washed with saturated aqueous NH₄Cl (3 × 30 ml) and brine (30 ml), dried with MgSO₄ and the solvent was removed *in vacuo* to give **56** as a pale yellow oil (6.50 g, 35.0 mmol, quant.).

¹H NMR (500 MHz, CDCl₃, δ/ppm): 3.65 (2H, t, *J* = 7.0 Hz, *H*-5), 2.41 (2H, t, *J* = 7.5 Hz, *H*-3), 1.90 (2H, tt, *J* = 7.5, 7.0 Hz, *H*-4), 1.43 (9H, s, C(CH₃)₃); ¹³C NMR (125 MHz, CDCl₃, δ/ppm): 174.2 (C-2), 150.2 (C(O)O), 82.6 (C(CH₃)₃), 46.4 (C-5), 32.9 (C-3), 29.9 (C(CH₃)₃), 17.4 (C-4); HRMS (ESI+) *m/z*: Calculated for C₉H₁₅NNaO₃ (M+Na⁺): 208.0944, found: 208.0954. Spectroscopic data consistent with literature values.¹¹³

***N*-Boc-4-(3'-Aminopropyl)-3,5-dimethyl-hepta-2,5-dien-4-ol (57)**

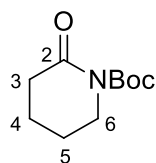


Prepared by a slightly modified version of the reported method of Ito *et al.*⁷⁰ as follows.

Lithium wire (340 mg, 48.6 mmol) was washed with hexane, cut into small pieces and suspended in Et₂O (10 ml). A solution of 2-bromo-2-butene (2.4 ml, 24 mmol, mixture of *cis* and *trans* isomers) in Et₂O (10 ml) was added dropwise and the suspension was stirred for 2 hours at RT. *N*-Boc-2-pyrrolidinone **56** (1.50 g, 8.10 mmol) dissolved in Et₂O (8.0 ml) was added dropwise, the mixture was stirred for 2 hours at RT and quenched with careful addition of saturated aqueous NH₄Cl (40 ml). The two phases were separated and the product was extracted with Et₂O (3 × 20 ml). The combined organic phases were dried with Na₂SO₄ and the solvent was removed under reduced pressure. Purification by flash chromatography (SiO₂, eluting with hexane-EtOAc (90:10 to 80:20)) gave **57** as a colourless oil as a mixture of *trans-trans* and *trans-cis* isomers (fraction major (*trans-cis*)/minor (*trans-trans*): 2/1) which was used without any other purification (1.10 g, 5.70 mmol, 70%).

R_f = 0.60 (hexane-EtOAc 70:30); ¹H NMR (500 MHz, CDCl₃, δ/ppm): 5.58 (2H, q, *J* = 6.5 Hz, 2CH for the *trans-trans* isomer), 5.35 (2H, dq, *J* = 1.0, 6.5 Hz, 2CH for the *trans-cis* isomer), 4.59 (2H, br s, 2NH), 3.14 (4H, br s, 2H-3'), 1.84-1.81 (2H, m, 2OH), 1.76-1.75 (4H, m, 2H-1'), 1.67-1.59 (24H, m, 8CH₃), 1.53-1.49 (4H, m, 2H-2'), 1.43 (18H, s, 2C(CH₃)₃); ¹³C NMR (125 MHz, CDCl₃, δ/ppm): 156.1 (C(O)), 140.0 (C_qCH₃), 139.5 (C_qCH₃), 138.0 (C_qCH₃), 122.7 (CH for the *trans-cis* isomer), 122.6 (CH for the *trans-cis* isomer), 118.3 (CH for the *trans-trans* isomer), 80.6 (C(CH₃)₃), 79.5 (C-4), 79.0 (C-4), 41.1 (C-3'), 36.8 (C-1'), 35.0 (C-1'), 28.4 (C(CH₃)₃), 24.5 (C-2'), 24.2 (C-2'), 23.4 (CH₃), 22.8 (CH₃), 14.7 (CH₃), 14.4 (CH₃), 13.2 (CH₃), 12.6 (CH₃); HRMS (ESI+) *m/z*: Calculated for C₁₇H₃₁NNaO₃ (M+Na⁺): 320.2196, found: 320.2200. Spectroscopic data consistent with literature values.⁷⁰

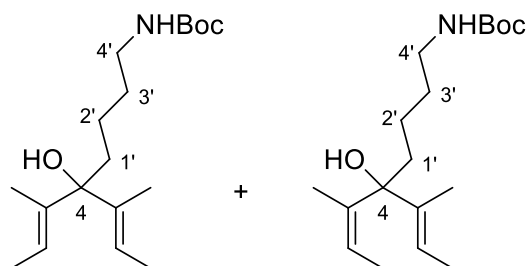
***N*-Boc-2-Piperidinone (59)**



Prepared by a slightly modified version of the reported method of Yoshitomi *et al.*¹¹² as follows. To a stirred solution of DMAP (8.50 g, 70.0 mmol) and di-*tert*-butyl dicarbonate (9.00 g, 42.0 mmol) in DCM (20 ml) was added *via* cannula a solution of δ -valerolactam **58** (3.50 g, 35.0 mmol) in DCM (30 ml). The resulting solution was stirred for 24 hours. The solvent was removed under reduced pressure, the residue was dissolved in EtOAc (30 ml) and saturated aqueous NH₄Cl (30 ml) and the two phases were separated. The product was extracted with EtOAc (2 \times 30 ml), the combined organic phases were washed with saturated aqueous NH₄Cl (2 \times 30 ml), dried with Na₂SO₄ and the solvent was removed under reduced pressure. Purification by flash chromatography (SiO₂, eluting with petrol-EtOAc (70:30)) gave **59** as a colourless oil (3.30 g, 16.6 mmol, 47%).

R_f = 0.44 (hexane-EtOAc 80:20); ¹H NMR (500 MHz, CDCl₃, δ /ppm): 3.65 (2H, t, J = 6.0 Hz, *H*-6), 2.51 (2H, t, J = 7.0 Hz, *H*-3), 1.86-1.80 (4H, m, 2CH₂), 1.53 (9H, s, C(CH₃)₃); ¹³C NMR (125 MHz, CDCl₃, δ /ppm): 171.3 (*C*-2), 152.8 (C(O)O), 82.8 (C(CH₃)₃), 46.3 (*C*-6), 34.9 (*C*-3), 28.0 (C(CH₃)₃), 22.8 (CH₂), 20.5 (CH₂); HRMS (ESI+) m/z : Calculated for C₁₀H₁₇NNaO₃ (M+Na⁺): 222.1101, found: 222.1110. Spectroscopic data consistent with literature values.¹¹⁴

***N*-Boc-4-(4'-Aminobutyl)-3,5-dimethyl-hepta-2,5-dien-4-ol (60)**

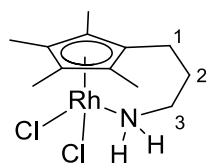


Lithium wire (4.37 mg, 63.0 mmol) was washed with hexane, cut into small pieces and suspended in Et₂O (10 ml). 2-Bromo-2-butene (1.3 ml, 13 mmol, mixture of *cis* and *trans* isomers) was added in one portion to the mixture and stirred until the reaction started, observed by the reflux of the solvent; another aliquot of 2-bromo-2-butene (2.0 ml, 20 mmol) in Et₂O (10 ml) was added dropwise and the suspension was stirred for 2 hours at RT. A solution of *N*-Boc-2-piperidinone **59** (3.00 g, 15.0 mmol) in Et₂O (20 ml) was added dropwise, the mixture was stirred for 1 hour and quenched with careful addition of saturated aqueous NH₄Cl (60 ml). The phases were separated and the product was extracted with Et₂O (2 \times 30 ml). The combined organic phases were dried with Na₂SO₄ and the solvent was removed under reduced pressure. Purification by flash

chromatography (SiO₂, eluting with hexane-EtOAc (90:10)) gave **60** as a colourless oil as a mixture of *trans-trans* and *trans-cis* isomers (fraction major (*trans-cis*)/minor (*trans-trans*): 3/2) which was used without any other purification (940 mg, 3.00 mmol, 20%).

R_f = 0.50 (hexane-EtOAc 70:30); ¹H NMR (500 MHz, CDCl₃, δ/ppm): 5.57 (2H, q, *J* = 6.5 Hz, 2CH for the *trans-trans* isomer), 5.34 (2H, dq, *J* = 1.3, 7.5 Hz, 2CH for the *trans-cis* isomer), 4.54 (2H, br s, 2NH), 3.12 (4H, br s, 2H-4'), 1.84-1.71 (6H, m, 2H-1' and 2OH), 1.69-1.60 (24H, m, 8CH₃), 1.53-1.46 (8H, m, 4CH₂), 1.44 (18H, s, 2C(CH₃)₃); ¹³C NMR (125 MHz, CDCl₃, δ/ppm): 156.1 (C(O)N), 140.2 (C_qCH₃), 139.6 (C_qCH₃), 138.1 (C_qCH₃), 122.5 (CH for the *trans-cis* isomer), 122.4 (CH for the *trans-cis* isomer), 118.9 (CH for the *trans-trans* isomer), 118.1 (CH for the *trans-trans* isomer), 80.8 (C(CH₃)₃), 79.4 (C-4), 79.1 (C-4), 40.4 (C-4'), 39.4 (C-1'), 37.6 (C-1'), 28.4 (C(CH₃)₃), 23.4 (CH₃), 22.8 (CH₃), 20.7 (CH₂), 20.5 (CH₂), 14.8 (CH₃), 14.4 (CH₃), 13.4 (CH₃), 13.2 (CH₃), 12.6 (CH₃), 12.4 (CH₃); IR (ν_{max}, neat, cm⁻¹): 3364 (N-H and O-H), 2975, 2933, 2865, 1695 (C=O), 1515, 1454, 1366, 1251, 1172, 1003; HRMS (ESI+) *m/z*: Calculated for C₁₈H₃₃NNaO₃ (M+Na⁺): 334.2353, found: 334.2357.

RhCl₂[η⁵:η¹-C₅(CH₃)₄(CH₂)₃NH₂] (**67**)



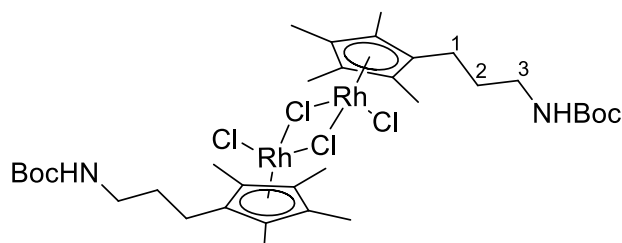
To a stirred solution of ligand **57** (850 mg, 2.86 mmol) in methanol (12 ml) was added RhCl₃·hydrate (300 mg, 1.44 mmol). The reaction mixture was heated at reflux for 20 hours and the solvent was removed

under reduced pressure. Purification by flash chromatography (SiO₂, eluting with DCM-MeOH (98:2)) gave **67** as a red solid (184 mg, 0.523 mmol, 36%). Single crystals were achieved by slow recrystallization from DCM.

R_f = 0.51 (DCM-MeOH 90:10); mp > 250 °C (DCM); ¹H NMR (500 MHz, CDCl₃, δ/ppm): 3.37 (2H, br s, NH₂), 2.68-2.65 (2H, m, H-3), 2.12-2.09 (2H, m, H-1), 2.04-2.03 (2H, m, H-2), 1.79 (6H, s, 2CH₃), 1.64 (6H, s, 2CH₃); ¹³C NMR (125 MHz, CDCl₃, δ/ppm): 99.1 (d, *J* = 8.0 Hz, C_qRh), 96.2 (d, *J* = 8.7 Hz, C_qRh), 86.6 (d, *J* = 8.7 Hz, C_qRh), 39.7 (C-3), 30.3 (C-2), 19.2 (C-1), 9.5 (CH₃), 9.0 (CH₃); IR (ν_{max}, neat, cm⁻¹): 3244 (N-H), 3162 (N-H), 2950, 1593, 1445, 1375, 1150, 1136, 1083, 1033; HRMS (ESI+) *m/z*: Calculated for C₁₂H₂₀³⁵ClNRh (M-Cl⁻): 316.0334, found: 316.0335; calculated for C₁₂H₂₀³⁷ClNRh (M-Cl⁻): 318.0307, found: 316.0304; Anal. Calcd. For C₁₂H₂₀Cl₂NRh:

C, 40.93; H, 5.73; N, 3.98; Found C, 40.85; H, 5.65; N, 3.90. Spectroscopic data consistent with literature values.⁷⁰

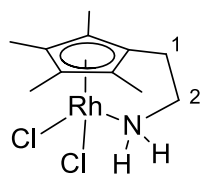
$[\eta^5\text{-C}_5(\text{CH}_3)_4(\text{CH}_2)_3\text{NHBoc}]_2\text{Rh}_2\text{Cl}_4$ (68**)**



To a stirred solution of ligand **57** (850 mg, 2.86 mmol) in methanol (12 ml) was added $\text{RhCl}_3\cdot\text{hydrate}$ (300 mg, 1.44 mmol). The reaction mixture was heated at reflux for 20 hours and the solvent was removed under reduced pressure. Purification by flash chromatography (SiO_2 , eluting with DCM-MeOH (98:2)) gave **68** as a dark red solid (160 mg, 0.178 mmol, 25%).

$R_f = 0.36$ (DCM-MeOH 90:10); mp 212.4-213.8 °C (DCM-hexane); $^1\text{H NMR}$ (500 MHz, CDCl_3 , δ/ppm): 4.68 (2H, br s, 2NH), 3.10 (4H, q, $J = 6.8$ Hz, 2H-3), 2.29 (4H, q, $J = 8.0$ Hz, 2H-1), 1.63 (12H, s, 4 CH_3), 1.62 (12H, s, 4 CH_3), 1.61-1.58 (4H, m, 2H-2), 1.42 (18H, s, 2C(CH_3)₃); $^{13}\text{C NMR}$ (125 MHz, CDCl_3 , δ/ppm): 155.8 (C(O)N), 95.0 (d, $J = 10.0$ Hz, C_qRh), 94.6 (d, $J = 6.3$ Hz, C_qRh), 79.4 (C(CH_3)₃), 40.3 (C-3), 28.4 (C(CH_3)₃), 27.4 (C-2), 21.5 (C-1), 9.6 (CH_3), 9.4 (CH_3), one carbon (C_qRh) not observed; IR (ν_{max} , neat, cm^{-1}): 3319 (N-H), 3003, 2970, 1738 (C=O), 1436, 1365, 1228, 1217, 1027; HRMS (ESI+) m/z : Calculated for $\text{C}_{34}\text{H}_{56}\text{N}_2\text{O}_4\text{Rh}_2^{35}\text{Cl}_3$ (M- Cl^- , 98%): 867.1410, found: 867.1410; calculated for $\text{C}_{34}\text{H}_{56}\text{N}_2\text{O}_4\text{Rh}_2^{35}\text{Cl}_2^{37}\text{Cl}$ (M- Cl^- , 100%): 869.1388, found: 869.1384; calculated for $\text{C}_{34}\text{H}_{56}\text{N}_2\text{O}_4\text{Rh}_2^{35}\text{Cl}^{37}\text{Cl}_2$ (M- Cl^- , 42%): 871.1370, found: 871.1366.

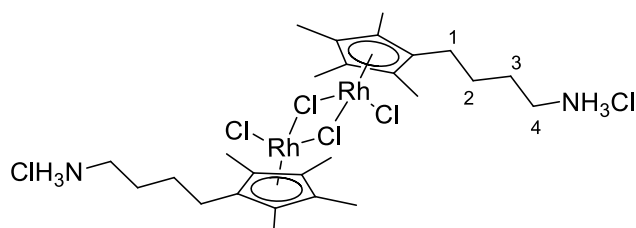
$\text{RhCl}_2[\eta^5:\eta^1\text{-C}_5(\text{CH}_3)_4(\text{CH}_2)_2\text{NH}_2]$ (64**)**



To a stirred solution of ligand **54** (272 mg, 0.961 mmol) in methanol (8.0 ml) was added $\text{RhCl}_3\cdot\text{hydrate}$ (100 mg, 0.481 mmol). The reaction mixture was heated at reflux for 22 hours, cooled to room temperature and the solvent was removed under reduced pressure. Purification by flash chromatography (SiO_2 , eluting with DCM-MeOH (97:3)) gave **64** as a red solid (15 mg, 44 μmol , 10%).

$R_f = 0.63$ (DCM-MeOH 80:20); $^1\text{H NMR}$ (500 MHz, CDCl_3 , δ/ppm): 3.93-3.87 (2H, m, $H-2$), 3.69 (2H, br s, NH_2), 2.41 (2H, t, $J = 6.5$ Hz, $H-1$), 1.89 (6H, s, 2CH_3), 1.69 (6H, s, 2CH_3); $^{13}\text{C NMR}$ (125 MHz, CDCl_3 , δ/ppm): 108.6 (d, $J = 7.5$ Hz, $C_q\text{Rh}$), 97.5 (d, $J = 6.3$ Hz, $C_q\text{Rh}$), 86.0 (d, $J = 8.8$ Hz, $C_q\text{Rh}$), 57.7 ($C-2$), 25.6 ($C-1$), 9.1 (CH_3), 8.8 (CH_3); HRMS (ESI+) m/z : Calculated for $\text{C}_{11}\text{H}_{18}\text{NRh}^{35}\text{Cl}$ ($\text{M}-\text{Cl}^-$, 100%): 302.0177, found: 302.0180, calculated for $\text{C}_{11}\text{H}_{18}\text{NRh}^{37}\text{Cl}$ ($\text{M}-\text{Cl}^-$, 35%): 304.0150, found: 304.0148. Spectroscopic data consistent with literature values.⁷⁰

$\text{Rh}_2\text{Cl}_4[\eta^5\text{-C}_5(\text{CH}_3)_4(\text{CH}_2)_4\text{NH}_3\text{Cl}]_2$ (**70**)

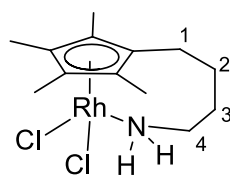


To a stirred solution of ligand **60** (298 mg, 0.964 mmol) in methanol (8.0 ml) was added $\text{RhCl}_3\cdot\text{hydrate}$ (100 mg, 0.478 mmol). The reaction

mixture was heated at reflux for 22 hours, then cooled to room temperature and the solvent was removed under reduced pressure. Crystallization from MeOH-Et₂O ($v/v = 1/2$) gave **70** as an orange solid (65 mg, 0.081 mmol, 34%). The formation of the hydrochloride salt was determined by comparing the NMR signals with a similar complex reported in the literature.⁷⁰

$^1\text{H NMR}$ (500 MHz, DMSO, δ/ppm): 8.05 (6H, br s, 2NH_3), 2.75 (4H, br s, $2H-4$), 2.15 (4H, br s, $2H-1$), 1.67 (12H, s, 4CH_3), 1.63-1.57 (16H, m, 2CH_2 and 4CH_3), 1.48 (4H, br s, 2CH_2); $^{13}\text{C NMR}$ (125 MHz, DMSO, δ/ppm): 99.4 (d, $J = 7.5$ Hz, $C_q\text{Rh}$), 99.3 (d, $J = 7.5$ Hz, $C_q\text{Rh}$), 99.1 (d, $J = 7.5$ Hz, $C_q\text{Rh}$), 38.3 ($C-4$), 26.9 (CH_2), 23.9 (CH_2), 22.7 ($C-1$), 8.7 (CH_3), 8.6 (CH_3); IR (ν_{max} , neat, cm^{-1}): 3370 (N-H), 3100 (N-H), 2965, 2914, 1706, 1591, 1567, 1479, 1400, 1367, 1024; HRMS (ESI+) m/z : Calculated for $\text{C}_{26}\text{H}_{44}\text{N}_2\text{Rh}_2^{35}\text{Cl}_3$ ($\text{M}-[2\text{HCl}]-\text{Cl}^-$, 100%): 695.0675, found: 695.0673, calculated for $\text{C}_{26}\text{H}_{44}\text{N}_2\text{Rh}_2^{35}\text{Cl}_2^{37}\text{Cl}$ ($\text{M}-[2\text{HCl}]-\text{Cl}^-$, 100%): 697.0649, found: 697.0647; calculated for $\text{C}_{26}\text{H}_{44}\text{N}_2\text{Rh}_2^{35}\text{Cl}^{37}\text{Cl}_2$ ($\text{M}-[2\text{HCl}]-\text{Cl}^-$, 33%): 699.0627, found: 699.0620.

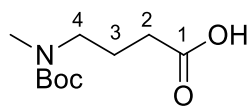
$\text{RhCl}_2[\eta^5:\eta^1\text{-C}_5(\text{CH}_3)_4(\text{CH}_2)_4\text{NH}_2]$ (**69**)



To a stirred solution of the dimer rhodium complex **70** (52 mg, 0.065 mmol) in DCM (10 ml) was added potassium *tert*-butoxide (16 mg, 0.14 mmol) and the mixture was stirred at room temperature for 72 hours. It was filtered through a pad of Celite®, washed with DCM and the solvent was removed under reduced pressure. Purification by flash chromatography (SiO₂, eluting with DCM-MeOH (97:3)) gave **69** as an orange solid (14 mg, 38 μmol, 29%).

$R_f = 0.53$ (DCM-MeOH 90:10); ¹H NMR (500 MHz, CDCl₃, δ/ppm): 3.23-3.19 (2H, m, *H*-4), 2.87 (2H, br s, NH₂), 2.11-2.09 (2H, m, CH₂), 2.07-2.01 (2H, m, CH₂), 1.86-1.79 (2H, m, CH₂), 1.66 (6H, s, 2CH₃), 1.64 (6H, s, 2CH₃); ¹³C NMR (125 MHz, CDCl₃, δ/ppm): 100.9 (d, $J = 11.3$ Hz, C_qRh), 96.7 (d, $J = 10.0$ Hz, C_qRh), 89.3 (d, $J = 10.0$ Hz, C_qRh), 43.9 (C-4), 28.9 (CH₂), 22.9 (CH₂), 21.5 (CH₂), 9.7 (CH₃), 9.0 (CH₃); HRMS (ESI+) m/z : Calculated for C₁₃H₂₂NRh³⁵Cl (M-Cl⁻, 100%): 330.0490, found: 330.0492, calculated for C₁₃H₂₂NRh³⁷Cl (M-Cl⁻, 33%): 332.0461, found: 332.0457.

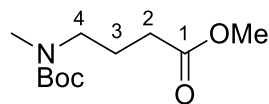
N-Boc-*N*-Methyl-4-aminobutanoic acid (**72**)



Prepared by a slightly modified version of the reported method of Heck *et al.*¹¹¹ as follows. To a stirred suspension of 4-methylaminobutyric acid hydrochloride **71** (1.40 g, 9.11 mmol) in DCM (20 ml) was added triethylamine (3.7 ml, 27 mmol) and it was cooled to 0 °C. A solution of di-*tert*-butyl dicarbonate (2.00 g, 9.17 mmol) in DCM (10 ml) was added and the reaction mixture was stirred at room temperature for 18 hours. The solvent was removed under reduced pressure, the residue was dissolved in EtOAc (40 ml) and 0.4 M aqueous HCl (30 ml) and the two phases were separated. The organic phase was washed with saturated aqueous NaHCO₃ (20 ml) and brine (30 ml), dried with Na₂SO₄ and the solvent was removed under reduced pressure to afford **72** as a white solid (1.70 g, 7.83 mmol, 89%). $R_f = 0.27$ (hexane-EtOAc 50:50); mp 64.2-65.4 °C (DCM-hexane, v/v = 1/2); ¹H NMR (500 MHz, CDCl₃, δ/ppm): 3.30 (2H, br s, *H*-4), 2.99 (3H, s, NCH₃), 2.37 (2H, t, $J = 7.0$ Hz, *H*-2), 1.86 (2H, ap quint, $J = 7.0$ Hz, *H*-3), 1.46 (9H, s, C(CH₃)₃); ¹³C NMR (125 MHz, CDCl₃, δ/ppm): 178.2 & 177.9 (C-1, rotamers), 156.1 & 155.9 (C(O)N, rotamers), 79.8 (C(CH₃)₃), 48.1 & 47.7 (C-4, rotamers), 34.2 (NCH₃), 31.3 & 30.9 (C-2, rotamers), 28.4 (C(CH₃)₃), 22.9 (C-3); IR (ν_{max}, neat, cm⁻¹): 3166 (O-H), 1728 (C=O),

1653, 1455, 1403, 1369, 1311, 1167; HRMS (ESI+) m/z : Calculated for $C_{10}H_{19}NNaO_4$ ($M+Na^+$): 240.1206, found: 240.1213. Spectroscopic data consistent with literature values.¹¹⁵

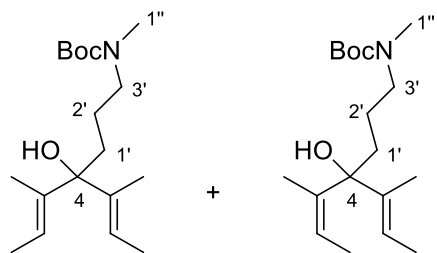
Methyl *N*-Boc-*N*-methyl-4-aminobutanoate (**73**)



To a stirred suspension of DMAP (1.30 g, 11.0 mmol) and *N*-(3-dimethylaminopropyl)-*N'*-ethylcarbodiimide hydrochloride (1.90 g, 10.0 mmol) in methanol (10 ml) at 0 °C was added *via* cannula a solution of *N*-Boc-*N*-methyl-4-aminobutanoic acid **72** (2.00 g, 9.21 mmol) in methanol (10 ml). The resulting solution was stirred at room temperature for 72 hours. The solvent was removed under reduced pressure, the residue was dissolved in EtOAc (60 ml) and water (50 ml) and the two phases were separated. The organic phase was washed with saturated aqueous $NaHCO_3$ (50 ml), 1 M aqueous HCl (50 ml) and brine (50 ml), dried with Na_2SO_4 and the solvent was removed under reduced pressure to give **73** as a pale yellow oil (2.00 g, 8.66 mmol, 97%).

R_f = 0.32 (hexane-EtOAc 80:20); 1H NMR (500 MHz, $CDCl_3$, δ/ppm): 3.67 (3H, s, OCH_3), 3.25 (2H, t, $J = 7.0$ Hz, $H-4$), 2.83 (3H, s, NCH_3), 2.31 (2H, t, $J = 7.0$ Hz, $H-2$), 1.84 (2H, ap quint, $J = 7.0$ Hz, $H-3$), 1.45 (9H, s, $C(CH_3)_3$); ^{13}C NMR (125 MHz, $CDCl_3$, δ/ppm): 173.8 ($C-1$), 155.8 ($C(O)N$), 79.4 ($C(CH_3)_3$), 51.6 (OCH_3), 48.3 & 47.8 ($C-4$, rotamers), 34.1 (NCH_3), 31.1 ($C-2$), 28.4 ($C(CH_3)_3$), 23.2 ($C-3$); HRMS (ESI+) m/z : Calculated for $C_{11}H_{21}NNaO_4$ ($M+Na^+$): 254.1363, found: 254.1372. Spectroscopic data consistent with literature values.¹¹⁶

N-Boc-*N*-Methyl-4-(3'-aminopropyl)-3,5-dimethyl-hepta-2,5-dien-4-ol (**74**)

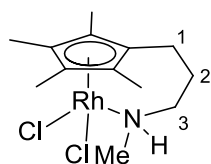


Lithium wire (150 mg, 22.0 mmol) was washed with hexane, cut into small pieces and suspended in Et_2O (10 ml). A solution of 2-bromo-2-butene (1.2 ml, 12 mmol, mixture of *cis* and *trans* isomers) in Et_2O (10 ml) was added dropwise and the suspension was stirred for 2 hours at RT. A solution of methyl *N*-Boc-*N*-methyl-4-aminobutanoate **73** (1.20 g, 5.19 mmol) in Et_2O (10 ml) was added dropwise, stirred for 90 minutes at RT

and quenched with careful addition of saturated aqueous NH_4Cl (40 ml). The phases were separated and the product was extracted with Et_2O (3×20 ml). The combined organic extracts were dried with Na_2SO_4 and the solvent was removed under reduced pressure. Purification by flash chromatography (SiO_2 , eluting with hexane-EtOAc (90:10)) gave **74** as a colourless oil in a 1 : 1 mixture of *trans-trans* and *trans-cis* isomers which was used without any other purification (540 mg, 1.74 mmol, 33%).

$R_f = 0.40$ (hexane-EtOAc 80:20); ^1H NMR (500 MHz, CDCl_3 , δ/ppm): 5.62-5.56 (2H, m, 2CH for the *trans-trans* isomer), 5.42-5.30 (2H, m, 2CH for the *trans-cis* isomer), 3.27-3.24 (4H, m, 2H-3'), 2.87 (6H, br s, 2H-1''), 1.86-1.76 (4H, m, 2H-1'), 1.74 (2H, s, 2OH), 1.69-1.61 (18H, m, 6CH₃), 1.62-1.59 (4H, m, 2CH₂), 1.46 (24H, s, 2CH₃ and 2C(CH₃)₃); ^{13}C NMR (125 MHz, CDCl_3 , δ/ppm): 156.0 (C(O)N), 140.1 (C_qCH₃), 139.6 (C_qCH₃), 138.1 (C_qCH₃), 122.5 (CH), 119.0 (CH), 118.2 (CH), 80.7 (C(CH₃)₃), 79.1 (C-4), 51.6 (C-3'), 34.0 (C-1''), 29.7 (C-1'), 28.4 (C(CH₃)₃), 23.4 (CH₃), 22.8 (CH₃), 21.9 (C-2'), 14.8 (CH₃), 14.4 (CH₃), 13.4 (CH₃), 13.2 (CH₃), 12.6 (CH₃), 12.4 (CH₃); IR (ν_{max} , neat, cm^{-1}): 3474 (O-H), 2973, 2931, 1759 (C=O), 1695 (C=C), 1481, 1454, 1395, 1365, 1171; HRMS (ESI+) m/z : Calculated for $\text{C}_{18}\text{H}_{33}\text{NNaO}_3$ (M+Na⁺): 334.2353, found: 334.2349.

RhCl₂[η^5 : η^1 -C₅(CH₃)₄(CH₂)₃N(CH₃)H] (75)

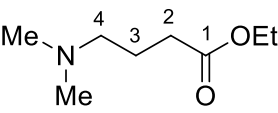


To a stirred solution of ligand **74** (210 mg, 0.68 mmol) in methanol (5.0 ml) was added $\text{RhCl}_3 \cdot \text{hydrate}$ (70 mg, 0.33 mmol). The mixture was heated at reflux for 18 hours and the solvent was removed under reduced pressure. Purification by flash chromatography (SiO_2 , eluting with DCM-MeOH (98:2)) gave **75** as a red solid (27 mg, 74 μmol , 30%). Single crystals were achieved by recrystallization from DCM and hexane ($v/v = 1/2$).

$R_f = 0.48$ (DCM-MeOH 90:10); mp 219.8-221.1 °C (DCM-hexane, $v/v = 1/2$); ^1H NMR (500 MHz, CDCl_3 , δ/ppm): 3.61 (1H, br s, NH), 2.85-2.80 (1H, m, H_A-3), 2.66-2.62 (1H, m, H_B-3), 2.59 (3H, d, $J = 6.5$ Hz, NCH₃), 2.24-2.16 (1H, m, CH₂), 2.12-2.03 (3H, m, CH₂), 1.77 (3H, s, CH₃), 1.72 (3H, s, CH₃), 1.66 (3H, s, CH₃), 1.62 (3H, s, CH₃); ^{13}C NMR (125 MHz, CDCl_3 , δ/ppm): 104.1 (d, $J = 8.8$ Hz, C_qRh), 93.8 (d, $J = 8.8$ Hz, C_qRh), 93.3 (d, $J = 8.8$ Hz, C_qRh), 92.0 (d, $J = 8.8$ Hz, C_qRh), 83.9 (d, $J = 11.3$ Hz, C_qRh), 51.6 (C-3), 39.9 (NCH₃), 26.1 (C-2), 19.4 (C-1), 9.9 (CH₃), 9.3 (CH₃), 9.2 (CH₃), 9.1 (CH₃); IR (ν_{max} , neat, cm^{-1}): 3504 (N-H), 3003, 2970, 1719, 1648, 1439, 1365, 1218, 902; HRMS (ESI+)

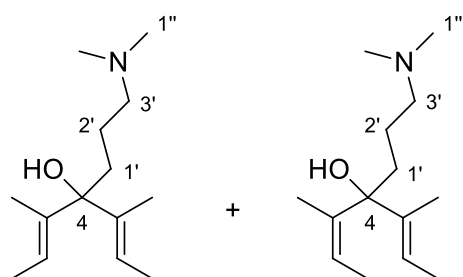
m/z : Calculated for $C_{13}H_{22}NRh^{35}Cl$ ($M-Cl^-$, 100%): 330.0490, found: 330.0489, calculated for $C_{13}H_{22}NRh^{37}Cl$ ($M-Cl^-$, 34%): 332.0464, found: 332.0462; Anal. Calcd. For $C_{13}H_{22}Cl_2NRh$: C, 42.65; H, 6.06; N, 3.83; Cl, 19.37; Found C, 42.30; H, 6.10; N, 3.70; Cl, 19.20.

Ethyl 4-dimethylaminobutanoate (**77**)


 Prepared by a slightly modified version of the reported method of Khan *et al.*¹¹⁷ as follows. To a stirred suspension of potassium carbonate (8.30 g, 60.0 mmol) in toluene (40 ml) were added dimethylamine hydrochloride (2.45 g, 30.0 mmol) and ethyl 4-bromobutyrate **76** (4.5 ml, 30 mmol). The reaction mixture was heated at reflux for 20 hours, then cooled to RT and filtered. The solvent was removed under reduced pressure to give **77** as a yellow oil (3.10 g, 19.0 mmol, 65%).

R_f = 0.26 (DCM-MeOH 90:10); 1H NMR (500 MHz, $CDCl_3$, δ/ppm): 4.10 (2H, q, J = 7.1 Hz, OCH_2), 2.30 (2H, t, J = 7.5 Hz, $H-2$ or $H-4$), 2.25 (2H, t, J = 7.3 Hz, $H-2$ or $H-4$), 2.19 (6H, s, $2NCH_3$), 1.76 (2H, ap quint, J = 7.4 Hz, $H-3$), 1.22 (3H, t, J = 7.1 Hz, CH_3); ^{13}C NMR (125 MHz, $CDCl_3$, δ/ppm): 173.5 ($C-1$), 60.2 (OCH_2), 58.8 ($C-2$ or $C-4$), 45.4 (NCH_3), 32.1 ($C-2$ or $C-4$), 23.0 ($C-3$), 14.2 (CH_3); IR (ν_{max} , neat, cm^{-1}): 2978, 2943, 2817, 2767, 1737 ($C=O$), 1464, 1372, 1256, 1188, 1032; HRMS (ESI+) m/z : Calculated for $C_8H_{18}NO_2$ ($M+H^+$): 160.1332, found: 160.1332.

4-(3'-Dimethylaminopropyl)-3,5-dimethyl-hepta-2,5-dien-4-ol (**78**)

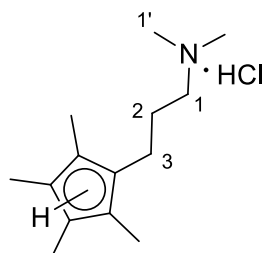


Lithium wire (530 mg, 76.0 mmol) was washed with hexane, cut into small pieces and suspended in Et_2O (10 ml). 2-Bromo-2-butene (1.5 ml, 15 mmol, mixture of *cis* and *trans* isomers) was added in one portion to the mixture and stirred until the reaction started, observed by the reflux of the solvent; another aliquot of 2-bromo-2-butene (2.5 ml, 25 mmol) in Et_2O (15 ml) was added dropwise and the suspension was stirred for 2 hours at RT. A solution of ethyl *N,N*-dimethyl-4-aminobutanoate **77** (2.80 g, 18.0 mmol) in Et_2O (15 ml) was added dropwise, stirred for 60 minutes at RT and quenched with careful addition of saturated

aqueous NH_4Cl (50 ml). The phases were separated and the product was extracted with Et_2O (2×40 ml). The combined organic phases were dried with Na_2SO_4 and the solvent was removed under reduced pressure. Purification by flash chromatography (SiO_2 , eluting with hexane-EtOAc (60:40 to 0:100)) gave **78** as a colourless oil as a 1 : 1 mixture of *trans-trans* and *trans-cis* isomers which was used without any other purification (1.70 g, 7.54 mmol, 41%).

$R_f = 0.38$ (DCM-MeOH 80:20); ^1H NMR (500 MHz, CDCl_3 , δ/ppm): 5.65 (2H, q, $J = 5.7$ Hz, 2CH for the *trans-trans* isomer), 5.58 (1H, q, $J = 6.5$ Hz, CH for the *trans-cis* isomer), 5.40 (1H, q, $J = 7.3$ Hz, CH for the *trans-cis* isomer), 2.33-2.28 (4H, m, 2 CH_2), 2.24 (6H, s, 2 H-1''), 2.20 (6H, s, 2 H-1''), 2.07-1.91 (4H, m, 2 CH_2), 1.83-1.61 (18H, m, 6 CH_3), 1.59-1.51 (4H, m, 2 CH_2), 1.49-1.46 (6H, m, 2 CH_3); ^{13}C NMR (125 MHz, CDCl_3 , δ/ppm): 139.8 (C_qCH_3), 139.0 (C_qCH_3), 138.8 (C_qCH_3), 122.9 (CH for the *trans-cis* isomer), 118.5 (CH for the *trans-trans* isomer), 117.5 (CH for the *trans-cis* isomer), 79.8 (C-4), 78.9 (C-4), 60.6 (C-3'), 45.1 (C-1''), 37.6 (C-1'), 36.4 (C-1'), 23.6 (CH_3), 22.1 (CH_2), 21.9 (CH_2), 14.8 (CH_3), 13.5 (CH_3), 13.3 (CH_3), 12.5 (CH_3), 12.4 (CH_3); IR (ν_{max} , neat, cm^{-1}): 3394 (O-H), 2944, 2919, 2859, 2821, 2779, 1459, 1378, 1039, 1014; HRMS (ESI+) m/z : Calculated for $\text{C}_{14}\text{H}_{28}\text{NO}$ ($\text{M}+\text{H}^+$): 226.2165, found: 226.2167.

***N,N*-Dimethyl-3-(tetramethylcyclopentadienyl)propan-1-amine hydrochloride (80)**

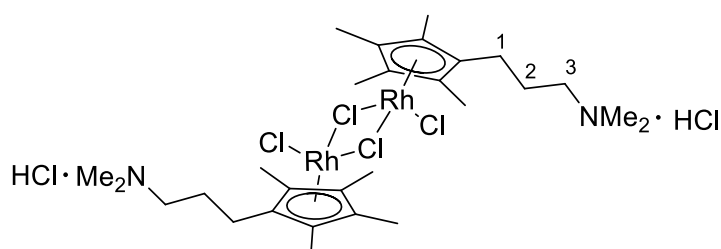


Prepared by a slightly modified version of the general method for the synthesis of cyclopentadienyls reported by Ito *et al.*⁷⁰ as follows. To a stirred solution of ligand **78** (970 mg, 4.30 mmol) in methanol (2.5 ml) was added a 2 M solution of HCl in Et_2O (2.6 ml, 5.2 mmol). The solution was stirred at room temperature for 2 hours and the solvent was removed under reduced pressure. The resulting yellow precipitate (1.14 g) was used in the following reactions without any other purification. Purification of a small amount of crude material (478 mg) by flash chromatography (SiO_2 , eluting with DCM-MeOH (90:10)) gave **80** as a pale yellow solid in an unresolved mixture of three isomers used for characterization (239 mg, 0.984 mmol, 55%).

$R_f = 0.50$ (DCM-MeOH 90:10); mp 117.5-118.6 °C (DCM- Et_2O); ^1H NMR (500 MHz, CDCl_3 , δ/ppm): 8.54 (1H, br s, NH), 2.73-2.66 (2H, m, H-1), 2.68-2.41 (1H, m, CH), 2.59-2.53 (6H, m, 2H-1'), 2.48-2.23 (2H, m, CH_2), 1.92-1.63 (2H, m, CH_2), 1.80-1.75 (9H, m, 3 CH_3), 0.98 (3H, d, $J = 7.5$ Hz, CH_3); ^{13}C NMR (125 MHz, CDCl_3 , δ/ppm): 139.7

(C_qCH_3), 139.6 (C_qCH_3), 139.0 (C_qCH_3), 136.7 (C_qCH_3), 136.4 (C_qCH_3), 136.1 (C_qCH_3), 134.5 (C_qCH_3), 133.9 (C_qCH_3), 132.9 (C_qCH_3), 58.6 (C-1), 58.2 (C-1), 55.3 (CH), 51.6 (CH), 49.1 (CH), 43.7 (C-1'), 43.6 (C-1'), 43.5 (CH₂), 43.3 (CH₂), 25.8 (CH₂), 25.1 (CH₂), 24.7 (CH₂), 23.3 (CH₂), 22.9 (CH₂), 14.2 (CH₃), 11.9 (CH₃), 11.8 (CH₃), 11.6 (CH₃), 11.3 (CH₃), 11.0 (CH₃); IR (ν_{max} , neat, cm^{-1}): 3403 (N-H), 2961, 2856, 2763, 2580, 2517, 2479, 1655, 1487, 1443, 1377, 1172, 1058, 1041, 1020, 1006; HRMS (ESI+) m/z : Calculated for C₁₄H₂₆N (M+H⁺): 208.2060, found: 208.2062.

Rh₂Cl₄[η^5 -C₅(CH₃)₄(CH₂)₃NMe₂·HCl]₂ (81**)**

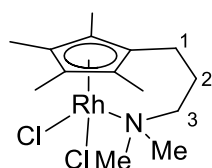


To a stirred solution of the ligand **80** hydrochloride (300 mg, 1.24 mmol) in methanol (7.0 ml) was added

RhCl₃·hydrate (130 mg, 0.622 mmol). The reaction mixture was heated at reflux for 20 hours, cooled to RT and the precipitate was filtered and washed with Et₂O (20 ml) to give **81** as a red solid (104 mg, 0.125 mmol, 40%). The formation of the hydrochloride salt was determined by comparing the NMR signals with a similar complex reported in the literature.⁷⁰

¹H NMR (500 MHz, DMSO, δ/ppm): 10.09 (2H, br s, 2NH), 3.10 (4H, t, $J = 8.0$ Hz, 2H-3), 2.71 (12H, s, 4NCH₃), 2.19 (4H, t, $J = 8.0$ Hz, 2H-1), 1.84-1.77 (4H, m, 2H-2), 1.69 (12H, s, 4CH₃), 1.63 (12H, s, 4CH₃); ¹³C NMR (125 MHz, DMSO, δ/ppm): 100.1 (d, $J = 8.8$ Hz, C_qRh), 99.1 (d, $J = 8.1$ Hz, C_qRh), 97.7 (d, $J = 8.8$ Hz, C_qRh), 55.9 (C-3), 42.1 (NCH₃), 21.9 (C-2), 20.4 (C-1), 8.7 (CH₃), 8.6 (CH₃); IR (ν_{max} , neat, cm^{-1}): 3629 (N-H), 3536 (N-H), 3016, 2716, 1738, 1593, 1460, 1367, 1231, 1161, 1021; HRMS (ESI+) m/z : Calculated for C₂₈H₄₈N₂Rh₂³⁵Cl₃ (M-[2HCl]-Cl⁻, 100%): 723.0988, found: 723.0986; Calculated for C₂₈H₄₈N₂Rh₂³⁵Cl₂³⁷Cl (M-[2HCl]-Cl⁻, 100%): 725.0962, found: 725.0960; Calculated for C₂₈H₄₈N₂Rh₂³⁵Cl³⁷Cl₂ (M-[2HCl]-Cl⁻, 35%): 727.0941, found: 727.0935.

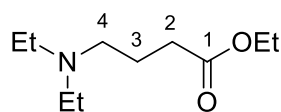
$\text{RhCl}_2[\eta^5:\eta^1\text{-C}_5(\text{CH}_3)_4(\text{CH}_2)_3\text{N}(\text{CH}_3)_2]$ (**79**)



To a suspension of rhodium dimer **81** (71 mg, 85 μmol) in DCM (5.0 ml) was added potassium *tert*-butoxide (20 mg, 0.17 mmol). The reaction mixture was stirred at RT for 72 hours, then filtered through a pad of Celite®, washed with DCM and the solvent was removed under reduced pressure. Crystallization from DCM-hexane (v/v = 1/5) gave **79** as a red solid (22 mg, 58 μmol , 34%). Single crystals were achieved by slow recrystallization from DCM-hexane (v/v = 1/2).

R_f = 0.60 (DCM-MeOH 90:10); mp 197.8-198.6 °C (DCM-hexane, v/v = 1/2); ^1H NMR (500 MHz, CDCl_3 , δ/ppm): 2.60 (6H, s, 2NCH₃), 2.55-2.53 (2H, m, *H*-3), 2.22-2.17 (2H, m, *H*-2), 2.07 (2H, t, J = 6.5 Hz, *H*-1), 1.69 (6H, s, 2CH₃), 1.61 (6H, s, 2CH₃); ^{13}C NMR (125 MHz, CDCl_3 , δ/ppm): 97.6 (d, J = 7.5 Hz, $C_q\text{Rh}$), 92.2 (d, J = 8.1 Hz, $C_q\text{Rh}$), 89.8 (d, J = 8.8 Hz, $C_q\text{Rh}$), 62.3 (*C*-3), 52.4 (NCH₃), 24.8 (*C*-2), 19.0 (*C*-1), 9.6 (CH₃), 9.4 (CH₃); IR (ν_{max} , neat, cm^{-1}): 3030, 2990, 2928, 1713, 1479, 1450, 1373, 1154, 1092, 1026, 1008; HRMS (ESI+) m/z : Calculated for $\text{C}_{14}\text{H}_{24}^{35}\text{ClNRh}$ ($\text{M}-\text{Cl}^-$, 100%): 344.0647, found: 344.0649; calculated for $\text{C}_{14}\text{H}_{24}^{37}\text{ClNRh}$ ($\text{M}-\text{Cl}^-$, 31%): 346.0620, found: 346.0619; Anal. Calcd. For $\text{C}_{14}\text{H}_{24}\text{Cl}_2\text{NRh}$: C, 44.23; H, 6.36; N, 3.68; Found C, 44.65; H, 6.40; N, 3.65. Elemental analysis data for C outside the expected range (\pm 0.4), but best value to date.

Ethyl 4-diethylaminobutanoate (**82**)

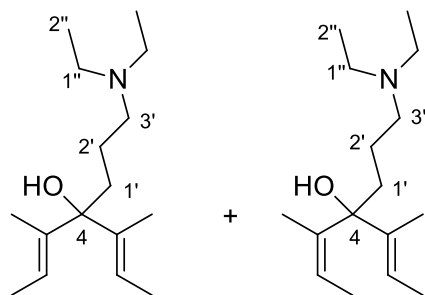


Prepared by a slightly modified version of the reported method of Khan *et al.*¹¹⁷ as follows. To a stirred suspension of potassium carbonate (4.10 g, 30.0 mmol) in toluene (40 ml) were added diethylamine (3.0 ml, 30 mmol) and ethyl 4-bromobutyrate **76** (4.5 ml, 30 mmol). The mixture was heated at 110 °C for 20 hours, cooled to room temperature and filtered. The solvent was removed under reduced pressure to give **82** as a yellow oil (5.20 g, 28.0 mmol, 93%).

R_f = 0.56 (DCM-MeOH 90:10); ^1H NMR (500 MHz, CDCl_3 , δ/ppm): 4.13 (2H, q, J = 7.3 Hz, OCH₂), 2.51 (4H, q, J = 7.2 Hz, 2NCH₂CH₃), 2.43 (2H, t, J = 7.4 Hz, *H*-4), 2.32 (2H, t, J = 7.5 Hz, *H*-2), 1.76 (2H, ap quint, J = 7.5 Hz, *H*-3), 1.25 (3H, t, J = 7.3 Hz, OCH₂CH₃), 1.01 (6H, t, J = 7.2 Hz, 2NCH₂CH₃); ^{13}C NMR (125 MHz, CDCl_3 , δ/ppm): 173.7 (*C*-1), 60.1 (OCH₂), 52.0 (*C*-4), 46.9 (NCH₂CH₃), 32.2 (*C*-2), 22.5 (*C*-3), 14.2

(OCH₂CH₃), 11.8 (NCH₂CH₃); IR (ν_{\max} , neat, cm⁻¹): 2985, 2941, 2735, 2663, 1735 (C=O), 1466, 1450, 1397, 1370, 1273, 1190, 1157, 1118, 1071, 1022; HRMS (ESI+) m/z : Calculated for C₁₀H₂₂NO₂ (M+H⁺): 188.1645, found: 188.1649.

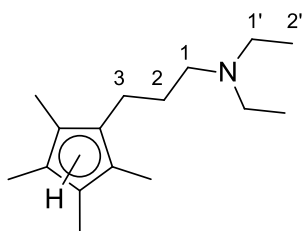
4-(3'-Diethylaminopropyl)-3,5-dimethyl-hepta-2,5-dien-4-ol (**83**)



Lithium wire (470 mg, 67.0 mmol) was washed with hexane, cut into small pieces and suspended in Et₂O (15 ml). 2-Bromo-2-butene (1.6 ml, 16 mmol, mixture of *cis* and *trans* isomers) was added in one portion to the mixture and stirred until the reaction started, observed by the reflux of the solvent; another aliquot of 2-bromo-2-butene (2.0 ml, 20 mmol) in Et₂O (15 ml) was added dropwise and the suspension was stirred for 2 hours at RT. A solution of ethyl *N,N*-diethyl-4-aminobutanoate **82** (3.00 g, 16.0 mmol) in Et₂O (10 ml) was added dropwise, stirred for 90 minutes at RT and quenched with careful addition of saturated aqueous NH₄Cl (100 ml). The phases were separated and the product was extracted with Et₂O (2 × 40 ml). The combined organic extracts were dried with Na₂SO₄ and the solvent was removed under reduced pressure. Purification by flash chromatography (SiO₂, eluting with hexane-EtOAc (80:20 to 0:100)) gave **83** as a colourless oil as a 1 : 1 mixture of *trans-trans* and *trans-cis* isomers which was used without any other purification (3.70 g, 14.7 mmol, 92%).

R_f = 0.39 (DCM-MeOH 90:10); ¹H NMR (500 MHz, CDCl₃, δ /ppm): 5.63 (2H, q, J = 6.7 Hz, 2CH for the *trans-trans* isomer), 5.59-5.55 (1H, m, CH for the *trans-cis* isomer), 5.38 (1H, q, J = 7.2 Hz, CH for the *trans-cis* isomer), 2.56-2.48 (8H, m, 4H-1''), 2.45-2.35 (4H, m, 2H-3'), 2.04-1.87 (4H, m, 2CH₂), 1.78-1.73 (4H, m, 2CH₂), 1.64-1.46 (24H, m, 8CH₃), 1.04-0.99 (12H, m, 4H-2''); ¹³C NMR (125 MHz, CDCl₃, δ /ppm): 139.9 (C_qCH₃), 139.3 (C_qCH₃), 122.5 (CH for the *trans-cis* isomer), 118.3 (CH for the *trans-trans* isomer), 117.4 (CH for the *trans-cis* isomer), 79.7 (C-4), 79.0 (C-4), 54.4 (C-3'), 54.1 (C-3'), 45.8 (C-1''), 45.6 (C-1''), 37.5 (C-1'), 36.4 (C-1'), 23.7 (CH₃), 21.8 (CH₂), 21.6 (CH₂), 14.8 (CH₃), 14.2 (CH₃), 13.4 (CH₃), 13.2 (CH₃), 12.6 (CH₃), 10.5 (C-2''), 10.2 (C-2''); IR (ν_{\max} , neat, cm⁻¹): 3408 (O-H), 2970, 2813, 2813, 1455, 1377, 1293, 1195, 1066; HRMS (ESI+) m/z : Calculated for C₁₆H₃₂NO (M+H⁺): 254.2478, found: 254.2484.

N,N-Diethyl-3-(tetramethylcyclopentadienyl)propan-1-amine (**85**)

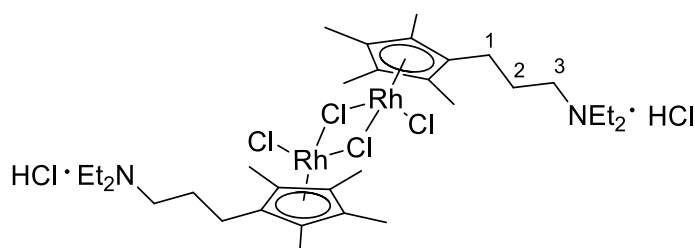


Prepared by a slightly modified version of the general method for the synthesis of cyclopentadienyls reported by Ito *et al.*⁷⁰ as follows. To a stirred solution of **83** (1.29 g, 5.09 mmol) in methanol (3.0 ml) was added a 2 M solution of HCl in Et₂O (3.0

ml, 6.0 mmol). The resulting solution was stirred at room temperature for 4 hours and the solvent was removed under reduced pressure. Purification by flash chromatography (Al₂O₃ pH 9.5 ± 0.5, eluting with DCM-MeOH (99:1)) gave **85** as a pale yellow oil in an unresolved mixture of three isomers (705 mg, 2.99 mmol, 60%).

R_f = 0.60 (Neutral aluminium oxide, DCM-MeOH 95:5); ¹H NMR (500 MHz, CDCl₃, δ/ppm): 2.65-2.40 (1H, m, CH), 2.52 (4H, q, *J* = 7.3 Hz, 2*H*-1'), 2.47-2.41 (2H, m, *H*-1), 2.35-2.11 (2H, m, *H*-3), 1.82-1.77 (9H, m, 3CH₃), 1.75-1.78 (2H, m, *H*-2), 1.05-0.96 (9H, m, CH₃ and 2*H*-2'); ¹³C NMR (125 MHz, CDCl₃, δ/ppm): 142.2 (C_qCH₃), 138.4 (C_qCH₃), 138.3 (C_qCH₃), 138.1 (C_qCH₃), 135.6 (C_qCH₃), 135.3 (C_qCH₃), 134.5 (C_qCH₃), 134.0 (C_qCH₃), 133.6 (C_qCH₃), 55.9 (CH), 53.4 (CH₂), 53.1 (CH₂), 52.7 (CH₂), 52.0 (CH₂), 51.5 (CH), 49.4 (CH), 46.9 (C-1'), 27.8 (CH₂), 26.7 (CH₂), 25.6 (CH₂), 24.3 (CH₂), 23.7 (CH₂), 22.4 (CH₂), 21.0 (CH₂), 14.2 (CH₃), 14.1 (CH₃), 11.8 (CH₃), 11.7 (CH₃), 11.6 (CH₃), 11.1 (CH₃), 11.0 (CH₃); IR (ν_{max}, neat, cm⁻¹): 2968, 2934, 2870, 2799, 1742, 1656, 1445, 1381, 1294, 1201, 1070; HRMS (ESI⁺) *m/z*: Calculated for C₁₆H₃₀N (M+H⁺): 236.2373, found: 236.2376.

Rh₂Cl₄[η⁵-C₅(CH₃)₄(CH₂)₃NEt₂·HCl]₂ (**86**)

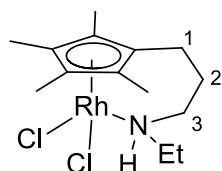


To a stirred solution of **85** hydrochloride (182 mg, 0.672 mmol) in methanol (5.0 ml) was added

RhCl₃·hydrate (70 mg, 0.33 mmol). The reaction mixture was heated at reflux for 22 hours, cooled to room temperature and the solvent removed under reduced pressure. Crystallization from DCM-hexane (v/v = 1/3) gave **86** as a red solid (130 mg, 0.147 mmol, 89%). The formation of the hydrochloride salt was determined by comparing the NMR signals with a similar complex reported in the literature.⁷⁰

mp >250 °C (MeOH); ^1H NMR (500 MHz, DMSO, δ/ppm): 10.14 (2H, br s, 2NH), 3.09-3.06 (12H, m, 6NCH₂), 2.22 (4H, t, $J = 8.3$ Hz, 2H-1), 1.84-1.80 (4H, m, 2H-2), 1.70 (12H, s, 4CH₃), 1.63 (12H, s, 4CH₃), 1.19 (12H, t, $J = 7.3$ Hz, 4NCH₂CH₃); ^{13}C NMR (125 MHz, DMSO, δ/ppm): 100.1 (d, $J = 8.8$ Hz, C_qRh), 99.1 (d, $J = 7.5$ Hz, C_qRh), 97.9 (d, $J = 8.0$ Hz, C_qRh), 50.2 (NCH₂), 46.0 (NCH₂), 21.4 (C-2), 20.5 (C-1), 8.6 (CH₃), 8.4 (CH₃), one carbon (CH₃) not observed; IR (ν_{max} , neat, cm⁻¹): 3214, 3140, 2933, 2856, 2756, 2724, 1581, 1491, 1453, 1370, 1355, 1309, 1263, 1157, 1114, 1070, 1023; Anal. Calcd. For C₃₂H₅₈Cl₆N₂Rh₂: C, 43.22; H, 6.57; N, 3.15; Found C, 43.65; H, 6.35; N, 2.90. Elemental analysis data for C outside the expected range (± 0.4), but best value to date.

RhCl₂[η^5 : η^1 -C₅(CH₃)₄(CH₂)₃N(CH₂CH₃)H] (**87**)

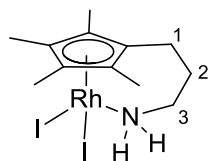


To a suspension of rhodium dimer **86** (40 mg, 50 μmol) in DCM (5.0 ml) was added potassium *tert*-butoxide (11 mg, 0.10 mmol). The mixture was stirred at room temperature for 72 hours, filtered through

a pad of Celite®, washed with DCM and the solvent was removed under reduced pressure. Purification by flash chromatography (SiO₂, eluting with DCM-MeOH (99:1)) gave **87** as an orange solid (6 mg, 16 μmol , 16%).

$R_f = 0.57$ (DCM-MeOH 90:10); mp 175.1-176.4 °C (DCM); ^1H NMR (500 MHz, CDCl₃, δ/ppm): 3.58-3.53 (1H, m, H_A-3), 3.30 (1H, br s, NH), 2.84-2.73 (2H, m, NCH₂), 2.68-2.61 (1H, m, H_B-3), 2.19-1.99 (4H, m, 2CH₂), 1.77 (3H, s, CH₃), 1.72 (3H, s, CH₃), 1.67 (3H, s, CH₃), 1.62 (3H, s, CH₃), 1.10 (3H, t, $J = 7.3$ Hz, CH₃); ^{13}C NMR (125 MHz, CDCl₃, δ/ppm): 105.1 (d, $J = 7.5$ Hz, C_qRh), 94.8 (d, $J = 8.8$ Hz, C_qRh), 93.1 (d, $J = 8.8$ Hz, C_qRh), 90.1 (d, $J = 7.5$ Hz, C_qRh), 83.8 (d, $J = 8.8$ Hz, C_qRh), 45.3 (NCH₂), 44.6 (NCH₂), 26.0 (C-2), 19.3 (C-1), 13.7 (CH₃), 9.9 (CH₃), 9.4 (CH₃), 9.3 (CH₃), 9.2 (CH₃); IR (ν_{max} , neat, cm⁻¹): 3469 (N-H), 3217 (N-H), 2917, 1651, 1448, 1374, 1063, 1028; HRMS (ESI+) m/z : Calculated for C₁₄H₂₄³⁵Cl₁NRh (M-Cl⁻, 100%): 344.0640, found: 344.0640.

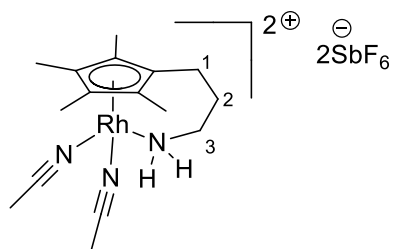
$\text{RhI}_2[\eta^5:\eta^1\text{-C}_5(\text{CH}_3)_4(\text{CH}_2)_3\text{NH}_2]$ (**92**)



To a stirred solution of rhodium complex **67** (30 mg, 85 μmol) in degassed acetone (5.0 ml) was added sodium iodide (28 mg, 0.19 mmol). The reaction mixture was heated at reflux for 20 hours, then cooled to RT and the solvent was removed under reduced pressure. The residue was dissolved in DCM (15 ml), washed with water (2×15 ml) and brine (15 ml). The organic phase was dried with Na_2SO_4 and the solvent was removed under reduced pressure. Purification by flash chromatography (SiO_2 , eluting with DCM-MeOH (98:2)) gave **92** as a dark red solid (27 mg, 0.050 mmol, 60%).

$R_f = 0.87$ (DCM-MeOH 90:10); mp > 250 $^\circ\text{C}$ (DCM-hexane, v/v = 1/2); ^1H NMR (500 MHz, CDCl_3 , δ/ppm): 3.17 (2H, br s, NH_2), 2.56-2.53 (2H, m, H -3), 2.17-2.13 (2H, m, H -1), 2.14 (6H, s, 2CH_3), 2.00 (6H, s, 2CH_3), 1.94-1.89 (2H, m, H -2); ^{13}C NMR (125 MHz, CDCl_3 , δ/ppm): 97.5 (d, $J = 7.5$ Hz, $C_q\text{Rh}$), 97.0 (d, $J = 7.5$ Hz, $C_q\text{Rh}$), 90.5 (d, $J = 7.5$ Hz, $C_q\text{Rh}$), 40.0 (C -3), 28.8 (C -2), 19.5 (C -1), 12.7 (CH_3), 10.6 (CH_3); IR (ν_{max} , neat, cm^{-1}): 3223 (N-H), 3149 (N-H), 2942, 2908, 1580, 1458, 1370, 1354, 1145, 1129, 1015, 924; HRMS (ESI+) m/z : Calculated for $\text{C}_{12}\text{H}_{20}\text{NRhI}$ ($\text{M}-\text{I}^-$): 407.9690, found: 407.9693; Anal. Calcd. For $\text{C}_{12}\text{H}_{20}\text{I}_2\text{NRh}$: C, 26.96; H, 3.77; N, 2.62; Found C, 27.50; H, 3.80; N, 2.50. Elemental analysis data for C outside the expected range (± 0.4), but best value to date.

$[\text{Rh}\{\eta^5:\eta^1\text{-C}_5(\text{CH}_3)_4(\text{CH}_2)_3\text{NH}_2\}\{\text{CH}_3\text{CN}\}_2][\text{SbF}_6]_2$ (**93**)

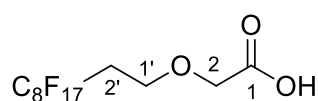


To a stirred solution of rhodium complex **67** (50 mg, 0.14 mmol) in acetonitrile (4.0 ml) was added silver hexafluoroantimonate (96 mg, 0.28 mmol). The mixture was heated at 70 $^\circ\text{C}$ for 24 hours, the crude was filtered through a pad of Celite®, washed with MeCN and the solvent was removed under reduced pressure. Purification by crystallization from MeCN-Et₂O (v/v = 1/2) gave **93** as a yellow powder (71 mg, 90 μmol , 61%). Single crystals were achieved by recrystallization from MeCN-Et₂O (v/v = 1/2).

mp > 250 $^\circ\text{C}$ (MeCN); ^1H NMR (500 MHz, DMSO, δ/ppm): 4.22 (2H, br s, NH_2), 2.59 (2H, br s, H -3), 2.17-2.11 (2H, m, H -1), 2.06-2.01 (8H, m, H -2 and $2\text{CH}_3\text{CN}$), 1.70 (6H, s, 2CH_3), 1.44 (6H, s, 2CH_3); ^{13}C NMR (125 MHz, DMSO, δ/ppm): 119.0 ($\text{C}\equiv\text{N}$),

102.7-101.4 (m, C_qRh), 86.1-85.2 (m, C_qRh), 41.3 ($C-3$), 29.8 ($C-2$), 18.7 ($C-1$), 7.4 (CH_3), 7.2 (CH_3), 2.1 (CH_3CN), one carbon (C_qRh) not observed; IR (ν_{max} , neat, cm^{-1}): 3328 (N-H), 3284 (N-H), 2321, 2291, 1594, 1455, 1370, 1163, 1083, 1021; HRMS (ESI+) m/z : Calculated for $C_{12}H_{20}F_6NRh^{121}Sb$ (M-[SbF₆⁻]-2MeCN, 100%): 515.9593, found: 515.9588; calculated for $C_{12}H_{20}F_6NRh^{123}Sb$ (M-[SbF₆⁻]-2MeCN, 68%): 517.9598, found: 517.9590; Anal. Calcd. For $C_{16}H_{26}F_{12}N_3RhSb_2$: C, 23.02; H, 3.14; N, 5.03; Found C, 23.20; H, 3.10; N, 4.90.

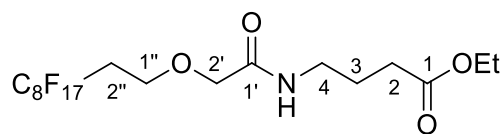
***1H',1H',2H',2H'*-Perfluorodecyloxyacetic acid (**98**)¹¹⁸**



To a stirred suspension of sodium hydride (3.89 g, 97.2 mmol, 60% in mineral oil) in THF (80 ml) at 0 °C was added dropwise a solution of *1H,1H,2H,2H*-perfluorodecanol (7.50 mg, 16.2 mmol) in THF (60 ml). The reaction mixture was stirred at 0 °C for 30 minutes, warmed at RT and stirred for 1 hour. A solution of bromoacetic acid (4.50 g, 32.4 mmol) in THF (70 ml) was added dropwise. The resulting reaction mixture was stirred at RT for 72 hours, water (100 ml) was slowly added to quench the excess of sodium hydride and the organic solvent was removed under reduced pressure. DCM (150 ml) and 6 M aqueous HCl (50 ml) were added and the two phases were separated. The product was extracted with DCM (2 × 150 ml), the combined organic phases were washed with brine (100 ml), dried with Na₂SO₄ and the solvent was removed under reduced pressure. Crystallization from hexane afforded **98** as a colourless solid (7.61 g, 14.6 mmol, 90%).

mp 51.5-52.7 °C (hexane) (lit. 47-48 °C¹¹⁸); ¹H NMR (500 MHz, CDCl₃, δ/ppm): 6.30 (1H, br s, OH), 4.18 (2H, s, *H-2*), 3.89 (2H, t, $J = 6.8$ Hz, *H-1'*), 2.55-2.44 (2H, m, *H-2'*); ¹³C NMR (125 MHz, CDCl₃, δ/ppm): 174.4 (*C-1*), 67.9 (*C-2*), 63.8 (*C-1'*), 31.5 (t, $J = 21.3$ Hz, *C-2'*), 8 carbons (7 x CF₂, 1 x CF₃) not observed; ¹⁹F NMR (282 MHz, CDCl₃, δ/ppm): -80.8 (t, $J = 10.7$ Hz), -113.4 (t, $J = 12.1$ Hz), -121.7, -121.9, -123.6, -126.1, 2 fluorines not observed; IR (ν_{max} , neat, cm^{-1}): 2925, 1726 (C=O), 1427, 1371, 1352, 1330, 1195, 1142, 1112, 1035; HRMS (ESI+) m/z : Calculated for $C_{12}H_6F_{17}Na_2O_3$ (M+2Na⁺-H⁺): 566.9835, found: 566.9837.

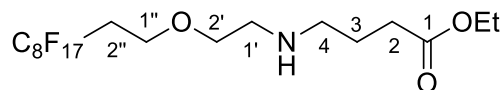
Ethyl 4-(2'-1H'',1H'',2H'',2H''-perfluorodecyloxyacetamido)butanoate (**96**)



To a stirred suspension of DMAP (3.48 g, 28.5 mmol), *N*-(3-dimethylaminopropyl)-*N'*-ethylcarbodiimide hydrochloride (2.73 g, 14.3 mmol) and ethyl 4-aminobutanoate hydrochloride **97** (1.59 g, 9.50 mmol) in DCM (160 ml) at 0 °C was added **98** in small aliquots (4.96 g, 9.50 mmol). The reaction mixture was warmed at RT and stirred for 18 hours. The solvent was removed under reduced pressure, the residue was dissolved in EtOAc (100 ml) and 1 M aqueous HCl (100 ml) and the two phases were separated. The product was extracted with EtOAc (3 × 100 ml) and the combined organic extracts were washed with brine (100 ml) and dried with Na₂SO₄. The solvent was removed under reduced pressure to afford **96** as a colourless oil (5.77 g, 9.09 mmol, 96%).

¹H NMR (500 MHz, CDCl₃, δ/ppm): 6.67 (1H, br s, NH), 4.13 (2H, q, *J* = 7.0 Hz, OCH₂), 3.98 (2H, s, *H*-2'), 3.83 (2H, t, *J* = 6.4 Hz, *H*-1''), 3.35 (2H, q, *J* = 7.0 Hz, *H*-4), 2.52-2.42 (2H, m, *H*-2''), 2.36 (2H, t, *J* = 7.2 Hz, *H*-2), 1.87 (2H, ap quint, *J* = 7.1 Hz, *H*-3), 1.25 (3H, t, *J* = 7.0 Hz, CH₃); ¹³C NMR (125 MHz, CDCl₃, δ/ppm): 173.2 (*C*-1 or *C*-1'), 168.9 (*C*-1 or *C*-1'), 70.5 (*C*-2'), 63.5 (*C*-1''), 60.5 (OCH₂), 38.3 (*C*-4), 31.7 (*C*-2), 31.4 (t, *J* = 21.7 Hz, *C*-2''), 24.6 (*C*-3), 14.1 (CH₃), 8 carbons (7 x CF₂, 1 x CF₃) not observed; ¹⁹F NMR (282 MHz, CDCl₃, δ/ppm): -80.8 (t, *J* = 10.0 Hz), -113.2 (quint, *J* = 14.4 Hz), -121.6, -121.9, -122.7, -123.6, -126.1, 1 fluororous not observed; IR (ν_{max}, neat, cm⁻¹): 3339 (N-H), 2938, 1732 (C=O), 1666 (C=O), 1536, 1446, 1372, 1348, 1325, 1235, 1199, 1144, 1116, 1029; HRMS (ESI+) *m/z*: Calculated for C₁₈H₁₉F₁₇NO₄ (M+H⁺): 636.1037, found: 636.1041.

Ethyl 4-((2'-1H'',1H'',2H'',2H''-perfluorodecyloxyethyl)amino)butanoate (**99**)

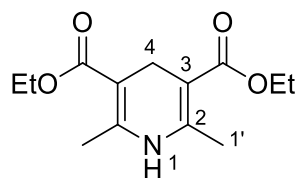


Following the general procedure for the amide reduction reported by Charette and co-workers,⁸⁰ to a stirred solution of amide **96** (2.20 g, 3.47 mmol) and 2-fluoropyridine (328 μl, 3.82 mmol) in DCM (8.0 ml) at -78 °C was added dropwise trifluoromethanesulfonic anhydride (613 μl, 3.64 mmol). The solution was stirred at -78 °C for 10 minutes and then warmed at 0 °C. Triethylsilane (610 μl, 3.82 mmol) was added dropwise, the solution was stirred at 0 °C for 10 minutes and for 5 hours at RT. Diethyl 2,6-dimethyl-1,4-dihydropyridine-3,5-dicarboxylate **100** (1.23 g, 4.86 mmol)

was added and the resulting mixture was stirred for 15 hours, before quenching with DCM (15 ml) and saturated aqueous NaHCO₃ (10 ml). The two phases were separated and the product was extracted with DCM (2 × 30 ml). The combined organic phases were dried with Na₂SO₄ and the solvent was removed under reduced pressure. Purification by flash chromatography (SiO₂, eluting with DCM-MeOH (95:5)) gave **99** as a colourless oil (688 mg, 1.11 mmol, 32%).

R_f = 0.35 (DCM-MeOH 90:10); ¹H NMR (500 MHz, CDCl₃, δ/ppm): 4.12 (2H, q, *J* = 7.0 Hz, OCH₂), 3.75 (2H, t, *J* = 6.8 Hz, *H*-1''), 3.61 (2H, t, *J* = 5.0 Hz, *H*-2'), 3.35 (1H, br s, NH), 2.84 (2H, t, *J* = 5.0 Hz, *H*-1'), 2.73 (2H, t, *J* = 7.2 Hz, *H*-4), 2.47-2.38 (2H, m, *H*-2''), 2.73 (2H, t, *J* = 7.2 Hz, *H*-2), 1.87 (2H, ap quint, *J* = 7.2 Hz, *H*-3), 1.24 (3H, t, *J* = 7.0 Hz, CH₃); ¹³C NMR (125 MHz, CDCl₃, δ/ppm): 173.4 (*C*-1), 69.8 (*C*-2'), 62.9 (*C*-1''), 60.4 (OCH₂), 48.8 (*C*-4 or *C*-1'), 48.6 (*C*-4 or *C*-1'), 32.0 (*C*-2), 31.5 (t, *J* = 21.3 Hz, *C*-2''), 24.6 (*C*-3), 14.1 (CH₃), 8 carbons (7 x CF₂, 1 x CF₃) not observed; ¹⁹F NMR (282 MHz, CDCl₃, δ/ppm): -80.8 (t, *J* = 9.9 Hz), -113.4, -121.7, -121.9, -122.7, -123.6, -126.1, 1 fluorine not observed; IR (ν_{max}, neat, cm⁻¹): 3342 (N-H), 2935, 1729 (C=O), 1656, 1543, 1444, 1370, 1348, 1199, 1145, 1134, 1016, 1029; HRMS (ESI+) *m/z*: Calculated for C₁₈H₂₀F₁₇NNaO₃ (M+Na⁺): 644.1064, found: 644.1066.

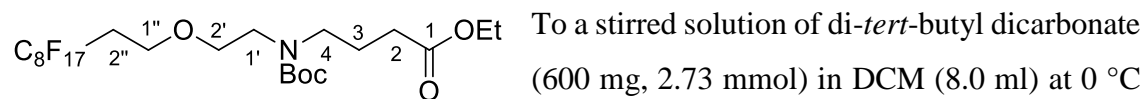
Diethyl 2,6-dimethyl-1,4-dihydropyridine-3,5-dicarboxylate (**100**)¹¹⁹



Paraformaldehyde (1.20 mg, 40.0 mmol), ammonium acetate (4.62 g, 60.0 mmol) and ethyl acetoacetate (10 ml, 80 mmol) were heated at 70 °C for 5 minutes, until a yellow solid was formed. The mixture was cooled at RT and water (60 ml) was added. The yellow suspension was filtered and washed with water (10 ml). Crystallisation from ethanol gave **100** as a pale yellow solid (10.1 g, 37.8 mmol, 95%).

¹H NMR (500 MHz, DMSO, δ/ppm): 8.24 (1H, br s, *H*-1), 4.04 (4H, q, *J* = 7.0 Hz, 2OCH₂), 3.10 (2H, s, *H*-4), 2.10 (6H, s, 2*H*-1'), 1.08 (6H, t, *J* = 7.0 Hz, 2CH₃); ¹³C NMR (125 MHz, DMSO, δ/ppm): 167.1 (C(O)), 146.5 (*C*-2), 97.0 (*C*-3), 58.9 (OCH₂), 24.7 (*C*-4), 17.9 (*C*-1'), 14.4 (CH₃); IR (ν_{max}, neat, cm⁻¹): 3347 (N-H), 2980, 2938, 2896, 2864, 1690, 1646, 1628, 1503, 1364, 1319, 1300, 1208, 1113, 1090, 1054, 1007; HRMS (ESI+) *m/z*: Calculated for C₁₃H₁₉NNaO₄ (M+Na⁺): 276.1206, found: 276.1204. Spectroscopic data consistent with literature values.¹¹⁹

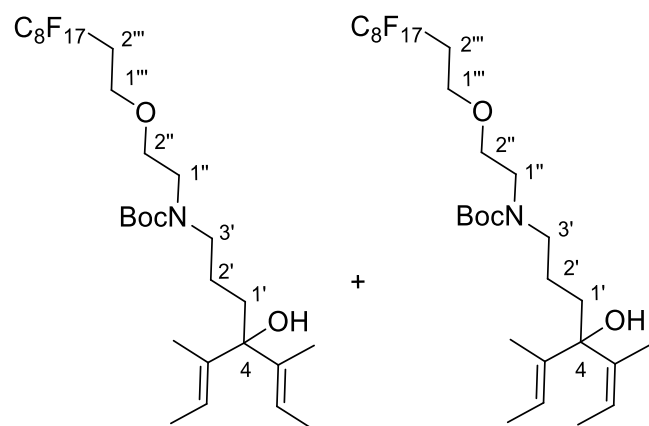
Ethyl 4-(*N*-Boc-(2'-1*H*'',1*H*'',2*H*'',2*H*''-perfluorodecyloxyethyl)amino)butanoate (95)



To a stirred solution of di-*tert*-butyl dicarbonate (600 mg, 2.73 mmol) in DCM (8.0 ml) at 0 °C was added a solution of **99** (1.54 g, 2.49 mmol) in DCM (4.0 ml). The solution was stirred at 0 °C for 30 minutes and then at RT for 16 hours. The solvent was removed under reduced pressure and a purification by flash chromatography (SiO₂, eluting with hexane-EtOAc (85:15)) gave **95** as a colourless oil (1.30 g, 1.80 mmol, 72%).

R_f = 0.36 (hexane-EtOAc 80:20); ¹H NMR (500 MHz, CDCl₃, δ/ppm): 4.12 (2H, q, J = 7.0 Hz, OCH₂), 3.72 (2H, t, J = 6.7 Hz, *H*-1''), 3.57 (2H, br s, *H*-1' or *H*-2'), 3.37 (2H, br s, *H*-1' or *H*-2'), 3.27 (2H, br s, *H*-4), 2.44-2.32 (2H, m, *H*-2''), 2.28 (2H, t, J = 7.3 Hz, *H*-2), 1.84 (2H, ap quint, J = 7.3 Hz, *H*-3), 1.45 (9H, s, C(CH₃)₃), 1.25 (3H, t, J = 7.0 Hz, CH₃); ¹³C NMR (125 MHz, CDCl₃, δ/ppm): 173.2 (*C*-1), 155.6 (C(O)N), 79.6 (C(CH₃)₃), 69.9 & 69.7 (CH₂, rotamers), 62.9 (CH₂), 60.3 (CH₂), 47.7 & 47.2 (CH₂, rotamers), 46.9 (CH₂), 31.6 (t, J = 21.2 Hz, *C*-2''), 31.5 (*C*-2), 28.4 (C(CH₃)₃), 23.9 & 23.5 (CH₂, rotamers), 14.2 (CH₃), 8 carbons (7 x CF₂, 1 x CF₃) not observed; ¹⁹F NMR (282 MHz, CDCl₃, δ/ppm): -80.8 (t, J = 10.0 Hz), -113.4 (quint, J = 15.5 Hz), -121.7, -121.9, -122.7, -123.6, -126.1, 1 fluorous not observed; IR (ν_{max} , neat, cm⁻¹): 2980, 2935, 1736 (C=O), 1729, 1693 (C=O), 1656, 1543, 1479, 1444, 1413, 1370, 1367, 1348, 1236, 1201, 1199, 1144, 1134, 1132, 1116, 1030; HRMS (ESI+) m/z : Calculated for C₂₃H₂₉F₁₇NO₅ (M+H⁺): 722.1769, found: 722.1778.

4-(*N*-Boc-(2''-1*H*'',1*H*'',2*H*'',2*H*''-Perfluorodecyloxyethyl)aminopropyl)-3,5-dimethyl-hepta-2,5-dien-4-ol (94)

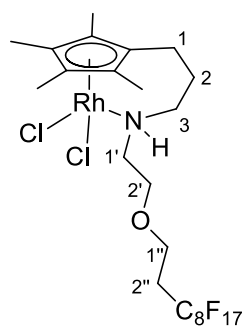


Lithium wire (300 mg, 43.2 mmol) was washed with hexane, cut into small pieces and suspended in Et₂O (10 ml). 2-Bromo-2-butene (1.0 ml, 10 mmol, mixture of *cis* and *trans* isomers) was added in one portion to the mixture and stirred until the reaction started, observed by the reflux of the solvent; another aliquot of 2-bromo-2-butene (1.33 ml, 13.0 mmol) diluted

in Et₂O (10 ml) was added dropwise and the suspension was stirred for 2 hours at RT. The concentration of the organolithium was determined by titration with menthol (1.0 mmol) and 2,2'-bipyridyl (0.1 mmol).¹²⁰ Ester **95** (1.35 g, 1.87 mmol) was dissolved in Et₂O (10 ml) and cooled at -78 °C. The titrated organolithium (7.48 mmol) was added dropwise and the solution was stirred for 30 minutes at -78 °C before warming up to RT for 60 minutes. Saturated aqueous NH₄Cl (15 ml) was added and the two phases were separated. The aqueous phase was extracted with Et₂O (3 × 50 ml), the combined organic extracts were dried with Na₂SO₄ and the solvent was removed under reduced pressure. Purification by flash chromatography (SiO₂, eluting with hexane-EtOAc (90:10 to 85:15)) gave **94** as a pale yellow oil as a 1 : 1 mixture of *trans-trans* and *trans-cis* isomers (849 mg, 1.08 mmol, 58%). A pure fraction of *trans-trans* isomer has been obtained after purification by chromatography and it has been used for characterisation.

R_f = 0.36 (hexane-EtOAc 80:20); ¹H NMR (500 MHz, CDCl₃, δ/ppm): 5.63-5.59 (2H, m, *H*-2 and *H*-6), 3.75-3.70 (2H, m, *H*-1'''), 3.57 (2H, br s, *H*-1'' or *H*-2''), 3.37 (2H, br s, *H*-1'' or *H*-2''), 3.26 (2H, br s, *H*-3'), 2.46-2.33 (2H, m, *H*-2'''), 1.86-1.58 (10H, m, 2CH₂ and 2CH₃), 1.55-1.44 (15H, m, 2CH₃ and C(CH₃)₃); ¹³C NMR (125 MHz, CDCl₃, δ/ppm): 155.7 (C(O)N), 138.1 (C_qCH₃), 118.9 (CH), 80.3 (C-4), 79.4 (C(CH₃)₃), 69.8 (CH₂), 62.9 (C-1'''), 48.8 (CH₂), 46.7 (CH₂), 31.6 (t, *J* = 21.2 Hz, C-2'''), 28.4 (C(CH₃)₃), 22.9 (CH₂), 12.3 (CH₃), 11.6 (CH₃), 9 carbons (1 x CH₂, 7 x CF₂, 1 x CF₃) not observed; ¹⁹F NMR (282 MHz, CDCl₃, δ/ppm): -80.7 (t, *J* = 9.7 Hz), -113.4, -121.7, -121.9, -122.7, -123.6, -126.1, 1 fluorine not observed; IR (ν_{max}, neat, cm⁻¹): 3449 (O-H), 2976, 1674 (C=O), 1479, 1416, 1367, 1237, 1202, 1170, 1144, 1006; HRMS (ESI+) *m/z*: Calculated for C₂₉H₃₈F₁₇NNaO₄ (M+Na⁺): 810.2422, found: 810.2417.

RhCl₂[η⁵:η¹-C₅(CH₃)₄(CH₂)₃N(CH₂CH₂OCH₂CH₂C₈F₁₇)H] (**101**)

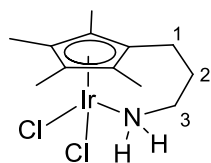


To a stirred solution of ligand **94** (386 mg, 0.490 mmol) in methanol (4.0 ml) was added RhCl₃·hydrate (51 mg, 0.25 mmol). The mixture was heated at reflux for 20 hours and the solvent was removed under reduced pressure. Purification by flash chromatography (SiO₂, eluting with DCM-MeOH (97:3 to 95:5)) gave **101** as a red solid (74 mg, 88 μmol, 35%).

R_f = 0.53 (DCM-MeOH 97:3); mp 133.3-134.6 °C (DCM-hexane, v/v = 1/2); ¹H NMR (500 MHz, CDCl₃, δ/ppm): 3.85-3.76 (1H, m, CH₂), 3.73-3.49 (4H, m, 2CH₂), 2.91-2.84

(1H, m, CH₂), 2.79-2.67 (2H, m, CH₂), 2.45-2.31 (2H, m, H-2''), 2.25-1.91 (4H, m, 2CH₂), 1.76 (3H, s, CH₃), 1.73 (3H, s, CH₃), 1.67 (3H, s, CH₃), 1.64 (3H, s, CH₃); ¹³C NMR (125 MHz, CDCl₃, δ/ppm): 103.0 (d, *J* = 7.5 Hz, C_qRh), 94.3 (d, *J* = 8.8 Hz, C_qRh), 93.2 (d, *J* = 8.0 Hz, C_qRh), 92.0 (d, *J* = 9.1 Hz, C_qRh), 85.1 (d, *J* = 9.6 Hz, C_qRh), 69.0 (C-3), 62.7 (CH₂), 50.7 (CH₂), 48.3 (CH₂), 31.4 (t, *J* = 21.2 Hz, C-2''), 27.0 (CH₂), 19.4 (CH₂), 9.9 (CH₃), 9.4 (CH₃), 9.1 (CH₃), 9.1 (CH₃), 8 carbons (7 x CF₂, 1 x CF₃) not observed; ¹⁹F NMR (282 MHz, CDCl₃, δ/ppm): -80.8 (t, *J* = 9.8 Hz), -113.3, -121.6, -121.9, -122.7, -123.5, -126.1, 1 fluorine not observed; IR (ν_{max}, neat, cm⁻¹): 3272 (N-H), 2918, 1487, 1440, 1370, 1331, 1243, 1200, 1145, 1114, 1006; HRMS (ESI+) *m/z*: Calculated for C₂₄H₂₇F₁₇³⁵CINORh (M-Cl⁻, 100%): 806.0559, found: 806.0552, calculated for C₂₄H₂₇F₁₇³⁷CINORh (M-Cl⁻, 35%): 808.0539, found: 808.0533; Anal. Calcd. For C₂₄H₂₇Cl₂F₁₇NORh: C, 34.22; H, 3.23; N, 1.66; Found C, 34.40; H, 3.20; N, 1.60.

IrCl₂[η⁵:η¹-C₅(CH₃)₄(CH₂)₃NH₂] (102)

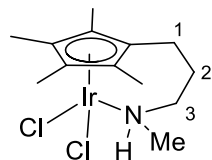


To a stirred suspension of IrCl₃·hydrate (670 mg, 2.24 mmol) and NaHCO₃ (190 mg, 2.24 mmol) in methanol (15 ml) was added the ligand **57** (1.34 g, 4.48 mmol). Microwave heating was applied to the reaction mixture with a set temperature of 130 °C for 2 hours with a pressure of 120 psi and, after cooling at RT, the solvent was removed under reduced pressure. Purification by flash chromatography (SiO₂, eluting with DCM-MeOH (98:2)) gave **102** as a yellow solid (427 mg, 0.968 mmol, 44%). Single crystals were achieved by recrystallization from DCM-hexane (v/v = 1/3).

R_f = 0.67 (DCM-MeOH 90:10); mp > 250 °C (DCM-hexane, v/v = 1/3); ¹H NMR (500 MHz, CDCl₃, δ/ppm): 3.94 (2H, br s, NH₂), 2.72-2.68 (2H, m, H-3), 2.18 (2H, t, *J* = 6.3 Hz, H-1), 1.96-1.91 (2H, m, H-2), 1.78 (6H, s, 2CH₃), 1.67 (6H, s, 2CH₃); ¹³C NMR (125 MHz, CDCl₃, δ/ppm): 90.8 (C_qIr), 88.7 (C_qIr), 41.9 (C-3), 30.7 (C-2), 19.2 (C-1), 9.2 (CH₃), 9.0 (CH₃), one carbon (C_qIr) not observed; IR (ν_{max}, neat, cm⁻¹): 3234 (N-H), 3153 (N-H), 2948, 2877, 1593, 1444, 1376, 1269, 1240, 1165, 1083, 1038; HRMS (ESI+) *m/z*: Calculated for C₁₂H₂₀³⁵Cl¹⁹¹IrN (M-Cl⁻, 50%): 404.0885, found: 404.0883; calculated for C₁₂H₂₀³⁷Cl¹⁹¹IrN and C₁₂H₂₀³⁵Cl¹⁹³IrN (M-Cl⁻, 100%): 406.0900, found: 406.0901; calculated for C₁₃H₂₂³⁷Cl¹⁹³IrN (M-Cl⁻, 26%): 408.0879, found: 408.0878;

Anal. Calcd. For $C_{12}H_{20}Cl_2IrN$: C, 32.65; H, 4.57; N, 3.17; Cl, 16.06; Found C, 32.95; H, 4.50; N, 3.00, Cl, 16.00.

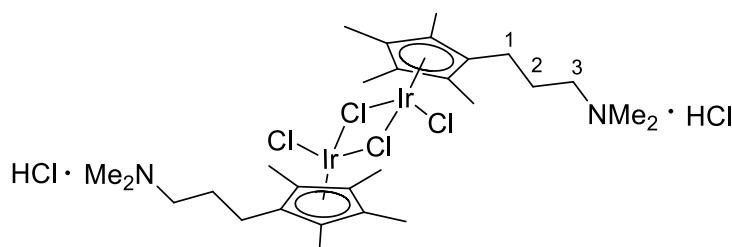
$IrCl_2[\eta^5\text{-}C_5(\text{CH}_3)_4(\text{CH}_2)_3\text{N}(\text{CH}_3)\text{H}]$ (103)



To a stirred suspension of $IrCl_3$ ·hydrate (70 mg, 0.23 mmol) and $NaHCO_3$ (20 mg, 0.23 mmol) in methanol (3.0 ml) was added the ligand **74** (143 mg, 0.46 mmol). Microwave heating was applied to the reaction mixture with a set temperature of 140 °C for 2 hours with a pressure of 200 psi and, after cooling at RT, the solvent was removed under reduced pressure. Purification by flash chromatography (SiO_2 , eluting with DCM-MeOH (98:2)) gave **103** as a yellow solid (32 mg, 0.070 mmol, 30%). Single crystals were achieved by slow recrystallization from DCM.

R_f = 0.47 (DCM-MeOH 90:10); mp 186.4-187.0 °C (DCM-hexane); 1H NMR (500 MHz, $CDCl_3$, δ /ppm): 4.22 (1H, br s, NH), 2.86-2.81 (1H, m, H_{A-3}), 2.77-2.73 (1H, m, H_{B-3}), 2.72 (3H, d, J = 6.0 Hz, NCH_3), 2.24-2.17 (1H, m, CH_2), 2.15-2.10 (2H, m, CH_2), 2.00-1.93 (1H, m, CH_2), 1.71 (3H, s, CH_3), 1.70 (3H, s, CH_3), 1.66 (3H, s, CH_3), 1.64 (3H, s, CH_3); ^{13}C NMR (125 MHz, $CDCl_3$, δ /ppm): 97.5 (C_qIr), 85.7 (C_qIr), 85.4 (C_qIr), 53.3 ($C-3$), 39.6 (NCH_3), 26.1 (CH_2), 19.3 (CH_2), 9.3 (CH_3), 9.2 (CH_3), 9.1 (CH_3), 9.0 (CH_3), two carbons (C_qIr) not observed; IR (ν_{max} , neat, cm^{-1}): 3178 (N-H), 2990, 2970, 2923, 1738, 1455, 1374, 1228, 1217, 1064, 1028; HRMS (ESI+) m/z : Calculated for $C_{13}H_{22}^{35}Cl^{191}IrN$ ($M-Cl^-$, 50%): 418.1041, found: 418.1044; calculated for $C_{13}H_{22}^{37}Cl^{191}IrN$ and $C_{13}H_{22}^{35}Cl^{193}IrN$ ($M-Cl^-$, 100%): 420.1056, found: 420.1052; calculated for $C_{13}H_{22}^{37}Cl^{193}IrN$ ($M-Cl^-$, 23%): 422.1035, found: 422.1029; Anal. Calcd. For $C_{13}H_{22}Cl_2IrN$: C, 34.28; H, 4.87; N, 3.08; Cl, 15.57; Found C, 34.40; H, 4.80; N, 3.00; Cl, 15.30.

$Ir_2Cl_4[\eta^5\text{-}C_5(\text{CH}_3)_4(\text{CH}_2)_3\text{NMe}_2 \cdot \text{HCl}]_2$ (104)

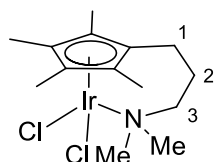


To a stirred suspension of $IrCl_3$ ·hydrate (100 mg, 0.334 mmol) in methanol (3.0 ml) was added the ligand **80** (321 mg, 1.32 mmol). Microwave heating was applied to the reaction mixture with a set

temperature of 120 °C for 1 hour with a pressure of 90 psi. From the resulting mixture, the orange solid was filtered and dried under reduced pressure to give **104** as an orange powder (155 mg, 0.153 mmol, 93%). The formation of the hydrochloride salt was determined by comparing the NMR signals with a similar complex reported in the literature.⁷⁰

¹H NMR (500 MHz, DMSO, δ /ppm): 10.11 (2H, br s, NH), 3.11-3.08 (4H, m, 2H-3), 2.72 (12H, s, 4NCH₃), 2.10 (4H, t, *J* = 8.3 Hz, 2H-1), 1.84-1.79 (4H, m, 2H-2), 1.70 (12H, s, 4CH₃), 1.64 (12H, s, 4CH₃); ¹³C NMR (125 MHz, DMSO, δ /ppm): 94.1 (C_qIr), 92.1 (C_qIr), 89.9 (C_qIr), 56.1 (C-3), 42.0 (NCH₃), 22.1 (C-2), 20.2 (C-1), 8.3 (CH₃), 8.2 (CH₃); IR (ν_{\max} , neat, cm⁻¹): 3011, 1453, 1406, 1375, 1031; HRMS (ESI+) *m/z*: Calculated for C₂₈H₄₈³⁵Cl₂³⁷Cl¹⁹¹Ir₂N₂ and C₂₈H₄₈³⁵Cl₃¹⁹¹Ir¹⁹³IrN₂ (M-[2HCl]-Cl⁻, 63%): 901.2102, found: 901.2112; calculated for C₂₈H₄₈³⁵Cl³⁷Cl₂¹⁹¹Ir₂N₂, C₂₈H₄₈³⁵Cl₂³⁷Cl¹⁹¹Ir¹⁹³IrN₂ and C₂₈H₄₈³⁵Cl³⁷Cl¹⁹³Ir₂N₂ (M-[2HCl]-Cl⁻, 100%): 903.2106, found: 903.2109; calculated for C₂₈H₄₈³⁷Cl₃¹⁹¹Ir₂N₂, C₂₈H₄₈³⁵Cl³⁷Cl₂¹⁹¹Ir¹⁹³IrN₂ and C₂₈H₄₈³⁵Cl₂³⁷Cl¹⁹³Ir₂N₂ (M-[2HCl]-Cl⁻, 65%): 905.2097, found: 905.2102; Anal. Calcd. For C₂₈H₅₀Cl₆Ir₂N₂: C, 33.24; H, 4.98; N, 2.77; Cl, 21.02; Found C, 33.10; H, 4.90; N, 2.60; Cl, 20.60.

IrCl₂[η^5 : η^1 -C₅(CH₃)₄(CH₂)₃N(CH₃)₂] (**105**)



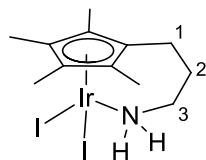
To a suspension of iridium dimer **104** (107 mg, 0.106 mmol) in DCM (10 ml) was added potassium *tert*-butoxide (25 mg, 0.22 μ mol) and the reaction mixture was stirred at room temperature for 15 hours. The

mixture was filtered through a pad of Celite®, washed with DCM and the solvent was removed under reduced pressure. Crystallization from DCM-hexane gave **105** as an orange solid (93 mg, 0.20 mmol, 90%). Single crystals were achieved by slow recrystallization from DCM-hexane (v/v = 1/2).

R_f = 0.90 (DCM-MeOH 90:10); mp 198.3-199.5 °C (DCM-hexane, v/v = 1/2); ¹H NMR (500 MHz, CDCl₃, δ /ppm): 2.77 (6H, s, 2NCH₃), 2.60-2.58 (2H, m, H-3), 2.15-2.08 (4H, m, 2CH₂), 1.60 (6H, s, 2CH₃), 1.59 (6H, s, 2CH₃); ¹³C NMR (125 MHz, CDCl₃, δ /ppm): 89.1 (C_qIr), 84.7 (C_qIr), 80.6 (C_qIr), 64.2 (C-3), 52.7 (NCH₃), 25.3 (CH₂), 19.0 (CH₂), 9.3 (CH₃), 9.1 (CH₃); IR (ν_{\max} , neat, cm⁻¹): 2917, 1477, 1448, 1435, 1375, 1029, 1002; HRMS (ESI+) *m/z*: Calculated for C₁₄H₂₄³⁵Cl¹⁹¹IrN (M-Cl⁻, 49%): 432.1198, found: 432.1197; calculated for C₁₄H₂₄³⁷Cl¹⁹¹IrN and C₁₄H₂₄³⁵Cl¹⁹³IrN (M-Cl⁻, 100%): 434.1213, found: 434.1215; calculated for C₁₄H₂₄³⁷Cl¹⁹³IrN (M-Cl⁻, 27%): 436.1195, found: 436.1193;

Anal. Calcd. For $C_{14}H_{24}Cl_2IrN$: C, 35.82; H, 5.15; N, 2.98; Cl, 15.10; Found C, 36.20; H, 5.15; N, 2.90; Cl, 14.75.

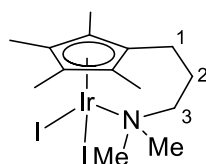
$IrI_2[\eta^5\text{-}\eta^1\text{-}C_5(\text{CH}_3)_4(\text{CH}_2)_3\text{NH}_2]$ (**106**)



To a stirred solution of iridium complex **102** (70 mg, 0.16 mmol) in degassed acetone (10 ml) was added sodium iodide (52 mg, 0.35 mmol). The reaction mixture was heated at reflux for 18 hours, cooled to RT and the solvent was removed under reduced pressure. The residue was dissolved in DCM (20 ml) and water (15 ml) and the two phases were separated. The product was extracted with DCM (2×20 ml) and the combined organic phases were washed with brine (40 ml) and dried with Na_2SO_4 . The solvent was removed under reduced pressure. Purification by crystallization from DCM-hexane (v/v = 1/2) gave **106** as an orange solid (72 mg, 0.12 mmol, 75%).

R_f = 0.88 (DCM-MeOH 90:10); mp > 250 °C (DCM); 1H NMR (500 MHz, $CDCl_3$, δ /ppm): 3.92 (2H, br s, NH_2), 2.58-2.54 (2H, m, $H-3$), 2.20 (2H, t, J = 6.3 Hz, $H-1$), 2.05 (6H, s, 2 CH_3), 1.92 (6H, s, 2 CH_3), 1.85-1.81 (2H, m, $H-2$); ^{13}C NMR (125 MHz, $CDCl_3$, δ /ppm): 89.8 (C_qIr), 89.7 (C_qIr), 81.1 (C_qIr), 42.5 ($C-3$), 29.1 ($C-2$), 19.3 ($C-1$), 12.2 (CH_3), 10.1 (CH_3); IR (ν_{max} , neat, cm^{-1}): 3214 (N-H), 3139 (N-H), 2908, 1579, 1458, 1371, 1309, 1262, 1157, 1070, 1022; HRMS (ESI+) m/z : Calculated for $C_{12}H_{20}I^{191}IrN$ ($M-I$, 64%): 496.0241, found: 496.0237; calculated for $C_{12}H_{20}I^{193}IrN$ ($M-I$, 100%): 498.0264, found: 498.0263; Anal. Calcd. For $C_{12}H_{20}I_2IrN$: C, 23.09; H, 3.23; N, 2.24; Found C, 23.55; H, 3.30; N, 2.20. Elemental analysis data for C outside the expected range (± 0.4), but best value to date.

$IrI_2[\eta^5\text{-}\eta^1\text{-}C_5(\text{CH}_3)_4(\text{CH}_2)_3\text{N}(\text{CH}_3)_2]$ (**107**)

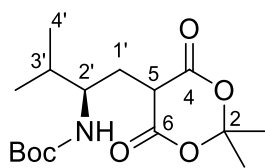


To a stirred solution of iridium complex **105** (93 mg, 0.20 mmol) in degassed acetone (12 ml) was added sodium iodide (66 mg, 0.44 mmol). The reaction mixture was heated at reflux for 17 hours, it was cooled to room temperature and the solvent was removed under reduced pressure. The residue was dissolved in DCM (30 ml) and water (30 ml) and the two phases were separated. The product was extracted with DCM (2×30 ml), the combined organic phases were dried with Na_2SO_4 and the solvent was removed under reduced pressure.

Purification by crystallization from DCM-hexane (v/v = 1/2) gave **107** as bright red crystals (125 mg, 0.192 mmol, 96%).

mp 203.0-204.7 °C (CHCl₃); ¹H NMR (500 MHz, CDCl₃, δ/ppm): 3.13 (6H, s, 2NCH₃), 2.57 (2H, br s, H-3), 2.05 (4H, s, 2CH₂), 1.87 (6H, s, 2CH₃), 1.82 (6H, s, 2CH₃); ¹³C NMR (125 MHz, CDCl₃, δ/ppm): 88.0 (C_qIr), 86.7 (C_qIr), 85.1 (C_qIr), 64.9 (C-3), 58.9 (NCH₃), 24.9 (CH₂), 18.4 (CH₂), 12.4 (CH₃), 11.0 (CH₃); IR (ν_{max}, neat, cm⁻¹): 2906, 1452, 1439, 1374, 1364, 1029; HRMS (ESI+) *m/z*: Calculated for C₁₄H₂₄I¹⁹¹IrN (M-I⁻, 54%): 524.0554, found: 524.0551; calculated for C₁₄H₂₄I¹⁹³IrN (M-I⁻, 100%): 526.0578, found: 526.0574; Anal. Calcd. For C₁₄H₂₄I₂IrN: C, 25.78; H, 3.71; N, 2.15; I, 38.91; Found C, 26.15; H, 3.70; N, 2.00; I, 38.45. Elemental analysis data for I outside the expected range (± 0.4), but best value to date.

(R)-5-[(2'-*t*-Butoxycarbonylamino-3'-methyl)-butyl]-2,2-dimethyl-1,3-dioxane-4,6-dione (110**)⁷⁸**

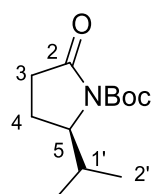


To a stirred solution of *N*-Boc-*L*-valine **108** (1.00 g, 4.60 mmol), DMAP (843 mg, 6.90 mmol) and *N*-(3-dimethylaminopropyl)-*N'*-ethylcarbodiimide hydrochloride (970 mg, 5.06 mmol) in DCM (40 ml) at 0 °C was added 2,2-dimethyl-1,3-dioxane-4,6-dione **109** (730 mg, 5.06 mmol). The resulting solution was stirred at RT overnight. Aqueous KHSO₄ (30 ml, 5%) was added and the two phases were separated. The organic phase was washed with aqueous KHSO₄ (3 × 40 ml, 5%) and brine (40 ml). The solution was dried with MgSO₄, filtered and cooled at 0 °C. Acetic acid (2.9 ml, 51 mmol) and sodium borohydride (435 mg, 11.5 mmol) were added to the filtrate and the reaction mixture was stirred overnight at 0 °C. Brine (40 ml) was added and the two phases were separated. The organic phase was washed with brine (2 × 40 ml) and water (2 × 40 ml), then dried with MgSO₄. The solvent was removed under reduced pressure. Crystallisation from EtOAc-hexane (v/v = 1/2) gave **110** as a white solid (860 mg, 2.61 mmol, 57%).

[α]_D = +9.5 (c = 0.65, CHCl₃) (lit. [α]_D = +12.5 (c = 3.0, EtOH)⁷⁸); mp 125.8-126.5 °C (DCM-hexane, v/v = 1/3); ¹H NMR (500 MHz, CDCl₃, δ/ppm): 4.47 (1H, d, *J* = 9.3 Hz, NH), 4.00-3.90 (1H, m, H-5), 3.80-3.71 (1H, m, H-2'), 2.33-2.21 (1H, m, H_A-1'), 2.18-2.07 (1H, m, H_B-1'), 1.85-1.78 (4H, m, CH₃ and H-3'), 1.76 (3H, s, CH₃), 1.42 (9H, s, C(CH₃)₃), 0.98-0.95 (6H, m, 2H-4'); ¹³C NMR (125 MHz, CDCl₃, δ/ppm): 166.1 (C-4), 165.7 (C-6), 156.9 (C(O)N), 104.9 (C-2), 79.5 (CCH₃), 54.4 (C-2'), 44.6 (C-5), 32.7

(C-3'), 29.2 (C-1'), 28.6 (CH₃), 28.3 (CCH₃), 25.9 (CH₃), 19.1 (C-4'), 17.9 (C-4'); IR (ν_{\max} , neat, cm⁻¹): 3367 (N-H), 2969, 2876, 1784, 1748, 1699, 1509, 1384, 1366, 1289, 1204, 1171; HRMS (ESI+) m/z : Calculated for C₁₆H₂₇NNaO₆ (M+Na⁺): 352.1731, found: 352.1735. Spectroscopic data consistent with literature values.⁷⁸

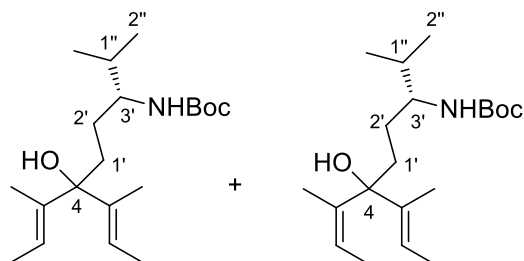
(R)-N-*t*-Butoxycarbonyl-5-isopropyl-2-pyrrolidinone (111)⁷⁸



A stirred solution of (R)-5-[(2-*t*-butoxycarbonylamino-3-methyl)-butyl]-2,2-dimethyl-1,3-dioxane-4,6-dione **110** (810 mg, 2.46 mmol) in toluene (20 ml) was heated at 110 °C for 5 hours. The reaction mixture was cooled down to RT and the solvent was removed under reduced pressure to afford **111** as a pale yellow oil (560 mg, 2.46 mmol, quant.), which was used and characterised without other purification.

$[\alpha]_D = +71.0$ ($c = 0.6$, CHCl₃) (lit. $[\alpha]_D = +77.4$ ($c = 1.4$, CHCl₃)⁷⁸); ¹H NMR (500 MHz, CDCl₃, δ /ppm): 4.01 (1H, ddd, $J = 9.1, 4.4, 2.3$ Hz, *H*-5), 2.49-2.31 (2H, m, *H*-3), 2.21-2.11 (1H, m, *H*-1'), 1.98-1.87 (1H, m, *H*_A-4), 1.80-1.72 (1H, m, *H*_B-4), 1.46 (9H, s, C(CH₃)₃), 0.87 (3H, d, $J = 7.0$ Hz, *H*-2'), 0.79 (3H, d, $J = 7.0$ Hz, *H*-2'); ¹³C NMR (125 MHz, CDCl₃, δ /ppm): 174.9 (C-2), 150.2 (C(O)N), 82.7 (C(CH₃)₃), 62.5 (C-5), 32.3 (C-3), 30.6 (C-1'), 28.0 (C(CH₃)₃), 19.0 (C-2'), 18.0 (C-4), 15.8 (C-2'); IR (ν_{\max} , neat, cm⁻¹): 2968, 1776 (C=O), 1712 (C=O), 1370, 1303, 1289, 1153, 905; HRMS (ESI+) m/z : Calculated for C₁₂H₂₁NNaO₃ (M+Na⁺): 250.1414, found: 250.1416. Spectroscopic data consistent with literature values.⁷⁸

(R)-N-Boc-4-(3'-Amino-3'-isopropyl)propyl-3,5-dimethyl-hepta-2,5-dien-4-ol (112)

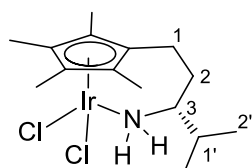


Lithium wire (300 mg, 43.2 mmol) was washed with hexane, cut into small pieces and suspended in Et₂O (10 ml). 2-Bromo-2-butene (1.0 ml, 10 mmol, mixture of *cis* and *trans* isomers) was added in one portion to the mixture and stirred until the reaction started, observed by the reflux of the solvent; another aliquot of 2-bromo-2-butene (1.3 ml, 13 mmol) in Et₂O (10 ml) was added dropwise and the suspension was stirred for 2 hours at RT. The concentration of the organolithium was determined by titration with menthol

(1.0 mmol) and 2,2'-bipyridyl (0.1 mmol).¹²⁰ Compound **111** (500 mg, 2.20 mmol) was diluted in Et₂O (6.0 ml) and cooled at 0 °C. The titrated organolithium (4.40 mmol) was added dropwise, the solution was stirred at 0 °C for 30 minutes before warming up to RT for 60 minutes. Saturated aqueous NH₄Cl (30 ml) was carefully added and the two phases were separated. The product was extracted with Et₂O (2 × 30 ml). The combined organic phases were dried with Na₂SO₄ and the solvent was removed under reduced pressure. Purification by flash chromatography (SiO₂, eluting with hexane-EtOAc (90:10)) gave **112** as a colourless oil in a mixture of *trans-trans* and *trans-cis* isomers (fraction major (*trans-cis*)/minor (*trans-trans*): 3/1) which was used without further purification (184 mg, 0.542 mmol, 25%).

R_f = 0.74 (hexane-EtOAc 80:20); [α]_D = +7.8 (*c* = 1.0, CHCl₃); ¹H NMR (500 MHz, CDCl₃, δ/ppm): 5.57 (2H, q, *J* = 6.2 Hz, 2CH for the *trans-trans* isomer), 5.43-5.27 (2H, m, 2CH for the *trans-cis* isomer), 4.30 (2H, br s, 2NH), 3.49-3.37 (2H, m, 2H-3'), 1.96-1.51 (30H, m, 8CH₃ and 2CH₂ and 2H-1''), 1.43 (18H, s, 2C(CH₃)₃), 1.39-1.16 (4H, m, 2CH₂), 0.91-0.85 (12H, m, 4H-2''); ¹³C NMR (125 MHz, CDCl₃, δ/ppm): 156.2 (C(O)), 140.2 (C_qCH₃), 139.7 (C_qCH₃), 138.2 (C_qCH₃), 122.6 (CH), 122.5 (CH), 122.4 (CH), 118.1 (CH), 80.8 (C(CH₃)₃), 79.5 (C-4), 78.8 (C-4), 56.1 (C-3'), 36.3 (CH₂), 34.3 (CH₂), 32.5 (CH₂), 28.4 (C(CH₃)₃), 27.0 (CH₂), 26.6 (CH₂), 23.5 (CH₂), 22.8 (CH₃), 19.2 (CH₂), 17.8 (CH₂), 14.8 (CH₃), 14.7 (CH₃), 14.4 (CH₃), 13.2 (CH₃), 12.6 (CH₃); HRMS (ESI+) *m/z*: Calculated for C₂₀H₃₇NNaO₃ (M+Na⁺): 362.2666, found: 362.2672.

(R)-IrCl₂[η⁵:η¹-C₅(CH₃)₄(CH₂)₂(CH(CH₃)₂)NH₂] (113**)**

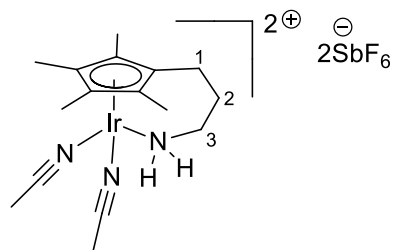


To a stirred suspension of IrCl₃·hydrate (80 mg, 0.27 mmol) and NaHCO₃ (23 mg, 0.27 mmol) in methanol (3.0 ml) was added diene **112** (184 mg, 0.542 mmol). Microwave heating was applied to the reaction mixture with a set temperature of 125 °C for 2 hours with a pressure of 130 psi and, upon cooling down to RT, the solvent was removed under reduced pressure. Purification by flash chromatography (SiO₂, eluting with DCM-MeOH (97:3)) followed by crystallisation from DCM-hexane (v/v = 1/3) gave **113** as a yellow solid (35 mg, 0.072 mmol, 27%). Single crystals were achieved by recrystallization from DCM-hexane (v/v = 1/3).

R_f = 0.71 (DCM-MeOH 95:5); [α]_D = -12.18 (*c* = 1.0, CHCl₃); mp 250.8-252.9 °C (decomposition, DCM-hexane, v/v = 1/3); ¹H NMR (500 MHz, CDCl₃, δ/ppm): 4.08 (1H,

br s, NH), 3.27 (1H, br s, NH), 2.43-2.30 (2H, m, $H-3$ and H_A-1), 2.19-2.02 (2H, m, H_B-1 and H_A-2), 1.94-1.82 (1H, m, $H-1'$), 1.78 (3H, s, CH_3), 1.77 (3H, s, CH_3), 1.69 (6H, s, $2CH_3$), 1.57-1.42 (1H, m, H_B-2), 0.98-0.95 (6H, m, $2H-2'$); ^{13}C NMR (125 MHz, $CDCl_3$, δ/ppm): 90.6 (C_qIr), 90.2 (C_qIr), 90.0 (C_qIr), 59.2 ($C-3$), 33.4 ($C-2$), 33.3 ($C-1'$), 20.3 ($C-1$), 18.2 ($C-2'$), 18.1 ($C-2'$), 9.3 (CH_3), 9.1 (CH_3), 9.0 (CH_3), 8.9 (CH_3), two carbons (C_qIr) not observed; IR (ν_{max} , neat, cm^{-1}): 3299 (N-H), 3207 (N-H), 2962, 2920, 2876, 1575, 1478, 1455, 1369, 1338, 1282, 1261, 1186, 1168, 1102, 1059, 1034; HRMS (ESI+) m/z : Calculated for $C_{15}H_{26}^{37}Cl^{191}IrN$ and $C_{15}H_{26}^{35}Cl^{193}IrN$ ($M-Cl^-$, 100%): 448.1369, found: 448.1368; Anal. Calcd. For $C_{15}H_{26}Cl_2IrN$: C, 37.26; H, 5.42; N, 2.90; Cl, 14.67; Found C, 37.60; H, 5.40; N, 2.80; Cl, 14.40.

[Ir{ η^5 : η^1 -C₅(CH₃)₄(CH₂)₃NH₂}{CH₃CN}₂][SbF₆]₂ (120**)**

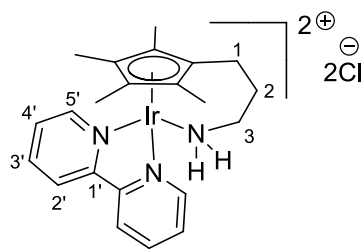


To a stirred solution of iridium complex **102** (120 mg, 0.272 mmol) in acetonitrile (8.0 ml) was added silver hexafluoroantimonate (200 mg, 0.582 mmol). The mixture was stirred at RT for 4 hours, the crude was

filtered through a pad of Celite®, washed with MeCN and the solvent was removed under reduced pressure. Purification by precipitation from DCM gave **120** as a pale yellow powder (174 mg, 0.188 mmol, 70%). Single crystals were achieved by recrystallization from MeCN-Et₂O ($v/v = 1/4$).

mp > 250 °C (MeCN-Et₂O, $v/v = 1/4$); 1H NMR (500 MHz, CD_3CN , δ/ppm): 4.38 (2H, br s, NH_2), 2.60-2.56 (2H, m, $H-3$), 2.30-2.25 (2H, m, $H-1$), 1.97 (6H, s, $2CH_3CN$), 1.92-1.87 (2H, m, $H-2$), 1.86 (6H, s, $2CH_3$), 1.65 (6H, s, $2CH_3$); ^{13}C NMR (125 MHz, CD_3CN , δ/ppm): 100.6 (C_qIr), 98.9 (C_qIr), 81.4 (C_qIr), 42.7 ($C-3$), 29.8 ($C-2$), 18.9 ($C-1$), 9.4 (CH_3), 9.1 (CH_3), two carbons ($C\equiv N$ and CH_3CN) not observed; IR (ν_{max} , neat, cm^{-1}): 3313 (N-H), 3274 (N-H), 2946, 2315, 1654, 1597, 1457, 1365, 1279, 1191, 1083, 1030; HRMS (ESI+) m/z : Calculated for $C_{12}H_{20}F_6N^{191}Ir^{121}Sb$ ($M-[SbF_6^-]-2MeCN$, 43%): 604.0139, found: 604.0139; calculated for $C_{12}H_{20}F_6N^{191}Ir^{123}Sb$ and $C_{12}H_{20}F_6N^{193}Ir^{121}Sb$ ($M-[SbF_6^-]-2MeCN$, 100%): 606.0156, found: 606.0157; calculated for $C_{12}H_{20}F_6N^{193}Ir^{123}Sb$ ($M-[SbF_6^-]-2MeCN$, 53%): 608.0167, found: 608.0164; Anal. Calcd. For $C_{16}H_{26}F_{12}N_3IrSb_2$: C, 20.80; H, 2.84; N, 4.55; Found C, 21.20; H, 2.80; N, 4.50.

[Ir{ η^5 : η^1 -C₅(CH₃)₄(CH₂)₃NH₂}{bipyridyl}][Cl]₂ (122**)**

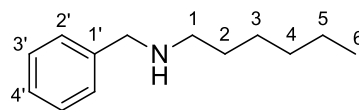


To a stirred solution of iridium complex **120** (70 mg, 0.16 mmol) in chloroform (3.0 ml) was added 2,2'-bipyridyl **121** (25 mg, 0.16 mmol). The reaction mixture was stirred overnight at RT and the solvent was slowly evaporated to half of its volume. The resulting precipitate was filtered to give **122** as pale yellow crystals (90 mg, 0.15 mmol, 94%). Single crystals were achieved by slow crystallization from chloroform.

mp 197.6-199.2 °C (decomposition, CHCl₃); ¹H NMR (500 MHz, MeOD, δ /ppm): 8.92 (2H, d, J = 5.7 Hz, 2*H*-5'), 8.65 (2H, d, J = 8.0 Hz, 2*H*-2'), 8.30 (2H, ap dt, J = 8.0, 1.4 Hz, 2*H*-3'), 7.84 (2H, ddd, J = 8.0, 5.7, 1.3 Hz, 2*H*-4'), 2.49-2.45 (2H, m, *H*-3), 2.44-2.41 (2H, m, *H*-1), 1.96-1.92 (2H, m, *H*-2), 1.80 (6H, s, 2*CH*₃), 1.41 (6H, s, 2*CH*₃); ¹³C NMR (125 MHz, MeOD, δ /ppm): 157.4 (*C*-1'), 153.6 (*C*-5'), 142.5 (*C*-3'), 130.6 (*C*-4'), 126.0 (*C*-2'), 101.2 (*C*_qIr), 97.5 (*C*_qIr), 80.3 (*C*_qIr), 43.1 (*C*-3), 29.7 (*C*-2), 19.4 (*C*-1), 8.2 (CH₃), 8.1 (CH₃); IR (ν _{max}, neat, cm⁻¹): 3448 (N-H), 3365 (N-H), 3116, 3043, 1698, 1607, 1472, 1446, 1314, 1210, 1162, 1076, 1033; HRMS (ESI+) m/z : Calculated for C₂₂H₂₈¹⁹¹IrN₃ (M-2Cl⁻, 56%): 262.5939, found: 262.5944; calculated for C₂₂H₂₈¹⁹³IrN₃ (M-2Cl⁻, 100%): 263.5951, found: 263.5960; Anal. Calcd. For C₂₂H₂₈Cl₂IrN₃ · 2H₂O : C, 41.70; H, 5.09; N, 6.63; Cl, 11.19; Found C, 41.60; H, 5.40; N, 6.20; Cl, 11.20. Elemental analysis data for N outside the expected range (\pm 0.4), but best value to date.

Preparation of secondary and tertiary amines using catalysts **102**, **103** and **120**

N-Benzylhexan-1-amine (124)



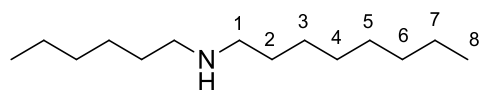
Following general procedure I, **124** was prepared from benzyl alcohol (103 μ l, 1.00 mmol) and 1-hexylamine (265 μ l, 2.00 mmol) at 130 °C. Purification by flash chromatography (Al_2O_3 pH 9.5 \pm 0.5, eluting with hexane-EtOAc (95:5 to 0:100)) gave **124** as a yellow oil (191 mg, 1.00 mmol, quant.).

Following general procedure J, **124** was prepared from benzyl alcohol (103 μ l, 1.00 mmol) and 1-hexylamine (132 μ l, 1.00 mmol) at 130 °C. Purification by filtration through a pad of Celite® washed with hexane gave **124** as a pale yellow oil (173 mg, 0.906 mmol, 91%).

Following general procedure L, **124** was prepared from benzyl alcohol (103 μ l, 1.00 mmol) and 1-hexylamine (132 μ l, 1.00 mmol) using 1.0 mol% of iridium catalyst **120** (9.2 mg, 0.010 mmol). Purification by flash chromatography (Al_2O_3 pH 9.5 \pm 0.5, eluting with DCM-MeOH (99:1 to 90:10)) gave **124** as a yellow oil (142 mg, 0.743 mmol, 74%).

R_f = 0.73 (Basic aluminium oxide, hexane-EtOAc 90:10); ^1H NMR (500 MHz, CDCl_3 , δ /ppm): 7.35-7.29 (4H, m, 4ArH), 7.27-7.22 (1H, m, ArH), 3.80 (2H, s, ArCH₂), 2.54 (2H, t, J = 7.3 Hz, H-1), 1.50 (1H, br s, NH), 1.47-1.39 (2H, m, H-2), 1.28-1.19 (6H, m, 3CH₂), 0.80 (3H, t, J = 7.0 Hz, H-6); ^{13}C NMR (125 MHz, CDCl_3 , δ /ppm): 140.7 (C-1'), 128.4 (Ar), 128.1 (Ar), 126.8 (Ar), 54.1 (ArCH₂), 49.6 (C-1), 31.8 (CH₂), 30.1 (CH₂), 27.1 (CH₂), 22.6 (CH₂), 14.1 (C-6); IR (ν_{max} , neat, cm^{-1}): 3314 (N-H), 3085, 3062, 3027, 2956, 2927, 2856, 2812, 1492, 1454, 1377, 1122, 1028; HRMS (ESI+) m/z : Calculated for $\text{C}_{13}\text{H}_{22}\text{N}$ (M+H⁺): 192.1747, found: 192.1749. Spectroscopic data consistent with literature values.³³

N-Hexyloctan-1-amine (126)



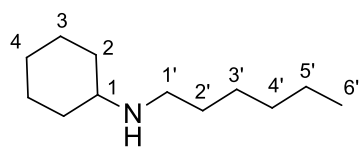
Following general procedure I, **126** was prepared from 1-octanol (157 μ l, 1.00 mmol) and 1-hexylamine (264 μ l, 2.00 mmol) at 130 °C.

Purification by flash chromatography (Al_2O_3 pH 9.5 ± 0.5 , eluting with DCM-MeOH (98:2 to 90:10)) gave **126** as a yellow oil (173 mg, 0.811 mmol, 81%).

Following general procedure J, **126** was prepared from 1-octanol (157 μl , 1.00 mmol) and 1-hexylamine (132 μl , 1.00 mmol). Purification by flash chromatography (Al_2O_3 pH 9.5 ± 0.5 , eluting with DCM-MeOH (99:1 to 95:5)) gave **126** as a yellow oil (179 mg, 0.839 mmol, 84%).

$R_f = 0.68$ (Basic aluminium oxide, DCM-MeOH 95:5); ^1H NMR (500 MHz, CDCl_3 , δ/ppm): 2.72 (1H, br s, NH), 2.59 (4H, t, $J = 7.3$ Hz, 2NCH_2), 1.50-1.46 (4H, m, 2CH_2), 1.28 (16H, br s, 8CH_2), 0.87-0.85 (6H, m, 2CH_3); ^{13}C NMR (125 MHz, CDCl_3 , δ/ppm): 49.8 (NCH_2), 31.8 (CH_2), 31.7 (CH_2), 29.8 (CH_2), 29.8 (CH_2), 29.5 (CH_2), 29.2 (CH_2), 27.4 (CH_2), 27.0 (CH_2), 22.6 (CH_2), 22.6 (CH_2), 14.0 (CH_3), 14.0 (CH_3), one carbon (NCH_2) not observed; IR (ν_{max} , neat, cm^{-1}): 3281 (N-H), 2957, 2926, 2856, 2810, 1466, 1407, 1378, 1130; HRMS (ESI+) m/z : Calculated for $\text{C}_{14}\text{H}_{32}\text{N}$ ($\text{M}+\text{H}^+$): 214.2529, found: 214.2537. Spectroscopic data consistent with literature values.³³

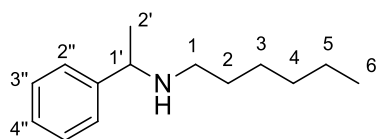
N-Hexylcyclohexanamine (127)



Following the general procedure I, **127** was prepared from cyclohexanol (106 μl , 1.00 mmol) and 1-hexylamine (132 μl , 1.00 mmol) at 125 $^\circ\text{C}$ using 2 mol% of iridium complex **102** (8.8 mg, 0.020 mmol). Purification by flash chromatography (Al_2O_3 pH 9.5 ± 0.5 , eluting with hexane-EtOAc (90:10 to 0:100)) gave **127** as a yellow oil (146 mg, 0.797 mmol, 80%).

$R_f = 0.67$ (Basic aluminium oxide, hexane-EtOAc 90:10); ^1H NMR (500 MHz, CDCl_3 , δ/ppm): 2.61 (2H, t, $J = 7.5$ Hz, $H-1'$), 2.44-2.38 (1H, tt, $J = 10.5, 3.7$ Hz, $H-1$), 1.90-1.88 (2H, m, CH_2), 1.74-1.70 (2H, m, CH_2), 1.66-1.55 (1H, m, CH_2), 1.50 (1H, br s, NH), 1.48-1.41 (2H, m, $H-2'$), 1.34-1.22 (8H, m, 4CH_2), 1.20-1.12 (1H, m, CH_2), 1.11-1.00 (2H, m, CH_2), 0.88 (3H, t, $J = 6.8$ Hz, $H-6'$); ^{13}C NMR (125 MHz, CDCl_3 , δ/ppm): 56.9 ($C-1$), 47.1 ($C-1'$), 33.6 (CH_2), 31.8 (CH_2), 30.4 (CH_2), 27.2 (CH_2), 26.2 (CH_2), 25.1 (CH_2), 22.6 (CH_2), 14.0 (CH_3); IR (ν_{max} , neat, cm^{-1}): 3276 (N-H), 2927, 2854, 1450, 1368, 1347, 1242, 1133; HRMS (ESI+) m/z : Calculated for $\text{C}_{12}\text{H}_{26}\text{N}$ ($\text{M}+\text{H}^+$): 184.2060, found: 184.2063. Spectroscopic data consistent with literature values.¹²¹

***N*-(1'-Phenylethyl)hexan-1-amine (128)**

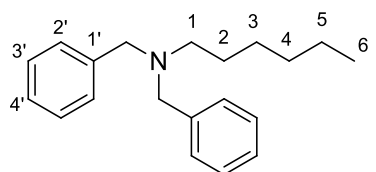


Following general procedure I, **128** was prepared from 1-phenylethanol (120 μ l, 1.00 mmol) and 1-hexylamine (132 μ l, 1.00 mmol) at 130 $^{\circ}$ C using 2 mol% of iridium complex **102** (8.8 mg, 0.020 mmol). Purification by flash chromatography (Al_2O_3 pH 9.5 ± 0.5 , eluting with hexane-EtOAc (95:5 to 0:100)) gave **128** as a yellow oil (177 mg, 0.862 mmol, 86%).

Following general procedure L, **128** was prepared from 1-phenylethanol (90 μ l, 0.75 mmol) and 1-hexylamine (66 μ l, 0.50 mmol) using 3 mol% of iridium complex **120** (14 mg, 0.015 mmol). Purification by flash chromatography (Al_2O_3 pH 9.5 ± 0.5 , eluting with DCM-MeOH (99:1)) gave **128** as a yellow oil (39 mg, 0.190 mmol, 38%).

$R_f = 0.60$ (Basic aluminium oxide, hexane-EtOAc 90:10); ^1H NMR (500 MHz, CDCl_3 , δ/ppm): 7.43-7.33 (4H, m, 4ArH), 7.30-7.25 (1H, m $H-4''$), 3.78 (1H, q, $J = 6.5$ Hz, $H-1'$), 2.55-2.50 (1H, m, H_A-1), 2.47-2.42 (1H, m, H_B-1), 1.54-1.42 (3H, m, CH_2 and NH), 1.39 (3H, d, $J = 6.5$ Hz, CH_3), 1.35-1.23 (6H, m, 3 CH_2), 0.90 (3H, t, $J = 6.8$ Hz, $H-6$); ^{13}C NMR (125 MHz, CDCl_3 , δ/ppm): 145.9 ($C-1''$), 128.3 (Ar), 126.7 (Ar), 126.5 (Ar), 58.4 ($C-1'$), 47.9 ($C-1$), 31.8 (CH_2), 30.3 (CH_2), 27.1 (CH_2), 24.4 (CH_3), 22.6 (CH_2), 14.1 ($C-6$); IR (ν_{max} , neat, cm^{-1}): 3308 (N-H), 3083, 3063, 2958, 2927, 2856, 1603, 1492, 1452, 1368, 1351, 1325, 1305, 1131; HRMS (ESI+) m/z : Calculated for $\text{C}_{14}\text{H}_{24}\text{N}$ ($\text{M}+\text{H}^+$): 206.1903, found: 206.1909. Spectroscopic data consistent with literature values.¹²¹

***N,N*-Dibenzylhexan-1-amine (125)**

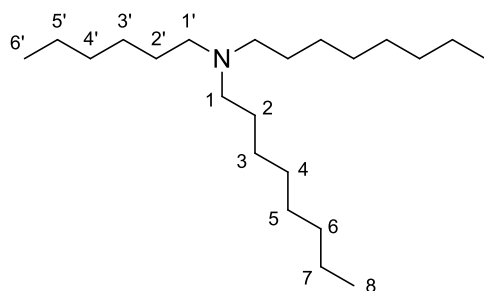


Prepared from benzyl alcohol (206 μ l, 2.00 mmol) and 1-hexylamine (132 μ l, 1.00 mmol) following general procedure I. Purification by flash chromatography (Al_2O_3 pH 9.5 ± 0.5 , eluting with hexane-EtOAc (95:5)) gave **125** as a colourless oil (237 mg, 0.842 mmol, 84%).

$R_f = 0.68$ (Basic aluminium oxide, hexane); ^1H NMR (500 MHz, CDCl_3 , δ/ppm): 7.40 (4H, d, $J = 7.5$ Hz, 4 $H-2'$), 7.33 (4H, ap t, $J = 7.5$ Hz, 4 $H-3'$), 7.25 (2H, t, $J = 7.3$ Hz, 2 $H-4'$), 3.58 (4H, s, 2Ar CH_2), 2.44 (2H, t, $J = 7.3$ Hz, $H-1$), 1.57-1.51 (2H, m, $H-2$), 1.33-1.26 (4H, m, 2 CH_2), 1.25-1.20 (2H, m, CH_2), 0.89 (3H, t, $J = 7.3$ Hz, $H-6$); ^{13}C NMR (125 MHz, CDCl_3 , δ/ppm): 140.2 ($C-1'$), 128.8 (Ar), 128.2 (Ar), 126.7 (Ar), 58.3

(ArCH₂), 53.5 (C-1), 31.8 (CH₂), 27.0 (CH₂), 27.0 (CH₂), 22.7 (CH₂), 14.1 (C-6); IR (ν_{max}, neat, cm⁻¹): 3085, 3063, 2954, 2929, 2857, 2794, 1494, 1453, 1365; HRMS (ESI+) *m/z*: Calculated for C₂₀H₂₈N (M+H⁺): 282.2216, found: 282.2225. Spectroscopic data consistent with literature values.³³

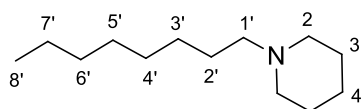
***N*-Hexyl-*N,N*-dioctylamine (129)**



Prepared from 1-octanol (314 μl, 2.00 mmol) and 1-hexylamine (132 μl, 1.00 mmol) following general procedure I. Purification by flash chromatography (Al₂O₃ pH 9.5 ± 0.5, eluting with hexane-EtOAc (95:5)) gave **129** as a colourless oil (221 mg, 0.679 mmol, 68%).

R_f = 0.83 (Basic aluminium oxide, hexane-EtOAc 95:5); ¹H NMR (500 MHz, CDCl₃, δ/ppm): 2.31 (6H, ap t, *J* = 7.8 Hz, 3NCH₂), 1.37-1.33 (6H, m, 3CH₂), 1.20 (26H, br s, 13CH₂), 0.81 (9H, ap t, *J* = 7.3 Hz, 3CH₃); ¹³C NMR (125 MHz, CDCl₃, δ/ppm): 54.3 (NCH₂), 31.9 (CH₂), 29.7 (CH₂), 29.4 (CH₂), 27.7 (CH₂), 27.1 (CH₂), 27.0 (CH₂), 22.7 (CH₂), 14.1 (CH₃), 14.1 (CH₃), four carbons (NCH₂ + 3CH₂) not observed; IR (ν_{max}, neat, cm⁻¹): 2955, 2926, 2796, 1467, 1378, 1094; HRMS (ESI+) *m/z*: Calculated for C₂₂H₄₈N (M+H⁺): 326.3781, found: 326.3786.

1-Octylpiperidine (130)

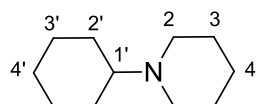


Prepared from 1-octanol (157 μl, 1.00 mmol) and piperidine (100 μl, 1.00 mmol) following general procedure I. Purification by filtration through a pad of Celite® washed with EtOAc gave **130** as a yellow oil (189 mg, 0.957 mmol, 96%), which was characterised without further purification.

R_f = 0.32 (Basic aluminium oxide, hexane-EtOAc 95:5); ¹H NMR (500 MHz, CDCl₃, δ/ppm): 2.29 (4H, br s, 2H-2), 2.20 (2H, t, *J* = 7.8 Hz, H-1'), 1.51 (4H, ap quint, *J* = 5.5 Hz, 2H-3), 1.44-1.39 (2H, m, CH₂), 1.38-1.33 (2H, m, CH₂), 1.24-1.15 (10H, m, 5CH₂), 0.81 (3H, t, *J* = 6.9 Hz, H-8'); ¹³C NMR (125 MHz, CDCl₃, δ/ppm): 59.7 (C-1'), 54.7 (C-2), 31.8 (CH₂), 29.6 (CH₂), 29.3 (CH₂), 27.8 (CH₂), 27.0 (CH₂), 26.0 (CH₂), 24.5

(CH₂), 22.6 (CH₂), 14.1 (C-8'); IR (ν_{\max} , neat, cm⁻¹): 2930, 2854, 2800, 2762, 1468, 1377, 1350, 1307; HRMS (ESI+) m/z : Calculated for C₁₃H₂₈N (M+H⁺): 198.2216, found: 198.2224. Spectroscopic data consistent with literature values.¹²²

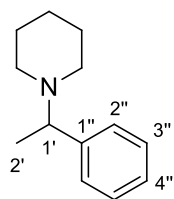
1-Cyclohexylpiperidine (131)



Prepared from cyclohexanol (106 μ l, 1.00 mmol) and piperidine (100 μ l, 1.00 mmol) at 130 °C following general procedure I. Purification by flash chromatography (Al₂O₃ pH 9.5 \pm 0.5, eluting with hexane-EtOAc (90:10 to 0:100)) gave **131** as a pale yellow oil (128 mg, 0.765 mmol, 77%).

R_f = 0.55 (Basic aluminium oxide, hexane-EtOAc 90:10); ¹H NMR (500 MHz, CDCl₃, δ /ppm): 2.44-2.43 (4H, m, 2H-2), 2.20-2.15 (1H, m, H-1'), 1.86-1.71 (4H, m, 2CH₂), 1.56-1.50 (5H, m, 2CH₂ and CH_A), 1.38-1.33 (2H, m, CH₂), 1.20-1.11 (5H, m, 2CH₂ and CH_B); ¹³C NMR (125 MHz, CDCl₃, δ /ppm): 64.4 (C-1'), 50.1 (C-2), 28.7 (CH₂), 26.5 (CH₂), 26.5 (CH₂), 26.2 (CH₂), 24.9 (CH₂); IR (ν_{\max} , neat, cm⁻¹): 3165, 2929, 2853, 2791, 1720, 1450, 1379, 1344, 1326, 1305, 1296, 1258, 1212, 1159, 1118, 1106; HRMS (ESI+) m/z : Calculated for C₁₁H₂₂N (M+H⁺): 168.1747, found: 168.1747. Spectroscopic data consistent with literature values.¹²³

1-(1'-Phenylethyl)piperidine (132)

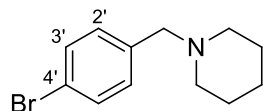


Prepared from 1-phenylethanol (180 μ l, 1.50 mmol) and piperidine (100 μ l, 1.00 mmol) at 130 °C using 2 mol% of iridium complex **102** (8.8 mg, 0.020 mmol) following general procedure I. Purification by flash chromatography (Al₂O₃ pH 9.5 \pm 0.5, eluting with hexane-EtOAc (95:5 to 90:10)) gave **132** as a pale yellow oil (136 mg, 0.718 mmol, 72%).

R_f = 0.72 (Neutral aluminium oxide, hexane-EtOAc 80:20); ¹H NMR (500 MHz, CDCl₃, δ /ppm): 7.24-7.22 (4H, m, 4ArH), 7.19-7.15 (1H, m, H-4''), 3.31 (1H, q, J = 6.8 Hz, H-1'), 2.31 (2H, br s, NCH₂), 2.26 (2H, br s, NCH₂), 1.47 (4H, m, 2CH₂), 1.33-1.26 (5H, m, H-2' and CH₂); ¹³C NMR (125 MHz, CDCl₃, δ /ppm): 144.0 (C-1''), 128.1 (Ar), 127.8 (Ar), 126.6 (Ar), 65.2 (C-1'), 51.5 (C-2), 26.3 (C-3), 24.6 (C-4), 19.4 (C-2'); IR (ν_{\max} , neat, cm⁻¹): 2971, 2933, 2852, 2791, 2751, 1601, 1491, 1451, 1372, 1321, 1302, 1228,

1200, 1156, 1134, 1117, 1026; HRMS (ES+) m/z : Calculated for $C_{13}H_{20}N$ ($M+H^+$): 190.1590, found: 190.1595. Spectroscopic data consistent with literature values.¹²³

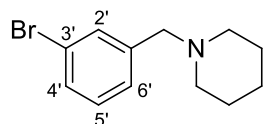
1-(4'-Bromobenzyl)piperidine (133)



Prepared from 4-bromobenzyl alcohol (187 mg, 1.00 mmol) and piperidine (100 μ l, 1.00 mmol) following general procedure I. Purification by filtration through a pad of Celite® washed with EtOAc gave **133** as a yellow oil (251 mg, 0.988 mmol, 99%), which was characterised without further purification.

1H NMR (500 MHz, $CDCl_3$, δ/ppm): 7.42 (2H, d, $J = 8.5$ Hz, $2H-2'$), 7.20 (2H, d, $J = 8.5$ Hz, $2H-3'$), 3.41 (2H, s, $ArCH_2$), 2.35 (4H, br s, $2H-2$), 1.57 (4H, ap quint, $J = 5.5$ Hz, $2H-3$), 1.47-1.39 (2H, m, $H-4$); ^{13}C NMR (125 MHz, $CDCl_3$, δ/ppm): 137.9 ($C-1'$), 131.2 ($C-2'$), 130.8 ($C-3'$), 120.6 ($C-4'$), 63.1 ($ArCH_2$), 54.5 ($C-2$), 26.0 ($C-3$), 24.4 ($C-4$); IR (ν_{max} , neat, cm^{-1}): 2932, 2853, 2784, 2753, 1485, 1440, 1341, 1297, 1112, 1094, 1011; HRMS (ESI+) m/z : Calculated for $C_{12}H_{17}^{79}BrN$ ($M+H^+$): 254.0539, found: 254.0540. Spectroscopic data consistent with literature values.¹²⁴

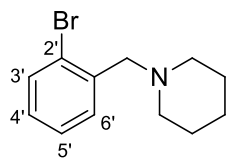
1-(3'-Bromobenzyl)piperidine (134)



Prepared from 3-bromobenzyl alcohol (120 μ l, 1.00 mmol) and piperidine (100 μ l, 1.00 mmol) following general procedure I. Purification by filtration through a pad of Celite® washed with EtOAc gave **134** as a yellow oil (239 mg, 0.940 mmol, 94%), which was characterised without further purification.

1H NMR (500 MHz, $CDCl_3$, δ/ppm): 7.49 (1H, s, $H-2'$), 7.37 (1H, dd, $J = 7.9, 1.0$ Hz, $H-4'$), 7.25 (1H, d, $J = 7.7$ Hz, $H-6'$), 7.17 (1H, dd, $J = 8.0, 7.7$ Hz, $H-5'$), 3.43 (2H, s, $ArCH_2$), 2.37 (4H, br s, $2H-2$), 1.58 (4H, ap quint, $J = 5.5$ Hz, $2H-3$), 1.47-1.41 (2H, m, $H-4$); ^{13}C NMR (125 MHz, $CDCl_3$, δ/ppm): 141.3 ($C-1'$), 132.0 ($C-2'$), 129.9 ($C-4'$ or $C-5'$), 129.8 ($C-4'$ or $C-5'$), 127.7 ($C-6'$), 122.4 ($C-3'$), 63.2 ($ArCH_2$), 54.5 ($C-2$), 26.0 ($C-3$), 24.3 ($C-4$); IR (ν_{max} , neat, cm^{-1}): 2932, 2852, 2790, 2753, 1594, 1569, 1469, 1441, 1426, 1341, 1301, 1195, 1087; HRMS (ESI+) m/z : Calculated for $C_{12}H_{17}^{79}BrN$ ($M+H^+$): 254.0539, found: 254.0539.

1-(2'-Bromobenzyl)piperidine (**135**)

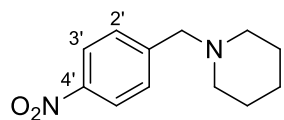


Prepared from 2-bromobenzyl alcohol (187 mg, 1.00 mmol) and piperidine (100 μ l, 1.00 mmol) following general procedure I. Purification by filtration through a pad of Celite® washed with

EtOAc gave **135** as a yellow oil (251 mg, 0.988 mmol, 99%), which was characterised without further purification.

R_f = 0.88 (Basic aluminium oxide, hexane-EtOAc 80:20); ^1H NMR (500 MHz, CDCl_3 , δ/ppm): 7.54-7.50 (2H, m, 2ArH), 7.28 (1H, dd, J = 7.7, 7.5 Hz, ArH), 7.09 (1H, dd, J = 7.7, 7.5 Hz, ArH), 3.57 (2H, s, ArCH₂), 2.47 (4H, br s, 2H-2), 1.60 (4H, ap quint, J = 5.6 Hz, 2H-3), 1.49-1.44 (2H, m, H-4); ^{13}C NMR (125 MHz, CDCl_3 , δ/ppm): 138.3 (C-1'), 132.6 (Ar), 130.6 (Ar), 128.1 (Ar), 127.1 (Ar), 124.6 (C-2'), 62.5 (ArCH₂), 54.7 (C-2), 26.1 (C-3), 24.4 (C-4); IR (ν_{max} , neat, cm^{-1}): 2932, 2851, 2795, 2755, 1465, 1438, 1344, 1301, 1265, 1154, 1124, 1114, 1103, 1039; HRMS (ESI+) m/z : Calculated for $\text{C}_{12}\text{H}_{17}^{79}\text{BrN}$ (M+H⁺): 254.0539, found: 254.0538.

1-(4'-Nitrobenzyl)piperidine (**136**)

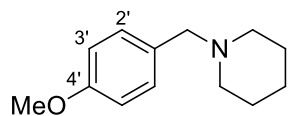


Prepared from 4-nitrobenzyl alcohol (153 mg, 1.00 mmol) and piperidine (100 μ l, 1.00 mmol) following general procedure I.

Purification by flash chromatography (Al_2O_3 pH 9.5 \pm 0.5, eluting with hexane-EtOAc (90:10)) gave **136** as a yellow oil (175 mg, 0.795 mmol, 80%).

R_f = 0.83 (Basic aluminium oxide, hexane-EtOAc 80:20); ^1H NMR (500 MHz, CDCl_3 , δ/ppm): 8.07 (2H, d, J = 9.0 Hz, 2H-3'), 7.42 (2H, d, J = 9.0 Hz, 2H-2'), 3.46 (2H, s, ArCH₂), 2.29 (4H, br s, 2H-2), 1.50 (4H, ap quint, J = 5.6 Hz, 2H-3), 1.39-1.30 (2H, m, H-4); ^{13}C NMR (125 MHz, CDCl_3 , δ/ppm): 147.1 (C-1' or C-4'), 147.0 (C-1' or C-4'), 129.4 (C-2'), 123.4 (C-3'), 62.9 (ArCH₂), 54.6 (C-2), 26.0 (C-3), 24.2 (C-4); IR (ν_{max} , neat, cm^{-1}): 2935, 2851, 2823, 2790, 2753, 2724, 1604, 1596, 1513, 1336, 1317, 1246, 1274, 1148, 1117, 1099; HRMS (ESI+) m/z : Calculated for $\text{C}_{12}\text{H}_{17}\text{N}_2\text{O}_2$ (M+H⁺): 221.1285, found: 221.1286. Spectroscopic data consistent with literature values.¹²⁴

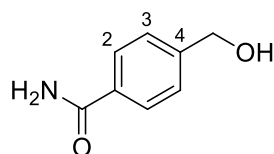
1-(4'-Methoxybenzyl)piperidine (**137**)



Prepared from 4-methoxybenzyl alcohol (138 mg, 1.00 mmol) and piperidine (100 μ l, 1.00 mmol) following general procedure I. Purification by flash chromatography (Al_2O_3 pH 9.5 ± 0.5 , eluting with hexane-EtOAc (95:5)) gave **137** as a colourless oil (184 mg, 0.896 mmol, 90%).

$R_f = 0.65$ (Basic aluminium oxide, hexane-EtOAc 80:20); ^1H NMR (500 MHz, CDCl_3 , δ/ppm): 7.13 (2H, d, $J = 8.5$ Hz, $2H-2'$), 6.76 (2H, d, $J = 8.5$ Hz, $2H-3'$), 3.70 (3H, s, OCH_3), 3.33 (2H, s, ArCH_2), 2.27 (4H, br s, $2H-2$), 1.48 (4H, ap quint, $J = 5.6$ Hz, $2H-3$), 1.39-1.30 (2H, m, $H-4$); ^{13}C NMR (125 MHz, CDCl_3 , δ/ppm): 158.6 ($C-4'$), 130.6 ($C-1'$), 130.4 ($C-2'$), 120.6 ($C-3'$), 63.3 (ArCH_2), 55.2 (OCH_3), 54.4 ($C-2$), 26.0 ($C-3$), 24.5 ($C-4$); IR (ν_{max} , neat, cm^{-1}): 2932, 2852, 2792, 2753, 1612, 1510, 1464, 1454, 1440, 1297, 1238, 1170, 1114, 1037; HRMS (ESI+) m/z : Calculated for $\text{C}_{13}\text{H}_{20}\text{NO}$ ($\text{M}+\text{H}^+$): 206.1539, found: 206.1544. Spectroscopic data consistent with literature values.¹¹⁰

4-(Hydroxymethyl)benzamide (**192**)

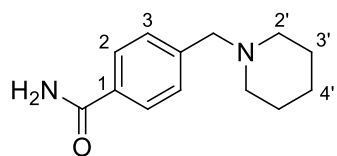


Following a modified procedure for the hydrolysis of nitriles reported by Wang *et al.*,¹²⁵ to a stirred solution of 4-cyanobenzyl alcohol (666 mg, 5.00 mmol) in ethanol (40 ml) was added hydrogen peroxide (1.7 ml, 15 mmol, 30% w.w. in H_2O) and 6 M aqueous NaOH (1.0 ml, 6.0 mmol). The mixture was heated at 60 $^\circ\text{C}$ for 3 hours and cooled at RT. DCM (100 ml) and 1 M aqueous HCl (50 ml) were added and the two phases were separated. The aqueous phase was washed with DCM (2×100 ml) and the solvent was removed under reduced pressure. The residue was dissolved in MeOH-EtOAc ($v/v = 2/1$) and the insoluble white solid was filtered through a pad of Celite $^\circledR$. The solvent was removed under reduced pressure and the crude was crystallized from MeOH-Et $_2$ O ($v/v = 1/3$) to give **192** as a colourless solid (443 mg, 2.93 mmol, 59%).

mp 130.6-131.7 $^\circ\text{C}$ (MeOH); ^1H NMR (500 MHz, DMSO, δ/ppm): 7.89 (1H, br s, NH), 7.82 (2H, d, $J = 8.2$ Hz, $2H-2$), 7.36 (2H, d, $J = 8.2$ Hz, $2H-3$), 7.26 (1H, s, NH), 4.53 (2H, s, CH_2); ^{13}C NMR (125 MHz, DMSO, δ/ppm): 167.8 (CO), 145.9 ($C-1$ or $C-4$), 132.6 ($C-1$ or $C-4$), 127.3 ($C-2$), 125.9 ($C-3$), 62.4 (CH_2); IR (ν_{max} , neat, cm^{-1}): 3276 (N-H), 3100 (N-H), 3055, 1680, 1614, 1510, 1413, 1369, 1043; HRMS (ES+) m/z :

Calculated for C₈H₁₀NO₂ (M+H⁺): 152.0706, found: 152.0706. Spectroscopic data consistent with literature values.¹²⁶

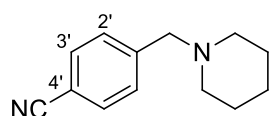
4-(Piperidin-1'-ylmethyl)benzamide (138)



Prepared from 4-(hydroxymethyl)benzamide **192** (151 mg, 1.00 mmol) and piperidine (100 μ l, 1.00 mmol) in *t*-amyl alcohol (0.5 ml) following general procedure I. Purification by flash chromatography (Al₂O₃ pH 9.5 \pm 0.5, eluting with DCM-MeOH (95:5)) gave **138** as a pale yellow solid (154 mg, 0.705 mmol, 71%).

R_f = 0.53 (Basic aluminium oxide, DCM-MeOH 90:10); mp 159.0-160.5 °C (DCM-MeOH, v/v = 5/1); ¹H NMR (500 MHz, CDCl₃, δ /ppm): 7.78 (2H, d, *J* = 8.0 Hz, 2*H*-2), 7.43 (2H, d, *J* = 8.0 Hz, 2*H*-3), 6.10 (2H, br s, NH₂), 3.53 (2H, s, ArCH₂), 2.40 (4H, br s, 2*H*-2'), 1.60 (4H, ap quint, *J* = 5.7 Hz, 2*H*-3'), 1.50-1.42 (2H, m, *H*-4'); ¹³C NMR (125 MHz, CDCl₃, δ /ppm): 169.5 (CO), 143.3 (*C*-1 or *C*-4), 131.9 (*C*-1 or *C*-4), 129.2 (*C*-2), 127.3 (*C*-3), 63.4 (ArCH₂), 54.6 (*C*-2'), 26.0 (*C*-3'), 24.3 (*C*-4'); IR (ν_{\max} , neat, cm⁻¹): 3395 (N-H), 3170 (N-H), 2931, 2797, 2756, 1647, 1616, 1570, 1396, 1368, 1153, 1108; HRMS (ESI+) *m/z*: Calculated for C₁₃H₁₉N₂O (M+H⁺): 219.1492, found: 219.1500.

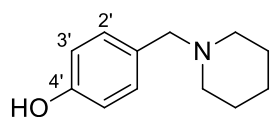
1-(4'-Cyanobenzyl)piperidine (139)



Prepared from 4-cyanobenzyl alcohol (133 mg, 1.00 mmol) and piperidine (100 μ l, 1.00 mmol) following general procedure I. Purification by flash chromatography (Al₂O₃ pH 9.5 \pm 0.5, eluting with hexane-EtOAc (90:10 to 80:20)) gave **139** as a colourless oil (163 mg, 0.815 mmol, 82%).

R_f = 0.60 (Basic aluminium oxide, hexane-EtOAc 80:20); ¹H NMR (500 MHz, CDCl₃, δ /ppm): 7.61 (2H, d, *J* = 8.2 Hz, 2*H*-3'), 7.47 (2H, d, *J* = 8.2 Hz, 2*H*-2'), 3.52 (2H, s, ArCH₂), 2.38 (4H, br s, 2*H*-2), 1.60 (4H, ap quint, *J* = 5.6 Hz, 2*H*-3), 1.49-1.43 (2H, m, *H*-4); ¹³C NMR (125 MHz, CDCl₃, δ /ppm): 144.8 (*C*-1'), 132.0 (*C*-3'), 129.5 (*C*-2'), 119.1 (*C*-4' or CN), 110.6 (*C*-4' or CN), 63.2 (ArCH₂), 54.6 (*C*-2), 26.0 (*C*-3), 24.2 (*C*-4); IR (ν_{\max} , neat, cm⁻¹): 2936, 2921, 2847, 2801, 2767, 2221 (C \equiv N), 1607, 1508, 1454, 1441, 1246, 1118, 1103, 1062; HRMS (ESI+) *m/z*: Calculated for C₁₃H₁₇N₂ (M+H⁺): 201.1386, found: 201.1392. Spectroscopic data consistent with literature values.¹²⁴

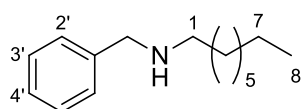
1-(4'-Hydroxybenzyl)piperidine (**140**)



Prepared from 4-hydroxybenzyl alcohol (124 mg, 1.00 mmol) and piperidine (100 μ l, 1.00 mmol) following general procedure I. Purification by flash chromatography (Al_2O_3 pH 9.5 ± 0.5 , eluting with DCM-MeOH (95:5 to 90:10)) followed by a crystallization from DCM-hexane ($v/v = 1/2$) gave **140** as a pale yellow solid (118 mg, 0.617 mmol, 62%).

$R_f = 0.81$ (Basic aluminium oxide, DCM-MeOH 90:10); mp 132.8-133.7 $^\circ\text{C}$ (DCM); ^1H NMR (500 MHz, CDCl_3 , δ/ppm): 7.08 (2H, d, $J = 8.4$ Hz, $2H-2'$), 6.57 (2H, d, $J = 8.4$ Hz, $2H-3'$), 3.43 (2H, s, ArCH_2), 2.51 (4H, br s, $2H-2$), 1.64 (4H, ap quint, $J = 5.5$ Hz, $2H-3$), 1.51-1.45 (2H, m, $H-4$); ^{13}C NMR (125 MHz, CDCl_3 , δ/ppm): 155.9 ($C-4'$), 131.2 ($C-2'$), 127.7 ($C-1'$), 115.7 ($C-3'$), 63.3 (ArCH_2), 54.3 ($C-2$), 25.2 ($C-3$), 24.1 ($C-4$); IR (ν_{max} , neat, cm^{-1}): 3049 (O-H), 3010, 2939, 2853, 2814, 2792, 2676, 2588, 1613, 1594, 1514, 1453, 1438, 1249, 1107, 1064, 1035; HRMS (ESI+) m/z : Calculated for $\text{C}_{12}\text{H}_{18}\text{NO}$ ($\text{M}+\text{H}^+$): 192.1383, found: 192.1383. Spectroscopic data consistent with literature values.¹²⁷

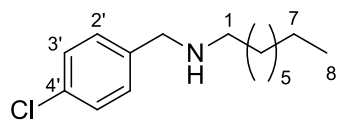
1-Benzyloctan-1-amine (**141**)



Prepared from *n*-octanol (157 μ l, 1.00 mmol) and benzylamine (218 μ l, 2.00 mmol) at 130 $^\circ\text{C}$ following general procedure I. Purification by flash chromatography (Al_2O_3 pH 9.5 ± 0.5 , eluting with DCM-MeOH (99:1)) gave **141** as a pale yellow oil (186 mg, 0.849 mmol, 85%).

$R_f = 0.62$ (Basic aluminium oxide, hexane-EtOAc 80:20); ^1H NMR (500 MHz, CDCl_3 , δ/ppm): 7.27-7.24 (4H, m, 4 ArH), 7.20-7.15 (1H, m, ArH), 3.72 (2H, s, ArCH_2), 2.55 (2H, t, $J = 7.5$ Hz, $H-1$), 1.53 (1H, br s, NH), 1.44 (2H, ap quint, $J = 7.2$ Hz, $H-2$), 1.26-1.15 (10H, m, 5 CH_2), 0.80 (3H, t, $J = 7.0$ Hz, $H-8$); ^{13}C NMR (125 MHz, CDCl_3 , δ/ppm): 140.5 ($C-1'$), 128.4 (Ar), 128.2 (Ar), 126.9 (Ar), 54.1 (ArCH_2), 49.5 ($C-1$), 31.9 (CH_2), 30.1 (CH_2), 29.5 (CH_2), 29.3 (CH_2), 27.4 (CH_2), 22.7 (CH_2), 14.1 ($C-8$); IR (ν_{max} , neat, cm^{-1}): 2923, 2853, 1454, 1259, 1119; HRMS (ESI+) m/z : Calculated for $\text{C}_{15}\text{H}_{26}\text{N}$ ($\text{M}+\text{H}^+$): 220.2060, found: 220.2065. Spectroscopic data consistent with literature values.¹²²

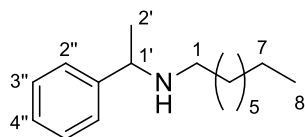
N-(4'-Chlorobenzyl)octan-1-amine (**142**)



Prepared from *n*-octanol (157 μ l, 1.00 mmol) and 4-chlorobenzylamine (244 μ l, 2.00 mmol) at 130 °C following general procedure I. Purification by flash chromatography (Al_2O_3 pH 9.5 ± 0.5 , eluting with DCM-MeOH (99:1)) gave **142** as a colourless oil (188 mg, 0.741 mmol, 74%).

R_f = 0.62 (Basic aluminium oxide, hexane-EtOAc 80:20); ^1H NMR (500 MHz, CDCl_3 , δ/ppm): 7.33-7.26 (4H, m, 4ArH), 3.78 (2H, s, ArCH₂), 2.63 (2H, t, $J = 7.2$ Hz, H-1), 1.59 (1H, br s, NH), 1.53 (2H, ap quint, $J = 7.2$ Hz, H-2), 1.36-1.26 (10H, m, 5CH₂), 0.91 (3H, t, $J = 7.2$ Hz, H-8); ^{13}C NMR (125 MHz, CDCl_3 , δ/ppm): 139.0 (C-1' or C-4'), 132.6 (C-1' or C-4'), 129.5 (C-2' or C-3'), 128.5 (C-2' or C-3'), 53.3 (ArCH₂), 49.3 (C-1), 31.8 (CH₂), 30.1 (CH₂), 29.6 (CH₂), 29.3 (CH₂), 27.4 (CH₂), 22.7 (CH₂), 14.1 (C-8); IR (ν_{max} , neat, cm^{-1}): 2954, 2923, 2853, 1490, 1457, 1089, 1015; HRMS (ESI+) m/z : Calculated for $\text{C}_{15}\text{H}_{25}^{35}\text{ClN}$ ($\text{M}+\text{H}^+$): 254.1670, found: 254.1670. Spectroscopic data consistent with literature values.¹²⁸

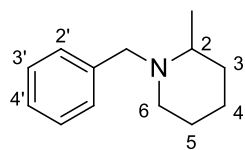
N-(1'-Phenylethyl)octan-1-amine (**143**)



Prepared from *n*-octanol (157 μ l, 1.00 mmol) and 1-phenylethylamine (130 μ l, 1.00 mmol) at 130 °C using 2 mol% of iridium complex **102** (8.8 mg, 0.020 mmol) following general procedure I. Purification by flash chromatography (Al_2O_3 pH 9.5 ± 0.5 , eluting with hexane-EtOAc (95:5 to 60:40)) gave **143** as a colourless oil (156 mg, 0.669 mmol, 67%).

R_f = 0.73 (Basic aluminium oxide, hexane-EtOAc 80:20); ^1H NMR (500 MHz, CDCl_3 , δ/ppm): 7.35-7.30 (4H, m, 4ArH), 7.26-7.21 (1H, m, ArH), 3.76 (1H, q, $J = 6.6$ Hz, H-1'), 2.50 (1H, ddd, $J = 11.3, 8.2, 6.5$ Hz, H_A-1), 2.42 (1H, ddd, $J = 11.3, 8.2, 6.5$ Hz, H_B-1), 1.52-1.41 (2H, m, H-2), 1.36 (3H, d, $J = 6.6$ Hz, H-2'), 1.33-1.22 (10H, m, 5CH₂), 0.88 (3H, t, $J = 6.6$ Hz, H-8); ^{13}C NMR (125 MHz, CDCl_3 , δ/ppm): 146.0 (C-1''), 128.4 (Ar), 126.8 (Ar), 126.6 (Ar), 58.4 (C-1'), 47.9 (C-1), 31.8 (CH₂), 30.3 (CH₂), 29.5 (CH₂), 29.3 (CH₂), 27.4 (CH₂), 24.4 (C-2'), 22.7 (CH₂), 14.1 (C-8); IR (ν_{max} , neat, cm^{-1}): 2957, 2923, 2853, 1451, 1130; HRMS (ESI+) m/z : Calculated for $\text{C}_{16}\text{H}_{28}\text{N}$ ($\text{M}+\text{H}^+$): 234.2216, found: 234.2220. Spectroscopic data consistent with literature values.¹²⁹

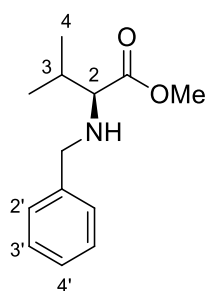
1-Benzyl-2-methylpiperidine (144)



Prepared from benzyl alcohol (103 μ l, 1.00 mmol) and 2-methylpiperidine (118 μ l, 1.00 mmol) following general procedure I. Purification by filtration through a pad of Celite® washed with EtOAc gave **144** as a yellow oil (181 mg, 0.956 mmol, 96%), which was characterised without further purification.

R_f = 0.89 (Basic aluminium oxide, hexane-EtOAc 90:10); ^1H NMR (500 MHz, CDCl_3 , δ/ppm): 7.40-7.32 (4H, m, 4ArH), 7.30-7.25 (1H, m, ArH), 4.06 (1H, d, J = 13.4 Hz, ArCH_A), 3.26 (1H, d, J = 13.4 Hz, ArCH_B), 2.79 (1H, dt, J = 11.5, 3.5 Hz, H-6), 2.40-2.33 (1H, m, H-2), 2.01 (1H, td, J = 11.5, 3.5 Hz, H-6), 1.75-1.66 (2H, m, CH₂), 1.62-1.26 (4H, m, 2CH₂), 1.23 (3H, d, J = 6.2 Hz, CH₃); ^{13}C NMR (125 MHz, CDCl_3 , δ/ppm): 139.5 (C-1'), 129.2 (Ar), 128.1 (Ar), 126.7 (Ar), 58.5 (ArCH₂), 56.4 (C-2), 52.2 (C-6), 34.8 (CH₂), 26.1 (CH₂), 24.1 (CH₂), 19.6 (CH₃); IR (ν_{max} , neat, cm^{-1}): 2931, 2854, 2785, 1450, 1372, 1278, 1222, 1116; HRMS (ESI+) m/z : Calculated for C₁₃H₂₀N (M+H⁺): 190.1590, found: 190.1589. Spectroscopic data consistent with literature values.¹³⁰

(S)-Benzyl-N-(methyl)valine ester (145)

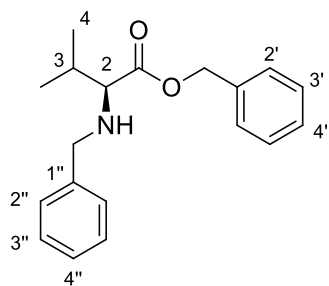


Prepared from benzyl alcohol (103 μ l, 1.00 mmol) and methyl-L-valine ester hydrochloride salt (168 mg, 1.00 mmol, 98% *e.e.*) with sodium hydrogen carbonate (168 mg, 2.00 mmol) using 2 mol% of iridium complex **102** (8.8 mg, 0.020 mmol) following general procedure I. Purification by flash chromatography (SiO_2 , eluting with hexane-EtOAc (90:10)) gave **145** as a colourless oil (158 mg, 0.715 mmol, 72%, 76% *e.e.*).

R_f = 0.58 (hexane-EtOAc 80:20); ^1H NMR (500 MHz, CDCl_3 , δ/ppm): 7.38-7.30 (4H, m, 4ArH), 7.27-7.22 (1H, m, H-4'), 3.84 (1H, d, J = 13.0 Hz, ArCH_A), 3.73 (3H, s, OCH₃), 3.60 (1H, d, J = 13.0 Hz, ArCH_B), 3.03 (1H, d, J = 6.5 Hz, H-2), 1.93 (1H, m, H-3), 1.80 (1H, br s, NH), 0.97-0.93 (6H, m, 2H-4); ^{13}C NMR (125 MHz, CDCl_3 , δ/ppm): 175.8 (C-1), 140.1 (C-1'), 128.3 (Ar), 128.3 (Ar), 127.0 (Ar), 66.6 (C-2), 52.6 (ArCH₂), 51.4 (OCH₃), 31.7 (C-3), 19.3 (C-4), 18.7 (C-4); IR (ν_{max} , neat, cm^{-1}): 3337 (N-H), 2960, 2873, 2841, 1731 (C=O), 1454, 1386, 1195, 1177, 1147; HRMS (ESI+) m/z : Calculated for

C₁₃H₂₀NO₂ (M+H⁺): 222.1489, found: 222.1489. The *e.e.* of the product was determined by HPLC using an AD-H column (*n*-hexane/EtOH = 90/10, flow rate = 0.3 ml/min, *t*_{major} = 12.7 min, *t*_{minor} = 16.3 min). Spectroscopic data consistent with literature values.¹³¹

(S)-Benzyl-N-(benzyl)valine ester (146)



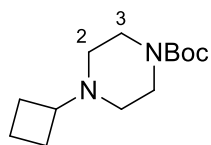
Following general procedure I, **146** was prepared from benzyl alcohol (103 μ l, 1.00 mmol) and benzyl-L-valine ester tosylate salt (380 mg, 1.00 mmol, 98% *e.e.*) using 2 mol% of iridium complex **102** (8.8 mg, 0.020 mmol). Purification by flash chromatography (SiO₂, eluting with hexane-EtOAc (90:10)) gave **146** as a colourless oil (187 mg, 0.629 mmol,

63%, 91% *e.e.*).

Following general procedure B, **146** was also prepared from benzyl alcohol (103 μ l, 1.00 mmol) and benzyl-L-valine ester tosylate salt (380 mg, 1.00 mmol, 98% *e.e.*) using 2 mol% of iridium complex **103** (9.0 mg, 0.020 mmol). Purification by flash chromatography (SiO₂, eluting with hexane-EtOAc (95:5)) gave **146** as a colourless oil (131 mg, 0.440 mmol, 44%, 98% *e.e.*).

*R*_f = 0.64 (hexane-EtOAc 90:10); ¹H NMR (500 MHz, CDCl₃, δ /ppm): 7.42-7.34 (5H, m, 5ArH), 7.33-7.30 (4H, m, 4ArH), 7.28-7.23 (1H, m, ArH), 5.22-5.16 (2H, m, ArCH₂O), 3.84 (1H, d, *J* = 13.0 Hz, ArCH_AN), 3.61 (1H, d, *J* = 13.0 Hz, ArCH_BN), 3.09-3.07 (1H, m, *H*-2), 2.00-1.93 (1H, m, *H*-3), 1.82-1.78 (1H, m, NH), 0.98-0.94 (6H, m, 2*H*-4); ¹³C NMR (125 MHz, CDCl₃, δ /ppm): 175.2 (*C*-1), 140.1 (*C*-1' or *C*-1''), 136.0 (*C*-1' or *C*-1''), 128.6 (*Ar*), 128.4 (*Ar*), 128.3 (*Ar*), 128.3 (*Ar*), 127.0 (*Ar*), 66.6 (*C*-2), 66.3 (ArCH₂O), 52.5 (ArCH₂N), 31.8 (*C*-3), 19.4 (*C*-4), 18.6 (*C*-4), one carbon (*Ar*) not observed; IR (ν _{max}, neat, cm⁻¹): 3336 (N-H), 2961, 1728 (C=O), 1496, 1454, 1174, 1141; HRMS (ESI⁺) *m/z*: Calculated for C₁₉H₂₄NO₂ (M+H⁺): 298.1802, found: 298.1807. The *e.e.* of the product was determined by HPLC using an AD-H column (*n*-hexane/EtOH = 90/10, flow rate = 0.3 ml/min, *t*_{major} = 14.5 min, *t*_{minor} = 18.5 min).

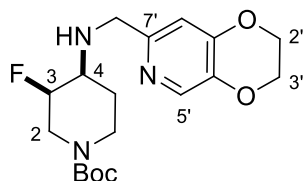
***N*-Boc-*N*-(Cyclobutyl)piperazine (151)**



Prepared from cyclobutanol **149** (157 μ l, 2.00 mmol) and *N*-Boc-piperazine **150** (373 mg, 2.00 mmol) in toluene (1.0 ml) using 1.5 mol% of iridium complex **102** (13 mg, 0.030 mmol) following general procedure K. Purification by flash chromatography (automatic purification system, 12 g column, eluting with DCM-MeOH (99:1 to 92:8)) gave **151** as a pale yellow oil (321 mg, 1.34 mmol, 67%).

R_f = 0.37 (DCM-MeOH 95:5); ^1H NMR (500 MHz, CDCl_3 , δ /ppm): 3.44 (4H, t, J = 5.0 Hz, 2*H*-3), 2.71 (1H, ap quint, J = 8.5 Hz, NCH), 2.26 (4H, t, J = 5.0 Hz, 2*H*-2), 2.07-2.00 (2H, m, CH_2), 1.92-1.82 (2H, m, CH_2), 1.76-1.64 (2H, m, CH_2), 1.46 (9H, s, $\text{C}(\text{CH}_3)_3$); ^{13}C NMR (125 MHz, CDCl_3 , δ /ppm): 154.8 (CO), 79.6 ($\text{C}(\text{CH}_3)_3$), 60.2 (NCH), 49.2 (C-2), 28.4 ($\text{C}(\text{CH}_3)_3$), 27.0 (CH_2), 14.3 (CH_2), one carbon (C-3) not observed; IR (ν_{max} , neat, cm^{-1}): 2974, 2938, 2861, 2806, 2761, 1693 (C=O), 1416, 1364, 1287, 1246, 1163, 1128, 1031, 1003; HRMS (ESI+) m/z : Calculated for $\text{C}_{13}\text{H}_{25}\text{N}_2\text{O}_2$ ($\text{M}+\text{H}^+$): 241.1911, found: 241.1911. Spectroscopic data consistent with literature values.¹²⁵

***N*-Boc-4-[(2',3'-Dihydro-[1',4']dioxino[2',3'-*c*]pyridin-7'-yl)methyl]amino}-3-fluoropiperidine (154)**

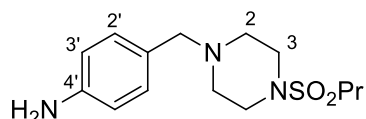


Prepared from (2,3-dihydro-[1,4]dioxino[2,3-*c*]pyridin-7-yl)methanol **153** (330 mg, 2.00 mmol) and *N*-Boc-4-amino-3-fluoropiperidine **152** (437 mg, 2.00 mmol) at 130 $^{\circ}\text{C}$ in toluene (1.0 ml) for 48 hours using 2 mol% of iridium complex **102** (17.6 mg, 0.0399 mmol) following general procedure K. Purification by flash chromatography (automatic purification system, 12 g column, eluting with DCM-MeOH (99:1 to 95:5)) gave **154** as a yellow oil (496 mg, 1.35 mmol, 68%).

R_f = 0.57 (DCM-MeOH 90:10); ^1H NMR (500 MHz, CDCl_3 , δ /ppm): 8.09 (1H, s, *H*-5'), 6.89 (1H, s, *H*-8'), 4.82-4.68 (1H, m, CH), 4.34-4.31 (3H, m, CH_2O and $\text{CH}_{2-\text{A}}$), 4.29-4.26 (2H, m, CH_2O), 4.10 (1H, br s, $\text{CH}_{2-\text{B}}$), 3.85 (2H, s, ArCH_2), 3.06-2.65 (3H, m, CH_2 and CH), 2.10 (1H, br s, NH), 1.80-1.73 (1H, m, CH_2), 1.72-1.64 (1H, m, CH_2), 1.45 (9H, s, $\text{C}(\text{CH}_3)_3$); ^{13}C NMR (125 MHz, CDCl_3 , δ /ppm): 155.1 (*Ar* or CO), 153.4 (*Ar* or CO), 150.3 (*Ar* or CO), 140.1 (*Ar*), 138.7 (C-5'), 110.5 (C-8'), 87.7 & 86.3 (CH, rotamers),

79.9 (C(CH₃)₃), 65.0 (CH₂O), 64.0 (CH₂O), 56.0 & 55.9 (CH, rotamers), 51.2 (ArCH₂), 47.0 & 46.0 (CH₂, rotamers), 42.5 & 41.8 (CH₂, rotamers), 28.3 (C(CH₃)₃), 26.9 (CH₂); IR (ν_{max}, neat, cm⁻¹): 3311 (N-H), 2976, 2931, 2887, 1683 (C=O), 1608, 1578, 1493, 1424, 1301, 1243, 1163, 1134, 1061; HRMS (ESI⁺) *m/z*: Calculated for C₁₈H₂₇FN₃O₄ (M+H⁺): 368.1980, found: 368.1985.

***N*-Propylsulfonyl-*N*-(4'-aminobenzyl)piperazine (**157**)**

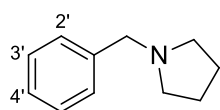


Following general procedure K, **157** was prepared from 4-aminobenzyl alcohol **155** (246 mg, 2.00 mmol) and 1-(propylsulfonyl)piperazine **156** (385 mg, 2.00 mmol) at 130 °C in *n*-butylacetate (1.0 ml). Purification by flash chromatography (automatic purification system, 12 g column, eluting with DCM-MeOH (99:1 to 90:10)) gave **157** as a pale yellow oil (492 mg, 1.66 mmol, 83%).

Following general procedure L, **157** was also prepared from 4-aminobenzyl alcohol **155** (123 mg, 1.00 mmol) and 1-(propylsulfonyl)piperazine **156** (385 mg, 2.00 mmol). Purification by flash chromatography (aluminium oxide basic, eluting with DCM-MeOH (99:1)) gave **62** as a yellow oil (283 mg, 0.954 mmol, 95%).

R_f = 0.81 (Basic aluminium oxide, DCM-MeOH 95:5); ¹H NMR (500 MHz, CDCl₃, δ/ppm): 7.08 (2H, d, *J* = 8.3 Hz, 2*H*-2'), 6.65 (2H, d, *J* = 8.3 Hz, 2*H*-3'), 3.65 (2H, br s, NH₂), 3.44 (2H, s, ArCH₂), 3.29 (4H, br s, 2*H*-2), 2.88-2.84 (2H, m, SO₂CH₂), 2.51 (4H, br s, 2*H*-3), 1.89-1.82 (2H, m, SO₂CH₂CH₂), 1.05 (3H, t, *J* = 7.4 Hz, CH₃); ¹³C NMR (125 MHz, CDCl₃, δ/ppm): 146.8 (C-1'), 130.4 (C-2'), 115.0 (C-3'), 113.4 (C-4'), 62.3 (ArCH₂), 52.4 (C-3), 50.8 (SO₂CH₂), 45.7 (C-2), 16.8 (SO₂CH₂CH₂), 13.2 (CH₃); IR (ν_{max}, neat, cm⁻¹): 3373 (N-H), 3231 (N-H), 2968, 2934, 2876, 2812, 2770, 1613, 1517, 1455, 1342, 1319, 1287, 1148; HRMS (ESI⁺) *m/z*: Calculated for C₁₄H₂₄N₃O₂S (M+H⁺): 298.1584, found: 298.1583. Spectroscopic data consistent with literature values.¹³²

1-Benzylpyrrolidine (158**)**



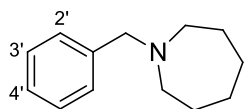
Following general procedure I, **158** was prepared from 1,4-butanediol (90 μl, 1.0 mmol) and benzylamine (110 μl, 1.00 mmol) using 2 mol% of iridium complex **102** (8.8 mg, 0.020 mmol) at 130 °C. Purification by flash

chromatography (Al_2O_3 pH 9.5 ± 0.5 , eluting with hexane-EtOAc (95:5 to 60:40)) gave **158** as a colourless oil (110 mg, 0.685 mmol, 69%).

Following general procedure J, **158** was also prepared from 1,4-butanediol (90 μl , 1.0 mmol) and benzylamine (110 μl , 1.00 mmol). Purification by flash chromatography (Al_2O_3 pH 9.5 ± 0.5 , eluting with hexane-EtOAc (95:5 to 60:40)) gave **158** as a colourless oil (81 mg, 0.50 mmol, 50%).

$R_f = 0.56$ (Basic aluminium oxide, hexane-EtOAc 80:20); ^1H NMR (500 MHz, CDCl_3 , δ/ppm): 7.37-7.30 (4H, m, 4ArH), 7.27-7.24 (1H, m, $H-4'$), 3.64 (2H, s, ArCH_2), 2.56-2.50 (4H, m, $2H-2$), 1.83-1.77 (4H, m, $2H-3$); ^{13}C NMR (125 MHz, CDCl_3 , δ/ppm): 139.5 ($C-1'$), 128.9 (Ar), 128.2 (Ar), 126.9 (Ar), 60.8 (ArCH_2), 54.2 ($C-2$), 23.5 ($C-3$); IR (ν_{max} , neat, cm^{-1}): 2963, 2908, 2781, 2732, 1493, 1453, 1375, 1348, 1141, 1125, 1074, 1028; HRMS (ESI+) m/z : Calculated for $\text{C}_{11}\text{H}_{16}\text{N}$ ($\text{M}+\text{H}^+$): 162.1277, found: 162.1281. Spectroscopic data consistent with literature values.¹³³

1-Benzylazepane (**159**)

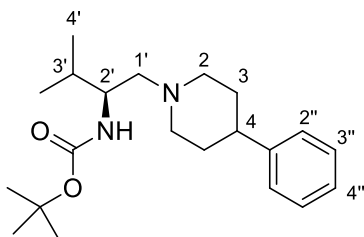


Following general procedure I, **159** was prepared from 1,6-hexanediol (118 mg, 1.00 mmol) and benzylamine (110 μl , 1.00 mmol) using 2 mol% of iridium complex **102** (8.8 mg, 0.020 mmol) at 130 °C. Purification by flash chromatography (Al_2O_3 pH 9.5 ± 0.5 , eluting with hexane-EtOAc (95:5 to 80:20)) gave **159** as a colourless oil (53 mg, 0.28 mmol, 28%).

Following general procedure J, **159** was prepared from 1,4-hexanediol (118 mg, 1.00 mmol) and benzylamine (110 μl , 1.00 mmol). Purification by flash chromatography (Al_2O_3 pH 9.5 ± 0.5 , eluting with hexane-EtOAc (95:5 to 80:20)) gave **159** as a colourless oil (85 mg, 0.45 mmol, 45%).

$R_f = 0.85$ (Basic aluminium oxide, hexane-EtOAc 90:10); ^1H NMR (500 MHz, CDCl_3 , δ/ppm): 7.36 (2H, dd, $J = 8.0, 1.0$ Hz, $2H-2'$), 7.34-7.29 (2H, m, $2H-3'$), 7.26-7.22 (1H, m, $H-4'$), 3.66 (2H, s, ArCH_2), 2.66-2.62 (4H, m, $2H-2$), 1.68-1.61 (8H, m, $4CH_2$); ^{13}C NMR (125 MHz, CDCl_3 , δ/ppm): 140.1 ($C-1'$), 128.8 (Ar), 128.1 (Ar), 126.7 (Ar), 62.8 (ArCH_2), 55.6 ($C-2$), 28.2 ($C-3$), 27.1 ($C-4$); IR (ν_{max} , neat, cm^{-1}): 2922, 2852, 2823, 1452, 1354, 1317; HRMS (ESI+) m/z : Calculated for $\text{C}_{13}\text{H}_{20}\text{N}$ ($\text{M}+\text{H}^+$): 190.1595, found: 190.1590. Spectroscopic data consistent with literature values.³³

(3'-Methyl-2'-(S)-N-Boc-amino)-N-butyl-(4-phenyl)piperidine (165)



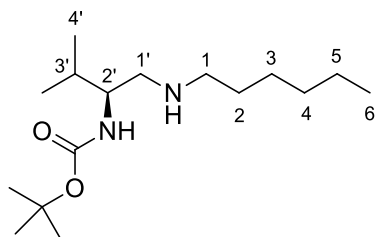
Prepared from *N*-Boc-*L*-valinol (203 mg, 1.00 mmol, 97% *e.e.*) and 4-phenylpiperidine (161 mg, 1.00 mmol) using 2 mol% of iridium complex **102** (8.8 mg, 0.020 mmol) following general procedure I. Purification

by flash chromatography (Al_2O_3 pH 9.5 ± 0.5 , eluting with hexane-EtOAc (90:10 to 60:40)) gave **165** as a colourless oil (267 mg, 0.771 mmol, 77%, 8% *e.e.*).

Following general procedure I, it was also prepared at 95 °C using the same conditions reported above. Purification by flash chromatography (Al_2O_3 pH 9.5 ± 0.5 , eluting with hexane-EtOAc (90:10 to 60:40)) gave **165** as a colourless oil (137 mg, 0.395 mmol, 40%, 13% *e.e.*).

$R_f = 0.67$ (Basic aluminium oxide, hexane-EtOAc 80:20); $^1\text{H NMR}$ (500 MHz, CDCl_3 , δ/ppm): 7.33-7.27 (2H, m, 2ArH), 7.24-7.17 (3H, m, 3ArH), 4.59 (1H, br s, NH), 3.66 (1H, br s, *H*-2'), 3.05 (1H, d, $J = 10.7$ Hz, *H*-2), 2.96 (1H, d, $J = 10.7$ Hz, *H*-2), 2.53-2.44 (1H, m, *H*-4), 2.35 (2H, d, $J = 6.2$ Hz, *H*-1'), 2.23-2.14 (1H, m, *H*-2), 2.06-2.00 (1H, m, *H*-2), 1.96-1.90 (1H, m, *H*-3'), 1.85-1.68 (4H, m, 2*H*-3), 1.47 (9H, s, $\text{C}(\text{CH}_3)_3$), 0.94 (3H, d, $J = 7.0$ Hz, *H*-4'), 0.89 (3H, d, $J = 7.0$ Hz, *H*-4'); $^{13}\text{C NMR}$ (125 MHz, CDCl_3 , δ/ppm): 156.3 (CO), 146.5 (*C*-1''), 128.4 (Ar), 126.9 (Ar), 126.1 (Ar), 78.9 ($\text{C}(\text{CH}_3)_3$), 59.9 (*C*-1'), 55.3 (*C*-2), 53.9 (*C*-2), 52.6 (*C*-2'), 42.6 (*C*-4), 33.6 (*C*-3), 33.5 (*C*-3), 30.4 (*C*-3'), 28.5 ($\text{C}(\text{CH}_3)_3$), 19.1 (*C*-4'), 17.3 (*C*-4'); IR (ν_{max} , neat, cm^{-1}): 3320 (N-H), 2967, 2949, 2934, 2804, 2746, 1699, 1675, 1538, 1388, 1364, 1269, 1250, 1173, 1093; HRMS (ESI+) m/z : Calculated for $\text{C}_{21}\text{H}_{35}\text{N}_2\text{O}_2$ ($\text{M}+\text{H}^+$): 347.2693, found: 347.2703. The *e.e.* of the product was determined by HPLC using a AD-H column (*n*-hexane/*i*-propanol = 95/5, flow rate = 0.5 ml/min, $t_{\text{minor}} = 13.3$ min, $t_{\text{major}} = 15.3$ min).

(3'-Methyl-2'-(S)-N-Boc-amino)-N-(butyl)hexylamine (167)



Prepared from *N*-Boc-*L*-valinol (203 mg, 1.00 mmol, 97% *e.e.*) and *n*-hexylamine (132 μ l, 1.00 mmol) using 2 mol% of iridium complex **102** (8.8 mg, 0.020 mmol) following general procedure I. Purification by flash chromatography (SiO₂, eluting with DCM-MeOH (95:5

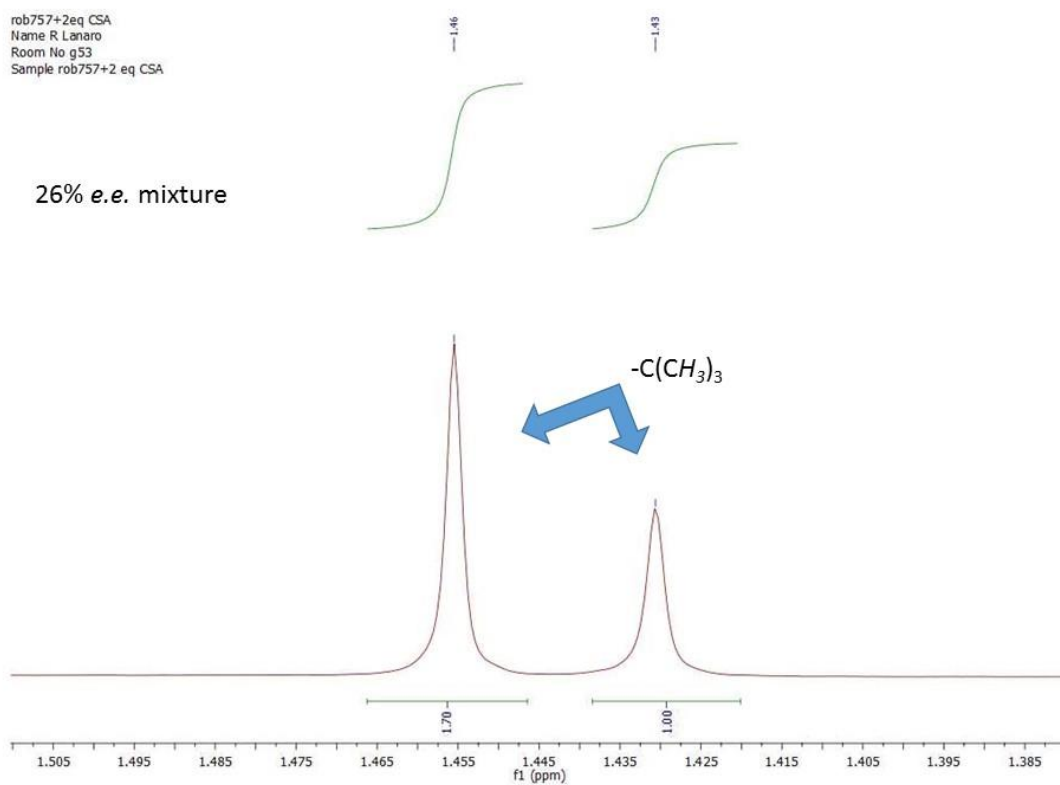
to 90:10)) gave **167** as a pale yellow oil (118 mg, 0.412 mmol, 41%, 26% *e.e.*).

R_f = 0.52 (DCM-MeOH 95:5); ¹H NMR (500 MHz, CDCl₃, δ /ppm): 4.80 (1H, br s, NH), 3.56 (1H, br s, *H*-2'), 2.76-2.67 (3H, m, *H*-1' and *H*_A-1), 2.65-2.57 (1H, br s, *H*_B-1), 1.85-1.76 (1H, m, *H*-3'), 1.58-1.49 (2H, m, *H*-2), 1.45 (9H, s, C(CH₃)₃), 1.37-1.25 (6H, m, 3CH₂), 0.95-0.85 (9H, m, 2*H*-4' and *H*-6); ¹³C NMR (125 MHz, CDCl₃, δ /ppm): 156.4 (CO), 79.3 (C(CH₃)₃), 54.7 (C-2'), 50.8 (C-1'), 49.3 (C-1), 31.7 (CH₂), 30.6 (C-3'), 29.2 (CH₂), 28.4 (C(CH₃)₃), 26.8 (CH₂), 22.6 (CH₂), 19.3 (C-4'), 18.2 (C-4'), 14.0 (C-6); IR (ν_{max} , neat, cm⁻¹): 3322 (N-H), 2958, 2932, 2872, 2857, 1694 (C=O), 1520, 1510, 1454, 1440, 1389, 1365, 1238, 1171; HRMS (ESI+) *m/z*: Calculated for C₁₆H₃₅N₂O₂ (M+H⁺): 287.2693, found: 287.2700. The *e.e.* of the product was determined by ¹H-NMR adding **194** (7.5 mg, 35.0 μ mol) to a solution of **167** (5.0 mg, 17.0 μ mol) in deuterated chloroform (0.5 ml). ¹H-NMR spectrum showed a shift of the signals near the amine and the carbamate, meaning that **194** formed a salt with **167**, separating the two enantiomers in two diastereoisomers. The *e.e.* of the product was determined comparing the areas of two singlets of *tert*-butyl groups in the two diastereoisomers, as shown in Figure 52.¹³⁴

Figure 52

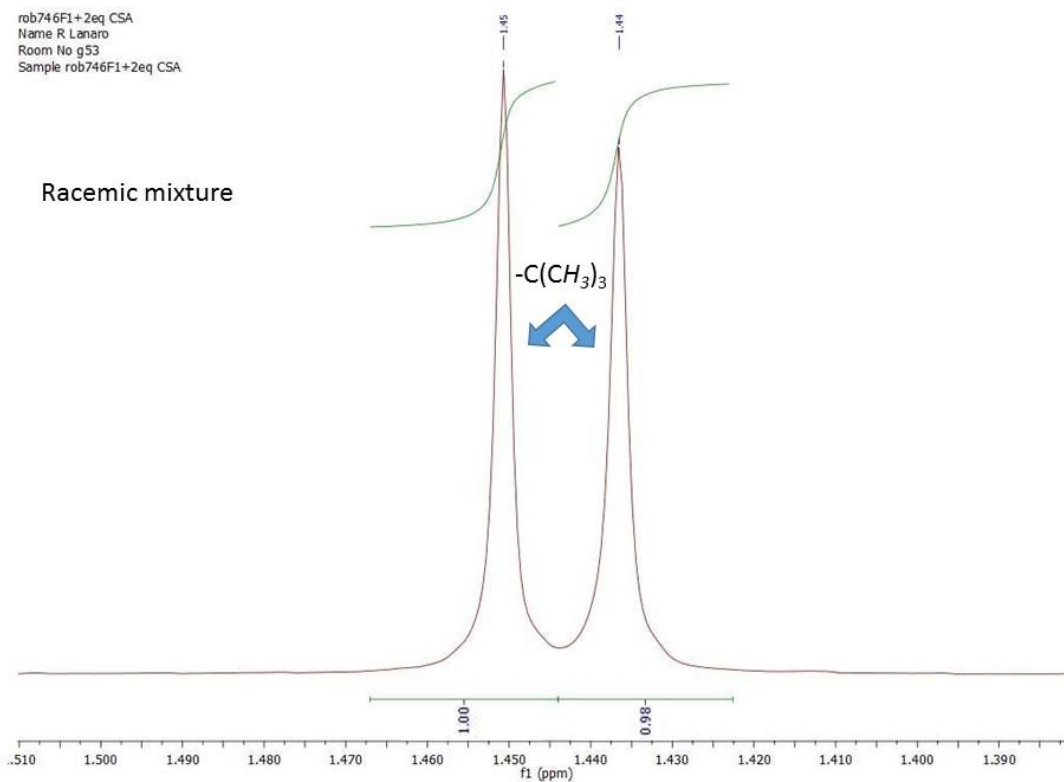
rob757+2eq CSA
Name R Lanaro
Room No g53
Sample rob757+2 eq CSA

26% *e.e.* mixture

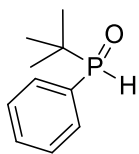


rob746F1+2eq CSA
Name R Lanaro
Room No g53
Sample rob746F1+2eq CSA

Racemic mixture



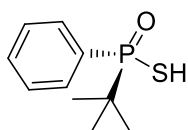
***tert*-Butyl(phenyl)phosphine oxide (**193**)**



Following the procedure reported by Gilheany *et al.*,¹³⁵ to a stirred solution of dichlorophenylphosphine (7.6 ml, 56 mmol) in THF (100 ml) at $-78\text{ }^{\circ}\text{C}$ was added dropwise a solution of *tert*-butylmagnesium chloride in THF (56 ml, 56 mmol, 1.0 M). The solution was warmed at RT, stirred for 1 hour and then cooled at $0\text{ }^{\circ}\text{C}$. Aqueous H_2SO_4 (30 ml, 10%) was added and the reaction mixture was stirred for 1 hour. The organic solvent was removed under reduced pressure, the residue was dissolved in DCM (100 ml) and the two phases were separated. The aqueous phase was extracted with DCM (2×100 ml) and the combined organic phases were washed with brine (150 ml), dried with MgSO_4 and the solvent was removed under reduced pressure to give **193** as a colourless oil (10.2 g, 56.0 mmol, quant.).

^1H NMR (500 MHz, CDCl_3 , δ/ppm): 7.71-7.66 (2H, m, 2ArH), 7.60-7.56 (1H, m, ArH), 7.52-7.49 (2H, m, 2ArH), 7.04 (1H, d, $J = 452.5$ Hz, PH), 1.15 (9H, d, $J = 16.6$ Hz, $\text{C}(\text{CH}_3)_3$); ^{13}C NMR (125 MHz, CDCl_3 , δ/ppm): 132.5 (d, $J = 2.9$ Hz, Ar), 131.0 (d, $J = 10.0$ Hz, Ar), 128.7 (d, $J = 90.0$ Hz, PCAr), 128.5 (d, $J = 12.5$ Hz, Ar), 32.0 (d, $J = 68.7$ Hz, PCCH_3), 23.5 (d, $J = 2.5$ Hz, $\text{C}(\text{CH}_3)_3$); ^{31}P NMR (121 MHz, CDCl_3 , δ/ppm): 47.4; IR (ν_{max} , neat, cm^{-1}): 3505, 3444, 3265, 2963, 2868, 1475, 1438, 1146, 1109; HRMS (ESI+) m/z : Calculated for $\text{C}_{10}\text{H}_{16}\text{OP}$ ($\text{M}+\text{H}^+$): 183.0933, found: 183.0936. Spectroscopic data consistent with literature values.¹³⁵

***(R)*-*tert*-Butyl(phenyl)phosphinothioic S-acid (**194**)**



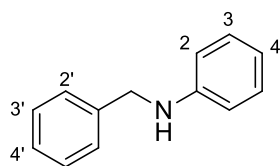
Following the procedure reported by Haynes *et al.*,¹³⁶ to a stirred solution of **193** (11.5 g, 63.0 mmol) in toluene (100 ml) was added sulfur (2.22 g, 69.3 mmol). The solution was heated at reflux for 22 hours and cooled at RT. The product was extracted with 0.7 M aqueous NaOH (6×50 ml). The combined aqueous phases were acidified with 6 M aqueous HCl until pH ~ 3 . The product was then extracted with DCM (6×60 ml), the combined organic phases were dried with Na_2SO_4 and the solvent was removed under reduced pressure to give (\pm)-*tert*-butyl(phenyl)phosphinothioic S-acid **194** (11.9 g, 55.6 mmol, 88%).

To a solution of the racemic **194** (11.9 g, 55.6 mmol) in Et_2O (100 ml) was added (*S*)-(-)- α -methylbenzylamine (7.2 ml, 56 mmol) and the resulting suspension was stirred

overnight. The reaction mixture was filtered and the precipitate was washed with cold Et₂O. The salt was dissolved in hot chloroform and diethyl ether was added to start the precipitation. The mixture was filtered and the filtrate was reduced to half of volume under reduced pressure to gain a second crop of the salt. The diastereomeric purity of the salt was checked with NMR spectroscopy and the recrystallization process was repeated until the other diastereoisomer was not visible in the spectrum. The salt was dissolved in 0.7 M aqueous NaOH (100 ml) and DCM (100 ml) was added. The two phases were separated, the aqueous phase was washed with DCM (2 × 50 ml) and it was acidified with 6 M aqueous HCl until pH ~ 3. The product was extracted with DCM (4 × 80 ml), the combined organic phases were dried with Na₂SO₄ and the solvent was removed under reduced pressure to give (*R*)-**194** as a white solid (3.76 g, 17.5 mmol, 32%).

$[\alpha]_{\text{D}} = +28.8$ ($c = 1.14$, MeOH) (lit. $[\alpha]_{\text{D}} = +30.1$ ($c = 2.36$, MeOH)¹³⁶ and $[\alpha]_{\text{D}} = +24.2$ ($c = 1.6$, MeOH)¹³⁷); mp 102.7-103.9 °C (DCM-hexane, v/v = 1/2) (lit. mp 95-96 °C¹³⁶); ¹H NMR (500 MHz, CDCl₃, δ/ppm): 7.80-7.72 (2H, m, 2*ArH*), 7.47-7.40 (1H, m, *ArH*), 7.38-7.32 (2H, m, 2*ArH*), 1.15 (9H, d, $J = 17.6$ Hz, C(CH₃)₃); ¹³C NMR (125 MHz, CDCl₃, δ/ppm): 132.3 (d, $J = 10.0$ Hz, *Ar*), 131.9 (d, $J = 93.8$ Hz, PC*Ar*), 131.5 (d, $J = 3.0$ Hz, *Ar*), 128.7 (d, $J = 12.4$ Hz, *Ar*), 36.3 (d, $J = 72.9$ Hz, PC(CH₃)₃), 24.2 (d, $J = 1.3$ Hz, C(CH₃)₃); ³¹P NMR (121 MHz, CDCl₃, δ/ppm): 97.8; IR (ν_{max} , neat, cm⁻¹): 2975, 2903, 2868, 1739, 1701, 1476, 1462, 1435, 1362, 1109; HRMS (ESI⁻) m/z : Calculated for C₁₀H₁₄OPS (M-H⁺): 213.0508, found: 213.0509. Spectroscopic data consistent with literature values.¹³⁶

N-Benzylaniline (**29**)



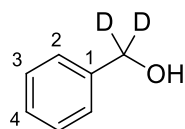
To a stirred suspension of iridium catalyst **102** (8.8 mg, 0.020 mmol) and (*S*)-(+)-1,1'-binaphthyl-2,2'-diyl hydrogen phosphate (14 mg, 0.040 mmol) in toluene (0.5 ml) in presence of 4 Å MS were added benzyl alcohol (103 μl, 1.00 mmol) and aniline (90 μl, 1.0 mmol). The reaction mixture was heated at 110 °C for 24 hours, then cooled at RT and the solvent was removed under reduced pressure. Purification by flash chromatography (Al₂O₃ pH 9.5 ± 0.5, eluting with hexane-EtOAc (90:10 to 60:40)) gave **29** as a pale yellow solid (164 mg, 0.895 mmol, 90%).

Following general procedure L, **29** was prepared from benzyl alcohol (103 μl, 1.00 mmol) and aniline (90 μl, 1.0 mmol). Purification by flash chromatography (Al₂O₃ pH 9.5 ± 0.5,

eluting with hexane-EtOAc (80:20)) gave **29** as a pale yellow solid (145 mg, 0.791 mmol, 79%).

R_f = 0.81 (Basic aluminium oxide, hexane-EtOAc 85:15); mp 30.2-31.1 °C (DCM); ^1H NMR (500 MHz, CDCl_3 , δ/ppm): 7.40-7.34 (4H, m, 4ArH), 7.31-7.27 (1H, m, ArH), 7.21-7.17 (2H, m, 2ArH), 6.73 (1H, t, $J = 7.3$ Hz, H-4), 6.65 (2H, d, $J = 7.5$ Hz, 2ArH), 4.35 (2H, s, ArCH₂), 4.03 (1H, br s, NH); ^{13}C NMR (125 MHz, CDCl_3 , δ/ppm): 148.2 (C-1' or C-1), 139.5 (C-1' or C-1), 129.3 (Ar), 128.6 (Ar), 127.5 (Ar), 127.2 (Ar), 117.6 (C-4), 112.9 (Ar), 48.4 (ArCH₂); IR (ν_{max} , neat, cm^{-1}): 3416 (N-H), 3079, 3051, 3022, 2925, 2847, 1600, 1507, 1492, 1448, 1431, 1327, 1274, 1178, 1151, 1117, 1105, 1026; HRMS (ESI+) m/z : Calculated for $\text{C}_{13}\text{H}_{14}\text{N}$ ($\text{M}+\text{H}^+$): 184.1121, found: 184.1119. Spectroscopic data consistent with literature values.¹²⁷

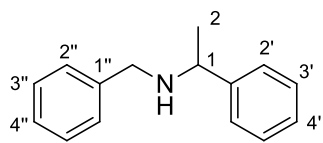
[1',1'-²H₂] Benzyl alcohol (**172**)⁹⁹



To a stirred suspension of LiAlD_4 (700 mg, 16.7 mmol) in THF (7.0 ml) at 0 °C was added dropwise a solution of benzoic acid (1.7 g, 14 mmol) in THF (7.0 ml). The mixture was stirred at RT for 5 hours, cooled at 0 °C and quenched with a careful addition of water. Diethyl ether (15 ml) and 1 M aqueous HCl (15 ml) were added and the two phases separated. The aqueous phase was extracted with diethyl ether (2×20 ml) and the combined organic extracts were dried with Na_2SO_4 . The solvent was removed under reduced pressure to give **87** as a pale yellow oil (1.40 g, 12.5 mmol, 90%).

R_f = 0.48 (hexane-EtOAc 80:20); ^1H NMR (500 MHz, CDCl_3 , δ/ppm): 7.41-7.24 (5H, m, 5ArH), 2.3 (1H, br s, OH); ^{13}C NMR (125 MHz, CDCl_3 , δ/ppm): 140.8 (C-1), 128.5 (Ar), 127.6 (Ar), 127.1 (Ar), 64.5 (t, $J = 21.7$ Hz, ArCD₂); IR (ν_{max} , neat, cm^{-1}): 3310 (O-H), 1495, 1148, 1228, 1092, 1058, 1024; HRMS (ES+) m/z : Calculated for $\text{C}_7\text{H}_6\text{D}_2\text{O}$ (M): 110.0732, found 110.0704. Spectroscopic data consistent with literature values.⁹⁹

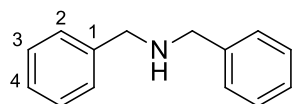
N-Benzyl-1-phenylethanamine (175)



Prepared from benzyl alcohol (124 μ l, 1.20 mmol) and 1-phenylethylamine (130 μ l, 1.00 mmol) following general procedure L. Purification by flash chromatography (Al_2O_3 pH 9.5 ± 0.5 , eluting with hexane-EtOAc (90:10 to 60:40)) gave **175** as a pale yellow oil (101 mg, 0.478 mmol, 48%).

R_f = 0.60 (Basic aluminium oxide, hexane-EtOAc 90:10); ^1H NMR (500 MHz, CDCl_3 , δ/ppm): 7.46-7.30 (10H, m, 10ArH), 3.90 (1H, q, J = 6.6 Hz, H-1), 3.75 (1H, d, J = 13.2 Hz, ArCH_A), 3.68 (1H, d, J = 13.2 Hz, ArCH_B), 1.72 (1H, br s, NH), 1.46 (3H, d, J = 6.6 Hz, H-2); ^{13}C NMR (125 MHz, CDCl_3 , δ/ppm): 145.7 (Ar), 140.8 (Ar), 128.6 (Ar), 128.5 (Ar), 128.2 (Ar), 127.1 (Ar), 126.9 (Ar), 126.8 (Ar), 57.6 (C-1), 51.8 (ArCH₂), 24.6 (C-2); IR (ν_{max} , neat, cm^{-1}): 3026, 2961, 2924, 2852, 1492, 1451, 1124, 1027; HRMS (ESI+) m/z : Calculated for $\text{C}_{15}\text{H}_{18}\text{N}$ ($\text{M}+\text{H}^+$): 212.1434, found: 212.1435. Spectroscopic data consistent with literature values.¹⁰¹

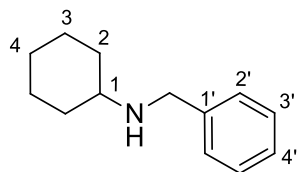
Dibenzylamine (176)



Prepared from benzyl alcohol (103 μ l, 1.00 mmol) and benzylamine (110 μ l, 1.00 mmol) following general procedure L. Purification by flash chromatography (Al_2O_3 pH 9.5 ± 0.5 , eluting with hexane-EtOAc (80:20 to 50:50)) gave **176** as a colourless oil (119 mg, 0.603 mmol, 60%).

R_f = 0.66 (Basic aluminium oxide, hexane-EtOAc 60:40); ^1H NMR (500 MHz, CDCl_3 , δ/ppm): 7.40-7.33 (8H, m, 8ArH), 7.32-7.25 (2H, m, 2ArH), 3.85 (4H, s, 2ArCH₂); ^{13}C NMR (125 MHz, CDCl_3 , δ/ppm): 140.3 (C-1), 128.4 (Ar), 128.2 (Ar), 127.0 (Ar), 53.2 (ArCH₂); IR (ν_{max} , neat, cm^{-1}): 3084, 3062, 3026, 2920, 2812, 1494, 1452, 1361, 1228, 1107, 1027; HRMS (ESI+) m/z : Calculated for $\text{C}_{14}\text{H}_{16}\text{N}$ ($\text{M}+\text{H}^+$): 198.1277, found: 198.1278. Spectroscopic data consistent with literature values.¹²⁷

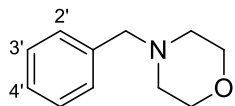
N-Benzylcyclohexanamine (177)



Prepared from benzyl alcohol (103 μ l, 1.00 mmol) and cyclohexylamine (115 μ l, 1.00 mmol) following general procedure L. Purification by flash chromatography (Al_2O_3 pH 9.5 ± 0.5 , eluting with hexane-EtOAc (80:20 to 0:100), followed by EtOAc-MeOH (95:5)) gave **177** as a pale yellow oil (161 mg, 0.851 mmol, 85%).

R_f = 0.66 (Basic aluminium oxide, hexane-EtOAc 70:30); ^1H NMR (500 MHz, CDCl_3 , δ/ppm): 7.34-7.29 (4H, m, 4ArH), 7.25-7.22 (1H, m, ArH), 3.81 (2H, s, ArCH₂), 2.53-2.45 (1H, m, H-1), 1.92 (2H, ap d, $J = 11.3$ Hz, CH₂), 1.80-1.58 (4H, m, CH₂ and NH), 1.31-1.11 (5H, m, CH₂); ^{13}C NMR (125 MHz, CDCl_3 , δ/ppm): 140.4 (C-1'), 128.4 (Ar), 128.2 (Ar), 126.9 (Ar), 56.2 (C-1), 50.9 (ArCH₂), 33.4 (CH₂), 26.2 (CH₂), 25.0 (CH₂); IR (ν_{max} , neat, cm^{-1}): 3062, 3027, 2923, 2851, 1495, 1450, 1361, 1347, 1122; HRMS (ESI+) m/z : Calculated for $\text{C}_{13}\text{H}_{20}\text{N}$ ($\text{M}+\text{H}^+$): 190.1590, found: 190.1591. Spectroscopic data consistent with literature values.¹²⁷

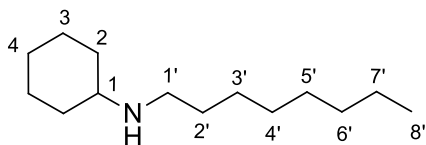
1-Benzylmorpholine (21)



Following general procedure L, **21** was prepared from benzyl alcohol (103 μ l, 1.00 mmol) and morpholine (90 μ l, 1.0 mmol). Purification by flash chromatography (Al_2O_3 pH 9.5 ± 0.5 , eluting with hexane-EtOAc (80:20)) gave **21** as a colourless oil (146 mg, 0.824 mmol, 82%).

R_f = 0.61 (Basic aluminium oxide, hexane-EtOAc 90:10); ^1H NMR (500 MHz, CDCl_3 , δ/ppm): 7.36-7.31 (4H, m, 4ArH), 7.29-7.24 (1H, m, H-4'), 3.72 (4H, t, $J = 4.5$ Hz, 2H-3), 3.51 (2H, s, ArCH₂), 2.46 (4H, t, $J = 4.5$ Hz, 2H-2); ^{13}C NMR (125 MHz, CDCl_3 , δ/ppm): 137.8 (C-1'), 129.2 (Ar), 128.3 (Ar), 127.2 (Ar), 67.1 (C-3), 63.5 (ArCH₂), 53.7 (C-2); IR (ν_{max} , neat, cm^{-1}): 2957, 2853, 2804, 2763, 1454, 1351, 1285, 1263, 1114, 1007; HRMS (ESI+) m/z : Calculated for $\text{C}_{11}\text{H}_{16}\text{NO}$ ($\text{M}+\text{H}^+$): 178.1226, found: 178.1226. Spectroscopic data consistent with literature values.¹²⁴

N-Octylcyclohexanamine (180)

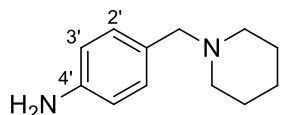


Prepared from 1-octanol (236 μ l, 1.50 mmol) and cyclohexylamine (115 μ l, 1.00 mmol) following general procedure L. Purification by flash

chromatography (Al_2O_3 pH 9.5 ± 0.5 , eluting with DCM-MeOH (98:2)) gave **180** as a yellow oil (150 mg, 0.710 mmol, 71%).

$R_f = 0.47$ (Basic aluminium oxide, hexane-EtOAc 70:30); ^1H NMR (500 MHz, CDCl_3 , δ/ppm): 2.54 (2H, t, $J = 7.2$ Hz, $H-1'$), 2.34 (1H, tt, $J = 10.5, 3.7$ Hz, $H-1$), 1.84-1.77 (2H, m, CH_2), 1.69-1.62 (2H, m, CH_2), 1.59-1.45 (1H, m, CH_2), 1.44-1.36 (2H, m, CH_2), 1.27-0.95 (15H, m, CH_2), 0.81 (3H, t, $J = 7.0$ Hz, $H-8'$); ^{13}C NMR (125 MHz, CDCl_3 , δ/ppm): 55.9 ($C-1$), 46.0 ($C-1'$), 32.6 (CH_2), 30.8 (CH_2), 29.4 (CH_2), 28.5 (CH_2), 28.3 (CH_2), 26.5 (CH_2), 25.2 (CH_2), 24.1 (CH_2), 21.7 (CH_2), 13.1 ($C-8'$); IR (ν_{max} , neat, cm^{-1}): 2922, 2852, 1619, 1450, 1402, 1366, 1307, 1255, 1131; HRMS (ESI+) m/z : Calculated for $\text{C}_{14}\text{H}_{30}\text{N}$ ($\text{M}+\text{H}^+$): 212.2373, found: 212.2375. Spectroscopic data consistent with literature values.³³

1-(4'-Aminobenzyl)piperidine (183)

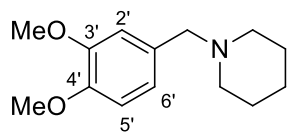


Prepared from 4-aminobenzyl alcohol **155** (123 mg, 1.00 mmol) and piperidine (200 μ l, 2.00 mmol) following general procedure

L. Purification by flash chromatography (Al_2O_3 pH 9.5 ± 0.5 , eluting with DCM-MeOH (99:1)) gave **183** as a yellow oil (163 mg, 0.858 mmol, 86%).

$R_f = 0.49$ (Basic aluminium oxide, DCM-MeOH 95:5); ^1H NMR (500 MHz, CDCl_3 , δ/ppm): 7.09 (2H, d, $J = 8.5$ Hz, $2H-2'$), 6.63 (2H, d, $J = 8.5$ Hz, $2H-3'$), 3.61 (2H, br s, NH_2), 3.37 (2H, s, ArCH_2), 2.35 (4H, br s, $2H-2$), 1.56 (4H, ap quint, $J = 5.8$ Hz, $2H-3$), 1.45-1.39 (2H, m, $H-4$); ^{13}C NMR (125 MHz, CDCl_3 , δ/ppm): 145.2 ($C-1'$), 130.4 ($C-2'$), 128.4 ($C-4'$), 114.8 ($C-3'$), 63.4 (ArCH_2), 54.3 ($C-2$), 26.0 ($C-3$), 24.5 ($C-4$); IR (ν_{max} , neat, cm^{-1}): 3310 (N-H), 3186 (N-H), 2933, 2790, 2749, 1632, 1612, 1516, 1437, 1341, 1289, 1268, 1099; HRMS (ESI+) m/z : Calculated for $\text{C}_{12}\text{H}_{19}\text{N}_2$ ($\text{M}+\text{H}^+$): 191.1543, found: 191.1542.

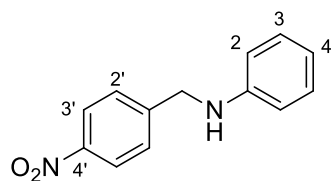
1-(3',4'-Dimethoxybenzyl)piperidine (**184**)



Prepared from 3,4-dimethoxybenzyl alcohol (145 μ l, 1.00 mmol) and piperidine (100 μ l, 1.00 mmol) following general procedure L. Purification by flash chromatography (Al_2O_3 pH 9.5 ± 0.5 , eluting with hexane-EtOAc (90:10)) gave **184** as a colourless oil (176 mg, 0.748 mmol, 75%).

R_f = 0.63 (Basic aluminium oxide, hexane-EtOAc 70:30); ^1H NMR (500 MHz, CDCl_3 , δ/ppm): 6.89 (1H, d, J = 1.5 Hz, H -2'), 6.82 (1H, dd, J = 8.2, 1.5 Hz, H -6'), 6.80 (1H, d, J = 8.2 Hz, H -5'), 3.89 (3H, s, OCH_3), 3.86 (3H, s, OCH_3), 3.41 (2H, s, ArCH_2), 2.36 (4H, br s, $2H$ -2), 1.57 (4H, ap quint, J = 5.5 Hz, $2H$ -3), 1.46-1.40 (2H, m, H -4); ^{13}C NMR (125 MHz, CDCl_3 , δ/ppm): 148.8 (C -3' or C -4'), 148.0 (C -3' or C -4'), 131.4 (C -1'), 121.3 (C -5' or C -6'), 112.4 (C -2'), 110.8 (C -5' or C -6'), 63.6 (ArCH_2), 55.9 (OCH_3), 54.5 (C -2), 26.0 (C -3), 24.5 (C -4), one carbon (OCH_3) not observed; IR (ν_{max} , neat, cm^{-1}): 2931, 2850, 2791, 2752, 1512, 1463, 1416, 1346, 1259, 1232, 1157, 1138, 1028; HRMS (ESI+) m/z : Calculated for $\text{C}_{14}\text{H}_{22}\text{NO}_2$ ($\text{M}+\text{H}^+$): 236.1645, found: 236.1646.

N-(4'-Nitrobenzyl)aniline (**185**)

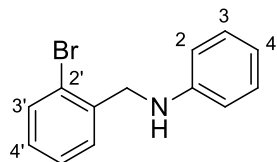


Prepared from 4-nitrobenzyl alcohol (153 mg, 1.00 mmol) and aniline (90 μ l, 1.0 mmol) following general procedure L. Purification by flash chromatography (Al_2O_3 pH 9.5 ± 0.5 , eluting with hexane-EtOAc (80:20)) gave **185** as a yellow oil (124 mg, 0.543 mmol, 54%).

R_f = 0.43 (Basic aluminium oxide, hexane-EtOAc 80:20); ^1H NMR (500 MHz, CDCl_3 , δ/ppm): 8.19 (2H, d, J = 8.5 Hz, $2H$ -3'), 7.54 (2H, d, J = 8.5 Hz, $2H$ -2'), 7.21-7.16 (2H, m, $2H$ -3), 6.76 (1H, t, J = 7.5 Hz, H -4), 6.60 (2H, d, J = 7.5 Hz, $2H$ -2), 4.49 (2H, s, ArCH_2), 4.28 (1H, br s, NH); ^{13}C NMR (125 MHz, CDCl_3 , δ/ppm): 147.5 (Ar), 147.3 (Ar), 147.2 (Ar), 129.4 (C -3), 127.7 (C -2'), 123.9 (C -3'), 118.3 (C -4), 113.0 (C -2), 47.7 (ArCH_2); IR (ν_{max} , neat, cm^{-1}): 3416 (N-H), 3052, 3020, 2922, 2850, 1599, 1504, 1340,

1317, 1264, 1108; HRMS (ESI+) m/z : Calculated for $C_{13}H_{13}N_2O_2$ ($M+H^+$): 229.0972, found: 229.0972. Spectroscopic data consistent with literature values.¹³⁸

***N*-(2'-Bromobenzyl)aniline (186)**

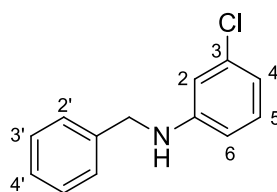


Prepared from 2-bromobenzyl alcohol (187 mg, 1.00 mmol) and aniline (90 μ l, 1.0 mmol) following general procedure L.

Purification by flash chromatography (Al_2O_3 pH 9.5 ± 0.5 , eluting with hexane-EtOAc (95:5)) gave **186** as a colourless oil (119 mg, 0.454 mmol, 45%).

R_f = 0.70 (Basic aluminium oxide, hexane-EtOAc 80:20); 1H NMR (500 MHz, $CDCl_3$, δ/ppm): 7.60 (1H, dd, J = 7.8, 1.2 Hz, $H-3'$), 7.43 (1H, d, J = 7.5 Hz, $H-6'$), 7.28 (1H, t, J = 7.8 Hz, ArH), 7.22-7.14 (3H, m, 3 ArH), 6.76 (1H, t, J = 7.2 Hz, $H-4$), 6.64 (2H, d, J = 7.5 Hz, 2 $H-2$), 4.43 (2H, s, $ArCH_2$), 4.22 (1H, br s, NH); ^{13}C NMR (125 MHz, $CDCl_3$, δ/ppm): 147.7 ($C-3'$), 138.2 (Ar), 132.9 (Ar), 129.3 (Ar), 129.2 (Ar), 128.7 (Ar), 127.6 (Ar), 123.3 (Ar), 117.8 ($C-4$), 113.0 ($C-2$), 48.5 ($ArCH_2$); IR (ν_{max} , neat, cm^{-1}): 3416 ($N-H$), 3052, 3019, 2917, 1600, 1504, 1439, 1323, 1262, 1023; HRMS (ESI+) m/z : Calculated for $C_{13}H_{13}^{79}BrN$ ($M+H^+$): 262.0226, found: 262.0224. Spectroscopic data consistent with literature values.¹³⁹

***N*-Benzyl-3-chloroaniline (187)**



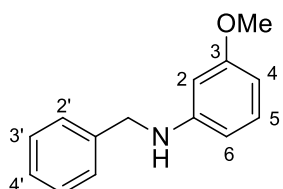
Prepared from benzyl alcohol (103 μ l, 1.00 mmol) and 3-chloroaniline (106 μ l, 1.00 mmol) following general procedure L.

Purification by flash chromatography (Al_2O_3 pH 9.5 ± 0.5 , eluting with hexane-EtOAc (90:10)) gave **187** as a colourless oil (130 mg, 0.597 mmol, 60%).

R_f = 0.76 (Basic aluminium oxide, hexane-EtOAc 80:20); 1H NMR (500 MHz, $CDCl_3$, δ/ppm): 7.42-7.37 (4H, m, 4 ArH), 7.35-7.30 (1H, m, $H-4'$), 7.10 (1H, ap t, J = 8.0 Hz, $H-5$), 6.72 (1H, dt, J = 8.0, 0.8 Hz, $H-4$), 6.65 (1H, ap t, J = 2.0 Hz, $H-2$), 6.52 (1H, dt, J = 8.0, 0.8 Hz, $H-6$), 4.33 (2H, s, $ArCH_2$), 4.13 (1H, br s, NH); ^{13}C NMR (125 MHz, $CDCl_3$, δ/ppm): 149.3 ($C-1'$), 138.8 (Ar), 135.1 (Ar), 130.3 (Ar), 128.8 (Ar), 127.5 (Ar), 127.5 (Ar), 117.5 ($C-4$), 112.6 ($C-2$), 111.2 ($C-6$), 48.2 (CH_2); IR (ν_{max} , neat, cm^{-1}): 3419

(N-H), 3063, 3028, 2853, 1594, 1494, 1484, 1324, 1074; HRMS (ESI+) m/z : Calculated for $C_{13}H_{13}^{35}ClN$ ($M+H^+$): 218.0731, found: 218.0732. Spectroscopic data consistent with literature values.¹⁴⁰

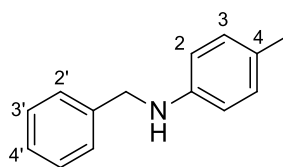
***N*-Benzyl-3-methylaniline (188)**



Prepared from benzyl alcohol (103 μ l, 1.00 mmol) and *m*-anisidine (112 μ l, 1.00 mmol) following general procedure L. Purification by flash chromatography (Al_2O_3 pH 9.5 \pm 0.5, eluting with hexane-EtOAc (90:10)) gave **188** as a colourless oil (96 mg, 0.45 mmol, 45%).

R_f = 0.61 (Basic aluminium oxide, hexane-EtOAc 80:20); 1H NMR (500 MHz, $CDCl_3$, δ/ppm): 7.43-7.34 (4H, m, 4ArH), 7.33-7.28 (1H, m, *H*-4'), 7.11 (1H, ap t, J = 8.1 Hz, *H*-5), 6.34-6.28 (2H, m, 2ArH), 6.23 (1H, ap t, J = 2.3 Hz, *H*-2), 4.34 (2H, s, ArCH₂), 4.10 (1H, br s, NH), 3.78 (3H, s, CH₃); ^{13}C NMR (125 MHz, $CDCl_3$, δ/ppm): 160.9 (*Ar*), 149.6 (*Ar*), 139.4 (*Ar*), 130.0 (*Ar*), 128.7 (*Ar*), 127.6 (*Ar*), 127.3 (*Ar*), 106.1 (*C*-4 or *C*-6), 102.8 (*C*-4 or *C*-6), 99.0 (*C*-2), 55.1 (CH₃), 48.4 (ArCH₂); IR (ν_{max} , neat, cm^{-1}): 3413 (N-H), 3061, 3028, 3000, 2932, 2834, 1611, 1595, 1509, 1494, 1452, 1206, 1159, 1039; HRMS (ESI+) m/z : Calculated for $C_{14}H_{16}NO$ ($M+H^+$): 214.1226, found: 214.1225. Spectroscopic data consistent with literature values.¹⁴¹

***N*-Benzyl-4-methylaniline (189)**

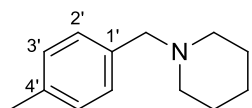


Prepared from benzyl alcohol (103 μ l, 1.00 mmol) and *p*-toluidine (107 mg, 1.00 mmol) following general procedure L. Purification by flash chromatography (Al_2O_3 pH 9.5 \pm 0.5, eluting with hexane-EtOAc (90:10)) gave **189** as a colourless oil (136 mg, 0.689 mmol, 69%).

R_f = 0.77 (Basic aluminium oxide, hexane-EtOAc 80:20); 1H NMR (500 MHz, $CDCl_3$, δ/ppm): 7.46-7.38 (4H, m, 4ArH), 7.35-7.31 (1H, m, *H*-4'), 7.05 (2H, d, J = 8.2 Hz, 2*H*-3), 6.62 (2H, d, J = 8.2 Hz, 2*H*-2), 4.36 (2H, s, ArCH₂), 3.94 (1H, br s, NH), 2.31 (3H, s, CH₃); ^{13}C NMR (125 MHz, $CDCl_3$, δ/ppm): 146.0 (*Ar*), 139.8 (*Ar*), 129.8 (*Ar*), 128.7

(Ar), 127.6 (Ar), 127.2 (Ar), 126.8 (Ar), 113.1 (C-2), 48.7 (ArCH₂), 20.5 (CH₃); IR (ν_{\max} , neat, cm⁻¹): 3415 (N-H), 3027, 2917, 2861, 1616, 1518, 1452, 1320, 1300, 1248; HRMS (ESI+) m/z : Calculated for C₁₄H₁₆N (M+H⁺): 198.1277, found: 198.1279. Spectroscopic data consistent with literature values.¹⁴²

1-(4'-Methyl)benzylpiperidine (190)



Following the general procedure reported by McHardy *et al.*,¹⁴³ to a stirred solution of 4-methylbenzaldehyde (2.0 ml, 17 mmol) and piperidine (1.7 ml, 17 mmol) in DCM (40 ml) were added acetic acid (200 μ l, 3.33 mmol) and sodium triacetoxyborohydride (5.40 g, 25.5 mmol) in small aliquots. The resulting mixture was stirred at RT overnight, quenched with H₂O (10 ml) and 6 M aqueous HCl until pH \sim 1. The two phases were separated and the aqueous phase was basified with 30% aqueous NaOH. DCM was added (100 ml) and the two phases were separated. The product was extracted with DCM (2 \times 100 ml), the combined organic phases were washed with brine and dried with Na₂SO₄. The solvent was removed under reduced pressure to give **190** as a colourless oil (1.26 g, 6.66 mmol, 39%).

R_f = 0.70 (hexane-EtOAc 60:40); ¹H NMR (500 MHz, CDCl₃, δ /ppm): 7.19 (2H, d, J = 8.0 Hz, 2ArH), 7.11 (2H, d, J = 8.0 Hz, 2ArH), 3.43 (2H, s, ArCH₂), 2.36 (4H, br s, 2H-2), 2.33 (3H, s, CH₃), 1.58-1.54 (4H, m, 2H-3), 1.42 (2H, br s, H-4); ¹³C NMR (125 MHz, CDCl₃, δ /ppm): 136.4 (C-1' or C-4'), 135.4 (C-1' or C-4'), 129.3 (C-2' or C-3'), 128.8 (C-2' or C-3'), 63.6 (ArCH₂), 54.4 (C-2), 26.0 (C-3), 24.4 (C-4), 21.1 (CH₃); IR (ν_{\max} , neat, cm⁻¹): 2932, 2853, 2790, 2752, 1514, 1441, 1343, 1269, 1153, 1101, 1039; HRMS (ESI+) m/z : Calculated for C₁₃H₂₀N (M+H⁺): 190.1590, found: 190.1596. Spectroscopic data consistent with literature values.¹²⁷

6.4 Supplementary data

Further supplementary data are included in the attached CD-ROM.

This material included the X-ray files for all the crystal structures reported above in Chapter 2 (complexes **67, 75, 79, 93, 102, 103, 105, 113, 120** and **122**).

It also included all the Excel or Origin files containing the data that have been used to make the graphs and to calculate the observed rate constants in Chapters 2, 4 and 5.

References

- 1 G. Guillena, D. J. Ramón and M. Yus, *Chem. Rev.*, 2010, **110**, 1611–1641.
- 2 J. S. Carey, D. Laffan, C. Thomson and M. T. Williams, *Org. Biomol. Chem.*, 2006, **4**, 2337–2347.
- 3 I. P. Andrews, R. J. Atkins, G. F. Breen, J. S. Carey, M. A. Forth, D. O. Morgan, A. Shamji, A. C. Share, S. A. C. Smith, T. C. Walsgrove and A. S. Wells, *Org. Process Res. Dev.*, 2003, **7**, 655–662.
- 4 G. E. Dobereiner and R. H. Crabtree, *Chem. Rev.*, 2010, **110**, 681–703.
- 5 C. Liu, S. Liao, Q. Li, S. Feng, Q. Sun, X. Yu and Q. Xu, *J. Org. Chem.*, 2011, **76**, 5759–5773.
- 6 M. H. S. A. Hamid, P. A. Slatford and J. M. J. Williams, *Adv. Synth. Catal.*, 2007, **349**, 1555–1575.
- 7 R. Martínez, G. J. Brand, D. J. Ramón and M. Yus, *Tetrahedron Lett.*, 2005, **46**, 3683–3686.
- 8 R. Martínez, D. J. Ramón and M. Yus, *Tetrahedron*, 2006, **62**, 8982–8987.
- 9 R. Martínez, D. J. Ramón and M. Yus, *Tetrahedron*, 2006, **62**, 8988–9001.
- 10 M. G. Edwards and J. M. J. Williams, *Angew. Chemie Int. Ed.*, 2002, **41**, 4740–4743.
- 11 R. Grigg, T. R. B. Mitchell, S. Sutthivaiyakit and N. Tongpenyai, *J. Chem. Soc., Chem. Commun.*, 1981, 611–612.
- 12 S.-I. Murahashi, K. Kondo and T. Hakata, *Tetrahedron Lett.*, 1982, **23**, 229–232.
- 13 Y. Watanabe, Y. Morisaki, T. Kondo and T. Mitsudo, *J. Org. Chem.*, 1996, **61**, 4214–4218.
- 14 M. H. S. A. Hamid and J. M. J. Williams, *Chem. Commun.*, 2007, 725–727.
- 15 M. H. S. A. Hamid, C. L. Allen, G. W. Lamb, A. C. Maxwell, H. C. Maytum, A. J. A. Watson and J. M. J. Williams, *J. Am. Chem. Soc.*, 2009, **131**, 1766–1774.
- 16 A. Tillack, D. Hollmann, D. Michalik and M. Beller, *Tetrahedron Lett.*, 2006, **47**, 8881–8885.
- 17 A. Tillack, D. Hollmann, K. Mevius, D. Michalik, S. Bähn and M. Beller, *European J. Org. Chem.*, 2008, **2008**, 4745–4750.

- 18 S. Bähn, A. Tillack, S. Imm, K. Mevius, D. Michalik, D. Hollmann, L. Neubert and M. Beller, *ChemSusChem*, 2009, **2**, 551–557.
- 19 K. Fujita and R. Yamaguchi, *Synlett*, 2005, 560–571.
- 20 T. Suzuki, *Chem. Rev.*, 2011, **111**, 1825–1845.
- 21 K. Fujita, Z. Li, N. Ozeki and R. Yamaguchi, *Tetrahedron Lett.*, 2003, **44**, 2687–2690.
- 22 K. Fujita, Y. Enoki and R. Yamaguchi, *Tetrahedron*, 2008, **64**, 1943–1954.
- 23 R. Yamaguchi, Z. Mingwen, S. Kawagoe, C. Asai and K. Fujita, *Synthesis*, 2009, 1220–1223.
- 24 M. A. Berliner, S. P. A. Dubant, T. Makowski, K. Ng, B. Sitter, C. Wager and Y. Zhang, *Org. Process Res. Dev.*, 2011, **15**, 1052–1062.
- 25 O. Saidi, A. J. Blacker, M. M. Farah, S. P. Marsden and J. M. J. Williams, *Chem. Commun.*, 2010, **46**, 1541–1543.
- 26 O. Saidi, A. J. Blacker, G. W. Lamb, S. P. Marsden, J. E. Taylor and J. M. J. Williams, *Org. Process Res. Dev.*, 2010, **14**, 1046–1049.
- 27 R. Kawahara, K. Fujita and R. Yamaguchi, *Adv. Synth. Catal.*, 2011, **353**, 1161–1168.
- 28 A. da Costa, M. Viciano, M. Sanaú, S. Merino, J. Tejada, E. Peris and B. Royo, *Organometallics*, 2008, **27**, 1305–1309.
- 29 A. Prades, R. Corberán, M. Poyatos and E. Peris, *Chem. – A Eur. J.*, 2008, **14**, 11474–11479.
- 30 D. Gnanamgari, E. L. O. Sauer, N. D. Schley, C. Butler, C. D. Incarvito and R. H. Crabtree, *Organometallics*, 2009, **28**, 321–325.
- 31 C. M. Crudden and D. P. Allen, *Coord. Chem. Rev.*, 2004, **248**, 2247–2273.
- 32 J.-Q. Li and P. G. Andersson, *Chem. Commun.*, 2013, **49**, 6131–6133.
- 33 A. Wetzel, S. Wöckel, M. Schelwies, M. K. Brinks, F. Rominger, P. Hofmann and M. Limbach, *Org. Lett.*, 2013, **15**, 266–269.
- 34 D. Balcells, A. Nova, E. Clot, D. Gnanamgari, R. H. Crabtree and O. Eisenstein, *Organometallics*, 2008, **27**, 2529–2535.
- 35 P. Fristrup, M. Tursky and R. Madsen, *Org. Biomol. Chem.*, 2012, **10**, 2569–2577.
- 36 G.-M. Zhao, H. Liu, X. Huang, D. Zhang and X. Yang, *RSC Adv.*, 2015, **5**, 22996–23008.

- 37 E. V Anslyn and D. A. Dougherty, *Modern Physical Organic Chemistry*, University Science, 2006.
- 38 S. Bähn, S. Imm, L. Neubert, M. Zhang, H. Neumann and M. Beller, *ChemCatChem*, 2011, **3**, 1853–1864.
- 39 A. Martínez-Asencio, M. Yus and D. J. Ramón, *Synthesis*, 2011, 3730–3740.
- 40 T. T. Dang, B. Ramalingam, S. P. Shan and A. M. Seayad, *ACS Catal.*, 2013, **3**, 2536–2540.
- 41 T. Yan, B. L. Feringa and K. Barta, *Nat Commun*, 2014, **5**, publish online 26 November 2014.
- 42 A. J. Rawlings, L. J. Diorazio and M. Wills, *Org. Lett.*, 2015, **17**, 1086–1089.
- 43 K. Fujita, T. Fujii and R. Yamaguchi, *Org. Lett.*, 2004, **6**, 3525–3528.
- 44 T. Naota, H. Takaya and S.-I. Murahashi, *Chem. Rev.*, 1998, **98**, 2599–2660.
- 45 L. U. Nordstrom and R. Madsen, *Chem. Commun.*, 2007, 5034–5036.
- 46 K. Yuan, F. Jiang, Z. Sahli, M. Achard, T. Roisnel and C. Bruneau, *Angew. Chemie Int. Ed.*, 2012, **51**, 8876–8880.
- 47 C. S. Cho, B. T. Kim, H.-J. Choi, T.-J. Kim and S. C. Shim, *Tetrahedron*, 2003, **59**, 7997–8002.
- 48 K. Taguchi, S. Sakaguchi and Y. Ishii, *Tetrahedron Lett.*, 2005, **46**, 4539–4542.
- 49 A. J. Blacker, M. M. Farah, M. I. Hall, S. P. Marsden, O. Saidi and J. M. J. Williams, *Org. Lett.*, 2009, **11**, 2039–2042.
- 50 K. Fujita, K. Yamamoto and R. Yamaguchi, *Org. Lett.*, 2002, **4**, 2691–2694.
- 51 H. Aramoto, Y. Obora and Y. Ishii, *J. Org. Chem.*, 2009, **74**, 628–633.
- 52 K. Fujita, A. Komatsubara and R. Yamaguchi, *Tetrahedron*, 2009, **65**, 3624–3628.
- 53 M. Zhu, K. Fujita and R. Yamaguchi, *Org. Lett.*, 2010, **12**, 1336–1339.
- 54 T. C. Nugent and M. El-Shazly, *Adv. Synth. Catal.*, 2010, **352**, 753–819.
- 55 M. Höhne, S. Köhl, K. Robins and U. T. Bornscheuer, *ChemBioChem*, 2008, **9**, 363–365.
- 56 R. Noyori, M. Yamakawa and S. Hashiguchi, *J. Org. Chem.*, 2001, **66**, 7931–7944.
- 57 W.-P. Liu, M.-L. Yuan, X.-H. Yang, K. Li, J.-H. Xie and Q.-L. Zhou, *Chem. Commun.*, 2015, **51**, 6123–6125.

- 58 C. Wang, X. Wu and J. Xiao, *Chem. – An Asian J.*, 2008, **3**, 1750–1770.
- 59 S. Gladiali and E. Alberico, *Chem. Soc. Rev.*, 2006, **35**, 226–236.
- 60 N. J. Oldenhuis, V. M. Dong and Z. Guan, *J. Am. Chem. Soc.*, 2014, **136**, 12548–12551.
- 61 Y. Zhang, C.-S. Lim, D. S. B. Sim, H.-J. Pan and Y. Zhao, *Angew. Chemie Int. Ed.*, 2014, **53**, 1399–1403.
- 62 Z.-Q. Rong, Y. Zhang, R. H. B. Chua, H.-J. Pan and Y. Zhao, *J. Am. Chem. Soc.*, 2015, **137**, 4944–4947.
- 63 T. D. Nixon, M. K. Whittlesey and J. M. J. Williams, *Dalt. Trans.*, 2009, 753–762.
- 64 N. N. Greenwood and A. Earnshaw, *Chemistry of the Elements*, 1990, Norwich, N. Y.: Knovel.
- 65 M. Cotton, F. Albert; Wilkinson, Geoffrey; Murillo, Carlos A.; Bochmann, *Advanced Inorganic Chemistry*, 1999, Wiley–Interscience.
- 66 B. Zhao, Z. Han and K. Ding, *Angew. Chemie Int. Ed.*, 2013, **52**, 4744–4788.
- 67 S. Hashiguchi, A. Fujii, J. Takehara, T. Ikariya and R. Noyori, *J. Am. Chem. Soc.*, 1995, **117**, 7562–7563.
- 68 R. Soni, K. E. Jolley, G. J. Clarkson and M. Wills, *Org. Lett.*, 2013, **15**, 5110–5113.
- 69 F. K. Cheung, C. Lin, F. Minissi, A. L. Crivillé, M. A. Graham, D. J. Fox and M. Wills, *Org. Lett.*, 2007, **9**, 4659–4662.
- 70 M. Ito, N. Tejima, M. Yamamura, Y. Endo and T. Ikariya, *Organometallics*, 2010, **29**, 1886–1889.
- 71 D. van Leusen, D. J. Beetstra, B. Hessen and J. H. Teuben, *Organometallics*, 2000, **19**, 4084–4089.
- 72 M. Ito, Y. Endo, N. Tejima and T. Ikariya, *Organometallics*, 2010, **29**, 2397–2399.
- 73 H. Adams, N. A. Bailey, M. Colley, P. A. Schofield and C. White, *J. Chem. Soc., Dalt. Trans.*, 1994, 1445–1451.
- 74 Q. Chu, W. Zhang and D. P. Curran, *Tetrahedron Lett.*, 2006, **47**, 9287–9290.
- 75 Q. Chu, M. S. Yu and D. P. Curran, *Org. Lett.*, 2008, **10**, 749–752.
- 76 H. Yu, L. Wan and C. Cai, *J. Fluor. Chem.*, 2012, **144**, 143–146.
- 77 W. Zhang and D. P. Curran, *Tetrahedron*, 2006, **62**, 11837–11865.

- 78 M. Smrcina, P. Majer, E. Majerová, T. A. Guerassina and M. A. Eissenstat, *Tetrahedron*, 1997, **53**, 12867–12874.
- 79 H. C. Brown and P. Heim, *J. Org. Chem.*, 1973, **38**, 912–916.
- 80 G. Pelletier, W. S. Bechara and A. B. Charette, *J. Am. Chem. Soc.*, 2010, **132**, 12817–12819.
- 81 T. Reiner, D. Jantke, A. Raba, A. N. Marziale and J. Eppinger, *J. Organomet. Chem.*, 2009, **694**, 1934–1937.
- 82 W. R. Esmieu, S. M. Worden, D. Catterick, C. Wilson and C. J. Hayes, *Org. Lett.*, 2008, **10**, 3045–3048.
- 83 C. Feng, Y. Liu, S. Peng, Q. Shuai, G. Deng and C.-J. Li, *Org. Lett.*, 2010, **12**, 4888–4891.
- 84 Y. Liu, W. Chen, C. Feng and G. Deng, *Chem. – An Asian J.*, 2011, **6**, 1142–1146.
- 85 A. Zanardi, J. A. Mata and E. Peris, *Chem. – A Eur. J.*, 2010, **16**, 10502–10506.
- 86 A. J. Blacker, S. Brown, B. Clique, B. Gourlay, C. E. Headley, S. Ingham, D. Ritson, T. Screen, M. J. Stirling, D. Taylor and G. Thompson, *Org. Process Res. Dev.*, 2009, **13**, 1370–1378.
- 87 A. J. Blacker, M. J. Stirling and M. I. Page, *Org. Process Res. Dev.*, 2007, **11**, 642–648.
- 88 S. R. S. Saibabu Kotti, C. Timmons and G. Li, *Chem. Biol. Drug Des.*, 2006, **67**, 101–114.
- 89 J. Burch, M. Corbett, C. Stock, K. Nicholson, A. J. Elliot, S. Duffy, M. Westwood, S. Palmer and L. Stewart, *Lancet Infect. Dis.*, 2015, **9**, 537–545.
- 90 D. J. Biedenbach and R. N. Jones, *J. Clin. Microbiol.*, 1994, **32**, 559–562.
- 91 N. J. Wheate, S. Walker, G. E. Craig and R. Oun, *Dalt. Trans.*, 2010, **39**, 8113–8127.
- 92 B. Blank, S. Michlik and R. Kempe, *Adv. Synth. Catal.*, 2009, **351**, 2903–2911.
- 93 S. Agrawal, M. Lenormand and B. Martín-Matute, *Org. Lett.*, 2012, **14**, 1456–1459.
- 94 J. Boström, H. Emtenäs, K. Granberg, M. Mogemark and A. Llinas, WO2012074469 A1, 2012.
- 95 W. Zhang, *Chem. Rev.*, 2004, **104**, 2531–2556.

- 96 S. J. Lucas, B. D. Crossley, A. J. Pettman, A. D. Vassileiou, T. E. O. Screen, A. J. Blacker and P. C. McGowan, *Chem. Commun.*, 2013, **49**, 5562–5564.
- 97 C. Li, B. Villa-Marcos and J. Xiao, *J. Am. Chem. Soc.*, 2009, **131**, 6967–6969.
- 98 R. I. Storer, D. E. Carrera, Y. Ni and D. W. C. MacMillan, *J. Am. Chem. Soc.*, 2006, **128**, 84–86.
- 99 J. Bialecki, J. Ruzicka and A. B. Attygalle, *J. Mass Spectrom.*, 2006, **41**, 1195–1204.
- 100 L. Neubert, D. Michalik, S. Bähn, S. Imm, H. Neumann, J. Atzrodt, V. Derdau, W. Holla and M. Beller, *J. Am. Chem. Soc.*, 2012, **134**, 12239–12244.
- 101 C. Wang, A. Pettman, J. Bacsá and J. Xiao, *Angew. Chemie Int. Ed.*, 2010, **49**, 7548–7552.
- 102 B. Ye and N. Cramer, *Science*, 2012, **338**, 504–506.
- 103 T. K. Hyster, L. Knörr, T. R. Ward and T. Rovis, *Science*, 2012, **338**, 500–503.
- 104 B. Ye and N. Cramer, *J. Am. Chem. Soc.*, 2013, **135**, 636–639.
- 105 M. Zhao, H.-B. Wang, L.-N. Ji and Z.-W. Mao, *Chem. Soc. Rev.*, 2013, **42**, 8360–8375.
- 106 K. Alfonsi, J. Colberg, P. J. Dunn, T. Fevig, S. Jennings, T. A. Johnson, H. P. Kleine, C. Knight, M. A. Nagy, D. A. Perry and M. Stefaniak, *Green Chem.*, 2008, **10**, 31–36.
- 107 S. Narayan, J. Muldoon, M. G. Finn, V. V Fokin, H. C. Kolb and K. B. Sharpless, *Angew. Chemie Int. Ed.*, 2005, **44**, 3275–3279.
- 108 R. Kawahara, K. Fujita and R. Yamaguchi, *J. Am. Chem. Soc.*, 2010, **132**, 15108–15111.
- 109 O. Soltani, M. A. Ariger, H. Vázquez-Villa and E. M. Carreira, *Org. Lett.*, 2010, **12**, 2893–2895.
- 110 G. A. Molander, P. E. Gormisky and D. L. Sandrock, *J. Org. Chem.*, 2008, **73**, 2052–2057.
- 111 T. Heck, A. Reimer, D. Seebach, J. Gardiner, G. Deniau, A. Lukaszuk, H.-P. E. Kohler and B. Geueke, *ChemBioChem*, 2010, **11**, 1129–1136.
- 112 Y. Yoshitomi, H. Arai, K. Makino and Y. Hamada, *Tetrahedron*, 2008, **64**, 11568–11579.
- 113 T. J. Harrison, J. A. Kozak, M. Corbella-Pané and G. R. Dake, *J. Org. Chem.*, 2006, **71**, 4525–4529.

- 114 E. C. Garnier and L. S. Liebeskind, *J. Am. Chem. Soc.*, 2008, **130**, 7449–7458.
- 115 M. A. DeWit and E. R. Gillies, *Org. Biomol. Chem.*, 2011, **9**, 1846–1854.
- 116 S. K. Agrawal, M. Sathe, A. K. Halve and M. P. Kaushik, *Tetrahedron Lett.*, 2012, **53**, 5996–5999.
- 117 G. S. Khan, B. D. Dickson and D. Barker, *Tetrahedron*, 2012, **68**, 1790–1801.
- 118 S. Elshani, E. Kobzar and R. A. Bartsch, *Tetrahedron*, 2000, **56**, 3291–3301.
- 119 G. Barbe and A. B. Charette, *J. Am. Chem. Soc.*, 2008, **130**, 18–19.
- 120 H.-S. Lin and L. A. Paquette, *Synth. Commun.*, 1994, **24**, 2503–2506.
- 121 D. Hollmann, A. Tillack, D. Michalik, R. Jackstell and M. Beller, *Chem. – An Asian J.*, 2007, **2**, 403–410.
- 122 Y. Fukumoto, H. Asai, M. Shimizu and N. Chatani, *J. Am. Chem. Soc.*, 2007, **129**, 13792–13793.
- 123 P. Spies, S. Schwendemann, S. Lange, G. Kehr, R. Fröhlich and G. Erker, *Angew. Chemie Int. Ed.*, 2008, **47**, 7543–7546.
- 124 O. O. Kovalenko, A. Volkov and H. Adolfsson, *Org. Lett.*, 2015, **17**, 446–449.
- 125 F. Wang, J. A. D. Good, O. Rath, H. Y. K. Kaan, O. B. Sutcliffe, S. P. Mackay and F. Kozielski, *J. Med. Chem.*, 2012, **55**, 1511–1525.
- 126 N. Murai, M. Yonaga and K. Tanaka, *Org. Lett.*, 2012, **14**, 1278–1281.
- 127 T. Zhang, Y. Zhang, W. Zhang and M. Luo, *Adv. Synth. Catal.*, 2013, **355**, 2775–2780.
- 128 R. P. Tripathi, N. Saxena, V. K. Tiwari, S. S. Verma, V. Chaturvedi, Y. K. Manju, A. K. Srivastva, A. Gaikwad and S. Sinha, *Bioorg. Med. Chem.*, 2006, **14**, 8186–96.
- 129 Q. Lei, Y. Wei, D. Talwar, C. Wang, D. Xue and J. Xiao, *Chem. – A Eur. J.*, 2013, **19**, 4021–4029.
- 130 Z. Liu and J. F. Hartwig, *J. Am. Chem. Soc.*, 2008, **130**, 1570–1571.
- 131 W. Russell Bowman and D. R. Coghlan, *Tetrahedron*, 1997, **53**, 15787–15798.
- 132 M. C. Carter, S. Cockerill, S. S. Flack and C. J. Wheelhouse, WO2009034390 A1, 2009.
- 133 B. Sezen and D. Sames, *J. Am. Chem. Soc.*, 2005, **127**, 5284–5285.

- 134 J. Omelańczuk and M. Mikolajczyk, *Tetrahedron: Asymmetry*, 1996, **7**, 2687–2694.
- 135 K. V Rajendran and D. G. Gilheany, *Chem. Commun.*, 2012, **48**, 817–819.
- 136 R. K. Haynes, T.-L. Au-Yeung, W.-K. Chan, W.-L. Lam, Z.-Y. Li, L.-L. Yeung, A. S. C. Chan, P. Li, M. Koen, C. R. Mitchell and S. C. Vonwiller, *European J. Org. Chem.*, 2000, **2000**, 3205–3216.
- 137 Z. Skrzypczynski and J. Michalski, *J. Org. Chem.*, 1988, **53**, 4549–4551.
- 138 R. He, P. H. Toy and Y. Lam, *Adv. Synth. Catal.*, 2008, **350**, 54–60.
- 139 M. Jiang, J. Li, F. Wang, Y. Zhao, F. Zhao, X. Dong and W. Zhao, *Org. Lett.*, 2012, **14**, 1420–1423.
- 140 X. Yu, C. Liu, L. Jiang and Q. Xu, *Org. Lett.*, 2011, **13**, 6184–6187.
- 141 Y. Zhang, T. F. Jamison, S. Patel and N. Mainolfi, *Org. Lett.*, 2011, **13**, 280–283.
- 142 D. B. Bagal, R. A. Watile, M. V Khedkar, K. P. Dhake and B. M. Bhanage, *Catal. Sci. Technol.*, 2012, **2**, 354–358.
- 143 S. F. McHardy, J. A. Bohmann, M. R. Corbett, B. Campos, M. W. Tidwell, P. M. Thompson, C. J. Bembien, T. A. Menchaca, T. E. Reeves, W. R. Cantrell, W. E. Bauta, A. Lopez, D. M. Maxwell, K. M. Brecht, R. E. Sweeney and J. McDonough, *Bioorg. Med. Chem. Lett.*, 2014, **24**, 1711–4.